Title
Human exposure to dynamic air pollutants: Ozone in airplanes and ultrafine particles in homes

Author
Bhangar, Seema Vijay

Publication Date
2010

Peer reviewed|Thesis/dissertation

Human Exposure to Dynamic Air Pollutants: Ozone in Airplanes and Ultrafine Particles in Homes

By

Seema Vijay Bhangar

A dissertation submitted in partial satisfaction of the

requirements for the degree of

Doctor of Philosophy
in

Engineering – Civil and Environmental Engineering

in the

GRADUATE DIVISION

of the

UNIVERSITY OF CALIFORNIA, BERKELEY

Committee in charge:

Professor William W Nazaroff, Chair
Professor Robert A. Harley
Professor Robert C. Spear

Fall 2010

Human exposure to dynamic air pollutants: Ozone in airplanes and ultrafine particles in homes

by Seema Vijay Bhangar

Abstract

Human exposure to dynamic air pollutants: Ozone in airplanes and ultrafine particles in homes

by

Seema Vijay Bhangar

Doctor of Philosophy in Engineering – Civil and Environmental Engineering

University of California, Berkeley

Professor William W Nazaroff, Chair

To effectively control health risks associated with an airborne contaminant we need to understand when, where, why, and how much humans come into contact with the contaminant. To answer these questions, the temporal and spatial variability in levels of species must be evaluated in relation to the locations of humans in space and time. Characterizing human exposure through the measurement of pollutant levels within occupied microenvironments where people spend time is particularly important for species that have sharp gradients owing to rapid environmental processing. This is especially true if the pollutant dynamics are influenced by the presence or activities of the occupants themselves.

This dissertation investigates inhalation exposures to two dynamic air pollutants in two important settings: ultrafine particles (UFP) in residences and ozone in aircraft cabins. New field data were acquired and observed pollutant trends were modeled to assess the importance for indoor concentrations and exposures of outdoor levels, ventilation characteristics, indoor sources, pollutant dynamics, human factors, and control strategies. Study findings can be applied to assess the risk associated with each exposure scenario and to suggest conditions under which interventions are likely to have the greatest public health impact.

In the first part of the dissertation, residential exposures to ultrafine particles were characterized and governing factors explored on the basis of field data collected from single-family houses in California. During the field study, time-resolved particle number (PN) concentrations were monitored indoors and outdoors over a multi-day period, and information was acquired concerning occupancy, source-related activities, and building operation. Technological challenges have limited prior efforts to acquire time-resolved data on UFP from homes under normal occupied conditions, data that are potentially important for understanding total daily exposures to ultrafine particles as people spend a majority of their time in their own homes.

Results showed levels of ultrafine particles in houses to be highest when residents were present and awake, mainly due to their cooking and other activities that constituted episodic indoor sources. On average, the contribution to residential exposures from indoor episodic sources was 150 percent of the contribution from particles of outdoor origin. A previously

unstudied continuous indoor source, unvented pilot lights, caused baseline particle levels to be significantly elevated in houses where present. Particle control devices – a filter or an electrostatic precipitator – were successful at mitigating exposure by reducing the persistence of particles indoors. We found that, owing to the importance of indoor sources, variations in the infiltration factor, and the influence of human behavior patterns on indoor UFP levels, residential exposures to ultrafine particles could not be characterized either by ambient levels or by average indoor levels alone.

The source characterization and exposure apportionment results from the study of ultrafine particles in residences were applied to quantify inhalation intake fractions (*iF*) for ultrafine particles emitted from indoor sources. Intake fraction is an exposure metric that quantifies the mass of pollution inhaled by all exposed persons per mass of pollution released. As such, *iF* estimates encapsulate the exposure effectiveness of a source under the exposure conditions considered. The analysis presented is one of only a few *iF* investigations focused on UFP and is also the first semi-empirical *iF* investigation for indoor sources to rely on experimental data resolved at the level of individual occupants and source-events.

For the continuous source (unvented pilot lights) and the episodic source events observed during the monitoring period at all study sites, estimated intake fractions ranged from 0.7×10^{-3} to 16×10^{-3}, consistent with previous estimates for contaminants released indoors. House-specific factors such as the volume and number of residents, and occupant-specific factors such as breathing rates and time-activity patterns, had a significant influence on *iF*. Particle loss rates and occupancy patterns did not vary markedly among source types. Consequently, source type did not have a significant, independent influence on intake fractions.

In the second part of the dissertation, ozone levels in airplane cabins and factors that influence them were studied on commercial passenger flights. Ozone levels in passenger aircraft had not been the subject of a full-scale time-resolved monitoring effort since 1980, when U.S. Federal Aviation Regulations limiting ozone in cabin air were adopted. Studies conducted prior to 1980 were in need of an update because, in the past three decades, the operating conditions of commercial aircraft have changed significantly. Moreover our understanding of ozone's reactions with cabin surfaces, including human surfaces, and of the health risks associated with exposure to ozone and ozone oxidation byproducts has grown. Findings on in-cabin ozone need to be interpreted in light of the new findings.

To close this knowledge gap real-time ozone data were collected within the cabins of commercial passenger aircraft on 76 flight segments. Sample mean ozone level, peak-hour ozone level, and flight-integrated ozone exposures were highly variable across U.S. domestic segments, with ranges of <1.5 to 146 ppb, 3 to 275 ppb, and <1.5 to 488 ppb-hour, respectively. On planes equipped with ozone catalysts, the mean peak-hour ozone level was substantially lower than on planes not equipped with catalysts. For aircraft with catalysts, levels were higher on transoceanic flights than on domestic routes. In addition, within the transoceanic sample, ozone levels were lower on newer aircraft, a pattern that may be explained by differences in converter efficiency. Seasonal variation on domestic routes without converters was modeled by a sinusoidal curve, predicting peak-hour levels approximately 70 ppb higher in Feb-March than in Aug-Sept. The temporal trend was broadly consistent with expectations, given the annual variation in tropopause height. Episodically elevated (>100 ppb) ozone levels on domestic flights were associated with winter-spring storms that were linked to enhanced exchange between the lower stratosphere and the upper troposphere.

As in-cabin ozone originates outside, findings from the field study were supplemented

with an analysis of atmospheric ozone levels collected through the Measurement of Ozone and Water Vapor by Airbus In-service Aircraft (MOZAIC) monitoring campaign. Temporal and spatial trends in ozone levels encountered by aircraft were investigated by analyzing the data from all MOZAIC flights between Munich and three U.S. destinations. In a finding that reinforced the in-cabin study results, the MOZAIC analysis showed ozone levels cycled through the year, and positive outliers to the mean cycle were spatially and temporally consistent with known patterns of stratosphere-to-troposphere exchange. A spatial analysis showed that, for the routes surveyed, there was no monotonic increase in atmospheric ozone with latitude. On average, ozone levels increased with altitude, though the relationship between altitude and ozone was highly variable within and between flights. The spatial analysis also showed that even in domestic US airspace ambient ozone concentrations greater than 100 ppb were routinely encountered. This result illustrated the potential benefit of equipping all U.S. passenger aircraft – not just the ones designed for transoceanic travel, as is standard practice – with ozone catalysts.

Acknowledgments

When I was a senior in college it dawned on me that I did not want to have anything more to do with the field – anthropology – that I had pursued for the previous three years. I was living in an environmental-themed co-op at the time and found myself increasingly compelled by the interests and pursuits of many of my housemates. If left to my own devices I might have assumed it was too late to make a change, and I am grateful to Morgan LaRue who brushed away my hesitations and marched me to her lab to seek a research project with her advisor; and I thank her advisor, Alfred Spormann, for giving me the break I needed to make a switch.

Holmes Hummel encouraged me to apply to Berkeley. I was sold on the environmental health program after an inspiring and encouraging meeting with Kirk Smith, who has since been a valued teacher, mentor and guide and to whom I owe a debt for introducing me to my true passion in environmental science: research on air quality and health.

Kara Nelson encouraged and facilitated my next move, to a PhD in environmental engineering. I owe the success of my subsequent doctoral career first and foremost to my advisor, Bill Nazaroff. His patient, steady coaching and the habits of mind he helped me to instill (or perhaps to undo) were crucial in helping me finish and will, I expect, have a long reach in aiding my future career. Most of all I appreciate Bill's integrity and wisdom and the complete trust I have been able to place in his support and judgment. It has been a privilege to have close access to his uncluttered, Sherlock Holmes-like, impeccably rational – and yet creative – mind.

The faculty on my dissertation and qualifying exam committees – Rob Harley, Bob Spear, David Sedlak and Allen Goldstein – provided guidance, a new lens through which to view my research and the encouragement that assured me I legitimately belonged in my new field. Rob's incisive comments and humor have been instrumental in providing a fresh perspective on my research and in fostering a warm and collegial tone at our Airheads group meetings. Jim Kirchner, Mark Nicas and Charlie Weschler have been additional sources of both research advice and personal encouragement. I have frequently availed of Shelley Okimoto's open door for help with paperwork, which always comes with the perk of a friendly chat.

I thank colleagues at the Lawrence Berkeley National Laboratory – Brett Singer, Rich Sextro, Hugo Destaillats, Doug Sullivan, Tom Kirchstetter, Tosh Hotchi and others – for being collaborators on, or otherwise facilitating, the studies in this dissertation. Shannon Cowlin laid the foundation for the ozone field study. The ultrafine particles field campaign was a collaborative effort with Susanne Hering and Nathan Kreisberg, our colleagues at Aerosol Dynamics, Inc.; with Nasim Mullen, my co-investigator on the ground; and with Bill Nazaroff, who was the principal investigator and the lead author of the final report that describes the work comprehensively. A California Air Resources Board contract and a Federal Aviation Administration Office of Aerospace Medicine grant funded much of the research contained in this dissertation.

I am grateful to my fellow graduate students, many of whom are now lifelong friends. Lisa Thompson and Manish Desai enlivened nights of work during my early years at Berkeley. Rengie Chan, Shannon Cowlin, Garvin Heath, Abby Hoats, Julian Marshall and Mark Sippola eased my transition into my new home in Davis Hall, a home I settled happily into thanks to the Airheads Josh Apte, Bev Coleman, Dev Millstein, Nasim Mullen, Arman Shehabi and especially Sharon Shearer, with whom I've shared an office, a commute and hundreds of tea, lunch and bathroom breaks during the difficult final year of dissertation writing.

Finally, my deep and most affectionate thanks go to:

My parents, Vijay and Nirupa, and my brothers, Sanjay and Sameer, for their unconditional love and for allowing me to be myself. The verbal fighting matches I can only have with Sameer have been a key stress relief tool. My parents have had, since my earliest school days, a masterful way of being boundlessly proud of my accomplishments while making it clear that the things that really matter lie elsewhere.

Nani for being the original source of my love of learning. All her grandchildren have had to tolerate, at least temporarily, being ignored while she was immersed in a book.

Jo Ann, Tom and John Downing, Heidi Hval, my Kothari and Kothari-Saura cousins nearby, and my extended families afar for forming the community that sustains me and keeps my life balanced. Daily phone calls with Jo Ann helped me make it through the crazy final months of being terminally pregnant and working on my dissertation.

Zac Unger and Shona Armstrong for providing me with a home near campus during my years living in Sacramento.

My dear friends Kathleen Bennett, Jaquelin Cochran, Ilya Druzhnikov, Susan Fischer, Jonah Holmes, Aine Keenan, Munira Khalil and Kritika Yegnashankaran for believing in me, for the endless hours spent brainstorming and commiserating with me or helping me pull my head out of the sand, and for the forthright, frank insights that keep me on track; and to my friend and former teacher, Anahita Devitre, who helped me develop the skills and self-confidence that led me to the United States.

And my husband, Jim Downing, who helps me grow by loving the best in me and embodying much that I admire and aspire to. He keeps me grounded and happy, gives my life a sense of purpose and makes me laugh when I least expect it. I work better and more efficiently for knowing that the end of a work day means going home to Jim.

Seema Bhangar
December 13, 2010

Table of Contents

Abstract 1
Acknowledgments i
Table of contents iii
List of tables vi
List of figures viii

Chapter 1: Introduction 1
1.1. Exposure 1
1.1.1. Exposure science: What it is and why it matters 1
1.1.2. Quantifying exposure 2
1.1.3. Exposure as a receptor-oriented science 3
1.1.4. History and current trends 4
1.1.5. Exposure assessment methods: Direct and indirect approaches 5
1.2. Dynamic air pollutants 7
1.3. Occupied microenvironments 9
1.4. Overview of dissertation 10
1.5. References 12

Chapter 2: Ultrafine particle concentrations and exposures in seven residences in northern California 16
2.1. Introduction 16
2.2. Methods 18
2.2.1. Site selection 18
2.2.2. Experimental protocols 21
2.2.3. Instruments and data acquisition 21
2.2.4. Quality assurance 22
2.2.5. Data analysis 22
2.3. Results and discussion 25
2.3.1. Particle number (PN) concentrations 25
2.3.2. Indoor episodic sources 30
2.3.3. Outdoor concentration pattern 36
2.3.4. Indoor proportion of outdoor particles (*f*) 40
2.3.5. Indoor emissions from unvented pilot lights 41
2.3.6. Exposure assessment 42
2.4. Conclusions 44
2.5. References 46
2.A. Appendix 50
2.A.1. Evaluating building ventilation rates with indoor and outdoor carbon dioxide measurements 50
2.A.1.1. Introduction 50
2.A.1.2. Data analysis 51
2.A.1.3. Results and discussion 52
2.A.1.4. References 53

Chapter 3: Inhalation intake fraction of ultrafine particles from indoor emissions in homes 54
3.1. Introduction 54
3.1.1. Issue 54
3.1.2. Inhalation intake fraction 55
3.1.3. Background and literature review 55
3.1.4. Study objectives 62
3.2. Methods 62
3.2.1. Evaluating intake fractions 62
3.2.2. Episodic sources 63
3.2.3. Continuous sources 64
3.2.4. Input parameters 65
3.2.4.1. Inhalation rate (Q_b) 65
3.2.4.2. House volume (V) 67
3.2.4.3. Particle first-order loss rate (k+a) 68
3.2.4.4. Occupancy and time-activity patterns 69
3.3. Results and discussion 69
3.3.1. Episodic sources 69
3.3.1.1. Individual and aggregate intake fractions 69
3.3.1.2. Assessment of uncertainty 73
3.3.1.3. House-specific characteristics 74
3.3.1.4. Influence of source type 77
3.3.1.5. Human factors 78
3.3.2. Continuous sources 80
3.4. Conclusions 81
3.5. References 83
3.A. Appendix 85
3.A.1. Comparing two sources of data for short-term inhalation rates 85
3.A.1.1. Results and discussion 85
3.A.1.2. References 86
3.A.2. Errors in input parameters 87
3.A.2.1. Inhalation rate 87
3.A.2.2. Volume 87
3.A.2.3. Particle first-order loss rate 87
3.A.2.4. Time-activity patterns 87
3.A.2.5. Reference 88

Chapter 4: Ozone levels in passenger cabins of commercial aircraft on North American and transoceanic routes 89
4.1. Introduction 89
4.2. Methods 90
4.2.1 In-flight sampling 90
4.2.2 Sampling method 91
4.2.3 Quality assurance 91
4.2.4 Data analysis 92
4.3. Results and discussion 92

4.4. References....102
4.A. Appendix....104
4.A.1. Determining an effective collection rate for the Ogawa passive ozone sampler for the aircraft cabin environment....104
4.A.1.1. Introduction....104
4.A.1.2. Methods....106
4.A.1.2.1. Experimental protocols....106
4.A.1.2.2. Data analysis....107
4.A.1.3. Results....107
4.A.1.4. Discussion....108
4.A.1.5. References....110
4.A.2. Flight-by-flight measurement results....111

Chapter 5: Atmospheric ozone levels encountered by commercial passenger aircraft on transatlantic routes....114
5.1. Introduction....114
5.2. Background: The tropopause....115
5.3. Methods....115
5.3.1 The MOZAIC project....115
5.3.2 Data acquisition....116
5.3.3 Data analysis....117
5.4. Results and discussion....117
5.4.1 Comparing means....117
5.4.2 Temporal effects....119
5.4.3 Spatial effects....123
5.5. Implications for in-cabin ozone exposures....133
5.6. Conclusions....134
5.7. References....135

Chapter 6: Conclusions....137
6.1. Summary of findings....137
6.2. Opportunities for future research....140
6.2.1. Indoor sources....141
6.2.1.1. Residential exposure to ultrafine particles from cooking....141
6.2.1.2. In-cabin exposure to ozone byproducts....142
6.2.2. Ultrafine particle emissions from natural gas appliance pilot lights....143
6.2.3. Direct versus indirect exposure assessment....143
6.2.4. Lessons from other disciplines....144
6.3. References....144

List of Tables

2-1a. Source-oriented attributes of study houses 18
2-1b. Characteristics of house sites studied 20
2-2. Average particle number concentrations (in units of 1000 particles cm^{-3}) measured during observational monitoring at the house sites 26
2-3. Appliances used or activities engaged in during observational monitoring, and whether they were associated with particle peaks 31
2-4. First-order decay constants and source strengths for peak events associated with identified single activities at the seven houses 32
2-5. Air-exchange rates determined at the seven house sites 41
2A-1. Air-exchange rate estimates for five house sites without indoor CO_2 sources, obtained on the basis of three alternate approaches 53
3-1. Summary of published research in peer-reviewed archived journals on intake fractions for indoor sources in homes 57-58
3-2. Short-term breathing rate estimates based on a metabolic approach, sorted by demographic group and activity level 66
3-3. Demographic classification of the 21 study subjects, for purposes of assigning breathing rate estimates. 67
3-4. House volume 68
3-5. Summary of $k+a$ estimates used to assess pilot lights iF at site H1 68
3-6. Individual and aggregate intake fractions for the 50 quantifiable episodic source events observed over 26 days of monitoring at the seven house sites 71-72
3-7. Summary statistics (arithmetic means and standard deviations) for aggregate and individual intake fractions assessed for the 50 episodic source events at the seven house sites 75
3-8. Aggregate and individual intake fractions for quantifiable peak events at the seven houses associated with identified single activities 78
3-9. Individual and aggregate intake fractions for UFP emissions from unvented natural gas pilot lights at sites H1 and H3 81
3A-1. Short-term breathing rate estimates based on direct-measurement techniques, sorted by demographic group 86
4-1. Summary of 76 flight segments monitored 93
4A-1. Flight-by-flight measurement results for the 11 segments on which passive sampling was conducted 106
4A-2. Flight-by-flight measurement results for domestic segments 111-112
4A-3. Flight-by-flight measurement results for transoceanic segments 113
5-1. Number of flight segments in the MOZAIC database during 1995-2005, by year, and by US city involved 116
5-2. Summary of least-squares best-fit parameters for the model in Equation (5.1) 121
5-3. The percentage of flights per month with peak 1-h or flight-average ozone model residuals greater than 100, 200, and 300 ppb 122

5-4. The fraction of flight time elapsed before the 1-h ozone peak is logged, by route 128
5-5. The mean “distance” from Munich when the 1-h ozone peak is logged, by route 128

List of Figures

2-1. Map of the approximate location of six of the seven house sites, in the East Bay Area of California. 19
2-2. Illustrative time series of indoor and outdoor particle number concentrations from the seven home sites 27-29
2-3. Ratios of mean indoor divided by mean outdoor (I/O) particle number concentrations measured during observational monitoring at the seven house sites, sorted according to occupancy status 30
2-4a. Cumulative distribution of particle source strength for 56 episodic events that were quantified from observational monitoring at the seven home sites 33
2-4b. Cumulative distribution of 51 determinations of first-order particle decay rate coefficient obtained from observational monitoring at the seven home sites 34
2-5. The particle number concentration associated with repeated uses of the furnace (natural gas, vented) at site H0....35
2-6. Diurnal variations in outdoor PN concentrations at sites H0-H6 38
2-7a. Time series of 1-h average outdoor particle number concentration, nitric oxide, carbon dioxide, and carbon monoxide levels at site H1 39
2-7b. Time series of 1-h average outdoor particle number concentration, nitric oxide, carbon dioxide, and carbon monoxide levels at site H3 40
2-8. Particle number concentrations versus time during the supplemental pilot-light experiments conducted at H1 and H3 42
2-9. The residential, average PN exposure for the 21 occupants of the seven houses studied 43
2A-1. Diurnal variation in outdoor CO_2 at sites H0-H6....51
3-1. Cumulative probability distribution of *iF* estimates for 50 episodic indoor source events observed during 26 days of observational monitoring over an ensemble of seven house sites 70
3-2. Aggregate *iF* estimates sorted by house site....75
3-3a. Average *iF* estimates sorted by house site, with each house identified by its approximate ventilation flow rate 76
3-3b. Average *iF* estimates sorted by house site, with each house identified by its estimated volume 76
3-4. Aggregate *iF* estimates sorted by source type 78
3-5. A comparison of "hypothetical" and "measured" *iF* for indoor peak source-use episodes....80
4-1. Weighted cumulative distributions of peak one-hour and sample-average ozone mixing ratios sampled in passenger cabins on 68 domestic US flight segments 94
4-2. Ozone levels sampled on eight transoceanic flights 95
4-3. Weighted cumulative distribution of ozone exposure levels from 68 domestic flight segments....97

4-4. Peak one-hour ozone for domestic flights without converters and with converters, plotted against time-of-year 99
4-5. Real-time ozone data from four consecutive domestic transcontinental US segments monitored within a 6-day interval in April 2007 100
4A-1. A comparison between background-corrected Ogawa passive sampler raw readings (in g nitrate), and ozone exposure values based on readings from the 2B Technologies' real-time ozone monitor when the two were simultaneously deployed 108
5-1. Weighted cumulative distributions of peak 1 h and sample-average ozone mixing ratios sampled outside passenger cabins of aircraft on six transatlantic routes.....118
5-2. Peak atmospheric 1-h ozone for aircraft on westbound and eastbound flights between Munich and each of three US cities, plotted against time-of-year.....120
5-3. Model residuals (measured ozone minus modeled ozone) versus time-of-year for peak 1-h and flight-average ozone (N = 865) 121
5-4a. Locations where peak ozone levels were encountered, for the 51 flights (out of 225) between Munich and Chicago, NY, and LA in Jan-Mar with peak 1-h ozone model residuals exceeding 100 ppb 124
5-4b. Ozone levels measured along flight tracks, for the 51 flights (out of 225) between Munich and Chicago, NY, and LA in Jan-Mar with peak 1-h ozone model residuals exceeding 100 ppb.....124
5-5. Ozone levels measured along flight tracks for the 66 MOZAIC flights between Munich and Chicago, NY, and LA monitored in June.....125
5-6a. Peak 1-h ozone model residuals versus the mean altitude corresponding to the 1-h peak on each flight segment 126
5-6b. Flight-average ozone model residuals versus the corresponding flight mean altitude.....126
5-7. Annual mean vertical distribution of ozone (10^{11} molecules per cubic centimeter) over North America (NRC, 2002) 127
5-8. The mean flight-average altitude and the mean altitude at which peak 1-h ozone levels are logged, for the six flight routes investigated.....128
5-9. Sample flight tracks for the route between Munich and each of three US cities.....130
5-10a. Ozone levels measured along flight tracks for the 66 MOZAIC flights between Munich and either Chicago, NY, or LA monitored in June, grouped according to altitude.....131
5-10b. Ozone levels measured along flight tracks for the 51 MOZAIC flights between Munich and either Chicago, NY, or LA with very high ozone, monitored in Jan-Mar, grouped according to altitude 132

4-4. Peak one-hour ozone for domestic flights without converters and with converters, plotted against time-of-year 99
4-5. Real-time ozone data from four consecutive domestic transcontinental US segments monitored within a 6-day interval in April 2007 100
4A-1. A comparison between background-corrected Ogawa passive sampler raw readings (in g nitrate), and ozone exposure values based on readings from the 2B Technologies' real-time ozone monitor when the two were simultaneously deployed 108
5-1. Weighted cumulative distributions of peak 1 h and sample-average ozone mixing ratios sampled outside passenger cabins of aircraft on six transatlantic routes.....118
5-2. Peak atmospheric 1-h ozone for aircraft on westbound and eastbound flights between Munich and each of three US cities, plotted against time-of-year.....120
5-3. Model residuals (measured ozone minus modeled ozone) versus time-of-year for peak 1-h and flight-average ozone (N = 865) 121
5-4a. Locations where peak ozone levels were encountered, for the 51 flights (out of 225) between Munich and Chicago, NY, and LA in Jan-Mar with peak 1-h ozone model residuals exceeding 100 ppb 124
5-4b. Ozone levels measured along flight tracks, for the 51 flights (out of 225) between Munich and Chicago, NY, and LA in Jan-Mar with peak 1-h ozone model residuals exceeding 100 ppb.....124
5-5. Ozone levels measured along flight tracks for the 66 MOZAIC flights between Munich and Chicago, NY, and LA monitored in June.....125
5-6a. Peak 1-h ozone model residuals versus the mean altitude corresponding to the 1-h peak on each flight segment 126
5-6b. Flight-average ozone model residuals versus the corresponding flight mean altitude.....126
5-7. Annual mean vertical distribution of ozone (10^{11} molecules per cubic centimeter) over North America (NRC, 2002) 127
5-8. The mean flight-average altitude and the mean altitude at which peak 1-h ozone levels are logged, for the six flight routes investigated.....128
5-9. Sample flight tracks for the route between Munich and each of three US cities.....130
5-10a. Ozone levels measured along flight tracks for the 66 MOZAIC flights between Munich and either Chicago, NY, or LA monitored in June, grouped according to altitude.....131
5-10b. Ozone levels measured along flight tracks for the 51 MOZAIC flights between Munich and either Chicago, NY, or LA with very high ozone, monitored in Jan-Mar, grouped according to altitude 132

Chapter 1: Introduction

The research presented in this dissertation explores factors influencing human inhalation exposure to dynamic air pollutants in occupied microenvironments such as transportation vehicles and buildings. In this chapter, background information that frames the research is presented, and an overview of topics covered in the remaining chapters is provided.

Three themes frame the present work: *exposure*, *dynamic air pollutants*, and *occupied microenvironments.* Each of these themes is considered below.

1.1. Exposure

1.1.1. Exposure science: What it is and why it matters

Exposure science is concerned with the interface between humans and chemical, physical and biological agents that are present in the environment. In a narrow sense, the aim of an exposure assessment is to describe the concentrations of an agent at the human-environment interface and the duration of contact between the human and the agent. Toxicological and epidemiological information can help to identify a biologically relevant time of contact, which in turn informs the appropriate time-scale to be considered in an exposure investigation. More broadly, the objective of exposure science is to not just quantify exposures, but also to assess factors influencing exposure, so as to provide a basis for developing exposure mitigation strategies for given exposure circumstances and also to evaluate the anticipated public health benefits associated with alternative interventions. Environmental agents are responsible for a substantial portion of the US and global burdens of disease (WHO, 2010). Human resources to control the exposures that lead to these burdens are necessarily finite, and their deployment frequently involves trade-offs. The judicious application of exposure science methods can help to promote the efficient allocation of resources to control environmental risks, by helping to prioritize amongst a range of pollutants, exposed populations, and potential interventions (Lioy, 2010; Klepeis and Nazaroff, 2006; Zartarian et al., 1997; Zartarian et al., 2005).

The broad exposure-science objectives noted above are best pursued by considering the whole system that links sources to health effects. The system comprises the following components, which can be conceived as a bridge between the environment and public health: sources, concentrations in environmental media (air, water, soil or dust), exposures (i.e., contact), intakes, doses, and health effects (Smith, 1993; Marshall and Nazaroff, 2004; Ott, 2006). The "exposure" component of the bridge constitutes, predictably, the central focus of the exposure scientist. However, attention to the other components is needed to fulfill the broad exposure-science objectives noted above. For instance, "downstream" components such as dose and health effects can aid in identifying exposure scenarios of potential health concern and in defining appropriate exposure metrics. "Upstream" components, such as source emission rates, and processes and mechanisms that transfer the agent to the human receptor, can be used to design control strategies, and to refine plans for the routine collection of exposure data.

Field monitoring is the standard method for assessing exposures. A whole-system approach to exposure science – using tools from a range of disciplines including science and engineering, statistics, and the health and social sciences – facilitates the generalization of

findings from field studies to environments and scenarios not directly studied (Ott, 2006). For example, the exposure effectiveness (*EE*) and intake fraction (*iF*) metrics link source emissions directly to exposure or intake, respectively (Evans et al., 2002; Bennett et al., 2002). Once estimates of *EE* or *iF* are defined (on the basis of models and/or measurements), and conditions under which they apply are described, they can be used to rapidly predict the expected exposure associated with a source without the need for costly and potentially intrusive measurements. Exposure involves humans, and studies involving humans are often complicated by ethical concerns, logistics, or the idiosyncratic nature of human behavior. These constraints add value to the innovation and application of exposure-science methods that rely on modeling, simulation, automatic sensors and other tools that enable exposure data to be collected and used more efficiently (Lioy, 2010).

Assessing exposure is an integral part of the risk assessment and management paradigm. It also plays a key role in epidemiological studies, and may be needed for clinical diagnosis and the prevention of disease (Lioy, 1990). As it is concerned with both risk analysis and control, exposure science is relevant for academics, the private sector, and government agencies. Regulators, health workers, policy makers, and the general public all draw on exposure knowledge to support environmental policy decisions or to make personal decisions relating to their health.

1.1.2. Quantifying exposure

Lioy (2010) defines an "equation" of exposure as follows:

$$E = \int_{t_0}^{t_1} C(t)dt \tag{1.1}$$

Exposure (E) is a function of both the concentration (C) of an agent of concern in contact with humans and intervals of time (dt) during which the contact occurs. Zartarian et al. (2005) present a quantitative definition of exposure assessment that asserts it is the process of estimating or measuring the magnitude, frequency, and duration of exposure to an agent, along with the number and characteristics of the population exposed (Zartarian et al., 2005). As is indicated by these definitions, an exposure assessment exercise has considerable flexibility in terms of defining the "exposure" to be quantified. The exposure of concern may be chronic or acute (or both). The subject of an exposure assessment can be an individual or a population and, in the case of the latter, the entire general public or discrete groups (subpopulations) defined on the basis of occupation, demographics, health status, or other criteria. The study can be designed to look at extant environmental conditions, historical data, or data from a controlled laboratory or field setting. An investigation may look at total exposure, or focus on a subset of sources, pathways, or routes. Moreover the usefulness of an exposure estimate is enhanced when it is paired with a description of its uncertainty and variability, and of the determinants of this variability (Zartarian et al., 2005; Paustenbach, 2000).

1.1.3. Exposure as a receptor-oriented science

Source-oriented approaches to assessing and controlling environmental risks require *a priori* identification of potential sources of concern, and thus treat the first component in the environment to public-health bridge as a focal point. While a source-based strategy may venture into explicit evaluation of exposures, by measuring or modeling factors that influence occupied microenvironmental concentrations, the human receptor is often missing from the analysis. In contrast, the "exposure" component – or human interface – is the focus of the receptor-oriented scientist. Like source-based strategies, the receptor-based approach is concerned with sources and environmental concentrations. It differs in that the focus is inverted so the receptor becomes the subject of the investigation, which can then proceed in both directions from the source to the receptor or the receptor to the source (Ott, 2006). A direct consequence of the change in focus is that importance is accorded to factors that influence exposure. These factors overlap with, but are not coincident with, the factors that influence emissions or environmental concentrations.

Receptor-based investigations have revealed that the exposure effectiveness (or intake fraction) of common pollution sources can vary over many orders of magnitude (Smith, 1988; Smith, 2002; Lai et al., 2000). The most obvious decoupling between exposure and environmental concentration occurs in relation to location or the use of personal protective equipment. Irrespective of environmental levels of an agent, exposure to it may be low if people are absent, or are shielded with efficacious protective devices (Nicas, 1995). No matter how detailed are the spatial and temporal maps of pollutant levels, they cannot give an indication of exposure without further information on the presence of humans, and their potential use of barriers against exposure. Knowledge about human attributes and behavior, referred to as "human activity patterns", is also important because these can influence pollutant sources or sinks. Activity pattern information must include details on location, attributes or behaviors that influence pollutant levels and inhalation intake rate. Owing to the variability amongst humans, putting the receptor into the story can thus complicate analyses and expand the uncertainty in results.

Despite challenges associated with the receptor-oriented approach, it has gained prominence as a tool for revealing novel sources and control measures, or evaluating the importance (from the perspective of exposure) of ones that were already known. As such, the approach is useful for setting priorities amongst potential exposure-mitigation strategies (Smith, 2002). The source-centered approach tends to accord central importance to controlling emissions from sources with the greatest *mass* emission rates to the outdoor atmosphere, such as industrial facilities and motor-vehicles. Through the use of the receptor-based method we now know that for a wide range of pollutants, exposure is dominated by emissions that may be smaller on an absolute scale, but that occur in close proximity to humans. Examples of such sources include building materials, consumer products (including cigarettes), appliances, and even the human body itself (Smith, 1988; Nazaroff, 2008). A focus on the receptor shifts priorities on which sources are most important to control and affords the opportunity to consider and compare a broader and more flexible range of strategies to protect humans from the harm associated with environmental agents. These strategies go beyond emissions controls to include dimensions such as enhanced ventilation, selective filtration, personal protection, or altering patterns of location and personal source-use.

1.1.4. History and current trends

Examples from the historical record show that concern with exposure predates its codification as a formal, quantitative field of study. Humans have always interacted closely with environmental media, relied on ecosystem goods for their livelihood and well-being, and endeavored to protect themselves from environmental hazards. In the most simple case, imagine a human tending a fire, who notes that exposure to the smoke is linked with respiratory discomfort; and that the discomfort can be mitigated by turning away from the direct plume. In this case, the magnitude of exposure could be qualitatively assessed by proxies such as the thickness of the smoke, the number of times it blows on the target, the size of the target population, and so on. A more formal example is from the early epidemiological literature. John Snow identified the cause of a cholera epidemic in London in 1854 by mapping the pattern of disease, and finding cases were clustered around a single water pump. By this process, the consumption of water from a contaminated pump was identified as the pathway of exposure, and the risk was mitigated by removing the pump and handle. (Lioy, 1990).

Pioneering work by Alice Hamilton and others in the early 1900s is cited as initiating the systematic analysis of exposure. In 1986 the USEPA drafted formal exposure assessment guidelines (Lioy, 1990). Early work in the 1990s addressed exposures that were marked by two criteria: they were visible or otherwise tangible, and they were relatively easily linked with a health outcome. These criteria were most often met by extreme pollution episodes, or occupational exposures, which made both an attractive choice for early exposure studies. Workplaces presented the exposure scientist with a discrete population, bounded physical environment, and clear sources and pathways of exposure for study. Moreover, exposures to individual pollutants was often especially high in workplaces, and resulting health effects were commonly acute. The temporal association between the exposure and health outcome facilitated the attribution of harm to one or more environmental agents.

The events that mark the establishment of exposure assessment or exposure science as a distinct field are described by Lioy (2008). As the tools of this field have become more sophisticated, the trend has been toward tackling scenarios where the associations between exposures and health outcomes are more subtle, variable, complex, or otherwise challenging to characterize. Current tools enable us to appreciate that small spatial and temporal scales can exert large effects on exposure (Ott, 2006; Smith, 1988), which motivates us to pay attention to microenvironments where people spend time, and to time-resolved trends in contaminant levels and exposures. Exposure scientists are now more likely to investigate exposures experienced in non-workplace settings, to investigate low-level or chronic exposures, and to consider a wider range of sources, pathways, routes, and variables influencing exposure. The study of exposure has become quantitative and measurement-based to a greater degree, and the use of statistical tools to define the precision of exposure estimates is now common. In looking ahead at future directions for exposure science, Lioy (2010) advocates a proactive view where the tools of exposure science are applied to evaluate the potential for harmful contacts to occur, and to prevent or minimize them in advance.

In the air pollution field, although it is still common for outdoor measurements to be used as proxies for estimates of exposure, new research findings challenge this convention and help to define its advantages and limitations. There is a certain logic to studying outdoor sources as these are in the public domain, and because they are the main anthropogenic driver for ambient air pollution, which falls under the purview of public regulation. Furthermore, under some

circumstances, outdoor sources dominate the health risk attributed to an agent, so controlling emissions from these sources can be an effective environmental health strategy. In contrast, trends that favor the following actions or factors diminishes the utility of ambient measurements for the management of environmental risk: (1) regulations that limit emissions from ambient sources, thus reducing outdoor air pollution over time; (2) buildings designed and operated to be more airtight in order to save energy; (3) the use in building ventilation systems of filters to treat outdoor air; (4) the use of health-damaging chemicals in building materials and consumer products, and the use of appliances that emit pollutants indoors; and (5) the high proportion of time spent indoors. (Lioy, 1990).

1.1.5. Exposure assessment methods: Direct and indirect approaches

Exposure can be quantified via "direct" or "indirect" methods. Both have been widely applied, and each possesses distinct advantages and limitations. The choice of one or the other strategy depends on many factors, including the underlying motivation (e.g., assessing the effectiveness of a potential intervention or designing a program to mitigate the exposure, establishing a dose-response relationship, assessing risk), properties of the contaminant of concern, available instruments, access to study subjects, the variability in exposure, study budget, and intended study duration. I argue that the two methods, rather than being viewed competitively, can complement each other when used judiciously to assess and manage environmental risk.

The direct method is so called because it characterizes by means of measurement the levels of an agent at the interface between the individual and the environment. The levels may be characterized by means of a personal sampling device (e.g., Palmes and Gunnison, 1973), or by identifying and measuring biomarkers of exposure (e.g., Lan et al., 2004). The application of the direct method requires a random sampling scheme, and the number of people sampled must be sufficient to allow inferences to be drawn, with known precision, about exposure of the larger population from which the sample is drawn. When combined with statistical analyses of human activity data, the direct method can aid in the identification of variables that contribute to exposure (Ott, 2006). The direct method has advantages in implicitly accounting for spatial and temporal variability in pollutant levels and human activity patterns, and in potentially measuring exposure from all sources and pathways. No *a priori* determination is needed about microenvironments where exposure occurs. The direct method is also a useful means for validating findings based on the indirect method (Klepeis, 1999).

The first practical personal samplers used photographic film to detect exposures to radiation. The Manhattan project provided an impetus for the development and use of monitoring badges for radiation detection, and by 1945 dosimeters that could be worn by workers to evaluate their exposure were commercially available (Poston, 2005). As reported by Silverman (1954), industrial hygienists also made advances in the 1930s and 1940s in developing equipment to sample gases and particles in workplaces. The Occupational Health and Safety Act, signed into law in 1970, formalized this use of personal sampling in the workplace.

Examples of early, direct exposure investigations relating to air quality reported in the literature include a study of the exposure of harvesters to pesticide residues (Popendor and Spear, 1974), and a study measuring personal carbon monoxide exposures (Cortese and Spengler, 1976). Examples of large-scale applications of the direct approach are the Total Exposure Assessment Methodology (TEAM) and National Human Exposure Assessment Survey

(NHEXAS) studies conducted by the US Environmental Protection Agency (EPA). In the 1979-1985 TEAM study, a stratified random sample of 600 people was monitored with specially developed personal samplers, to estimate the volatile organic compound (VOC) exposure of urban residents in selected US cities (Wallace, 1987). In the Particle TEAM (PTEAM) study, conducted in 1990, exposure to airborne particulate matter in Riverside, California, was surveyed (Ozkaynak et al., 1996). Beginning in the 1990s, the NHEXAS group of studies combined personal monitoring with the sampling of biomarkers to further explore and develop exposure assessment methods.

In the indirect approach, exposure is assessed using information on pollutant concentrations in microenvironments and human activity pattern data (Yoshida et al., 1980; Duan, 1982). Instead of installing a monitor on a person who then transports it through space and time, monitors are placed in fixed locations (or pollutant concentrations are predicted using mathematical models), and the movements of the individual are tracked. The indirect approach can be used to predict individual personal exposures without the problems of cost, logistics, access, and feasibility involved in measuring exposure directly. When combined with Monte-Carlo methods (Macintosh et al., 1995) or the use of input parameters with well-defined variances (Klepeis, 1999), the indirect exposure framework can be used to generate population frequency distributions of exposure. A virtue of the indirect approach is that it can be employed to rapidly and inexpensively generate estimates of exposure over a wide range of scenarios; and the sensitivity of exposure to quantifiable parameters can be readily assessed (Klepeis, 1999).

The indirect method is ideally suited to identifying and evaluating the relative importance of factors that influence exposure, which is necessary to fulfill the purpose of intervening with effective controls. Investigations in this dissertation rely on the indirect method. Consequently, the remainder of this section looks more closely at methods and emerging trends in indirect exposure research. Core components of the indirect method are assessing pollutant levels in microenvironments and assessing human time-activity patterns. Each is discussed in turn below.

Data on levels of a contaminant in microenvironments can be generated empirically by means of environmental measurements, or theoretically by means of mathematical models such as those based on the material balance principle. Varying levels of complexity may be brought to bear on the definition of a microenvironment. At the simplest level, microenvironments are defined on the level of their function, at a predetermined spatial scale, resulting in designations such as residence, vehicle, office, library, school. In a more sophisticated treatment, microenvironments are further defined on the basis of criteria such as time of day, season, weather conditions, geographic regions, demographic group under consideration; or the microenvironment itself may be defined on the basis of a finer spatial scale, such as kitchen instead of house. Such classifications aid in the generalization of findings to conditions outside the ones directly studied. A single microenvironment may be chosen as the focus of an exposure investigation on the basis of criteria such as high exposures, the presence of a vulnerable population, being previously understudied, or being the potential target of an intervention. Or, for a total exposure assessment, all locations where a population of interest spends significant time must be considered (Klepeis, 1999).

Several tools exist for collecting data on human activity patterns. These tools can be broadly categorized as population-based or individual-based. Population-based activity pattern data are collected through randomized surveys and may be used in the place of individual measurements when the subjects of an exposure study are drawn from the population that was surveyed. Such surveys typically include a range of questions relating to activities, locations,

and the use of and proximity to potential pollution sources. The Consolidated Human Activity Database (CHAD), maintained by the USEPA's National Exposure Research Laboratory (NERL), is a source of such data, with ~23,000 person-days of activity spanning disparate cohorts (McCurdy et al., 2000). NERL sponsored the National Human Activity Pattern Survey (NHAPS), which was carried out from 1992-1994 and included 9,386 respondents recruited via a random sampling methodology from across the contiguous United States (Klepeis et al., 2001). CHAD also includes data from two large surveys conducted in California in 1987-1990 (Jenkins et al., 1992). Survey-based activity data can be helpful for predicting the frequency distribution of exposures in a population.

Individual-based approaches monitor the real-time, location-activity profile of subjects in an exposure study, with the aid of written records or sensors. Written records include questionnaires, surveys, or time-activity diaries, and typically depend on recall. Sensors can provide information about location and, in limited cases, about specific activities relating to exposure. Advantages of sensors include their accuracy relative to recall and their potential for being less intrusive than a diary or questionnaire. The requirement to keep a record of location and activities may cause a subject to unconsciously alter his or her behavior; this bias risk is reduced when the data are collected automatically.

Emerging research explores the use of automated sensors for obtaining location and activity data. Ultrasound transmitter/receiver pairs developed by Allen-Piccolo et al. (2009) represent an inexpensive means of indicating when a subject in present in a microenvironment (e.g., various rooms in a house). Global Positioning System (GPS) tools were used to successfully quantify time-location trends at a relatively high spatial resolution (typically about 2-3 m outdoors and 4-5 m indoors), for a cohort of 11 children in Seattle (Elgethun et al., 2003). The GPS units were integrated into the children's clothing, and data were transferred into GIS software for analysis. GPS profiles and diaries were also used to estimate individual exposure to $PM_{2.5}$ in a study by Gerharz et al. (2009).

Location and activity patterns can also be tracked via indirect indicators, such as the open or closed state of doors, or the temperature near a source. This approach was applied in this dissertation. "State" sensors were installed on windows and doors, and served as indicators of when these were opened and closed. Temperature sensors were installed on potential indoor sources that heat up when operated (e.g. furnace, cooking range, toaster oven), and served as indicators of their use (Nazaroff et al., 2010). New research on sensors includes expanding their use to collect population-level data on exposure-relevant variables, such as stove use.

1.2. Dynamic air pollutants

When a species is released from a source into air it is subject to physical and chemical processes that cause it to be transformed, removed to a surface, or transported to a different airborne location. Potential species transformation processes include phase change and partitioning, and acid-base or redox reactions. Removal occurs by transport in the bulk fluid, or contaminant flux to fixed surfaces or to airborne particles, which occurs by mechanisms such as gravitational settling, diffusion, dispersion, inertial drift, and drift owing to electrostatic or thermophoretic forces (Nazaroff and Alvarez-Cohen, 2001). In this dissertation, a "dynamic" airborne species is defined as one that undergoes rapid chemical or physical processing following its release. "Rapid" in this context implies that the species is transformed or removed from the air at timescales faster than the residence time of the air mass in the region or indoor

environment. Typical residence times for air in an urban airshed are on the order of a day; indoors, residence times depend on the air exchange rate and are typically on the order of an hour.

The groupings "airborne particles" and "airborne gases" each contain conserved and dynamic components. For particles, the significance of dynamic behaviors tend to correspond with size. This class of contaminants is often divided into three groups, based on particle diameter, that receive separate consideration (Nazaroff, 2004). Particles in the largest (coarse mode) and smallest (ultrafine mode) size groups have a shorter lifetimes in air than do particles in the middle size range or accumulation mode (0.1-1 μm). Airborne gases span a wide range of lifetimes. At one extreme are long-lived, highly conserved species such as chlorofluorocarbons, nitrous oxide and carbon dioxide whose atmospheric residence times are on the order of years and longer. At the other limit are dynamic, short-lived radicals such as $NO_3^{\cdot}$, $OH^{\cdot}$ and $HO_2^{\cdot}$ which have midday lifetimes of seconds or less (Seinfeld and Pandis, 1998). Between these two extremes lie the relatively stable carbon monoxide, and less stable ozone, nitrogen oxides, sulfur dioxide, and volatile or semivolatile organic compounds.

In a mixed aerosol, elements that can be characterized as dynamic under the extant set of environmental conditions are preferentially removed. The result of uneven atmospheric processing is that air masses that are under the influence of fresh emissions are more likely to be enriched with dynamic components, while aged air masses are more likely to contain species that are relatively conserved. This trend has potential implications for public health, as it confers distinct features on fresh and aged air masses, which may in turn be linked with distinct health effects. Assessing exposure to dynamic species also poses special challenges (Sioutas et al., 2005), as it requires strategies that are sensitive to potentially sharp spatial and temporal gradients. Where dynamic species are concerned, the use of ambient monitoring data as a proxy for exposure in interior microenvironments is particularly inadequate. On the contrary, the need for high-frequency measurements is especially acute for characterizing exposures to dynamic air pollutants, as time-dependent phenomena that are relevant for assessing health effects and identifying sources would be masked by integrated sampling.

Conditions and processes that act on a species rendering it dynamic depend on the environment and on the species. Outdoor and indoor environments, discussed in turn below, each have attributes that amplify the relative importance of distinct physical and chemical processes. In outdoor air, species are subject to shortwave solar radiation, which can provide primary energy initiating chemical transformations; strong variations in meteorological conditions such as temperature and relative humidity that can, for instance, influence the activation of particles into cloud condensation nuclei; and transport by wind (Seinfeld and Pandis, 1998). Indoors, species are subject to transport between zones, and across the indoor/outdoor interface; sorptive reactions with surfaces; and reactive chemistry fueled by oxidants such as ozone or nitrates (Nazaroff, 2004; Nazaroff and Weschler, 2004). Five features distinct to indoor (versus outdoor) environments are: (1) the lack of a strong source of short-wave radiation; hence species that are rapidly broken down in the atmosphere during the daytime can persist indoors; (2) a high surface-area to volume ratio, which implies that species amenable to surface uptake will have a shorter lifetime indoors; (3) more stable environmental conditions (such as temperature, relative humidity, wind speed), which retards environmental transformations dependent on extremes in these measures; (4) typically, a higher occupant density, which amplifies the importance of processes that are directly linked with humans; and (5) dilution flows and volumes that are significantly smaller (Nazaroff et al., 2003).

Understanding pollutant dynamics is useful as it enables the construction of deterministic models of expected contaminant trends, on the basis of the principle of material balance. Once constructed, an effective model can be used to make *forward* predictions of exposure when emissions are known, or can work *backwards* to characterize sources that were responsible for the concentration in a monitored location. When applied in conjunction with an indirect exposure assessment study, models can aid in identifying conditions to which findings do or don't apply. For example, models may be used to evaluate the degree to which conclusions from data on one contaminant might apply to another, to predict changes in exposure owing to expected variations in environmental conditions or patterns of behavior, and to investigate the significance of the proximity effect. While these goals can also be realized through a well-designed direct exposure study, the use of deterministic models allows the influence of a range of variables to be tested rapidly and at much lower cost. Such models have been used as tools in planning, owing to their usefulness in predicting the effect of an intervention or change. They are also widely used for guiding the establishment of regulations and for ensuring compliance.

1.3. Occupied microenvironments

Occupied environments under normal-use conditions are those where modes of operation are not under the control of a researcher, but allowed instead to follow habitual, undisturbed patterns. Conducting exposure assessments under such conditions is desirable because they represent reality rather than an idealized case. However, studies conducted under "normal" conditions pose challenges because the presence of research equipment necessarily creates an interference with the usual state of affairs at a site. Exposure assessments must seek to reduce bias associated with this interference.

Several features distinguish environments under normal occupied conditions from those that are vacant or controlled. Most importantly, the presence and habitual actions of occupants may exert direct and indirect effects on exposure. Direct effects include, for example, providing a substrate for chemical reactions (Coleman et al., 2008; Wisthaler et al., 2005; Corsi et al., 2007; Rim et al., 2009), or serving as a direct emission source for species (e.g., bioeffluents or infectious agents as described by Batterman and Peng, 1995 and Nicas et al., 2005). Indirect effects include manipulation of airflow conditions (e.g., by opening doors and windows or generating turbulence through movement as discussed in Klepeis and Nazaroff, 2006 and Zhang et al., 2008), or the operation of sources and sinks (e.g., cooking or turning on a fan-filter unit). Cumulatively, such "human" effects result in an association between human occupancy and pollutant trends in many common environments, which is of central interest for exposure science owing to the fundamental link between occupancy and exposure. This association between occupancy and environmental concentrations is likely to be more pronounced for dynamic species. Therefore, it is especially important to study pollutant dynamics in conjunction with human dynamics, as the two are intimately linked; and because the dynamics of greatest relevance for exposure assessment are the ones associated with the presence and behavior patterns of humans.

Occupied environments in a normal-use mode are more difficult to monitor than corresponding vacant or controlled sites because of problems of access or intrusion. The two environments sampled for the research presented in this dissertation both posed such challenges. For the study in aircraft, bureaucratic and practical challenges had to be overcome to monitor in commercial passenger cabins during flight. Owing partly to such issues, prior work to

understand in-cabin exposures has been conducted in laboratory chambers or simulated cabins. Almost no other published data were available since 1980 reporting real-time monitoring of ozone in ordinary aircraft cabins during flight. Two large surveys of time resolved ozone from aircraft cabin were conducted prior to 1980 (Brabets et al., 1967; Nastrom et al., 1980) but their current usefulness is limited by the following factors: (1) the design of aircraft ventilation systems has changed significantly so less outdoor air is drawn into the cabin and more is recirculated; (2) occupant densities are systematically higher due to an increase in load factors and reduction in floor space per passenger in economy cabins; and (3) the introduction of control devices. The data presented in this dissertation represent the largest published set of ozone levels measured in the location of interest for most aircraft passengers – the general (i.e. economy) seating area. In previous large surveys ozone levels were measured in the cockpit close to an incoming airstream (Brabets et al., 1967), on the outside wall of the staircase in a B747 airplane (Nastrom et al., 1980), or in the first-class cabin (Spengler et al., 2004). As findings from laboratory and simulated-cabin studies have shown ozone reacts with human skin oils, forming byproducts, the monitoring location relative to locations of exposed humans might matter.

The ultrafine particles study was conducted in houses in northern California. Though residences themselves are relatively easy to access, sampling ultrafine particles in occupied indoor environments has been challenging owing to health concerns associated with butanol, the common working fluid of condensation particle counters (CPC), which are the instruments typically used to measure UFP. While a CPC that uses isopropyl alcohol instead of butanol (the P-Trak) has been developed and is commercially available, information on the reliability and precision of the P-Trak is limited and evidence indicates that it significantly underestimates ultrafine particles smaller than 25-30 nm (Zhu et al., 2006). The present study pioneers the use of a water-based condensation particle counter (TSI Model 3781, Hering et al., 2005), which is free of toxic components, and relatively small, lightweight, and low cost, and is therefore likely to gain prominence as a tool for monitoring indoor UFP.

1.4. Overview of dissertation

This dissertation presents two indirect exposure investigations, of a particulate and a gaseous dynamic pollutant, in two common occupied microenvironments subject to normal use conditions: ozone in passenger cabins of commercial aircraft, and ultrafine particles in residences. The two studies are unified by the central aim of quantifying concentrations and exposures, and characterizing variables that govern trends in exposure. In each investigation, air concentrations were sampled at high frequency (at least 1/min) to capture peak exposures and to assess pollutant dynamic behaviors; levels in ambient air and levels in adjacent indoor exposure microenvironments were compared; and models based on principles of material balance were used to interpret and generalize findings.

Chapters 2 and 3 address the theme of residential exposure to ultrafine particles. During a field monitoring campaign in the East Bay area near San Francisco, California, UFP and copollutant levels were monitored at seven houses that span a range of expected source conditions. In Chapter 2, key findings from the field investigation are presented and explored. The dependence of concentration profiles on occupancy is elucidated, and the exposures of household occupants to UFP during the time spent at home is quantified. A dynamic particle material balance model is used to apportion exposures between outdoor and indoor source categories. Variables that significantly influence indoor PN concentrations and exposures for

study subjects are identified, and their degree of influence is quantified. The investigation of variables that influence residential UFP concentrations and exposures encapsulates four components: (1) indoor episodic source characterization, including the quantification of source-specific emission and loss rates; (2) understanding trends in the outdoor particle number (PN) concentration, which are responsible for baseline particle trends indoors; (3) estimating the indoor proportion of outdoor particles (IPOP or infiltration factor *f*) for various sites and operating conditions, and assessing the influences on *f* of variables such as the air-exchange rate and active particle removal; and (4) analyzing the influence of unvented pilot lights, when present, on the baseline indoor PN concentration.

The analysis presented in Chapter 2 shows that indoor sources are the main cause of indoor particle peaks and also of the between-home variability in occupants' at-home PN exposures. In Chapter 3, therefore, an important question relating to indoor source use is explored: What fraction of UFP emitted from indoor sources is inhaled, and what are the variables that influence this fraction? The question is explored by assessing semi-empirical intake fractions (*iF*) associated with the peak events and continuous sources observed in the field study. The intake fraction metric allows inferences about exposure to be made on the basis of information on source emission rates. For each source category or event, individual and aggregate *iF* are assessed, the uncertainty associated with each estimate is described, and drivers of the variability in *iF* are explored.

Chapters 4 and 5 explore exposures to ozone in aircraft cabins during flight. The broad objective of the research presented in these chapters is to assess in-cabin ozone levels and factors that influence them, on northern hemisphere commercial passenger flights originating from or terminating in the United States, in all seasons. Chapter 4 presents results from a field investigation where ozone levels were measured in the passenger cabins of 76 commercial flight segments in 2006-2007. Measurements were made using a portable UV-photometric monitor on many flights across the United States and on several transatlantic and transpacific routes. A range of narrow and wide body aircraft, with or without ozone converters, was sampled. Flight selection was substantially opportunistic, with some flights intentionally chosen to augment seasons or flight routes not otherwise well represented. The analysis in Chapter 4 explores the dependence of in-cabin ozone on cabin occupant density, the presence or absence of a control device, and variables that are expected to influence levels of ozone in the air outside the aircraft, such as flight altitude, latitude, season, and meteorological processes that affect vertical mixing between the lower stratosphere and the upper troposphere. To put the results in context, findings on in-cabin ozone levels and exposures are compared with federally mandated limits, and with results from related published work. In an appendix to Chapter 4, estimates of the effective collection rate (ECR) for the Ogawa ozone passive sampler are presented for the air cabin environment. These ECR estimates were calculated based on field calibration tests.

Outdoor ozone levels are of key importance for in-cabin ozone exposures, as the ozone in cabins during flight originates outdoors (NRC, 2002). Hence, in Chapter 5, atmospheric ozone levels in the US and transatlantic air-traffic corridors are analyzed, for further insight into ozone levels and factors that influence them along these routes. The analysis in Chapter 4 is based on a field investigation of in-cabin ozone conducted by our research team. The analysis in Chapter 5 relies on data on outdoor ozone that were obtained as part of an ongoing European campaign known as the Measurement of Ozone by Airbus In-service air Craft (MOZAIC) project. MOZAIC investigators have, since 1993, collected ambient ozone data along a range of flight routes via automatic measurements by sensors installed on five long-range passenger aircraft

(Marenco et al., 1998). So far, more than 20,000 flights have been sampled. These represent a rich source of data that has not yet been used to expand understanding of in-cabin ozone exposure. The analysis of MOZAIC data in Chapter 5 complements the investigation reported in Chapter 4 by providing additional insight into spatial and temporal patterns in levels of ozone encountered by aircraft. Results from the analysis are combined with predicted ratios of in-cabin to outdoor ozone (which are in turn based on studies of the dynamic behavior of ozone in the cabin) to model the implications for in-cabin exposures. On the basis of these findings, the potential for controlling in-cabin ozone through the use of flight route planning and ozone converters (the control strategies recommended for compliance with federal standards) is evaluated.

Chapter 6 summarizes findings from this research, and outlines future research directions.

1.5. References

Allen-Piccolo G, Rogers JV, Edwards R, Clark MC, Allen TT, Ruiz-Mercado I, Shields KN, Canuz E, Smith KR, 2009. An ultrasound personal locator for time-activity assessment. *International Journal of Occupational and Environmental Health* **15**, 122-132.

Batterman S, Peng CU, 1995. TVOC and CO_2 concentrations as indicators in indoor air-quality studies. *American Industrial Hygiene Association Journal* **56**, 55-65.

Bennett DH, McKone TE, Evans JS, Nazaroff WW, Margni MD, Jolliet O, Smith KR, 2002. Defining intake fraction. *Environmental Science and Technology* **36**, 206A-211A.

Brabets RI, Hersh CK, Klein MJ, 1967. Ozone measurement survey in commercial jet aircraft. *Journal of Aircraft* **4**, 59-64.

Coleman BK, Destaillats H, Hodgson AT, Nazaroff WW, 2008. Ozone consumption and volatile byproduct formation from surface reactions with aircraft cabin materials and clothing fabrics. *Atmospheric Environment* **42**, 642-654.

Corsi RL, Siegel J, Karamalegos A, Simon H, Morrison GC, 2007. Personal reactive clouds: introducing the concept of near-head chemistry. *Atmospheric Environment* **41**, 3161-3165.

Cortese AD, Spengler JD, 1976. Ability of fixed monitoring stations to represent personal carbon monoxide exposure. *Journal of the Air Pollution Control Association* **26**, 1144-1150.

Duan N, 1982. Models for human exposure to air pollution. *Environment International* **8**, 305-309.

Elgethun K, Fenske RA, Yost MG, Palcisko GJ, 2003. Time-location analysis for exposure assessment studies of children using a novel global positioning system instrument. *Environmental Health Perspectives* **111**, 115-122.

Evans JS, Wolff SK, Phonboon K, Levy JI, Smith KR, 2002. Exposure efficiency: an idea whose time has come? *Chemosphere* **49**, 1075-1091.

Gerharz LE, Kruger A, Klemm O, 2009. Applying indoor and outdoor modeling techniques to estimate individual exposure to PM2.5 from personal GPS profiles and diaries: a pilot study. *Science of the Total Environment* **407**, 5184-5193.

Hering SV, Stolzenburg MR, Quant FR, Oberreit DR, Keady PB, 2005. A laminar-flow, water-based condensation particle counter (WCPC). *Aerosol Science and Technology* **39**, 659-672.

Jenkins PL, Phillips TJ, Mulberg EJ, Hui SP, 1992. Activity patterns of Californians – use of and proximity to indoor pollutant sources. *Atmospheric Environment Part A-General Topics* **26**, 2141-2148.

Klepeis NE, 1999. An introduction to the indirect exposure assessment approach: modeling human exposure using microenvironmental measurements and the recent National Human Activity Pattern Survey. *Environmental Health Perspectives* **107 (Suppl 2)**, 365-374.

Klepeis NE, Nelson WC, Ott WR, Robinson JP, Tsang AM, Switzer P, Behar JV, Hern SC, Engelmann WH, 2001. The National Human Activity Pattern Survey (NHAPS): a resource for assessing exposure to environmental pollutants. *Journal of Exposure Analysis and Environmental Epidemiology* **11**, 231-252.

Klepeis NE, Nazaroff WW, 2006. Modeling residential exposure to secondhand tobacco smoke. *Atmospheric Environment* **40**, 4393-4407.

Lai ACK, Thatcher TL, Nazaroff WW, 2000. Inhalation transfer factors for air pollution health risk assessment. *Journal of the Air and Waste Management Association* **50**, 1688-1699.

Lan Q, Zhang LP, Li GL, Vermeulen R, Weinberg RS, Dosemeci M, Rappaport SM, Shen M, Alter BP, Wu YJ, Kopp W, Waidyanatha S, Rabkin C, Guo WH, Chanock S, Hayes RB, Linet M, Kim S, Yin SN, Rothman N, Smith MT, 2004. Hematotoxicity in workers exposed to low levels of benzene. *Science* **306**, 1774-1776.

Lioy PJ, 1990. Assessing total human exposure to contaminants – a multidisciplinary approach. *Environmental Science and Technology* **24**, 938-945.

Lioy PJ, 2008. Time for a change: from exposure assessment to exposure science. *Environmental Health Perspectives* **116**, A282-A283.

Lioy PJ, 2010. Exposure science: a view of the past and milestones for the future. *Environmental Health Perspectives* **118**, 1081-1090.

Macintosh DL, Xue JP, Ozkaynak H, Spengler JD, Ryan PB, 1995. A population-based exposure model for benzene. *Journal of Exposure Analysis and Environmental Epidemiology* **5**, 375-403.

Marenco A, Thouret V, Nedelec P, Smit H, Helten M, Kley D, Karcher F, Simon P, Law K, Pyle J, Poschmann G, Von Wrede R, Hume C, Cook T, 1998. Measurement of ozone and water vapor by Airbus in-service aircraft: the MOZAIC airborne program, an overview. *Journal of Geophysical Research-Atmospheres* **103**, 25631-25642.

Marshall JD, Nazaroff WW, 2004. Using intake fraction to guide ARB policy choices: the case of particulate matter. Report to the Research Division of the California Air Resources Board, Sacramento, CA.

McCurdy T, Glen G, Smith L, Lakkadi Y, 2000. The National Exposure Research Laboratory's consolidated human activity database. *Journal of Exposure Analysis and Environmental Epidemiology* **10**, 566-578.

Nastrom GD, Holdeman JD, Perkins PJ, 1980. Measurements of cabin and ambient ozone on B747 airplanes. *Journal of Aircraft* **17**, 246-249.

Nazaroff WW, Alvarez-Cohen L. *Environmental Engineering Science*. John Wiley and Sons, New York, 2001.

Nazaroff WW, Weschler CJ, Corsi RL, 2003. Editorial: indoor air chemistry and physics. *Atmospheric Environment* **37**, 5451-5453.

Nazaroff WW, 2004. Indoor particle dynamics. *Indoor Air* **17 (Suppl 7)**, 175-183.

Nazaroff WW, Weschler CJ, 2004. Cleaning products and air fresheners: exposure to primary and secondary air pollutants. *Atmospheric Environment* **38**, 2841-2865.

Nazaroff WW, 2008. New directions: it's time to put the human receptor into air pollution control policy. *Atmospheric Environment* **42**, 6565-6566.

Nazaroff WW, Bhangar S, Mullen NA, Hering SV, Kreisberg NM, 2010. Ultrafine particle concentrations in schoolroom and homes, Final Report, Contract No. 05-305, California Air Resources Board, Sacramento, CA.

Nicas M, 1995. Respiratory protection and the risk of *Mycobacterium-tuberculosis* infection. *American Journal of Industrial Medicine* **27**, 317-333.

Nicas M, Nazaroff WW, Hubbard A, 2005. Toward understanding the risk of secondary airborne infection: emission of respirable pathogens. *Journal of Occupational and Environmental Hygiene* **2**, 143-154.

NRC (National Research Council) Committee on air quality in passenger cabins of commercial aircraft. *The Airliner Cabin Environment and the Health of Passengers and Crew.* National Academy Press, Washington, DC, 2002.

Ott WR. Exposure analysis: a receptor-oriented science. In Ott WR, Steinemann AC, Wallace LA, Eds., *Exposure Analysis*, CRC Press, Boca Raton, 2006.

Ozkaynak H, Xue J, Spengler J, Wallace L, Pellizzari E, Jenkins P, 1996. Personal exposure to airborne particles and metals: results from the Particle TEAM study in Riverside, California. *Journal of Exposure Analysis and Environmental Epidemiology* **6**, 57-78.

Palmes ED, Gunnison AF, 1973. Personal monitoring device for gaseous contaminants. *American Industrial Hygiene Association Journal* **34**, 78-81.

Paustenbach DJ, 2000. The practice of exposure assessment: a state-of-the-art review. *Journal of Toxicology and Environmental Health, Part B* **3**, 179-291.

Popendor WJ, Spear RC, 1974. Preliminary survey of factors affecting exposure of harvesters to pesticide-residues. *American Industrial Hygiene Association Journal* **35**, 374-380.

Poston JW, 2005. External dosimetry and personnel monitoring. *Health Physics* **88**, 289-296.

Rim D, Novoselec A, Morrison G, 2009. The influence of chemical interactions at the human surface on breathing zone levels of reactants and products. *Indoor Air* **19**, 324-334.

Seinfeld JH, Pandis SN. *Atmospheric Chemistry and Physics: From Air Pollution to Climate Change*, Wiley, New York, 1998.

Silverman L, 1954. Sampling instruments for air pollution surveys. *Public Health Reports* **69**, 914-924.

Sioutas C, Delfino RJ, Singh M, 2005. Exposure assessment for atmospheric ultrafine particles (UFPs) and implications in epidemiologic research. *Environmental Health Perspectives* **113**, 947-955.

Smith KR, 1988. Air pollution: assessing total exposure in developing countries. *Environment* **30**, 16-35.

Smith KR, 1993. Fuel combustion, air pollution exposure, and health: the situation in developing countries. *Annual Review of Energy and the Environment* **18**, 529-566.

Smith KR, 2002. Place makes the poison: Wesolowski Award Lecture – 1999. *Journal of Exposure Analysis and Environmental Epidemiology* **12**, 167-171.

Spengler JD, Ludwig S, Weker RA, 2004. Ozone exposures during trans-continental and trans-pacific flights. *Indoor Air* **14 (Suppl 7)**, 67-73.

Wallace LA, 1987. The Total Exposure Assessment Methodology (TEAM) study: Summary and analysis, Volume 1, Office of Research and Development, US Environmental Protection Agency, Washington, D.C.

WHO, 2010. World Health Organization. Global burden of disease (GBD). http://www.who.int/healthinfo/global_burden_disease/en/index.html. Accessed on February 10, 2010.

Wisthaler A, Tamás G, Wyon DP, Strøm-Tejsen P, Space D, Beauchamp J, Hansel A, Märk TD, Weschler CJ, 2005. Products of ozone-initiated chemistry in a simulated aircraft environment. *Environmental Science and Technology* **39**, 4823-4832.

Yoshida M, Yamauchi H, Arai F, Yamamura Y, 1980. Mercury exposure monitoring comparison of environmental monitoring and personal monitoring. *Japanese Journal of Hygiene* **35**, 543-549.

Zartarian VG, Ott WR, Duan NH, 1997. A quantitative definition of exposure and related concepts. *Journal of Exposure Analysis and Environmental Epidemiology* **7**, 411-437.

Zartarian VG, Bahadori T, McKone T, 2005. Adoption of an official ISEA glossary. *Journal of Exposure Analysis and Environmental Epidemiology* **15**, 1-5.

Zhang XY, Ahmadi G, Qian J, Ferro A, 2008. Particle detachment, resuspension and transport due to human walking in indoor environments. *Journal of Adhesion Science and Technology* **22**, 591-621.

Zhu YF, Yu N, Kuhn T, Hinds WC, 2006. Field comparison of P-Trak and condensation particle counters. *Aerosol Science and Technology* **40**, 422-430.

Chapter 2: Ultrafine particle concentrations and exposures in seven residences in northern California

Reproduced in part from Bhangar S, Mullen NA, Hering SV, Kreisberg NM, Nazaroff WW, Ultrafine particle concentrations and exposures in seven residences in northern California, *Indoor Air*, in press (doi: 10.1111/j.1600-0668.2010.00689), with permission from Wiley-Blackwell.

2.1. Introduction

Inhalation exposure to airborne fine particles poses significant health risks (Pope and Dockery, 2006). Since populations cumulatively spend most of their time in their own homes (Klepeis et al., 2001), understanding exposure to particles indoors at home is needed to quantify total exposure. Particles measured on the basis of a mass concentration metric (particulate matter per unit air volume smaller than 2.5 or 10 μm in diameter for $PM_{2.5}$ and PM_{10}, respectively) have well established health risks, and their levels in ambient air are commonly subject to government regulations. On the other hand, ultrafine particles (UFP, smaller than 100 nm in diameter) may pose independent cardiovascular, respiratory, and neurological health hazards (Hoek et al., 2010; Knol et al., 2009; Weichenthal et al., 2007a; Delfino et al., 2005; Crüts et al., 2008; Ibald-Mulli et al., 2002) but are not separately regulated. They typically contribute little to and correlate poorly with $PM_{2.5}$ levels (Morawska et al., 2003; Jeong et al., 2004; Watson et al., 2006). In fact, under common conditions, particle number and mass may be negatively correlated (Ban-Weiss et al., 2009). Consequently, ultrafine particles are inefficiently controlled with mass-based standards, and $PM_{2.5}$ is a poor proxy for understanding the behavior and effects of the ultrafine fraction of airborne particulate matter.

Uncertainties exist in our understanding of pathways that link inhalation exposure to ultrafine particles with adverse health effects. In a recent "expert elicitation" (Knol et al., 2009), short-term UFP exposures were linked with adverse outcomes including mortality, hospital-admissions, lung-function decrements, and asthma aggravation more strongly than long-term exposures. Respiratory inflammation and thrombotic effects were proposed as key links in the mechanism considered most important in causing these adverse health outcomes. Whether all ultrafine particles pose similar hazards, or whether their toxicity is mediated by composition and varies by source, remains an open question. Studies that informed the early base of knowledge on UFP health effects were conducted with surrogate particles such as titanium dioxide and carbon black and emphasized effects linked to their small size and high surface area to volume ratio, rather than to their origin (Donaldson and Stone, 2003; Nel et al., 2006). In contrast most epidemiological studies on UFP have relied on outdoor levels or exposures and the comments by Knol et al. (2009) are specifically directed at *ambient* ultrafine particles.

Two studies where effects of indoor and outdoor exposures were independently evaluated suggested particles of outdoor origin were more potent than uncharacterized indoor UFP at generating the adverse effects investigated (Delfino et al., 2008; Vinzents et al., 2005). However both studies were designed to assess the effect of outdoor rather than indoor particles. One was conducted in a retirement community where indoor sources appear to have been minimal. The other prescribed a bicycling activity for exposure subjects to ensure they were exposed to fresh

traffic emissions outdoors, with no similar intervention to ensure sustained exposure to particles emitted indoors. To properly evaluate the hazard posed by ultrafine particles from indoor sources there is a need for either epidemiological studies that link indoor source exposures to health outcomes, or studies that characterize the composition of ultrafine particles emitted from various sources, and link individual components to health outcomes (e.g., Garza et al., 2008).

UFP exhibit dynamic characteristics in indoor and outdoor air. Owing to their small size, they have a high Brownian diffusion coefficient (approximately 0.0005 $cm^2 s^{-1}$ for 10 nm particles) and consequently high deposition velocity. Due to their high surface area to volume ratio and small diameter, ultrafine particles are also particularly susceptible to alteration via phase-change processes (Nazaroff, 2004; Zhang and Wexler, 2002). Previous work confirms that ultrafine particles are more subject to dynamic processing than species that are relatively stable such as carbon monoxide (CO) or accumulation mode particles measured on a mass basis ($PM_{2.5}$) (Zhu et al., 2002; Wallace et al., 2008). As a consequence, for a polydisperse aerosol emitted from a source, nanosized particles are preferentially altered, or removed to fixed surfaces or to the surfaces of other particles (via coagulation), relative to particles between 0.1 and 1 μm in diameter.

Concentrations of ultrafine particles in houses are affected by the intrusion of airborne particles from outdoors, removal processes from indoor air such as deposition and air filtration, and emissions from indoor sources. Two known major sources of UFP in outdoor air – motor vehicles and secondary photochemical formation – have been explored in many studies (Kulmala et al., 2004; Spracklen et al., 2006; Zhu et al., 2002). Dynamic particle parameters that mediate the impact of outdoor sources on indoor levels have also been identified and investigated (Liu and Nazaroff, 2001; Riley et al., 2002; Zhu et al., 2005; Zhao et al., 2009). Several studies have characterized indoor sources of ultrafine particles through experiments or observations in a chamber, laboratory, or field setting. Despite the steady emergence of new studies on ultrafine particles, so far very few have investigated levels in homes under normal occupied conditions. Since populations cumulatively spend most of their time in their own homes (Klepeis et al., 2001), understanding exposure to particles indoors at home is particularly important for quantifying total exposure.

Of eight studies of detached, single-family houses we identified in the archival literature, four focused on US conditions. Wallace (2006) collected and analyzed extensive size- and time-resolved particle data in one townhouse in suburban Virginia over a period of 37 months. Wallace and Ott (in press) collected data at close proximity to residential sources for the purpose of simulating personal exposures in a townhouse in Virginia and a house in California. Long et al. (2000) and Abt et al. (2000), respectively, studied nine and four houses in Boston, Massachusetts. Other studies have been conducted in a suburb of Brisbane, Australia (Morawska et al., 2003; He et al., 2004), in Canadian cities (Weichenthal et al., 2007b), in Mysore, India (Monkkonen et al., 2005), and in Sweden (Matson, 2005). A majority of the studies cited present simultaneous indoor and outdoor concentration data and characterize particle dynamic behaviors. However, only two studies included a source characterization component (Wallace, 2006; Morawska et al., 2003), and none have apportioned occupant residential PN exposures amongst indoor and outdoor source categories. In addition to detached, single-family houses, occupied interior spaces in which UFP levels have been characterized include apartments (Balasubramanian and Lee, 2007; Diapouli et al., 2007; Hussein et al., 2005; Mitsakou et al., 2007), retirement communities (Delfino et al., 2009), ice-rinks (Rundell, 2003), offices (Matson, 2005), schools (Weichenthal et al., 2008; Morawska et al., 2009; Mullen et al., in press), and the

cabins of motor vehicles (Fruin et al., 2008; Wallace and Ott, in press; Zhang and Zhu, 2010; Knibbs et al., 2010). In combination with the high potential health risks and the high proportion of time spent in one's home across most populations, the small number of studies of ultrafine particles in occupied houses under normal use indicates the need for further research in this area.

The present study was undertaken to measure levels of ultrafine particles and to investigate factors that influence them in several occupied single-family houses in northern California. Particle number (PN) concentration is the metric used to quantify UFP levels, though health effects may also be linked to other particle parameters, such as surface area concentration and chemical composition (Nel et al., 2006). Houses that span a range of expected UFP source conditions were studied in moderate detail so as to elucidate important information about underlying physical processes that affect UFP levels and the resulting exposures of occupants.

2.2. Methods

2.2.1. Site selection

Seven occupied, single-family houses located in urban and suburban Alameda County, California, were included in this study. Monitoring was undertaken between November 2007 and October 2008 with supplementary experiments completed by February 2009. In aggregate, sampling was distributed across all four seasons. The study sites were a convenience sample and were intended to have UFP levels that were higher than average but within a normal range. House recruitment was based on the presence and occupants' utilization of potential indoor UFP sources, the proximity of the house to traffic, and occupants' willingness to cooperate with the research team. The realization of various specific source-oriented criteria in the study houses is described in Table 2.1a. We excluded households with smokers or other unusually heavy indoor sources, such as extreme candle use. Protocols for recruitment and study procedures were reviewed and approved by the Committee for the Protection of Human Subjects at the University of California, Berkeley.

Table 2.1a. Source-oriented attributes of study houses

Attribute	**Houses with attribute**
Proximity to (within 150 m of) a freeway	H3, H4
Gas cooking	H1, H2, H3, H4, H6
Unvented pilot lights	H1, H3
Vented natural-gas appliances	All
Use of terpene-containing cleaning products	H4, H5, H6
Candle use	H1, H6

Table 2.1b provides a brief summary of the monitored houses, designated H0-H6. The 21 residents of these seven houses comprised 14 adults and seven children. All houses were single-family detached units and spanned a range of ages, reflecting different construction styles and degrees of airtightness. On average, houses in this study were older than the overall housing stock in California. This outcome resulted from a deliberate choice to emphasize urban core housing, which tends to be older, rather than suburban sites, which is where California's population growth in recent decades has been concentrated. The occupant-weighted geometric

mean household volume per occupant was approximately 100 m^3, lower than the estimate for all US single-family residences, 160 m^3 (Nazaroff, 2008). Five of the seven houses had central forced-air heating (and in two cases cooling) systems that were used during the observational monitoring period. For the forced-air systems, the recirculating fan was coupled to heating or cooling, and was activated either on-demand or according to thermostatic control. At two sites, the central air system included a particle filter, and at a third it was equipped with an electrostatic particle control device. Houses H1 and H3 had unvented pilot lights associated with their kitchen ranges.

Approximate locations of six of the seven sites are presented in a map, in Figure 2.1. H0 and H5 were at an elevation of ~150 m above sea level, and H5 was the only suburban site. The two houses that were sited within 150 m of freeways were downwind of the freeway during ~60% of the observational monitoring period.

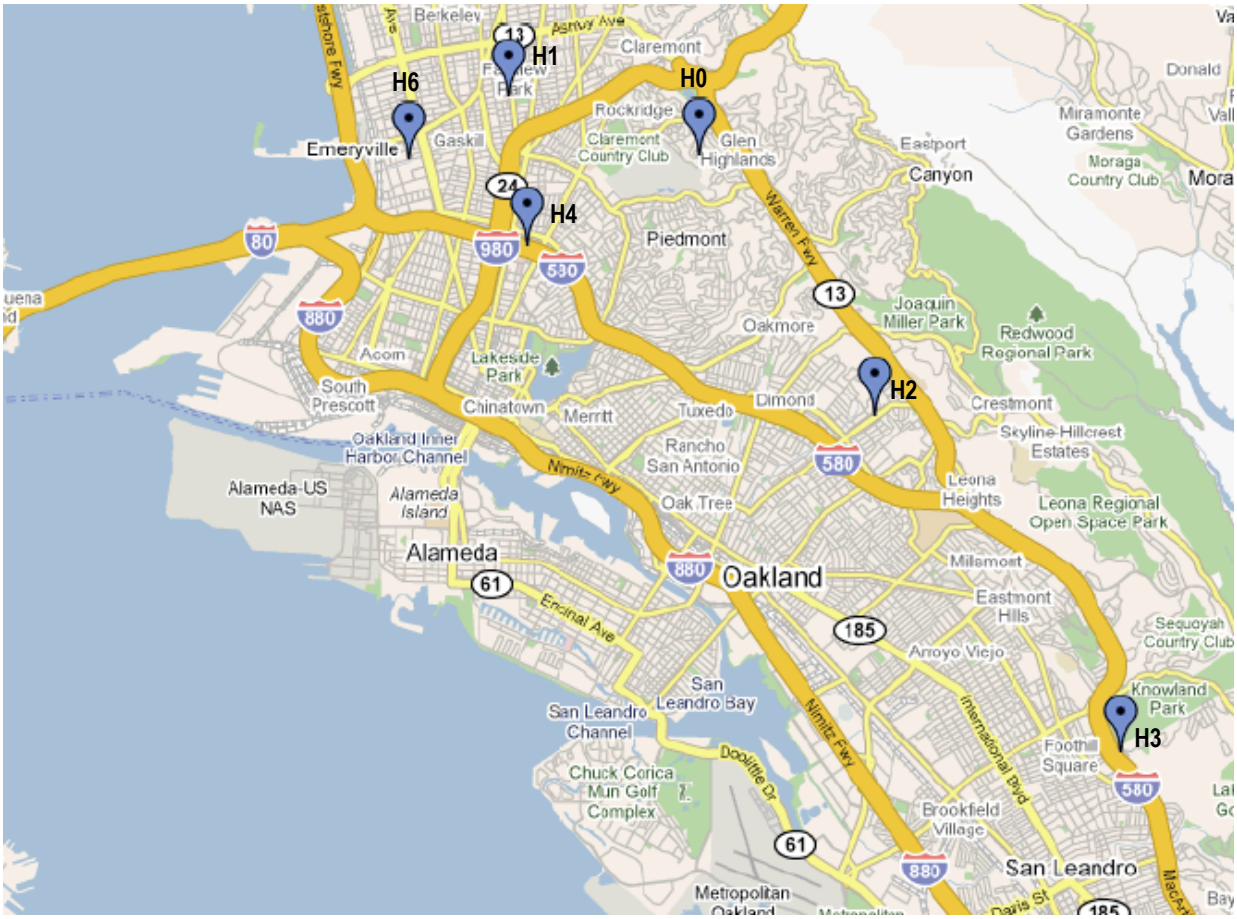

Figure 2.1. This map shows the approximate location of six of the seven house sites, in the East Bay Area of California. One site, H5, was located to the east in Livermore, outside the frame of this map.

Table 2.1b. Characteristics of house sites studied. [a]

Site	Residents [b]	Y [c]	*V* [d]	Monitoring period	Nearest freeway [e]	Description of heating and air-conditioning system and its use patterns during observational monitoring
H0	2 (M, F)	1938	320	Oct-Nov 07	500 m E (0.62)	Heating by central, natural convection, natural gas furnace. Used sporadically.
H1	4 (M, F, m, m)	1910	315	Dec 2007	600 m SE (0.55)	Forced air, natural gas furnace, equipped with particle filter. Thermostat control.
H2	4 (M, F, m, m)	1949	328	Feb 2008	500 m NE (0.51)	Natural gas, vented wall-furnace. Used sporadically.
H3	3 (M, F, m)	1928	200	Mar 2008	120 m SW (0.58)	Forced air, natural gas furnace. Used sporadically.
H4	4 (M, F, m, m)	1904	386	Apr 2008	< 50 m S (0.61)	Separate forced air systems upstairs and downstairs for heating and cooling, with particle filters. Upstairs recirculating fan on continuously; downstairs fan coupled to heat/air-conditioning (AC). Used sporadically for heating.
H5	1 (F)	1993	420	Jun-July 08	1.25 km N (0.43)	Forced air, natural gas furnace with AC. Electrostatic particle filter. Recirculating fan coupled to heat/AC. Used sporadically for cooling.
H6	3 (M, F, M)	1996	314	Sep-Oct 08	800 m W (0.80)	Forced air system, natural gas furnace. Not used during monitoring period.

[a] H0-H4 are in Oakland; H5 is in Livermore; H6 is in Emeryville.

[b] M = male adult; F = female adult; m = male child (3 – 11 y).

[c] Estimated year built data from www.zillow.com except for H6.

[d] *V* = volume (m^3); estimate based on geometric measurement of occupied spaces. Unoccupied spaces such as unfinished basements or garages not included. Not corrected for volume of furniture or cabinetry.

[e] Numbers in parentheses indicate the fraction of the observational monitoring period during which the house site was downwind of the freeway (based on hourly data from the Bay Area Air Quality Management District). The annual average daily traffic frequency on the freeways near H3 and H4 is 170,000 and 202,000 vehicles per day, respectively (Caltrans, 2007). Heavy-duty trucks are banned from the freeway stretch close to H3 but allowed on the nearest freeway for all other sites.

2.2.2. Experimental protocols

Observational monitoring at each site was conducted for durations of 67-140 h during 3- to 9-day periods and included at least one weekday and one weekend day. At H2 and H5 field complications resulted in one or two breaks of 8.5-54 h duration within the monitoring period; each of the other sites was monitored for a single, contiguous period. During observational monitoring, the 21 occupants of the seven houses were asked to follow normal behavior patterns. Time resolved particle and copollutant levels were measured indoors and outdoors, simultaneously. The main indoor instrument enclosure was placed in a central location (e.g. living or dining room), but not in the kitchen to avoid proximity to cooking-associated UFP sources. A supplementary indoor particle monitor was placed in a second indoor location to provide information about the spatial variability of UFP levels in the house. The outdoor enclosure was placed within 10 m of the house, under a shade for protection from rain and sunlight. Questionnaires, diaries, and direct observation and measurement by the field research team were used to collect information about building features and dimensions, occupant demographics and activity patterns, and potential sources. Additional information pertaining to ventilation and source-use was obtained with the aid of supplementary sensors. Details are reported in Nazaroff et al. (2010).

In addition to observational monitoring, approximately 20 h was spent in each house while it was unoccupied to conduct manipulation experiments to measure air-exchange rates (AER) and to characterize emissions and dynamic behavior of UFP from selected indoor sources. The air-exchange rate was determined by means of tracer-gas decay. Carbon dioxide was used as the tracer gas and was released by sublimating dry ice until the indoor concentration reached a level of about 2000 ppm. The AER measurements were conducted for key conditions of the building as observed during ordinary occupancy. A few potentially significant indoor UFP emission sources were tested at each house site. The tests entailed the researchers initiating a source activity and allowing it to continue for a predetermined period. Once the source was terminated, the house was left unoccupied until particle levels indoors returned to the baseline. At two sites with unvented pilot lights, additional manipulation experiments were conducted to quantify the emissions from this source.

2.2.3. Instruments and data acquisition

Air sampling instruments were assembled into two rigid, weatherproof enclosures that sampled air through masts at a height of 1.5-1.6 m, corresponding approximately to the breathing zone of a standing person. The particle line airflow rates were 8-9 L/min to minimize diffusion losses to the walls of the sampling tubes. Each enclosure contained a laptop computer for logging data and instruments to measure particle number concentration (TSI, model 3781); ozone (2B Technologies, model 202); nitric oxide (2B Technologies, model 400); and carbon dioxide, carbon monoxide, temperature, and relative humidity (TSI, model Q-Trak Plus 8554). The indoor enclosure was equipped with a supplementary carbon dioxide monitor (LI-COR, model 820). Data were averaged over 1-min intervals, either by configuring units accordingly or via post-processing of data collected over shorter periods.

The TSI Model 3781 water-based condensation particle counter detects airborne particles larger than 6 nm in diameter. Though particles larger than the nominal 100-nm upper bound for

the ultrafine size range are not excluded, these typically contribute little to the total PN concentration. Hence, total PN concentration is considered to be a good proxy for UFP levels. The instrument uses single-particle detection with live-time coincidence correction. Accuracy decreases with increasing particle concentrations; according to the manufacturer, the minimum accuracy is ± 10% at 5×10^5 particles cm^{-3}. The units used in the study were configured to log full data records, including raw counts, live time, and status flags. The analyzer has a response time (T_{95}) of 2 s, and can log data at the frequency of 1 Hz.

Two types of supplementary sensors were deployed indoors. "State" sensors (Onset, HOBO U9) recorded time-series data to indicate whether frequently used doors and windows were open or closed. Temperature sensors (Onset, HOBO U12) provided evidence about source-related activities by registering a rapid change of temperature owing to operation of the monitored appliance (e.g. toaster, cooking range, or a central heating or air-conditioning system).

2.2.4. Quality assurance

Instrument calibrations and performance checks were conducted throughout the period of field monitoring, approximately once per site. In addition, side-by-side testing of the instrument packages was done for several hours, indoors and outdoors, at each field site. For the WCPCs, instrument flow rates were checked with an external flow meter (BIOS, model Defender 510). Measured flow rates were used to adjust instrument responses to the target flow of 0.12 L/min. The absence of sampling leaks inside the WCPC was confirmed by the measurement of zero particle concentrations when air was sampled through a particle filter placed at the inlet. Artifacts were identified by means of scrutinizing values marked by an error code in the "status flags" field. For each site, one of the WCPCs was designated as the reference device; side-by-side comparison data were used to adjust the readings of the other instruments to match as closely as possible the results from this reference instrument. At the level of one-minute resolved data, the adjusted instrument responses agreed to better than 10%. Detailed quality control protocols and outcomes are presented in Nazaroff et al. (2010).

For a portion of the time at houses H2-H5, the temperature of the WCPC saturators rose above the design specification. Theoretical and empirical evidence indicates that the effect on data quality was small, so no adjustments were made to compensate. Once the problem was thoroughly diagnosed, it was corrected by adding active thermoelectric cooling devices to the instrument enclosures to offset the internal heat loads and maintain the enclosure temperature at close to ambient conditions.

2.2.5. Data analysis

The evolution of the indoor PN concentration (N, particles cm^{-3}) was interpreted using a material-balance approach (equation (2.1)), and assuming well-mixed conditions and steady values of dynamic particle parameters.

$$\frac{dN(t)}{dt} = \frac{E(t)}{V} + N_O(t)aP - (k + a)N(t) \qquad (2.1)$$

In equation (2.1), $E(t)$ is the rate of particle emissions (particles h^{-1}) from indoor sources at time t, V is the volume of the indoor mixed zone (estimated using physical dimensions, in units of cm^3), $N_O(t)$ is the outdoor concentration (particles cm^{-3}) at time t, a is the air-exchange rate (h^{-1}), P is the particle penetration efficiency (–), and k is the cumulative first-order particle loss-rate coefficient for processes other than air exchange (h^{-1}). The model presented in equation (2.1) relies on the conservation of particle number rather than particle mass. Particle loss, in this treatment, implies either removal from the air owing to processes such as filtration and deposition on fixed surfaces, or coagulation with existing particles, a process that changes particle size and number concentration but not mass.

In keeping with the terminology of prior studies, an infiltration factor (f) is defined as the ratio of the time-averaged indoor particle concentration in the absence of indoor emission sources ($E = 0$), divided by the time-averaged outdoor particle concentration (Wallace and Williams, 2005). Based on the time-average of the terms in equation (2.1), to a good approximation, f can be expressed as a function of the air-exchange rate, particle penetration efficiency, and particle loss parameter as summarized in equation (2.2).

$$f = \frac{\overline{N[E=0]}}{\overline{N_o}} \sim \frac{Pa}{k+a} \tag{2.2}$$

At most sites, f estimates were obtained by analyzing indoor and outdoor concentrations from the observational monitoring data, when the house was vacant and there was no evident influence of indoor sources on indoor PN levels. At H1 and H3, indoor sources always impacted indoor PN levels owing to the presence of continuously burning, unvented, natural-gas pilot lights. At these sites, the contribution to indoor PN from pilots was assessed and subtracted from the indoor trace prior to assessing f. For H6, data from periods when occupants were asleep were included in the assessment of f. Estimates of f_1 and f_2 were obtained for the primary and secondary indoor monitoring locations, respectively, and for one or more common house configurations.

Values of the AER and source-specific emission and loss rates were obtained under controlled conditions from manipulation experiments and under normal-use conditions from the observational monitoring data. AER values from observational monitoring data were estimated from periods when a change in state from occupied to unoccupied resulted in the decay of the indoor CO_2 level. Assessments of particle emission rates from unvented pilot lights (E_{pilot}) were based on study of H1 while vacant, with and without the pilot lights, and regression analysis at H3 using indoor and outdoor observational monitoring data (Nazaroff et al., 2010). To characterize episodic indoor sources, a parameter N_{net} was defined as the residual indoor PN concentration, computed as the difference between the indoor PN concentration and the expected concentration owing to outdoor particles (fN_o) and, where present, unvented pilot lights ($E_{pilot}/[(k+a)V]$). Event-specific first-order loss-rate coefficients were estimated as the slope of the natural log of $N_{net}(t)$ versus time during the immediate post-emissions period. Cumulative emissions per house volume per event were obtained by integrating both sides of equation (2.1), and solving for $\int[E(t)/V]\,dt$.

For episodic source events, the ability to attribute an indoor PN peak to an activity or appliance depended on the amplitude of fluctuations in the baseline PN concentration at a site at the time the activity was conducted. The detection limit for an instantaneous release of particles is estimated as $\sim 2\sigma V$, where σ is the maximum standard deviation of 30-min time-averaged

baseline PN concentrations. If we further estimate that 10 min is a reasonable representation of "instantaneous" (as it is smaller than the typical time for removal of particles from house air and also smaller than the duration of emissions from most source events), the minimum detectable emission *rate* can be estimated to be $2\sigma V \div 10$ min. Based on this approach, for the conditions in this study, an indoor source would need to emit at a rate of at least ~ 10^{10} particles min^{-1} (range: 1×10^{10} min^{-1} at H2 and H5 to 5×10^{10} min^{-1} at H6) for a period of at least 10 min to be clearly discernible.

Contributions to indoor PN concentrations from outdoor particles, from indoor continuous sources, and from indoor episodic sources were separately quantified. The concentration owing to outdoor particles was modeled, for each 1-min time interval, as $f N_O(t)$. The concentration owing to unvented pilot lights was modeled as $E_{pilot}/[V \times (k+a)]$. During periods under the influence of episodic indoor sources, the contribution of these episodic sources was set equal to $N_{net}(t)$. At all other times, the contribution of the episodic sources was set to zero. The causes of indoor episodic source events were identified by associating, whenever feasible, peaks in $N_{net}(t)$ with a known activity, taking into account information from occupant questionnaires, measurements of copollutants, and supplementary sensor data (such as a temperature sensor and data logger placed on a toaster).

The exposure of individual household occupants to PN while they were at home was assessed using indoor concentration data from the primary monitoring location; when the supplementary indoor WCPC was placed in the sleeping zone, concentration data from the supplementary monitor were used to estimate exposures during sleep. For the purposes of this chapter, I use two primary exposure metrics. For both, the first step involves assessing an "integrated exposure" (Zartarian et al., 2005; Lioy, 2010), by integrating the concentration over time (units: particles cm^{-3} h) for periods of occupancy considered separately for each resident. The *average exposure concentration* was then assessed by dividing the integrated exposure by the exposure duration, and has units of particles cm^{-3}. The *daily integrated exposure* was calculated by dividing the integrated exposure by the monitoring duration (in days), and has units of particles cm^{-3} h/d. The daily integrated exposure is a normalized form of the integrated exposure, and serves as a useful single metric to compare the relative importance of indoor and outdoor sources in contributing to indoor exposure.

Each occupant's daily integrated residential UFP exposure was apportioned into contributions from outdoor particles, episodic indoor sources, and continuous indoor sources. Exposures owing to outdoor sources were estimated as the product of the time spent at home, the average outdoor concentration during that time, and an appropriate infiltration factor. Exposure attributable to episodic indoor sources was estimated by summing contributions from individual indoor source events during which the occupant was present. Specifically, the exposure associated with each event was estimated as the time integral of $N_{net}(t)$ for the period of time that person was present. Exposure attributable to unvented pilot lights was estimated as the product of the time-average attributable indoor concentration times the duration of occupancy. The difference between measured and modeled values was designated as of unknown cause.

2.3. Results and discussion

2.3.1. Particle number (PN) concentrations

Reported in Table 2.2 are average PN concentrations measured at each site, indoors and outdoors, for the total observational monitoring period, as well as for times when all occupants were (i) awake or (ii) asleep at home, and when the house was (iii) vacant. Considered over the full monitoring period there is no simple pattern with respect to whether average particle levels are greater indoors or outdoors. At H0 and H1 the difference between the indoor and outdoor average is less than 10%. At H3 and H6 average indoor levels are 40-50% greater than outdoors. For ease of discussion, these four sites, with average indoor PN concentrations approximately equal to or greater than average outdoor PN, are clustered as Group 1. The other three sites — H2, H4, and H5 — are designated as Group 2; these houses had average indoor levels 30-40% below the average outdoor levels.

When time-resolved data are considered, the pattern across sites exhibits greater coherence. Figure 2.2 presents illustrative time-series plots of the diurnal trends for indoor and outdoor PN levels, from 48 h of monitoring at each of the seven sites. As illustrated, there are sharp, intermittent peaks in the indoor trace, when the indoor level rises to as much as an order of magnitude above the outdoor level. During periods between these episodic peaks, indoor PN typically drops to a value below the outdoor concentration. The occupancy-sorted PN averages and indoor/outdoor (I/O) ratios in Table 2.2 and Figure 2.3 demonstrate that high indoor levels and high I/O ratios coincide with periods when occupants are awake at home. In contrast, during quiescent (asleep or vacant) periods, indoor levels are significantly lower and the I/O ratio is consistently less than one.

Insight is gained into the causes of indoor PN trends by considering four factors that significantly influence indoor PN concentrations (§2.3.2-2.3.5). Implications for exposure are explored in §2.3.6.

Table 2.2. Average particle number concentrations (in units of 1000 particles cm^{-3}) measured during observational monitoring at the house sites. [a]

	Full monitoring period				**All occupants at home, awake**				**All occupants at home, asleep**				**House vacant**			
Site	**In1**	**In2**	**Out**	***t*(h)**	**In1**	**In2**	**Out**	***t*(h)**	**In1**	**In2**	**Out**	***t*(h)**	**In1**	**In2**	**Out**	***t*(h)**
H0	10	9.2	9.9	140	15	13	12	15	5.1	4.1	5.9	17	4.2	4.2	12	31
H1	21	27	23	67	81	110	27	6.5	5.4	9.4	17	22	9.8	17	20	14
H2	11	8.9	18	92	19	12	20	17	5.6	6.0	9.9	36	11	11	26	28
H3	28	35	19	77	64	73	30	16	6.1	12	7.0	13	12	11	12	9.9
H4	12	2.6	18	74	17	3.0	17	20	7.7	1.2	12	23	11	2.9	24	20
H5	3.7	4.1 [b]	5.5	100	5.6	5.8 [b]	6.5	39	2.6	2.9 [b]	3.4	32	2.2	2.7 [b]	6.5	30
H6	16	21	11	74	32	36	8.2	8.5	2.8	2.7	6.8	13	13	19	19	9.9

[a] "In1" is the primary indoor monitor; "In2" is the supplementary indoor monitor; "Out" is the outdoor monitor; "*t*(h)" is the duration of monitoring under the conditions indicated. The monitoring periods at H2 and H5 are non-contiguous, with breaks of 8.5-54 h.

[b] These averages are based on the first 40 h of observational monitoring, only.

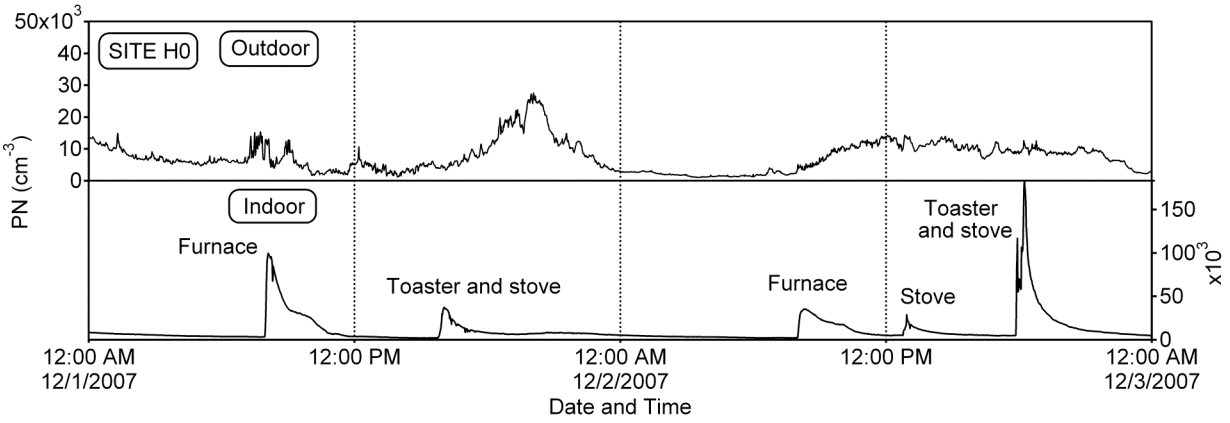
SITE H0
Outdoor
Indoor
PN (cm-3)
50x10^3
40
30
20
10
0
150
100
50
0
x10^3
Furnace
Toaster and stove
Furnace
Stove
Toaster and stove
12:00 AM 12/1/2007
12:00 PM
12:00 AM 12/2/2007
12:00 PM
12:00 AM 12/3/2007
Date and Time

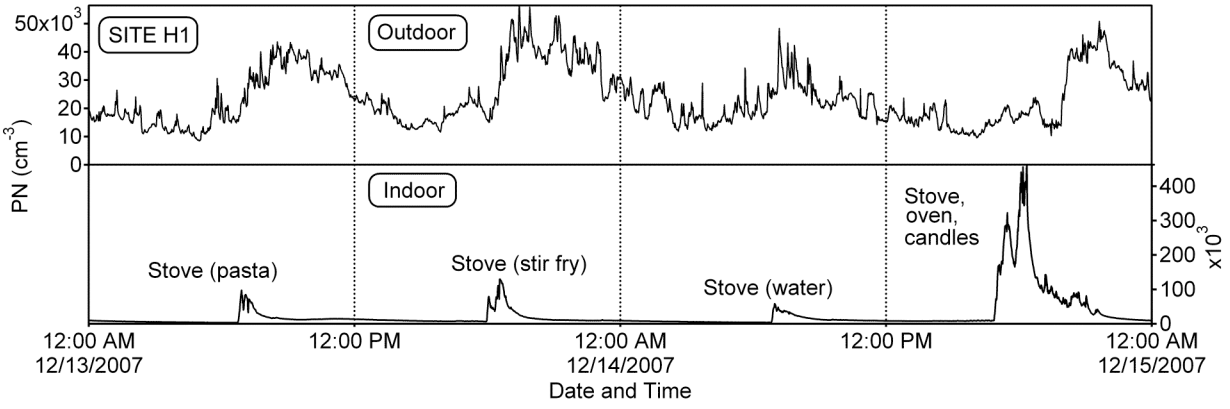
SITE H1
Outdoor
Indoor
PN (cm-3)
50x10^3
40
30
20
10
0
400
300
200
100
0
x10^3
Stove (pasta)
Stove (stir fry)
Stove (water)
Stove, oven, candles
12:00 AM 12/13/2007
12:00 PM
12:00 AM 12/14/2007
12:00 PM
12:00 AM 12/15/2007
Date and Time

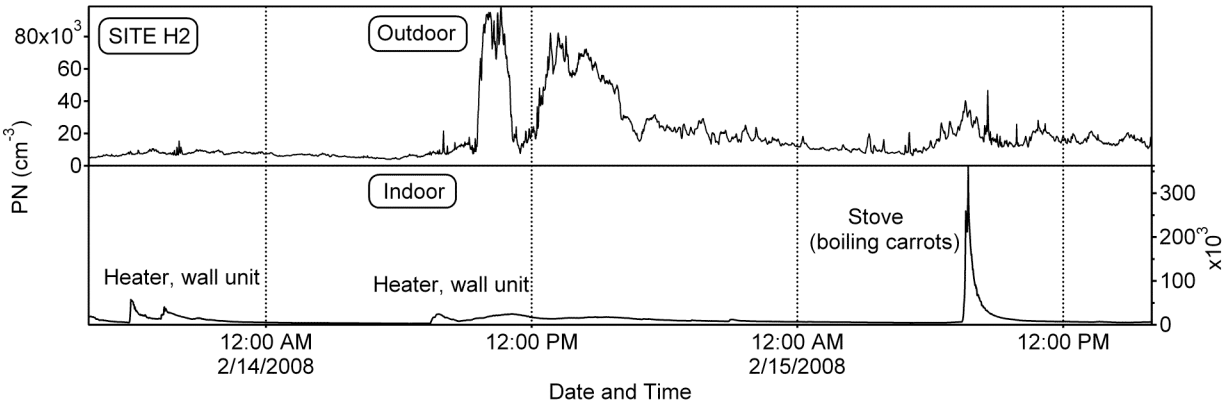
SITE H2
Outdoor
Indoor
PN (cm-3)
80x10^3
60
40
20
0
300
200
100
0
x10^3
Heater, wall unit
Heater, wall unit
Stove (boiling carrots)
12:00 AM 2/14/2008
12:00 PM
12:00 AM 2/15/2008
12:00 PM
Date and Time

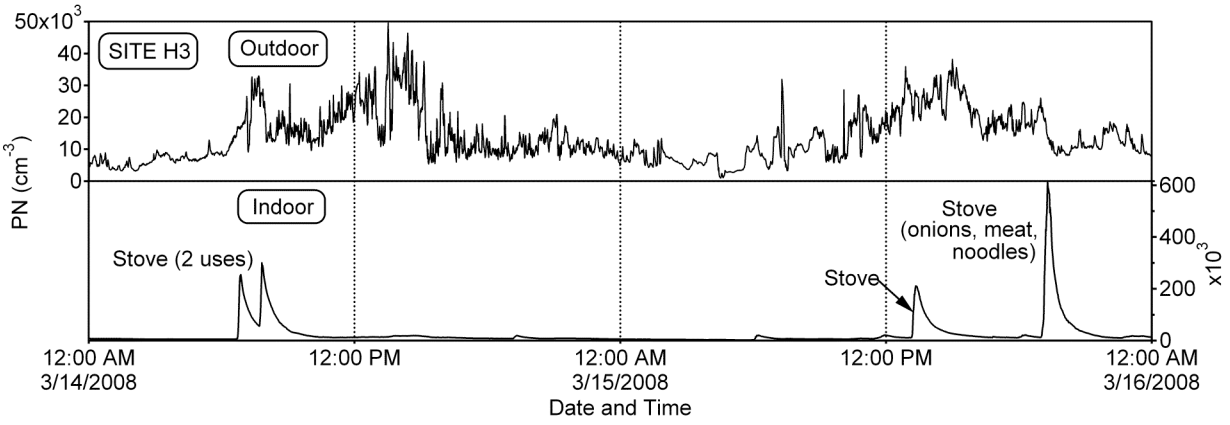
SITE H3
Outdoor
Indoor
PN (cm-3)
50x10^3
40
30
20
10
0
600
400
200
0
x10^3
Stove (2 uses)
Stove
Stove
(onions, meat,
noodles)
12:00 AM
3/14/2008
12:00 PM
12:00 AM
3/15/2008
12:00 PM
12:00 AM
3/16/2008
Date and Time

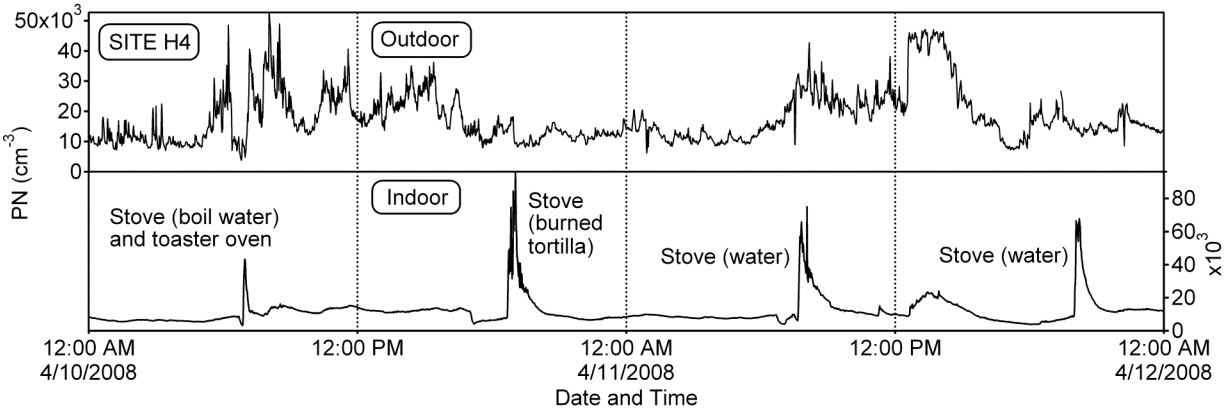
SITE H4
Outdoor
Indoor
PN (cm-3)
50x10^3
40
30
20
10
0
80
60
40
20
0
x10^3
Stove (boil water)
and toaster oven
Stove
(burned
tortilla)
Stove (water)
Stove (water)
12:00 AM
4/10/2008
12:00 PM
12:00 AM
4/11/2008
12:00 PM
12:00 AM
4/12/2008
Date and Time

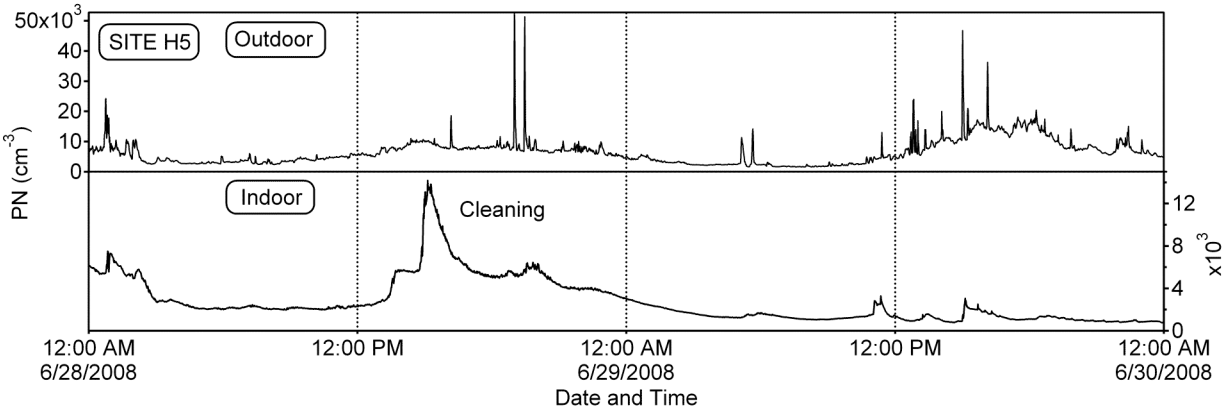
SITE H5
Outdoor
Indoor
PN (cm-3)
50x10^3
40
30
20
10
0
12
8
4
0
x10^3
Cleaning
12:00 AM
6/28/2008
12:00 PM
12:00 AM
6/29/2008
12:00 PM
12:00 AM
6/30/2008
Date and Time

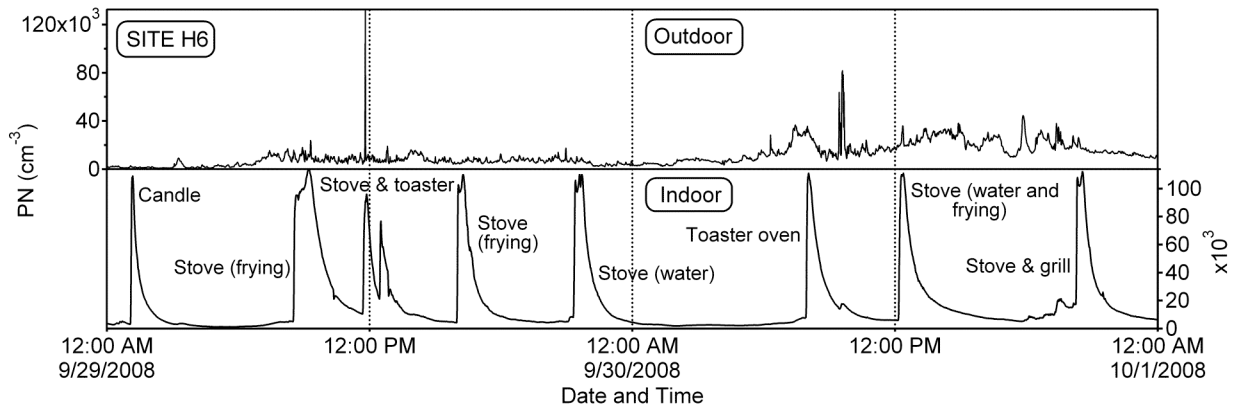

Figure 2.2. Illustrative time series of indoor and outdoor particle number concentrations from the seven home sites. At each site, 48 hours of continuous observational monitoring data are shown, for periods that start at midnight. The site H2 time series starts at 16:00 instead of midnight because 48 h of contiguous data starting at midnight were not available for this site. Vertical dashed lines demarcate noon and midnight and are intended to guide the eye. The indoor source activities associated with the peaks in the indoor trace are individually labeled. The vertical scales vary over orders of magnitude for the representations of "indoor" time series data. Vertical scales for the "outdoor" time series data are consistent, with the exception of sites H2 and H6.

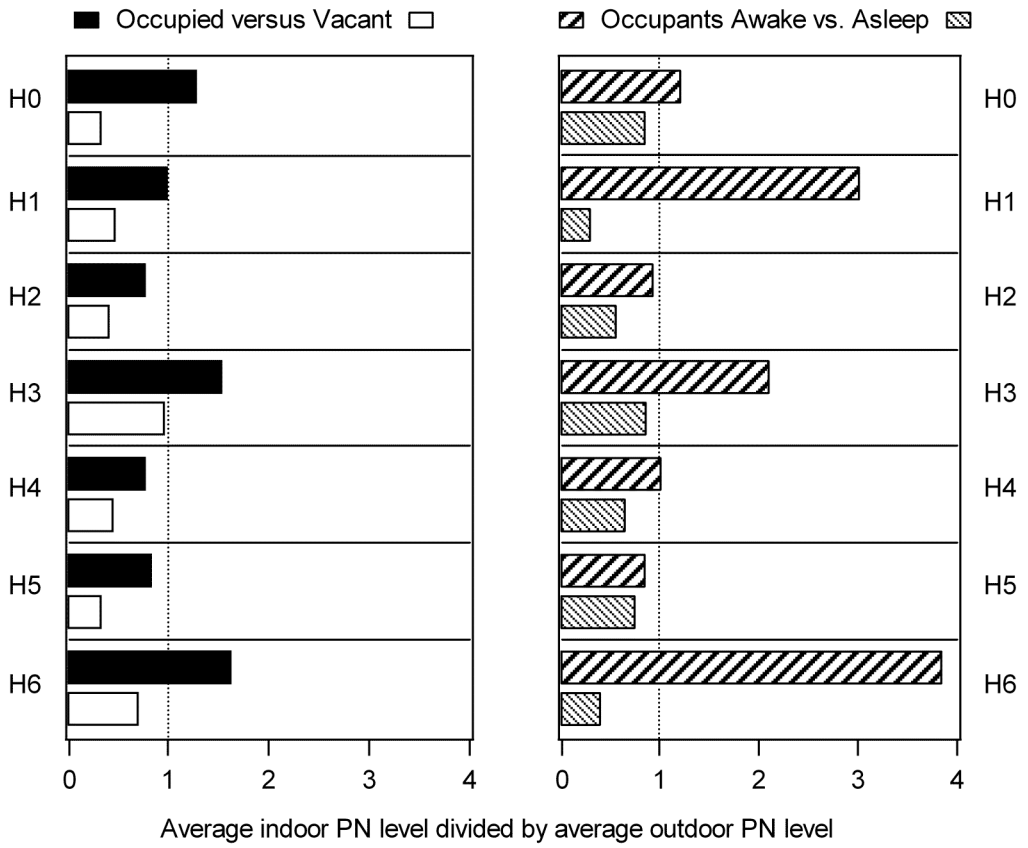

Figure 2.3. Ratios of mean indoor divided by mean outdoor (I/O) particle number concentrations measured during observational monitoring at the seven house sites, sorted according to occupancy status (Occupied = at least one occupant present; Vacant = all occupants absent; Awake = all occupants at home and awake; Asleep = all occupants at home and asleep). The vertical dashed lines at I/O = 1 are intended to guide the eye.

2.3.2. Indoor episodic sources

Indoor PN concentration peaks were consistently associated with occupant activities and were absent when occupants were away from home or asleep. An indoor peak is defined here as a sharp excursion in the indoor PN concentration that cannot be explained by a corresponding change in the outdoor concentration or in the building configuration or operation that would influence *f*. When use of an appliance or some other activity was linked with a peak, it is referred to in this chapter as an "indoor source event."

During the cumulative observational monitoring periods for all seven houses, there were 59 instances when an indoor source event resulted in a PN peak. The 59 peaks correspond to an average of about 2.4 peaks per day monitored. We identified one or two likely causes of the peaks for 57 events, and a single likely source factor was associated with 42 events. The following activities and appliances were sources of UFP each time they were used at one or more of the home sites (see Table 2.3): (i) cooking on a gas or electric stove, (ii) using candles, and (iii) ironing clothes. The following activities were associated with a particle peak at some sites

but not at others: the use of (iv) an electric toaster oven, (v) a vented natural-gas appliance, and (vi) terpene-based cleaning products. In addition to identifying activities that were sources of UFP, we noted that the following activities never led to a discernible increase in indoor PN levels: vacuuming; sweeping; clothes washing; the use of several electric appliances, such as a blender, dishwasher, coffeemaker, rice cooker, kettle, and clothes dryer; and the use of non-terpene cleaning products.

Our classification of activities into source and nonsource categories is broadly consistent with published reports of investigations in homes (He et al., 2004; Wallace, 2006; Long et al., 2000; Wallace and Ott, in press). For activities that were seen to be sources at some sites but not at others, a potential explanation is that low emission rates were insufficient to markedly disturb the baseline PN concentration. Furthermore, vented natural gas appliances may act as a source in some cases, such as when the exhaust gases are not perfectly captured by the flue, but may not be a source with better venting. Analogously, terpene-based cleaning products are expected to be particle sources only in the presence of sufficient ozone.

Table 2.3. Appliances used or activities engaged in during observational monitoring, and whether they were associated with particle peaks.

Source	H0	H1	H2	H3	H4	H5	H6	N,Y,M [a]
Gas stove or oven [b]	—					—		0, 20, 9
Gas clothes dryer	N	N		—	N	—	—	10, 1, 1
Furnace (gas fired, central or wall)		—		—	N	—	—	2, 9, 1
Electric stove or oven		—	—	—	—		—	0, 5, 7
Toaster or toaster oven		N	—	—		—		3, 4, 5
Ironing clothes, electric steam iron	—	—	—	—	—		—	0, 2, 0
Microwave oven	N	N	—	N	N			11, 0, 3
Candles	—		—	—	—	—		0, 1, 1
Terpene-based cleaning product use	—	—	—	—	N		N	2, 0, 2
Vacuum cleaners	N	N	—	—	—	N	—	4, 0, 0
Sweeping	—	—	—	N	—	—	—	1, 0, 0
Clothes washing	N	N	—	N	N	N	—	7, 0, 0
Other electric appliances [c]	N	N	—	N	—	N		25, 0, 6
Non-terpene cleaning product use	—	N	—	N	N	N	N	7, 0, 1

[a] Number of episodes, summed over all sites, that fit into three categories in the form: N, Y, M; N = reported use with no clear evidence of emissions; Y = reported use alone associated with an indoor peak; M = reported use along with another potential source associated with an indoor peak.

[b] The stoves at sites H1 and H3 were equipped with unvented pilot lights that emitted particles continuously. Stoves at all sites emitted particles episodically, during use.

[c] Examples: blender, dishwasher, coffeemaker, rice cooker, kettle, and clothes dryer.

— = Not reported as used, or not present
N = Used, no clear evidence of emissions
= Used, individual use associated with an indoor peak
= Not used alone; however, joint use with another potential source was associated with an indoor peak

Table 2.4 presents a summary of the statistical attributes of the source strengths (41 instances) and decay constants (39 instances) for the peak events that were associated with identifiable single events. The source strength is defined as the total number of particles emitted per event. As presented in Figure 2.4a, the emissions source strength for all 56 quantifiable events conform well to a lognormal distribution with a geometric mean (GM) of 18×10^{12} particles per event and a geometric standard deviation (GSD) of 3.7. The overall arithmetic mean (AM) is 36×10^{12} particles per event. The source strength estimates presented in this paper only represent contributions to PN that we could measure, limited at the lower end of the particle size range by the 6 nm instrument cutoff. The results indicate a high degree of dispersion among source strengths, which vary by more than an order of magnitude between the low-emissions source types (steam iron, clothes dryer, and wall furnace) and the high-emissions sources (use of a gas stove, central forced-air furnace, or candle).

Table 2.4. First-order decay constants and source strengths for peak events associated with identified single activities at the seven houses. [a]

	Decay constant (k+a) (h^{-1})			Source strength ($\times 10^{12}$ particles)		
Emission source	***N***	**GM (GSD)**	**AM ± SD**	***N***	**GM (GSD)**	**AM ± SD**
Gas stove	20	1.8 (1.4)	1.9 ± 0.7	19	38 (2.1)	48 ± 34
Furnace, central air	2	1.6 (1.5)	1.7 ± 0.6	2	41 (1.1)	41 ± 5
Candles [b]	1	1.9	1.9	1	26	26
Toaster oven	4	1.7 (1.2)	1.7 ± 0.3	4	9 (2.8)	13 ± 15
Electric stove	5	1.1 (1.3)	1.2 ± 0.3	4	10 (2.1)	12 ± 10
Furnace, wall	3	1.3 (1.7)	1.4 ± 0.6	7	3.1 (2.7)	4.6 ± 4.5
Clothes dryer [b]	1	2.2	2.2	1	2.2	2.2
Steam iron	2	1.5 (1.2)	1.6 ± 0.6	2	1.9 (1.4)	2.0 ± 0.6

[a] N = number of episodes; GM = geometric mean; GSD = geometric standard deviation; AM = arithmetic mean; SD = arithmetic standard deviation.
[b] Since N = 1 for these sources, values reported are determinations for single events, not means.

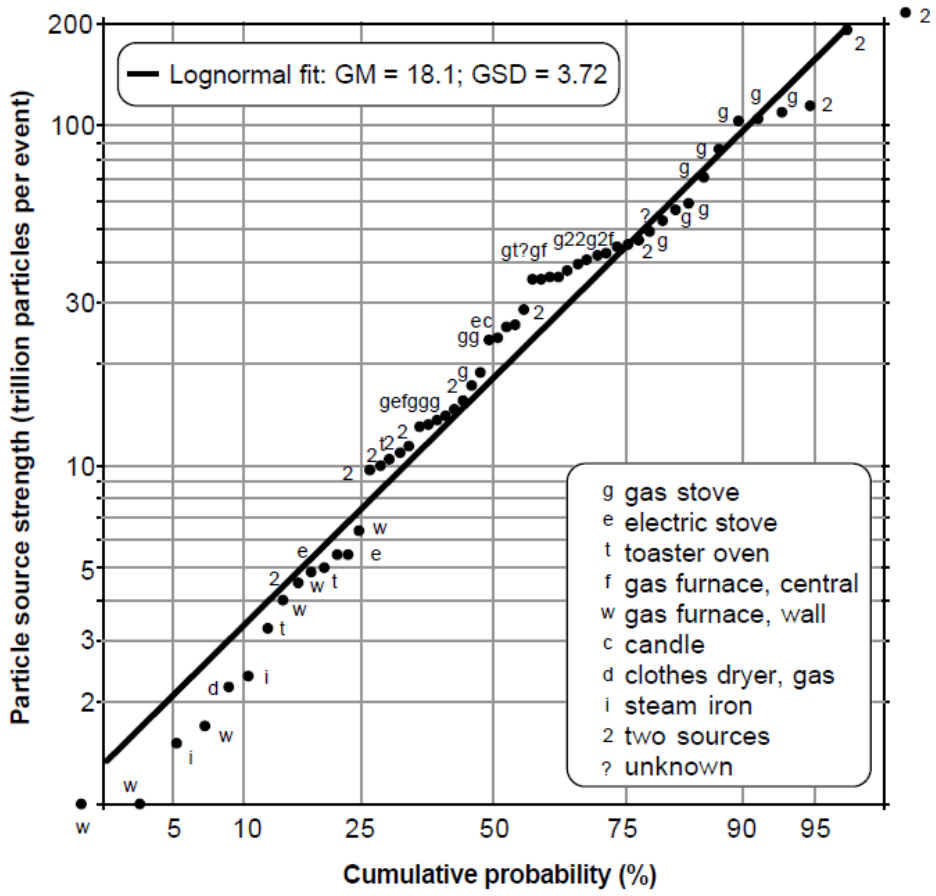

Figure 2.4a. Cumulative distribution of particle source strength for 56 episodic events that were quantified from observational monitoring at the seven home sites. With our protocol, it is difficult to quantify sources that emit far fewer than 10^{12} particles.

Decay constants represent the influence of processes both that remove particles from the air and also that cause them to coagulate. For most peaks, the rate of decay conformed well to first-order dynamics. However, in several cases, the rate of decay was faster at the start than at the end of the decay period. In these instances, the overall decay rate was estimated as a weighted average of the two individual estimates. Overall, as presented in Figure 2.4b, the decay constants for 51 of the events that we could quantify conform well to a lognormal distribution with a GM of 1.6 h^{-1} and a GSD of 1.5; no systematic variability in the decay rate was observed among source types. Three much higher decay constants (9.5, 10 and 11 h^{-1}) are excluded from this distribution; these occurred at H4 and appear to be dominated by the high rate of removal in the recirculating air-filtration systems at that site. Excluding these three events, the AM value of $k+a$ was 1.7 h^{-1}.

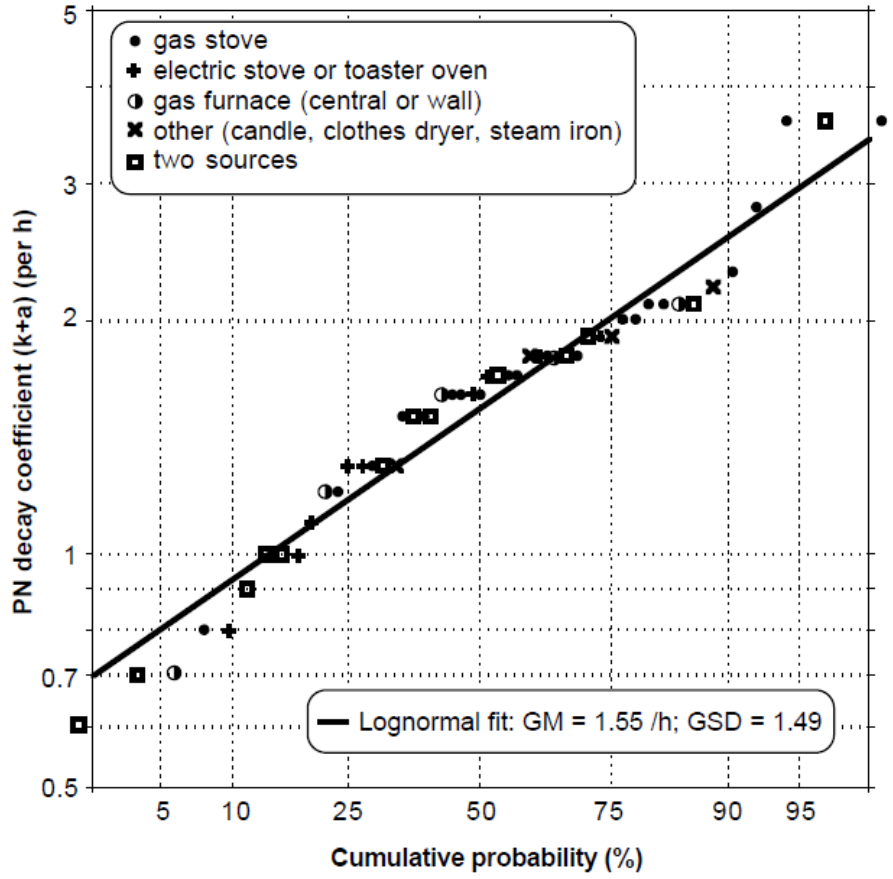

Figure 2.4b. Cumulative distribution of 51 determinations of first-order particle decay rate coefficient obtained from observational monitoring at the seven home sites. For five peaks, the decay coefficient could not be determined (typically because the peaks were too small). For three peaks at H4, the decay coefficients were much higher than the values in this distribution (9-11 h^{-1}).

Sources varied in terms of their temporal behavior and could be described as "continuous" or "sudden burst" emitters. For a combustion source, such as a gas stove or a candle, emissions continued until the activity was terminated, so that the total source strength was sensitive to the duration of use. In contrast, for sources that can be classified as heated surfaces, such as the furnace at H0 and electric stove at H0 and H5, particle concentration decay typically commenced before appliance use ended and total emissions were relatively insensitive to use duration. Moreover, as demonstrated in Figure 2.5, for furnace emissions at H0, an "aging" effect was apparent, whereby the source strength declined during subsequent uses that followed the first use closely in time. A similar aging effect was observed by Wallace and Ott (in press) for emissions from heated surfaces such as a toaster oven and electric oven. An explanation offered by those authors is that emissions could be associated with a coating of a chemical or dust on heating coils, which would become depleted during use.

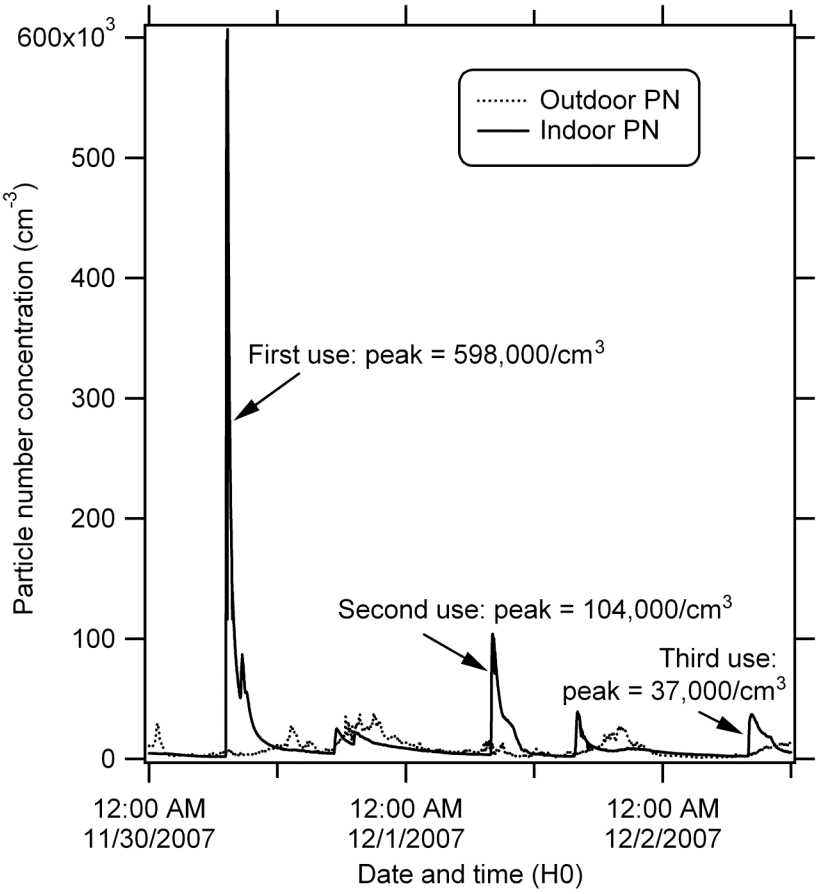

Figure 2.5. The particle number (PN) concentration associated with repeated uses of the furnace (natural gas, vented) at site H0. The first use of the winter season (after months without use) resulted in a very high indoor PN level. Subsequent uses over the following 2 days resulted in progressively dampened peaks.

For most of the PN peaks associated with gas cooking, copollutant monitoring provides corroborating evidence. At four of the five house sites where natural gas appliances were used, we obtained coincident NO and CO data. There is a discernible NO peak associated with 21 of the 22 particle peaks that were linked with gas cooking at these sites. Some but not all of these peaks were also associated with evident increases in CO levels. Relative to baseline pollutant levels, significant NO emissions likely occur more consistently from gas combustion appliances than do emissions of CO, which, being a product of incomplete combustion, is not significantly emitted from well-tuned gas appliances.

Manipulation experiments were helpful for confirming that a particular activity was (or was not) a source at a given house site. In total, we ran 20 tests, 13 of which produced an analyzable peak. The loss-rate coefficients ($k+a$) obtained from manipulation experiments were similar to those inferred from observational monitoring, with a GM = 1.6 h^{-1} and GSD = 1.4. The source strengths from the manipulation experiments were lower than those inferred from observational monitoring.

To assess the spatial variability of indoor concentrations during indoor source-use

periods, mean PN concentrations from the two indoor locations during the "awake" period were compared. At four of the five sites for which the two monitors were placed in the main indoor zone (H0, H3, H5, H6), mean "awake" PN concentrations were similar at the two locations, differing by only 4-15%. House H1 was an exception, with a mean difference of 31% between the two indoor monitors. At the remaining two sites (H2, H4), the two monitors were placed in zones that were treated in the analysis as decoupled. Based on these comparisons, we expect the indoor concentration data employed in the analysis to be reasonably representative of exposures, particularly as occupants tend to move about in a manner that is likely to take them both closer to and farther away from each active source. However, our results would not likely be representative of extreme cases, such as the exposure of occupants who remain consistently proximate to a source, or consistently distant such as on a decoupled floor or behind a closed door.

Only a few prior studies have characterized PN sources in homes under normally occupied conditions. He et al. (2004) characterized the sources of particles larger than 7 nm in 15 houses in a Brisbane suburb in the winter. They reported median PN emission rates that range from 1.1×10^{10} particles min^{-1} for hair drying to 73×10^{10} particles min^{-1} for grilling. Activity durations were not reported, but assuming that hair drying lasted for 10 min, and grilling for 1 h, these emission rates would correspond to source strengths of ~ $(0.1 – 44) \times 10^{12}$ particles per event. Wallace (2005, 2006) investigated the sources of particles larger than 10 nm in a suburban Virginia townhouse. PN source strengths were reported to be in the range from (5 to 39) $\times 10^{12}$ particles for common cooking events, and to be 6×10^{12} particles per use for a natural-gas dryer. Wallace and Ott (in press) measured particles larger than 10 nm in a suburban Virginia townhouse, and a home in California. For the California home, reported source strengths range from 0.4×10^{12} particles from boiling water on a gas stove for 1 min in a stainless steel pan, to 68×10^{12} particles from toasting an English muffin in an electric toaster. For the Virginia home, mean reported PN emission rates range from 0.003×10^{12} particles min^{-1} from a fireplace, to 5.1×10^{12} particles min^{-1} from a gas stove and toaster oven. Source strength results from these three studies are similar to the source-specific central tendencies reported in Table 2.4.

2.3.3. Outdoor concentration pattern

Whereas indoor episodic sources influence indoor PN intermittently, outdoor particles influence indoor PN continuously. They are responsible, in conjunction with indoor continuous sources at H1 and H3, for the "baseline" indoor PN concentration. In this study, we found that the cumulative contribution from the baseline to average indoor PN levels was substantial owing to its continuous influence. Hence, an understanding of the variability in outdoor particle levels is important for understanding indoor particle levels.

Figure 2.6 presents time-series plots of the diurnal variations in outdoor PN at each site. The values shown were calculated by averaging the concentrations measured at each clock minute, for all days monitored. As demonstrated in Figure 2.6, at all sites, outdoor levels are lower overnight than during the daytime. The overnight lows lead to lower indoor concentrations during "asleep" periods relative to "away" periods at all sites except H0 and H5 (Table 2.2).

Figure 2.6 also demonstrates that at H0 and H5, which are the two sites at the greatest

remove from the heavily trafficked urban core, the daily outdoor PN profile is relatively flat. At the remaining five sites, there is a marked diurnal cycle in outdoor PN, with two types of peaks in evidence. An afternoon peak occurred most distinctively at H2, H3 and H4, sites monitored between February and April. Rush-hour peaks at ~ 6:00 and ~ 18:00 were most prominently observed at H1, a site measured in the winter and marked by the lowest average outdoor air temperature in our sample (7 °C). These findings are consistent with observations made based on yearlong monitoring in Rochester, NY (Jeong et al., 2004), which showed that peaks related to strong afternoon nucleation events were most prevalent in the springtime, whereas traffic-related UFP peaks were common during cold, stagnant winter days.

Diurnal variations in outdoor levels of gaseous copollutants substantiate the hypothesis that there are two distinct sources of elevated outdoor PN evident in our data set. At H1, strong peaks in levels of copollutants accompanied the peaks in PN (Figure 2.7a). Moreover, the average wind speed was low (1.5 m s^{-1}), and peaks occurred twice a day in the morning and evening, indicating that primary emissions from traffic and stagnant atmospheric conditions are a plausible explanation. At this site 1-h CO, CO_2, and NO maxima of 2.4 ppm, 550 ppm, and 210 ppb, respectively, were observed.

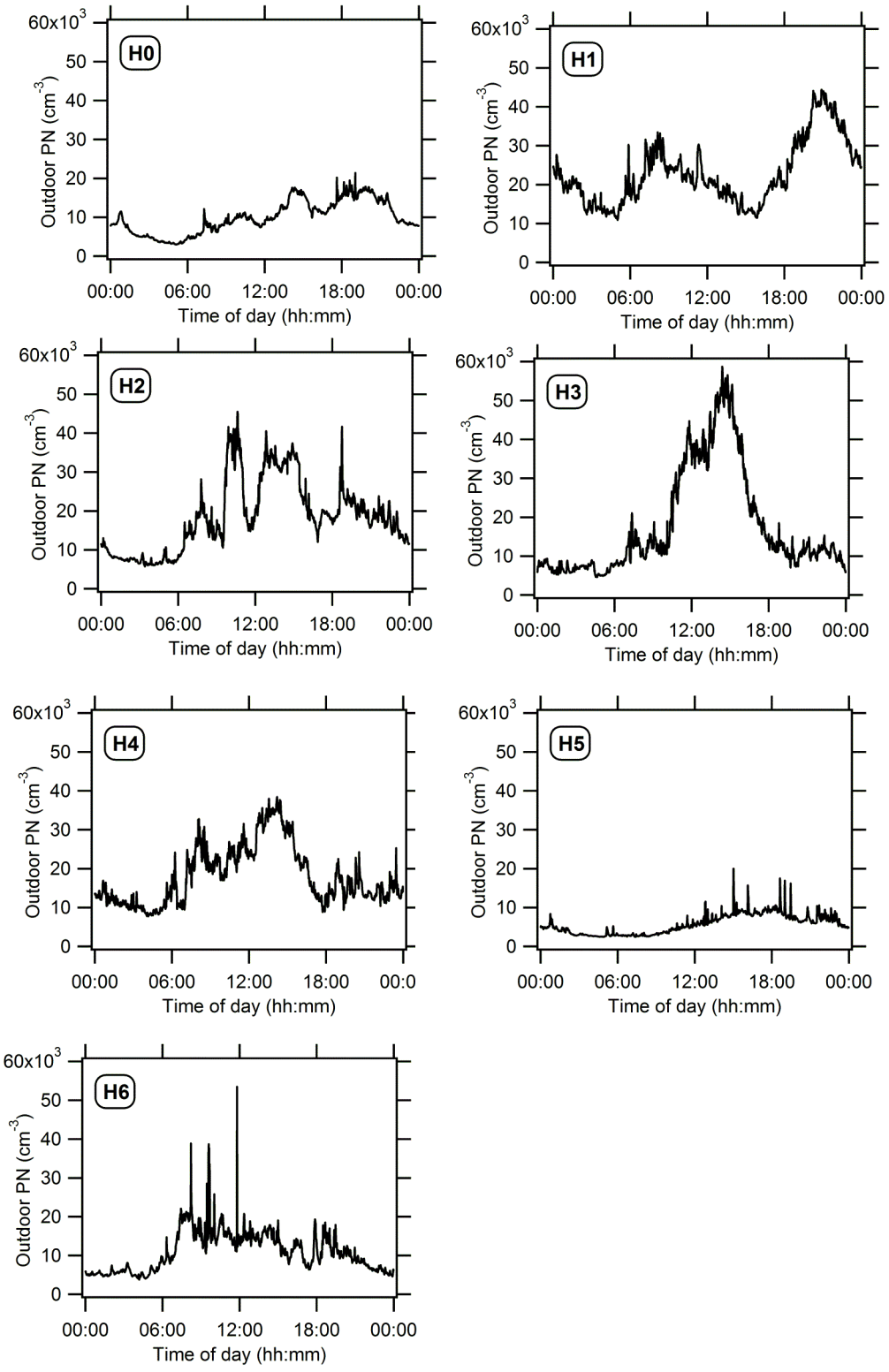

Figure 2.6. Diurnal variations in outdoor PN concentrations at sites H0-H6. Values shown represent the averages of 67-140 h of observational data at each site.

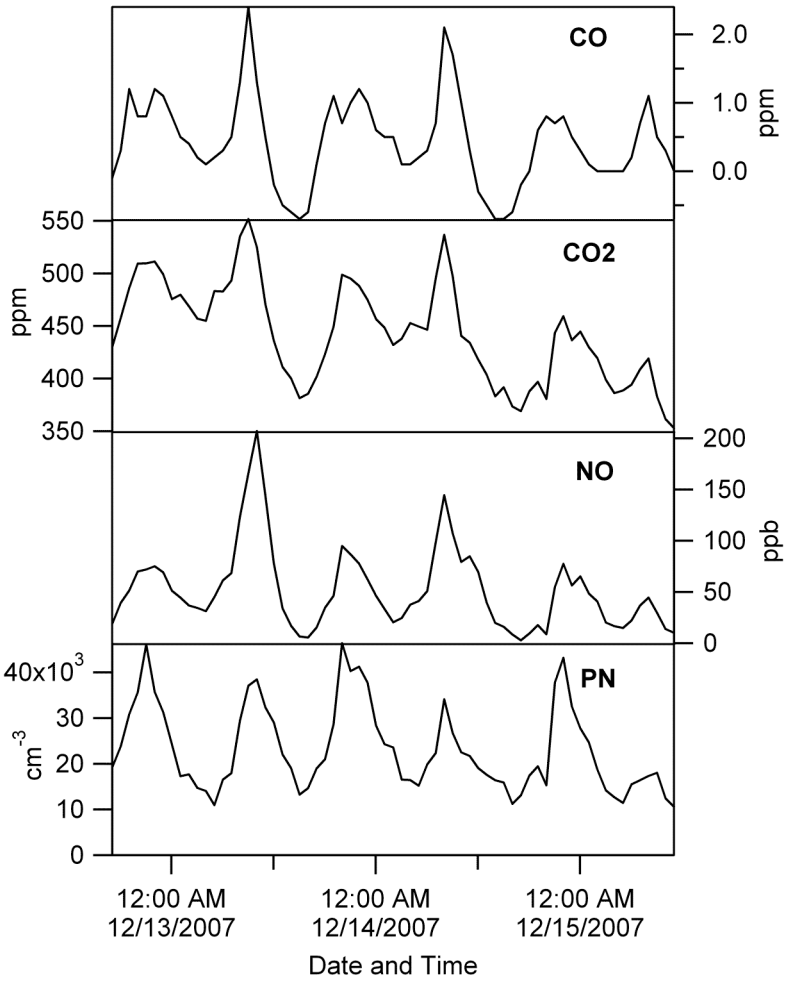

Figure 2.7a. Time series of 1-h average outdoor particle number (PN) concentration, nitric oxide (NO), carbon dioxide (CO2), and carbon monoxide (CO) levels at site H1. Levels of the four pollutants are strongly correlated. The average wind speed at a nearby central monitoring station during the period was relatively low, 1.5 m/s.

In contrast to conditions at H1, afternoon PN peaks at sites H2, H3, and H4 were decoupled from levels of gaseous copollutants, indicating that secondary formation via nucleation may be the source of these peaks. The decoupling was most clearly evident at H3. As illustrated by Figure 2.7b, PN levels at H3 are highest during the time of day when gaseous copollutants are at their lowest. Levels of 1-h CO, CO_2, and NO are relatively flat, with maxima of 0.5 ppm, 400 ppm, and 12 ppb, respectively. The absence of significant primary gaseous copollutant peaks at this site may be partly explained by the atmospheric ventilation conditions. The mean wind speed outdoors during the monitoring period was high (4.2 m s^{-1}). Since the secondary formation of ultrafine particles has been found to be a regional phenomenon (Kulmala et al., 2004), the relatively strong winds would not dampen peaks associated with this source, as it would peaks owing to local primary emissions.

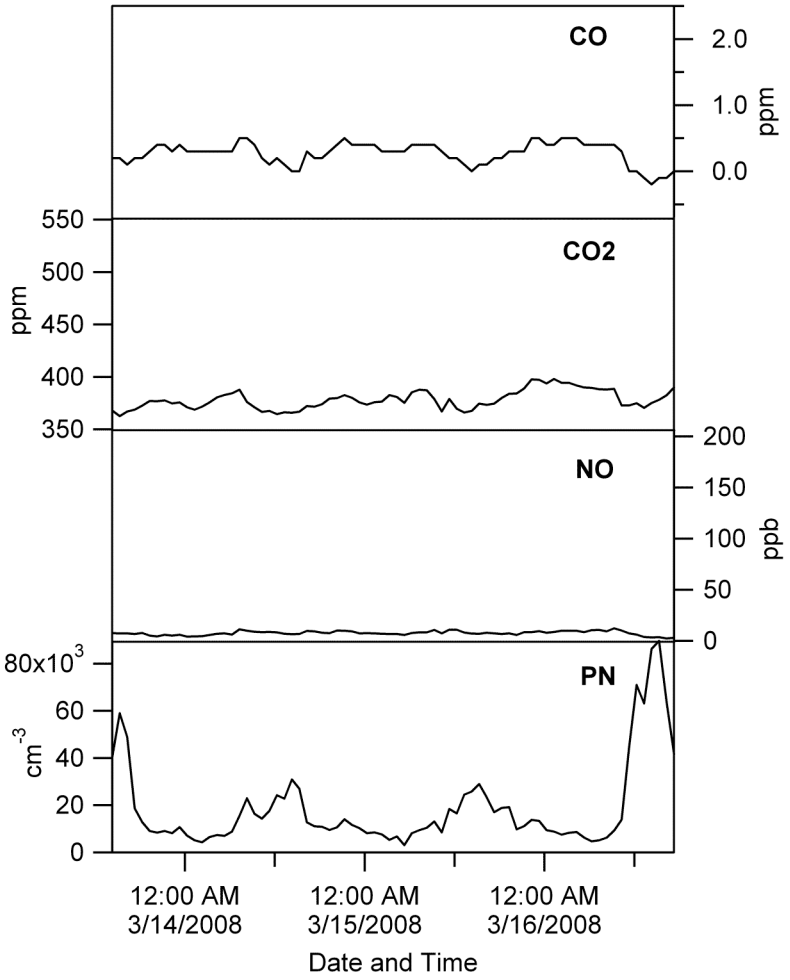

Figure 2.7b. Time series of 1-h average outdoor particle number (PN) concentration, nitric oxide, carbon dioxide and carbon monoxide levels at site H3. Levels of gaseous copollutants are relatively flat. Gas and particle peaks are decoupled. The average wind speed at this site during the monitoring period was relatively high, 4.2 m/s.

2.3.4. Indoor proportion of outdoor particles (f)

A key parameter describing the influence on indoor PN concentrations exerted by outdoor particles is the infiltration factor, *f*, also referred to as the "indoor proportion of outdoor particles" (Riley et al., 2002). This factor, which can assume values between 0 and 1, indicates the degree of protection from outdoor particles conferred to occupants of an indoor environment owing to removal processes such as deposition onto indoor surfaces, filtration, and deposition of particles during air leakage through the building shell.

Time-averaged *f* estimates obtained for the primary indoor monitoring location at six of the seven sites span a relatively small range, from 0.30 to 0.47. The estimate for H1 is much

lower, at 0.11. The significance of filters or air treatment devices in the mechanical ventilation system is evident in comparing *f* estimates made under varying house configurations at two sites. At H1, the estimated value of *f* was 0.16 when the ventilation system, including filtration, was off and 0.074 when it was on. At H5, the value of *f* was 0.43 when air filtration was off and 0.11 when it was operated. Both cases illustrate that active particle removal systems can significantly reduce indoor particle levels, in these cases by factors of ~ 2 and ~ 4.

The extent to which particles are able to penetrate from outdoors and persist in houses is expected to be associated with the air-exchange rate. All else being equal, a higher AER should increase *f*. Table 2.5 presents a summary of the statistical attributes of 37 AER determinations made at the seven house sites. The harmonic mean of per-site AER estimates ranged from 0.18 h^{-1} at H0 to 1.1 h^{-1} at H6. The high value at H6 was at least partly attributable to occupants habitually having windows partially open. The distribution of arithmetic average AERs for the seven house sites has a GM of 0.59 h^{-1} and a GSD of 2.0, similar to the distribution parameters of a large data set from across the US (N = 2844, GM = 0.50 h^{-1}, GSD = 2.1) (Murray and Burmaster, 1995; Nazaroff, 2004).

Details on air-exchange rate assessments were reported by Nazaroff et al. (2010). Results reported there have been reanalyzed here using measured outdoor CO_2 data, as discussed in Appendix 2.A.

Table 2.5. Air-exchange rates determined at the seven house sites.

Site	*N*	HM (h^{-1}) [a]	Avg (h^{-1})	Range (h^{-1})
H0	1	0.18	0.18	n/a
H1	4	0.25	0.26	0.20-0.34
H2	5	0.38	0.70	0.14-1.0
H3	6	0.75	0.99	0.45-2.2
H4	7	0.79	0.87	0.44-1.2
H5	11	0.30	0.75	0.16-3.3
H6	3	1.1	1.2	0.79-1.6
Avg.	5.3	0.53	0.70	0.36-1.6

[a] The harmonic mean is the reciprocal of the arithmetic mean of the reciprocals.

2.3.5. Indoor emissions from unvented pilot lights

Indoor sources that emit continuously elevate the baseline indoor PN concentration. However, unlike particles of outdoor origin, the influence of continuous indoor emissions should vary inversely with the air-exchange rate. The only continuous sources that we detected were pilot lights associated with gas cooking appliances. At the two sites where pilots were present, persistently elevated indoor CO_2 levels served as an indicator of the significance of pilot lights. The emission of particles from pilot lights at these houses was confirmed through controlled experiments. As presented in Figure 2.8, when the pilot lights were extinguished and all other conditions remained unchanged, the indoor PN concentration instantly started to decay (H3) or underwent an increase in the rate of decay (H1). A similar, instantaneous decrease in levels of gaseous copollutants was observed upon extinguishing pilot lights at these houses.

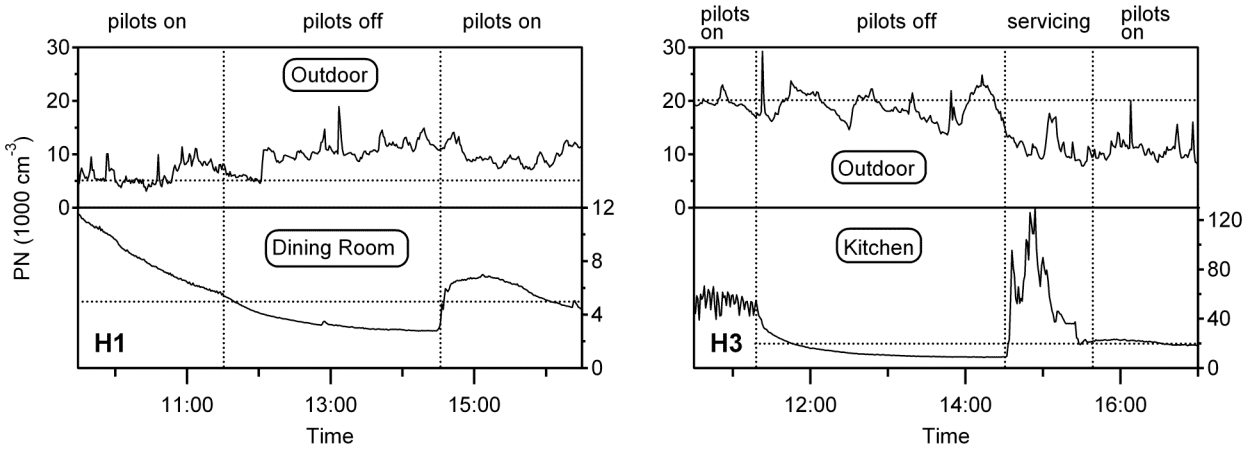

Figure 2.8. Particle number concentrations versus time during the supplemental pilot-light experiments conducted on 12 February 2009 at H1 (left), and on 8 July 2008 at H3 (right). The vertical dashed lines separate different operational states of the cook-stove pilot lights. During "servicing" at H3, a technician called in to relight the pilots conducted routine maintenance on the burners. Horizontal dashed lines at 5,000 and 20,000 cm^{-3} are intended to guide the eye.

Inferred PN emission rates from the pilot lights associated with the gas cooking appliances were 0.58×10^{12} particles h^{-1} for H1, and 1.6×10^{12} particles h^{-1} for H3. Based on field observations, the stove with lower emissions was in better repair, but the exact cause underlying the difference in emission rates was not discerned. Estimated steady-state indoor concentration increments attributable to the pilot lights for the dominant house configurations were 2.7×10^3 and 4.2×10^3 particles cm^{-3} at H1 and H3, respectively (Nazaroff et al., 2010).

2.3.6. Exposure assessment

Residential PN exposures of the 21 occupants of the seven houses, and the apportionment of exposures among sources, are summarized in Figure 2.9. The geometric mean of the average exposure concentration was 14.5×10^3 particles cm^{-3} (GSD = 1.8). The average exposure duration was 17 ± 1.7 hours per day (mean ± standard deviation). The geometric mean daily integrated exposure per person was 244×10^3 particles cm^{-3} h/d (GSD = 1.9). The corresponding arithmetic mean ± standard deviation are $296 \times 10^3 \pm 195 \times 10^3$ particles cm^{-3} h/d. On average, more than 95% of the observed exposure was attributed to known source categories.

At every site, there were substantial contributions to exposure both from the penetration and persistence of outdoor particles and from episodic indoor emissions. Furthermore, at each site and for every occupant, these two source categories dominated. The distribution of residential PN daily integrated exposures caused by particles from episodic indoor sources and by particles of outdoor origin each conform reasonably well to lognormal distributions, with GM = 129×10^3 particles cm^{-3} h/d (GSD = 2.4) for exposures attributable to episodic sources and GM = 77.2×10^3 particles cm^{-3} h/d (GSD = 1.6) for residential exposures attributable to particles of outdoor origin. At two sites with unvented gas pilot lights, H1 and H3, the average daily integrated exposures associated with this source were 63.1×10^3 and 79.1×10^3 cm^{-3} h/d (or 16 and 12% of total exposure from all sources at these two sites), respectively.

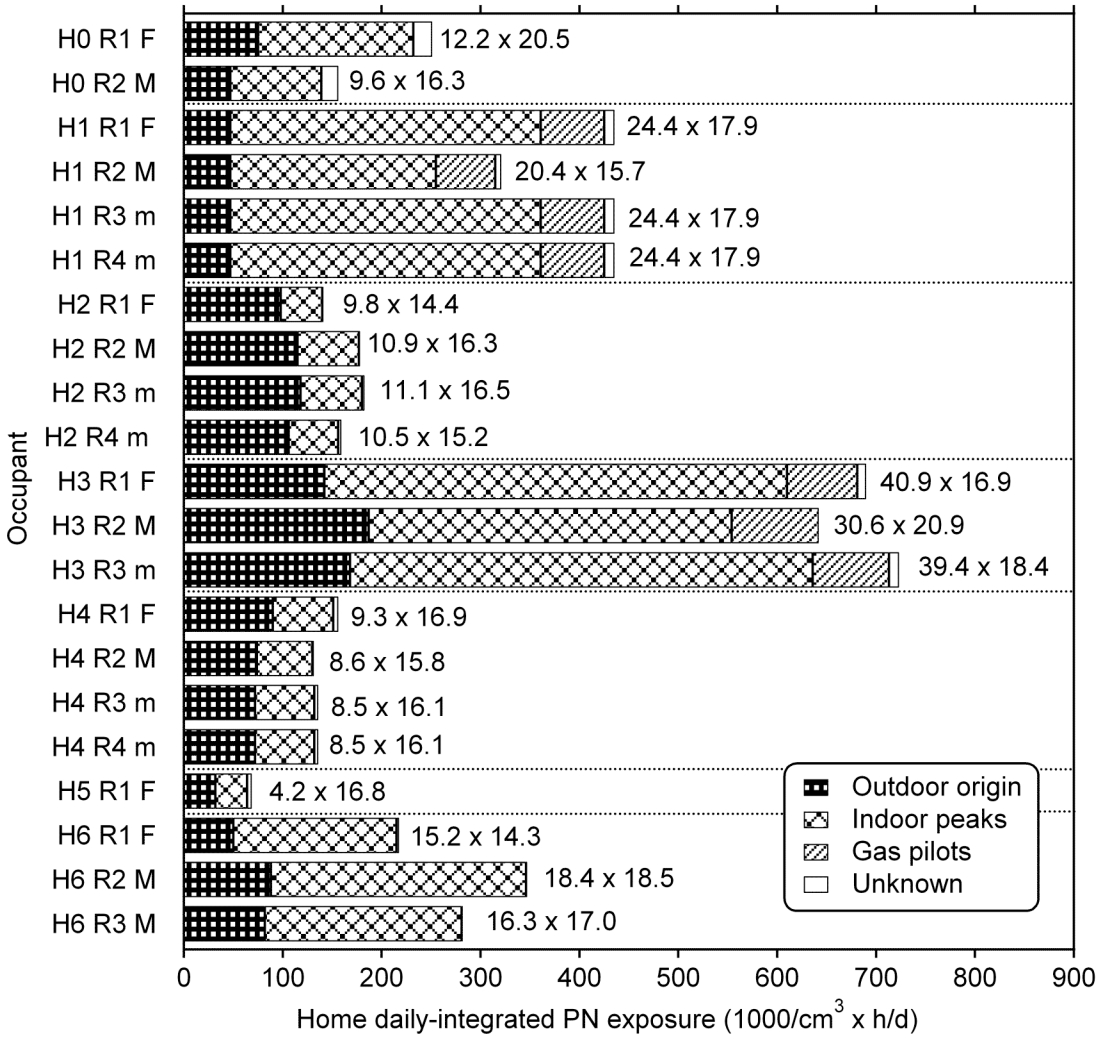

Figure 2.9. The residential, average PN exposure for the 21 occupants of the seven houses studied. The bars indicate the daily integrated exposure (1000/cm^3 h/d) and its apportionment amongst source categories. The length of the bars can be understood as the average exposure concentration per person × the daily average time spent indoors at home, which are listed to the right of each bar with units of 1000/cm^3 × h/d.

Variation in exposure, as indicated by the relative standard deviation of individual average exposure concentration estimates, was greater between houses than among occupants of the same house. The within-house RSD ranged from 0.05 at H3 (N = 3) to 0.2 (N = 2) at H0. The RSD for all occupants was 0.6 (N = 21). An explanation for this observation is that key factors that influence indoor concentrations are site-specific. Moreover, occupancy patterns are correlated for family members. In addition, the inter-individual variability owing to within-house spatial variability of particle concentrations and variability in individual location patterns was not characterized in this study. As a consequence, the true within-household variability in exposures is likely to be greater than is indicated by our RSD estimates.

Insight into the primary cause of exposure variation between sites can be gained by analyzing the two sets of sites that were clustered earlier as Group 1 (H0, H1, H3, H6) and Group 2 (H2, H4, H5). The average residential PN exposure concentration is, on average, almost 2.5× greater for the 12 occupants of Group 1 sites, compared to the 9 occupants of Group 2 sites. This difference is mainly caused by the contribution from indoor sources. Whereas for Group 2 sites indoor sources contribute an average of 38% to the daily integrated exposure, for Group 1 sites emissions from indoor sources are more important, with a mean contribution of 76%.

The frequency with which the cooking range (gas or electric) was used to prepare food was the single most important determinant of exposure from episodic indoor sources. Subjects cooked in the monitored households at an average frequency that ranged from 0.3 to 2 times per day. A single-parameter linear regression analysis showed a high degree of correlation ($r^2 = 0.7$) between the average number of times per day that the stove (alone or in combination with another source) was used for cooking in the presence of an occupant, and the indoor episodic source exposure of that occupant.

To put the exposure results in context, four other studies of ultrafine particles in interior environments are briefly discussed. In a companion study to the present one, conducted in six schools in northern California, Mullen et al. (in press) found the mean within-classroom daily integrated exposure for students was 50×10^3 particles cm^{-3} h/d. Two factors account for the at-school exposure being substantially lower than the residential exposure estimate: (1) less time is spent at school than at home by children; and (2) there was a much lower prevalence of indoor source events in the monitored classrooms as compared with households. In a multiyear study conducted in an occupied suburban Virginia townhouse with gas appliances (but with no pilots), Wallace (2006) attributed 55% of indoor UFP concentrations to indoor sources. This estimate is similar to our mean estimated exposure owing to indoor episodic sources (59%). Fruin et al. (2008) measured in-vehicle UFP concentrations in Los Angeles. Their modeled on-road exposure to UFP during 1.5 h/d spent driving was 119×10^3 cm^{-3} h/d, an average daily integrated exposure that is about 40% as large as the average residential estimate from our study. Based on a scenario describing a "typical, suburban, nonsmoker house," and data from a study in two houses in Virginia and California, Wallace and Ott (in press) attributed an integrated daily exposure of 62×10^3 particles cm^{-3} h/d to cooking at home. Their estimate is similar to the geometric mean daily exposure attributable to residential cooking in our study, 88×10^3 particles cm^{-3} h/d (GSD = 2.6).

2.4. Conclusions

Indoor and outdoor sources were both found to contribute substantially to PN concentrations and exposures in seven monitored northern California houses. Indoor concentrations are, on average, 1.7× greater during occupied relative to unoccupied hours because occupants, when present and awake, engage in activities that emit particles. If the occupied period is further segregated into "all occupants asleep" or "all occupants awake" hours, we find that "awake" PN levels are on average 6.6× greater than "asleep" PN levels, both because indoor peaks are linked with human activities and because outdoor PN concentrations were lower overnight than during the day for the conditions studied.

Indoor episodic sources are the cause of peak indoor concentrations and also the main cause of variability in occupants' residential exposure among the houses. On average, indoor

sources contributed more to the individual residential daily integrated exposures than did particles originating outdoors. The most important indoor episodic source activity is cooking, and the frequency of cooking food on either a gas or electric range is therefore an important variable influencing exposure to PN in houses.

Intrusion of outdoor particles and emissions from indoor continuous sources such as unvented pilot lights determine the baseline particle level indoors. Making houses more airtight would tend to provide some protection from outdoor particles but would also lead to higher exposure to particles generated indoors. When present, active filtration or air treatment was seen to be an effective means of reducing the persistence of particles from outdoors and indoors alike. Completing the switch away from the use of unvented pilot lights on cooking appliances would be an effective intervention for reducing indoor PN levels and exposures.

Our study focused on a relatively small number of houses in one state in the US. Different regions have different outdoor air pollution levels, climatic conditions, building stocks, and demographics. Each of these features could influence the indoor PN and resulting exposures. Also, because the lower size-cut of our instrument is 6 nm, we may have underestimated the importance of sources like a gas or electric stovetop burner, which have been found to emit smaller particles under some conditions (Wallace et al., 2008). Our study relies on microenvironmental monitoring and diary data on time-activity patterns to model personal exposure. As such, reported exposures do not fully account for spatial variability in concentrations within a residence.

Spatial variability likely plays a minor role for exposures from particles that originate outdoors. However for particles generated indoors, the short-term exposure of a person proximate to a source can be significantly higher than is indicated by our estimates (Klepeis, 1999). The degree to which exposure is underestimated by the area measurements made in this study is likely to be greatest for indoor sources that require close proximity while active emissions are underway, as the spatial heterogeneity in concentrations is expected to be greatest during the emissions phase. For example for cooking, which was the most important indoor source observed in this study, the "active" version (e.g., stir-frying) requires the cook to remain close to the stove during the emissions period and thus to be exposed to freshly emitted particle plumes. In contrast during "passive" cooking (such as boiling rice or baking in the oven) the cook may be in the near-neighborhood of the source only intermittently or not at all.

Although limited in scope, this study reinforces and substantiates the expectation that residential exposure to ultrafine particles cannot be characterized by ambient (outdoor air) measurements alone. Reasons include the importance of indoor sources, and variations in the indoor proportion of outdoor particles across sites and as a function of several variables, including meteorology, house configuration, and house operating conditions. Therefore, characterizing indoor sources, assessing their frequency of use, investigating the parameter f, and monitoring spatial and temporal trends in outdoor PN are all important aspects on which we need better knowledge so that we may understand well the levels of human exposure to ultrafine particles and their determinants.

2.5. References

Abt E, Suh HH, Catalano P, Koutrakis P, 2000. Relative contribution of outdoor and indoor particle sources to indoor concentrations. *Environmental Science and Technology* **34**, 3579-3587.

Ban-Weiss GA, Lunden MM, Kirchstetter TW, Harley RA, 2009. Measurement of black carbon and particle number emission factors from individual heavy-duty trucks. *Environmental Science and Technology* **43**, 1419-1424.

Balasubramanian R, Lee SS, 2007. Characteristics of indoor aerosols in residential homes in urban locations: a case study in Singapore. *Journal of the Air and Waste Management Association* **57**, 981-990.

Caltrans, 2007. Traffic volumes on California state highways. State of California Department of Transportation, Division of Traffic Operations, Sacramento, CA. Accessed at http://www.dot.ca.gov/traffops/saferest/trafdata/2007TrafficVolumes.pdf.

Crüts B, van Etten L, Törnqvist H, Blomberg A, Sandström T, Mills NL, Borm PJA, 2008. Exposure to diesel exhaust induces changes in EEG in human volunteers. *Particle and Fibre Toxicology* **5**, article 4, doi:10.1186/1743-8977-5-4.

Delfino RJ, Sioutas C, Malik S, 2005. Potential role of ultrafine particles in associations between airborne particle mass and cardiovascular health. *Environmental Health Perspectives* **113**, 934-946.

Delfino RJ, Staimer N, Tjoa T, Polidori A, Arhami M, Gillen DL, Kleinman MT, Vaziri ND, Longhurst J, Zaldivar F, Sioutas C, 2008. Circulating biomarkers of inflammation, antioxidant activity, and platelet activation are associated with primary combustion aerosols in subjects with coronary artery disease. *Environmental Health Perspectives* **116**, 898-906.

Delfino RJ, Staimer N, Tjoa T, Gillen DL, Polidori A, Arhami M, Kleinman MT, Vaziri ND, Longhurst J, Sioutas C, 2009. Air pollution exposures and circulating biomarkers of effect in a susceptible population: clues to potential causal component mixtures and mechanisms. *Environmental Health Perspectives* **117**, 1232-1238.

Diapouli E, Chaloulakou A, Spyrellis N, 2007. Levels of ultrafine particles in different microenvironments – implications to children exposure. *Science of the Total Environment* **388**, 128-136.

Donaldson K, Stone V, 2003. Current hypotheses on the mechanisms of toxicity of ultrafine particles. *Ann 1st Super Sanità* **39**, 405-410.

Fruin S, Westerdahl D, Sax T, Sioutas C, Fine PM, 2008. Measurements and predictors of on-road ultrafine particle concentrations and associated pollutants in Los Angeles. *Atmospheric Environment* **42**, 207-219.

Garza KM, Soto KF, Murr LE, 2008. Cytotoxicity and reactive oxygen species generation from aggregated carbon and carbonaceous nanoparticulate materials. *International Journal of Nanomedicine* **3**, 83-94.

He CR, Morawska L, Hitchins J, Gilbert D, 2004. Contribution from indoor sources to particle number and mass concentrations in residential houses. *Atmospheric Environment* **38**, 3405-3415.

Hoek G, Boogaard H, Knol A, de Hartog J, Slottje P, Ayres JG, Borm P, Brunekreef B, Donaldson K, Forastiere F, Holgate S, Kreyling WG, Nemery B, Pekkanen J, Stone V, Wichmann HE, van der Sluijs J, 2010. Concentration response functions for ultrafine particles and all-cause mortality and hospital admissions: Results of a European expert panel

elicitation. *Environmental Science and Technology* **44**, 476-482.
Hussein T, Korhonen H, Herrmann E, Hämeri K, Lehtinen KEJ, Kulmala M, 2005. Emission rates due to indoor activities: indoor aerosol model development, evaluation, and applications. *Aerosol Science and Technology* **39**, 1111-1127.
Ibald-Mulli A, Wichmann HE, Kreyling W, Peters A, 2002. Epidemiological evidence on health effects of ultrafine particles. *Journal of Aerosol Medicine* **15**, 189-201.
Jeong CH, Hopke PK, Chalupa D, Utell M, 2004. Characteristics of nucleation and growth events of ultrafine particles measured in Rochester, NY. *Environmental Science and Technology* **38**, 1933-1940.
Klepeis NE, 1999. Validity of the uniform mixing assumption: determining human exposure to environmental tobacco smoke. *Environmental Health Perspectives* **107 (S2)**, 357-363.
Klepeis NE, Nelson WC, Ott WR, Robinson JP, Tsang AM, Switzer P, Behar JV, Hern SC, Engelmann WH, 2001. The National Human Activity Pattern Survey (NHAPS): a resource for assessing exposure to environmental pollutants. *Journal of Exposure Analysis and Environmental Epidemiology* **11**, 231-252.
Knibbs LD, de Dear RJ, Morawska L, 2010. Effect of cabin ventilation rate on ultrafine particle exposure inside automobiles. *Environmental Science and Technology* **44**, 3546-3551.
Knol AB, de Hartog JJ, Boogaard H, Slottje P, van der Sluijs JP, Lebret E, Cassee FR, Wardekker A, Ayres JG, Borm PJ, Brunekreef B, Donaldson K, Forastiere F, Holgate ST, Kreyling WG, Nemery B, Pekkanen J, Stone V, Wichmann HE, Hoek G, 2009. Expert elicitation on ultrafine particles: Likelihood of health effects and causal pathways. *Particle and Fibre Toxicology* **6**, article 19, doi:10.1186/1743-8977-6-19.
Kulmala M, Vehkamäki H, Petäjä T, Dal Maso M, Lauri A, Kerminen VM, Birmili W, McMurry PH, 2004. Formation and growth rates of ultrafine atmospheric particles: a review of observations. *Journal of Aerosol Science* **35**, 143-176.
Lioy PJ, 2010. Exposure science: a view of the past and milestones for the future. *Environmental Health Perspectives* **118**, 1081-1090.
Liu DL, Nazaroff WW, 2001. Modeling pollutant penetration across building envelopes. *Atmospheric Environment* **35**, 4451-4462.
Long CM, Suh HH, Koutrakis P, 2000. Characterization of indoor particle sources using continuous mass and size monitors. *Journal of the Air and Waste Management Association* **50**, 1236-1250.
Matson U, 2005. Indoor and outdoor concentrations of ultrafine particles in some Scandinavian rural and urban areas. *Science of the Total Environment* **343**, 169-176.
Mitsakou C, Housiadas C, Eleftheriadis K, Vratolis S, Helmis C, Asimakopoulos D, 2007. Lung deposition of fine and ultrafine particles outdoors and indoors during a cooking event and a no activity period. *Indoor Air* **17**, 143-152.
Monkkonen P, Pai P, Maynard A, Lehtinen KEJ, Hameri K, Rechkemmer P, Ramachandran G, Prasad B, Kulmala M, 2005. Fine particle number and mass concentration measurements in urban Indian households. *Science of the Total Environment* **347**, 131-147.
Morawska L, He CR, Hitchins J, Mengersen K, Gilbert D, 2003. Characteristics of particle number and mass concentrations in residential houses in Brisbane, Australia. *Atmospheric Environment* **37**, 4195-4203.
Morawska L, He CR, Johnson G, Guo H, Uhde E, Ayoko G, 2009. Ultrafine particles in indoor air of a school: possible role of secondary organic aerosols. *Environmental Science and Technology* **43**, 9103-9109.

Mullen NA, Bhangar S, Hering SV, Kreisberg NM, Nazaroff WW, in press. Ultrafine particle concentrations and exposures in six elementary school classrooms in northern California. *Indoor Air*, doi: 10.1111/j.1600-0668.2010.00690.

Murray DM, Burmaster DE, 1995. Residential air exchange rates in the United States: empirical and estimated parametric distributions by season and climatic region. *Risk Analysis* **15**, 459-465.

Nazaroff WW, 2004. Indoor particle dynamics. *Indoor Air* **14 (Suppl. 7)**, 175-183.

Nazaroff WW, 2008. Inhalation intake fraction of pollutants from episodic indoor emissions. *Building and Environment* **43**, 267-277.

Nazaroff WW, Bhangar S, Mullen NA, Hering SV, Kreisberg NM, 2010. Ultrafine particle concentrations in schoolroom and homes, Final Report, Contract No. 05-305, California Air Resources Board, Sacramento, CA. Available at http://www.arb.ca.gov/research/apr/past/indoor.htm.

Nel A, Xia T, Mädler L, Li N, 2006. Toxic potential of materials at the nanolevel. *Science* **311**, 622-627.

Pope CA, Dockery DW, 2006. Health effects of fine particulate air pollution: lines that connect. *Journal of the Air and Waste Management Association* **56**, 709-742.

Riley WJ, McKone TE, Lai ACK, Nazaroff WW, 2002. Indoor particulate matter of outdoor origin: importance of size-dependent removal mechanisms. *Environmental Science and Technology* **36**, 200-207.

Rundell KW, 2003. High levels of airborne ultrafine and fine particulate matter in indoor ice arenas. *Inhalation Toxicology* **15**, 237-250.

Spracklen DV, Carslaw KS, Kulmala M, Kerminen VM, Mann GW, Sihto SL, 2006. The contribution of boundary layer nucleation events to total particle concentrations on regional and global scales. *Atmospheric Chemistry and Physics* **6**, 5631-5648.

Vinzents PS, Møller P, Sørensen M, Knudsen LE, Hertel O, Jensen FP, Schibye B, Loft S, 2005. Personal exposure to ultrafine particles and oxidative DNA damage. *Environmental Health Perspectives* **113**, 1485-1490.

Wallace L, 2005. Ultrafine particles from a vented gas clothes dryer. *Atmospheric Environment* **39**, 5777-5786.

Wallace L, Williams R, 2005. Use of personal-indoor-outdoor sulfur concentrations to estimate the infiltration factor and outdoor exposure factor for individual homes and persons. *Environmental Science and Technology* **39**, 1707-1714.

Wallace L, 2006. Indoor sources of ultrafine and accumulation mode particles: size distributions, size-resolved concentrations, and source strengths. *Aerosol Science and Technology* **40**, 348-360.

Wallace L, Wang F, Howard-Reed C, Persily A, 2008. Contribution of gas and electric stoves to residential ultrafine particle concentrations between 2 and 64 nm: size distributions and emission and coagulation rates. *Environmental Science and Technology* **42**, 8641-8647.

Wallace L, Ott W, in press. Personal exposure to ultrafine particles. *Journal of Exposure Science and Environmental Epidemiology*, doi: 10.1038/jes.2009.59.

Watson JG, Chow JC, Park K, Lowenthal DH, Park K, 2006. Nanoparticle and ultrafine particle events at the Fresno Supersite. *Journal of the Air and Waste Management Association* **56**, 417-430.

Weichenthal S, Dufresne A, Infante-Rivard C, 2007a. Indoor ultrafine particles and childhood asthma: exploring a potential public health concern. *Indoor Air* **17**, 81-91.

Weichenthal S, Dufresne A, Infante-Rivard C, Joseph L, 2007b. Indoor ultrafine particle exposures and home heating systems: a cross-sectional survey of Canadian homes during the winter months. *Journal of Exposure Science and Environmental Epidemiology* **17**, 288-297.
Weichenthal S, Dufresne A, Infante-Rivard C, Joseph L, 2008. Characterizing and predicting ultrafine particle counts in Canadian classrooms during the winter months: model development and evaluation. *Environmental Research* **106**, 349-360.
Zartarian V, Bahadori T, McKone T, 2005. Adoption of an official ISEA glossary. *Journal of Exposure Analysis and Environmental Epidemiology* **17**, 1-5.
Zhang KM, Wexler AS, 2002. Modeling the number distributions of urban and regional aerosols: theoretical foundations. *Atmospheric Environment* **36**, 1863-1874.
Zhang QF, Zhu YF, 2010. Measurements of ultrafine particles and other vehicular pollutants inside school buses in South Texas. *Atmospheric Environment* **44**, 253-261.
Zhao B, Chen C, Tan ZC, 2009. Modeling of ultrafine particle dispersion in indoor environments with an improved drift flux model. *Journal of Aerosol Science* **40**, 29-43.
Zhu YF, Hinds WC, Kim S, Shen S, Sioutas C, 2002. Study of ultrafine particles near a major highway with heavy-duty diesel traffic. *Atmospheric Environment* **36**, 4323-4335.
Zhu YF, Hinds WC, Krudysz M, Kuhn T, Froines J, Sioutas C, 2005. Penetration of freeway ultrafine particles into indoor environments. *Journal of Aerosol Science* **36**, 303-322.

2.A. Appendix

2.A.1. Evaluating building ventilation rates with indoor and outdoor carbon dioxide measurements

2.A.1.1. Introduction

Building ventilation conditions can be evaluated through techniques that rely on the measurement and analysis of a tracer gas. The analysis typically relies on the principle of material balance. From a scientific point of view, an ideal tracer gas is one that has no indoor sources, and is present only in trace quantities outdoors. When such a species (e.g., SF_6) is released continuously or as a pulse indoors, a material balance equation may be used to model the rate of change of the tracer as a function of ventilation conditions and the (known) emission conditions. By comparing measured concentrations to those modeled, the unknown ventilation rate may be determined.

Carbon dioxide is a commonly used tracer species. In this case, the tracer may be deliberately released indoors, or opportune use may be made of CO_2 released from respiration and from combustion appliances. Persily (1997) and Persily and Dols (1990) have explored approaches to assess ventilation on the basis of CO_2 measurements. Their discussion, and other examples of the application of this technique identified in the peer-reviewed literature, relies on the assumption that outdoor CO_2 levels remain constant during the ventilation assessment period.

As demonstrated by Figure 2.A.1, observations from our field study show that carbon dioxide levels at some urban sites exhibit significant temporal variability. The pattern in outdoor CO_2 levels depicted in Figure 2.A.1 – midday minima flanked by morning and evening peaks – are supported by investigations of outdoor CO_2 conducted in Baltimore by George et al. (2007). In light of the observed temporal variability in outdoor CO_2 levels, we evaluated air-exchange rates on the basis of time-varying data on indoor and outdoor CO_2. We compared our results with those obtained when outdoor CO_2 is treated as constant during each assessment period, to evaluate the importance of incorporating temporal variability in outdoor CO_2 to assess ventilation conditions, for the conditions in our study.

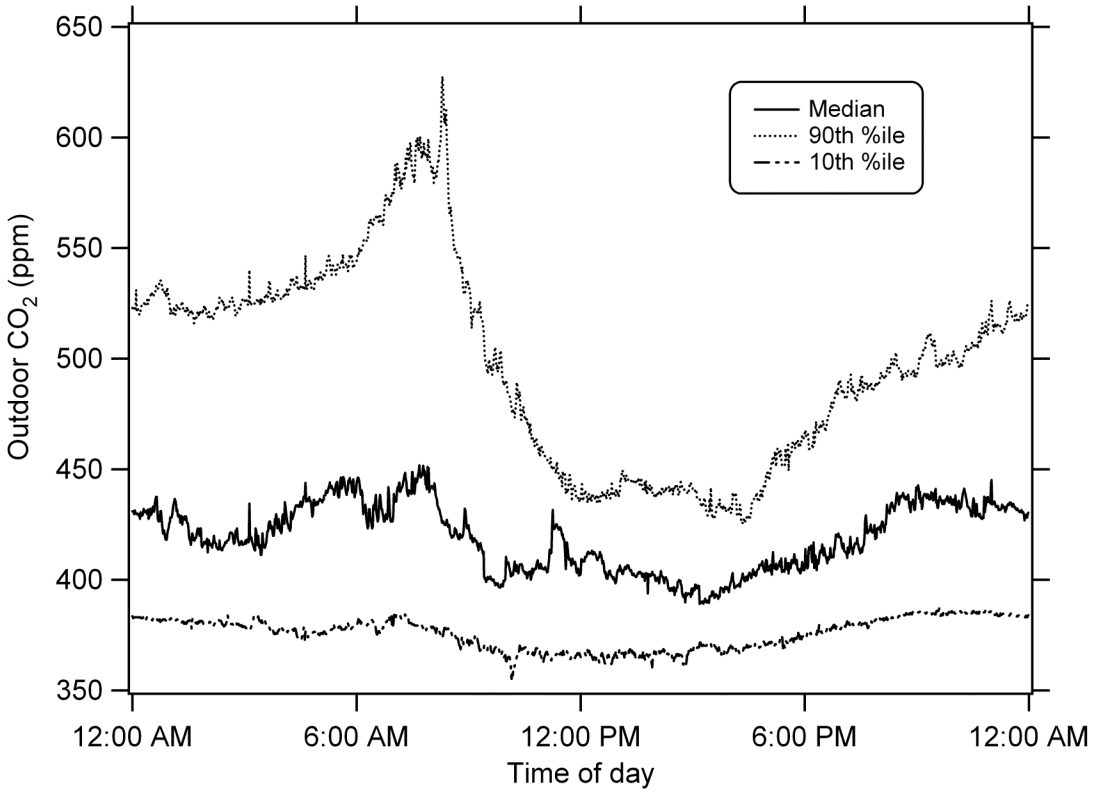

Figure 2.A.1. Diurnal variation in outdoor CO_2 at sites H0-H6. The median, 10th percentile and 90th percentile of 1-min carbon dioxide data collected during observational monitoring at all sites are plotted against the time of day when the data were acquired. The number of days monitored varies from 22 to 28 (average = 26) per clock minute.

2.A.1.2. Data analysis

The governing material balance equation for the evolution of CO_2 levels indoors in the absence of indoor sources is presented as equation (2.A.1):

$$\frac{dY}{dt} = \lambda Y_O(t) - \lambda Y(t) \qquad (2.A.1)$$

where Y is the indoor CO_2 level (ppm) at time t; λ is the air exchange rate (h^{-1}), which is assumed to stay constant during the decay period; Y_O is the outdoor CO_2 level (ppm) at time t. Since the model equation assumes that there are no indoor sources of carbon dioxide, it is applicable only when the building is unoccupied and unvented pilot lights are absent. The house is treated as a single, well-mixed compartment.

When the outdoor CO_2 level can be treated as approximately constant, equation (2.A.1) can be solved analytically, with the result shown in equation (2.A.2):

$$Y_d = Y_d(0)e^{-\lambda t} \quad (2.A.2)$$

where $Y_d = Y\text{-}Y_O$. For this case, λ can be calculated as the negative slope of ln ($Y_d(t)$) regressed against t. When the outdoor CO_2 level is variable, a solution to equation (2.A.1) can be approximated using a numerical or an integral approach. The numerical approach involves transforming equation (2.A.1) into a difference equation, shown as equation (2.A.3):

$$Y_{i+1} \cong Y_i + \lambda(Y_{O,i} - Y_i)\Delta t \quad (2.A.3)$$

A best-fit value for λ can be obtained by minimizing the sum of squared deviations between predicted and measured values of ln(Y), where predicted values are obtained via equation (2.A.3).

Alternatively, an integral approach can be used in analysis. Integrate both sides of equation (2.A.1) and solve for λ. The result is shown as equation (2.A.4):

$$\lambda = \frac{(Y_{t_2} - Y_{t_1})}{(Y_{O,avg} - Y_{avg}) \times (t_2 - t_1)} \quad (2.A.4)$$

In equation 2.A.4, time t_2 represents the end of the air-exchange rate assessment period, and t_1 represents the start of the period.

2.A.1.3. Results and discussion

Table 2.A.1 presents results for 27 air-exchange rate assessments from the five house sites without unvented pilot lights. For comparison, air exchange rates are calculated using the numerical approach (equation (2.A.3)), the integral approach (equation (2.A.4)), and based on the assumption that outdoor levels remain constant (equation (2.A.2)). When the latter assumption was invoked, a representative outdoor CO_2 level was obtained as the average outdoor CO_2 during the decay period. The mean (± standard deviation) relative standard deviation of air-exchange rate estimates obtained by the three methods is low: 5 ± 4%. If, however, the global annual average value of ~385 ppm is used as a representative outdoor CO_2 level, the air exchange rate estimates obtained from observational monitoring data are biased (compared to the average estimate obtained using the other three methods) by, on average, 42%. Air exchange rates assessed on the basis of manipulation experiments remain robust irrespective of the method or representative outdoor CO_2 level employed.

On the basis of these findings, we concluded that the choice of method is not important for the ventilation assessments made via manipulation experiments (where CO_2 levels indoors were deliberately elevated to ~2000 ppm). For unbiased results from observational monitoring data, however, while the choice of method is not of key importance, it is important to rely on measured outdoor CO_2 levels rather than the global annual mean. This is especially true for urban areas where outdoor CO_2 levels can be significantly elevated.

Summary statistics reported in this chapter are based on the integral method.

Table 2.A.1. Air-exchange rate estimates for five house sites without indoor CO_2 sources, obtained on the basis of three alternate approaches. [a,b]

ID	$CO_{2,\,out,\,avg}$ (ppm)	AER (h^{-1}) Fixed CO_2	AER (h^{-1}) Integral	AER (h^{-1}) Numerical	RSD (%)
H0 M1	341	0.19	0.18	0.18	3.1
H2 O1	494	1.0	1.0	1.0	1.5
H2 O2	536	0.93	0.98	0.93	3.0
H2 O3	435	1.2	1.0	1.1	9.5
H2 M1	413	0.20	0.14	0.21	21
H2 M2	Missing	0.32	0.34	n/a	4.3
H4 O2	417	1.1	1.1	1.1	0.9
H4 O3	497	0.89	0.78	0.74	9.7
H4 O4	429	0.44	0.44	0.45	1.3
H4 M1	431	1.3	1.2	1.2	1.6
H4 M2	422	0.77	0.73	0.73	3.1
H4 M3	431	1.2	1.1	1.1	4.7
H4 M4	418	0.67	0.73	0.75	5.8
H5 O2	370	0.89	0.96	0.84	6.7
H5 O3	366	0.25	0.24	0.24	2.4
H5 M1	Missing	0.19	0.18	n/a	3.8
H5 M2	Missing	0.31	0.31	n/a	0.0
H5 M3	Missing	0.19	0.18	n/a	3.8
H5 M4	Missing	0.33	0.34	n/a	2.1
H5 M5	Missing	0.17	0.16	n/a	4.3
H5 M6	Missing	0.56	0.55	n/a	1.3
H5 M7	Missing	1.9	2.1	n/a	7.1
H5 M8	Missing	0.19	0.18	n/a	3.8
H5 M9	Missing	2.8	3.0	n/a	5.6
H6 O1	449	1.3	1.6	1.6	12
H6 M1	449	1.0	1.1	1.1	5.4
H6 M2	359	0.73	0.79	0.82	5.9

[a] Each experiment is labeled with a two-part code that identifies that site, and whether the data are from the observational monitoring period (O), or from a deliberate experiment (M).

[b] In instances when time-varying CO_2 levels were not measured during the decay period, the numerical approach could not be applied. In these cases, the following outdoor CO_2 levels were used to evaluate λ: H2M2, 528 ppm, the CO_2 level measured outdoors just before AER assessment; H5, 367 ppm, the average of observational data 1-min averages from 11:00 to 17:00.

2.A.1.4. References

George K, Ziska LH, Bunce JA, Quebedeaux B, 2007. Elevated atmospheric CO_2 concentration and temperature across an urban-rural transect. *Atmospheric Environment* **41**, 7654-7665.

Persily AK, Dols WS, 1990. The relation of CO_2 concentration to office building ventilation. *Air Change Rate and Airtightness in Buildings*, MH Sherman, Ed, pp. 77-92. ASTM STP 1067. Philadelphia: American Society for Testing and Materials.

Persily AK, 1997. Evaluating building IAQ and ventilation with indoor carbon dioxide. *ASHRAE Transactions* **103 Pt. 2**, 1-12.

Chapter 3: Inhalation intake fraction of ultrafine particles from indoor emissions in homes

3.1. Introduction

3.1.1. Issue

Indoor sources dominate exposures to peak concentrations of ultrafine particles (UFP) in homes. On average, for 21 occupants of seven houses monitored in the field study reported in Chapter 2, indoor sources also dominated cumulative at-home UFP exposures. As people spend most of their time at home, the importance of indoor sources to at-home exposure suggests that they have the potential to contribute major proportions of overall daily integrated exposures as well.

The human health risk posed by indoor sources of UFP depends not only on their contributions to exposure, but also on the adverse health effects associated with their emissions. The most important indoor source observed in the field study described in Chapter 2 was cooking, which contributed, on average, 74% of exposures attributed to indoor episodic sources. During cooking, emissions are caused by the cooking fuel, electrically heated element, or the food itself. Modern cooking in the US and developed countries has been shown to be associated with adverse outcomes such as respiratory symptoms from nitrogen dioxide exposure (Neas et al., 1991). Fumes from Chinese-style cooking with hot oil have been shown to be mutagenic (Chiang et al., 1997) and this cooking style has also been reported to be a risk factor for lung cancer in nonsmoking women in Taiwan (Ko et al., 1997). The human health effects associated with the ultrafine particle emissions from cooking have not been directly investigated. However, individual components of particles emitted from cooking – such as elemental and organic carbon, polycyclic aromatic hydrocarbons, aldehydes, and metals – have been linked with adverse outcomes (e.g., Garza et al., 2008; See and Balasubramanian, 2008). Moreover, toxicological studies on ultrafine particles have emphasized effects linked to the small size and high surface area to volume ratio, rather than to their origin (Donaldson and Stone, 2003; Nel et al., 2006).

We know more about indoor sources of UFP than we do about exposures owing to their use. As emphasized in Chapter 2, there have been few studies published on ultrafine particles in occupied homes under normal-use conditions. Several studies have characterized emission rates for indoor sources via laboratory or controlled field investigations. A few studies have modeled the anticipated relationship between emissions and exposure for airborne contaminants released in residences (or other interior environments such as motor vehicles), and have used the intake fraction metric (or an equivalent concept) to present and discuss findings. However, as is demonstrated by the literature review to be presented in this chapter, the concerted characterization of sources of and exposure to ultrafine particles, in indoor environments, is comparatively rare. Increasing our understanding of the source-to-exposure relationship for ultrafine particles under real-world conditions puts us in a position to leverage our emerging knowledge about sources to draw inferences that have relevance for epidemiological studies, environmental planning, and risk assessment.

In the subsections to follow, the intake fraction (*iF*) metric is discussed (§3.1.2), a literature review is presented of previous *iF* assessments in homes (§3.1.3), and objectives of the

study are outlined (§3.1.4). Then, an intake fraction lens is applied to reinterpret the field data described in Chapter 2.

3.1.2. Inhalation intake fraction

Intake fraction was proposed, and has been widely adopted, as a consistent concept to discuss emissions-to-intake relationships, when emissions and intake are linearly related as is the case for most primary pollutants (Bennett et al., 2002). Other articulations of the linkage between emissions and intake or exposure have been variously named as exposure effectiveness, committed dose, inhalation transfer factor, or fate factor, to name a few examples (Bennett et al., 2002). Intake fraction is defined, for a species, emission source, and exposure scenario, as the ratio of attributable intake to attributable emissions (Bennett et al., 2002; Marshall et al., 2003). An intake fraction can also be conceptualized as the ratio of the probability of a pollutant entering a human body before it is removed from the local environment (Nazaroff, 2008). The relationship between emissions and exposures depends on several source-specific, environment-specific and population-specific factors that complicate precise *iF* evaluations under real-world scenarios. However, *iF* estimates often represent a useful starting point, an approximate and preliminary but efficient tool for comparing exposure scenarios, prioritizing efforts to reduce risk, and assessing whether further study is needed (Lai et al., 2000).

The intake fraction metric is unitless by design. The original definition presents it as a ratio of two masses (mass inhaled to mass emitted). In the present work, *iF* is assessed as a ratio of two numbers, as ultrafine particles are conventionally quantified on a number rather than a mass basis. When unqualified, *iF* encapsulates intake via all pathways and routes. The calculations here are limited to the inhalation route because that is the only known route of potential health concern for ultrafine particles emitted from environmental sources. While dermal uptake and ingestion routes have been explored for synthetic nanoparticles (such as may be incorporated, for instance, into consumer or medical products), these alternate routes do not make known contributions of health significance for environmental UFP intake. Finally, *iF* can be defined on an individual or a population basis. This analysis does both, as each formulation has distinct merits. Individual intake fractions are useful for identifying high-risk groups or inferring a dose from information on emissions. Population intake fractions are useful for assessing the total impact associated with a source as might be required, for example, for a comparative risk assessment (Ilacqua et al., 2007).

3.1.3. Background and literature review

The ideas underlying the intake fraction concept were conceived and developed independently by a number of research groups, as reviewed by Evans et al. (2002). The use of a consistent term to unify the development of related ideas was proposed by Bennett et al. (2002).

Attention to the intake fraction concept has had the effect of highlighting – from the perspective of environmental risk – the importance of indoor sources. When emission strength is the sole criterion for ranking sources, outdoor sources such as power plants and refineries are typically clear winners. But if exposure or intake is considered in addition to source strength, indoor sources emerge as potential cost-effective targets for intervention. An early study that illustrated the importance of indoor sources is the USEPA Total Exposure Assessment

Methodology (TEAM) survey. In the TEAM study, personal samplers were used to directly measure exposure to volatile organic compounds of 600 urban residents in selected US cities. Results showed that sources previously considered to be important – for example, for benzene, petroleum refining operations and manufacturing, oil storage tanks and underground leaks, groundwater contamination, and service stations – were unimportant compared to personal activities such as cigarette smoking, driving, and using attached garages (Wallace, 1989). A key reason for the observed dichotomy between sources associated with large emissions and sources leading to high exposures is that, according to magnitude estimates, intake fractions for indoor sources are roughly 1000 times greater than intake fractions for outdoor sources. This observation comparing indoor and outdoor sources has been dubbed the "Rule of 1000" (Smith, 1993).

Magnitude estimates of *iF* for indoor sources presented in the literature are semi-empirical. They rely on a combination of data, deterministic models, and simplifying assumptions, as illustrated by an early investigation of environmental tobacco smoke (ETS) exposure by Smith (1993). In that study, dose effectiveness was modeled as a function of mean occupancy, breathing rate, attributable exposure (i.e. attributable concentration × exposure duration) per cigarette, and a per-cigarette emission factor. Nominal values were assigned to model parameters via approximation or from the literature. For example, data on attributable exposures and emissions on a per-cigarette basis were taken from Dockery and Spengler (1967), who in turn based their estimates on an analysis of simultaneous indoor and outdoor field measurements, questionnaire data from 68 homes sampled in six US cities, and a model of the house as a single, well-mixed zone with steady penetration efficiency, volumetric air flow, and particle first order loss rate.

Subsequent investigations of indoor intake fractions, summarized in Table 3.1, have also been semi-empirical, relying on tools and resources that include material-balance models, values for input parameters drawn from the literature or generated via models or measurements, and simplifying assumptions. The most basic case has the following elements: (1) conserved pollutant; (2) steady occupancy, with steady and uniform breathing rate; and (3) indoor space modeled as a single, well-mixed compartment with a steady ventilation rate. These three elements can be generalized as relating to pollutant dynamics, human factors and building-specific factors, respectively (Nazaroff, 2008). When conditions (1)-(3) are invoked, the *iF* is independent of the rate and schedule of emissions and reduces to the expression in equation (3.1), which is a ratio of the amount of air breathed by occupants (number of occupants, N × breathing rate, Q_b) to the air available for dilution and removal of the pollutant (volume, V × air-exchange rate, *a*).

$$iF = \frac{NQ_b}{Va} \tag{3.1}$$

Results based on this basic approach are presented by Bennett et al. (2002) for benzene in California homes, Nazaroff (2008) and Lai et al. (2000) for US residences, and Meijer et al. (2005) for organic compounds in building materials released to the first or second floor of a house. In each of these cases, values of the input parameters are selected from the literature to match the geographical region and demographic group under consideration. Intake fraction results for this group of investigations range from 3-31 × 10^{-3}.

Table 3.1. Summary of published research in peer-reviewed archived journals on intake fractions for indoor sources in homes (*page 1 of 2*).

Reference	Source/Agent	*iF* ($\times 10^{-3}$)	Topic [a]			Comment
			S	P	O	
Bennett et al., 2002	ETS: Benzene	7				Parameter values applicable to California residences.
Hellweg et al., 2009	Household indoors	1~30	√			*iF* estimates include a correction factor for incomplete mixing.
Ilacqua et al., 2007	Indoor VOC sources: Individual *iF* Aggregate *iF*	Mean: 1.5-4.5 4.6-11.8			√	Monte-Carlo simulations based on distributions of residence volume, air exchange rate and time-activity data from the EXPOLIS dataset. Inhalation rates at rest and during light activity from the literature.
Klepeis and Nazaroff, 2006a	ETS: Particles Nicotine Carbon monoxide	GM: 0.66-2.5 0.26-1.2 1.4	√	√	√	Model incorporates influence of contaminant transport and occupant location in a multizone residential environment. Human activity pattern scenarios for *iF* assessments based on scripts (phase I) and on an NHAPS cohort (phase II).
Klepeis and Nazaroff, 2006b	ETS: Particles (scripted scenarios)	0.23-2.6	√	√	√	Influence of mitigation strategies such as opening and closing interior doors and windows on ETS *iF* in a multizone simulated house investigated. Scripted and NHAPS cohort scenarios considered (results for former shown).
Lai et al., 2000	Conserved pollutant Aerosol, low air-exchange rate Aerosol, high air-exchange rate Multizone home, two scenarios	1-10 1-20 0.2-1.2 0.5-40	√	√		Modifications of the basic expression investigated are: nonconserved pollutant, multi-compartment residence. Individual *iF* results shown here.
Meijer et al., 2005	Organic compounds in building materials	26-31	√			Two *iF* estimates, for compounds emitted to the first or second floor, respectively.
Nazaroff, 2008	Particles Sorbing species (acrolein, ethylbenzene, *o*-cresol)	3.6-5.2 0.6-6.2	√	√	√	Modifications of the basic expression owing to incomplete mixing, time-varying occupancy, deposition and sorptive interactions explored.
Russo and Khalifa, 2010	Conserved gas emitted from the floor, wall, desk, human body.	n/a	√			"Normalized" *iF* modeled to compare influence of ventilation system and proximity to source on exposure in office space.
Smith, 1993 [b]	ETS Stove unvented Stove vented	1-10 1-10 1-2		√		Magnitude estimates generated for less developed country (LDC) cities.

Table 3.1. *cont.* (*page 2 of 2*).

Reference	Source/Agent	*iF* ($\times 10^{-3}$)	Topic [a]			Comment
			S	P	O	
Zhang et al., 2010	UFP (particle number concentration)	0.55-2.3		√		Empirical concentration data used to assess intake and emissions. Effect of stove fuel (electric or gas), stove temperature (medium or high) and exhaust fan (on or off) on *iF* assessed.

[a] Topic code indicates the investigation considered: S = spatial variation, P = pollutant dynamics, O = occupant dynamics.
[b] Early research that led to the development of the intake fraction concept is reviewed in Evans et al. (2002) and Bennett et al. (2002) and has not been comprehensively reexamined here.

More sophisticated *iF* analyses consider the influence of relaxing one or more of the pollutant-related, human-related and building-related elements noted in (1)-(3) above. Table 3.1 summarizes studies on *iF* in homes, and classifies studies according to the factor explored. Though the influence of each class of factors is discussed in turn below, the influence of factors is interdependent. For example, the extent to which the well-mixed assumption will yield results that vary relative to a model with higher spatial resolution depends on spatial distributions of the agents and of the exposed people throughout a house. Or, in another example, the impact on *iF* of a dynamic behavior such as deposition depends on the ventilation rate. Comments on these dependencies are woven into the discussion of individual factors below.

Pollutant dynamics that have the potential to influence inhalation intake fractions include deposition on fixed surfaces, coagulation with other particles, removal on filter media, sorptive interactions, phase change and resuspension (Nazaroff, 2004). If a pollutant is lost via first-order processes, a loss-rate coefficient associated with each process is added to the air-exchange rate, *a*, in equation (3.1). Sorption, when fully reversible, has the effect of shifting the time-dependent concentration profile and can alter the *iF* when other factors such as the ventilation rate, occupancy, or occupant breathing rate also vary in time (Nazaroff, 2008). Intake fraction assessments that include particle deposition or reversible sorption are discussed in turn below. The influence of phase change on *iF*, though potentially significant, has not been explicitly studied. Resuspension is expected to be unimportant for ultrafine particles.

Lai et al. (2000) present particle size-specific *iF* estimates, by associating each particle size fraction with a first-order deposition loss rate derived from prior research. Individual *iF* values for particles 0.001-10 μm in diameter vary in the range (1-20) $\times 10^{-3}$ under low ventilation conditions (0.2 h^{-1}), and are (0.2-1.2) $\times 10^{-3}$ under high ventilation conditions (2 h^{-1}). In the only published study that has assessed indoor intake fractions for UFP semi-empirically, Zhang et al. (2010) estimated individual *iF* in the range (0.55-2.3) $\times 10^{-3}$. The highest individual intakes were attributed to high-temperature cooking on a gas stove with the exhaust fan turned off.

Nazaroff (2008) explored the influence of reversible sorption on *iF* estimates, for the pulsed release of three species into an indoor environment that is occupied for various time horizons after the release. According to the model parameters chosen in that work, the ultimate *iF* for a nonsorbing contaminant would be 6.25×10^{-3}. When the effect of sorption is incorporated, *iF* estimates reduce to 0.38, 0.33, and 0.10 of the baseline value for acrolein, ethylbenzene, and *o*-cresol, for 1-h exposure periods. In 24 hours, intake fractions increase to 0.95, 0.94, and 0.24, respectively, of the baseline values for the three contaminants. These numbers are based on sorption parameters from previous research, and a model implemented with the aid of numerical integration. Klepeis and Nazaroff (2006a) also account for the reversible sorption of nicotine, in a model that also accounts for spatial heterogeneity of indoor concentrations and occupant movement. For simulations based on activity patterns from the National Human Activity Pattern Survey (NHAPS), the geometric mean *iF* was found to be 0.26 $\times 10^{-3}$ for a clean-wall scenario. The predicted GM *iF* increased to 1.2×10^{-3} for the case where the wall was preloaded with nicotine (as would occur with repeated indoor smoking over months to years).

Occupant-related factors constitute the second category of elements influencing *iF*. They include presence or absence in the house, and activities such as cooking, resting, or sleeping that influence the breathing rate and location within the house (the latter being significant if concentrations are spatially variable). Occupant-related factors are at once a pivotal element for *iF* – as exposure depends on the presence of people – and the most difficult to characterize

owing to the non-deterministic nature of human behavior, and the complexity of intra- and inter-individual differences. Hence, the influence of human factors is less-well studied than the influence of pollutant- and building-related elements. For example, no indoor *iF* studies were identified in the peer-reviewed literature that incorporate activity-specific inhalation rates as inputs. The presence or absence of occupants indoors during part or all of a peak associated with an episodic source has also not been previously addressed. Intake fraction assessments that incorporate, to varying degrees, information on fractional time spent at home, variable breathing rates, and/or location and activities within the home are discussed below.

Nazaroff (2008) presents deterministic expressions for intake fractions associated with partial occupancy that are applicable for steady emission rates with a well-defined start and stop time. Klepeis and Nazaroff (2006a) incorporate detailed information from the NHAPS on the daily duration and sequence of time spent by Americans in locations that include the rooms of their home; results from their simulations are discussed below. NHAPS lacks, however, details on the configuration of individual homes, and on the timing and location of indoor smoking events. Ilacqua et al. (2007) include separate inhalation rates for "rest" and "light" activity. Values for the fraction of time spent in each state are based on time-activity data from the EXPOLIS dataset, but are applied independently of other parameters such as ventilation rate and the schedule of emissions. This independence assumption is problematic because occupant activity patterns typically have distinct diurnal patterns (e.g. sleeping at night, leaving the home during the day, cooking in the morning and evening). The ventilation rate and the schedule of emissions are also likely to vary diurnally, either owing to variations in meteorological conditions, or because both may be strongly linked to human activities such as the manipulation of air handling systems, or the use of appliances.

Building-related factors that influence intake fractions include volumetric ventilation rate and interzonal mixing. The use of the well-mixed assumption may be appropriate in cases where the release is not immediately proximate to an exposed individual and the characteristic time for mixing (τ_{mix}) is shorter than the time for removal (τ_{decay}) via ventilation and other processes. On the other hand, when τ_{mix} is similar to or larger than τ_{decay}, spatial variation must be understood and addressed. Approaches to characterize spatial variation in pollutant levels and removal rates indoors include computational fluid dynamics (CFD) and multizone transport models (Chen, 2009). A semi-empirical technique involves multiplying the expression for *iF* in equation 3.1 by a 'mixing factor,' derived as a ratio of time-averaged concentration in the breathing zone of the exposed individual to the time-averaged concentration in the ventilation exhaust air. If the ventilation rate and breathing rate are correlated with pollutant concentrations, the *iF* expression is altered so NQ_b and Va are each included within integrals of concentrations in the breathing zone and exhaust air, respectively (Nazaroff, 2008). Applications of these techniques and consequences for *iF* are discussed below.

Lai et al. (2000) use the multizone indoor air quality model MIAQ4 to assess individual intake fractions for exposure to a conserved species in a six-zone, single-floor residence with a steady ventilation rate and steady interzonal air flows, with variations in the location of the source and state of internal doors and external windows. Under these conditions, the *iF* is heterogeneous across the six zones and varies in the range $(0.5\text{-}40) \times 10^{-3}$ for the configurations considered. Hellweg et al. (2009) assess intake fractions for use in life cycle impact assessments, and suggest values of the mixing factor ranging from 1 to 10. Russo and Khalifa (2010) use a CFD model to explore the effects on *iF* of body temperature, proximity, and personal ventilation systems (relative to conventional mixing and displacement systems) in an office room. Body

temperature was found to have a negligible effect on *iF*. Emissions from all sources were determined to be poorly mixed prior to inhalation. The occupant-associated thermal plume had the effect of enhancing exposure to pollutants emitted from the floor and from the body and protecting against exposure to pollutants emitted from the wall and desk. Under the conditions modeled, personal ventilation systems were effective at reducing *iF*. The size of the reduction ranged from 59% for a wall-emitted pollutant to 83% for a desk-emitted pollutant.

The multizone exposure model employed to assess nonsmoker ETS intake fractions by Klepeis and Nazaroff (2006a, b) considers the interplay between the multicompartment nature of homes, intermittent emissions, the dynamic nature of pollutants, and the movement of human beings. A standard house configuration (with windows always closed), volume, and air exchange rate were chosen as inputs in the model. Building-configuration parameters such as the state (open or closed) of interior doors, interior airflow pattern, and operation of the central air handling system were varied among simulations. The movement of occupants was also varied, either according to scripts or according to nationally representative data from NHAPS. Finally, three classes of ETS pollutants were chosen to assess the influence of variations in pollutant dynamics. A correction factor *f* was quantified for each simulation. This parameter, *f*, is analogous to the mixing factor but also incorporates differences owing to not only the single-zone model relative to a multizone model, but also due to occupant presence/absence and movements within the house. Results showed that *f* for particles ranged from 0.1 to 1.3 for scripted scenarios. The geometric mean *f* (GM_f) ranged from 0.4 to 0.8 for NHAPS scenarios. Results indicated that the lowest exposure ($iF = 0.23 \times 10^{-3}$) was experienced by a nonsmoking occupant who systematically avoided the smoking occupant. The highest *iF* was an order of magnitude greater, 2.6×10^{-3}, and corresponded to a nonsmoker who consistently occupied the same room as the smoker.

To date, there has been no reported indoor *iF* assessment that is purely empirical, that is, where emissions and intake are measured simultaneously using direct methods under normal field conditions. It is possible to imagine such an empirical study in theory. It could be achieved via time-resolved monitoring of breathing rates and personal exposure concentrations, and time-resolved or integrated measurements of emissions, in the field. However, in practice we lack instrumentation for continuous, passive monitoring of breathing rates and we rely on models to assess emissions from sources under normal operating conditions in the field.

Excluding mainstream cigarette smoke, intake fraction estimates for indoor sources in homes reviewed in this section span more than two orders of magnitude, from 0.2×10^{-3} for small particles with a high indoor deposition efficiency, under high ventilation, well-mixed conditions, to 40×10^{-3} for a conserved species in a multizone model, with the source and receptor in the same room. The high and low estimates are both presented by Lai et al. (2000). To be included in this review an "indoor source" had to meet the criterion of emitting pollutants directly into an occupied indoor space. Hence, for example, a fireplace venting to the outdoors or VOCs infiltrating into the house from the crawl space were excluded. The range in *iF* estimates, though broad, supports the *Rule of 1000* concept as – irrespective of the approach, assumptions, and input parameters employed – intake fractions for indoor sources are orders of magnitude greater than those commonly obtained for outdoor releases (Humbert et al., 2009). The range in *iF* estimates indicates that for some exposure scenarios, intake may be mitigated via means that aim to reduce *iF*, rather than or in addition to aiming to reduce emissions from sources.

3.1.4. Study objectives

This investigation explores factors that influence the relationship between emissions of ultrafine particles from indoor sources and intake during a field study in seven California homes. In Chapter 2 indoor sources were characterized, and the role of indoor and outdoor sources and the infiltration factor in influencing particle number concentrations and exposures in homes was explored, with the aid of a material-balance model. The present work builds on that analysis. The objective of this research is to present a distribution of empirical intake fraction estimates, both individual and aggregate, for the population of episodic and continuous indoor sources identified during the field investigation. Episodic indoor emissions are linked with sporadic human activities that result in UFP emissions. For this source type, intake fractions are assessed on a per-peak basis, and average values per source type are summarized. Continuous UFP emissions are linked to the presence of unvented pilot lights (associated with some older, gas-fired cooking ranges), and lead to an elevated indoor particle baseline. The intake fraction for this source is considered on a per-house, per-occupant basis, for the full duration of the monitoring period, at the two sites where such a source was observed to be active. The dependence of *iF* on building factors (ventilation), human factors (occupancy, asleep/awake state, breathing rate), and pollutant dynamics (particle removal or loss, timing of emissions) is explored for the range of sources and exposure scenarios observed in the field study.

This is one of very few intake fraction analyses focused on ultrafine particles (Zhang et al., 2010; Zhou and Levy, 2008) and also the first semi-empirical intake fraction investigation for indoor sources to rely on experimental data resolved at the level of individual occupants and source-events.

3.2. Methods

3.2.1. Evaluating intake fractions

The present investigation builds on the data acquired and analysis reported in Chapter 2. Indoor UFP concentrations attributable to identified indoor sources, source-specific particle first-order loss-rate coefficients, and episode start- and end- times assessed and presented in Chapter 2 serve as inputs in the analysis described below. Occupant exposures reported in Chapter 2 were reanalyzed by using sensor data (when available) instead of recall to assess exposure durations.

Individual *iF* values are defined as the attributable fraction of particles emitted from a source that are inhaled by a single occupant. Aggregate intake fractions are computed by summing individual intake fractions over all exposed occupants. This approach for assessing aggregate *iF* values assumes that a negligible number of particles emitted from indoor sources are inhaled by people other than household occupants. This assumption is reasonable owing to the rapid dilution of air as it is removed from a building. Though it is possible to imagine circumstances when, for instance, an open window carries a direct particle plume into the breathing zone of someone outside and nearby, on a cumulative basis, the exposure associated with such an occurrence is likely to be small relative to the exposure of in-house occupants. Further, *iF* estimates do not incorporate the influence of unrecorded, short entries and exits (such as may occur to take out the garbage or pick up the mail), or the presence of transient occupants such as guests.

The influence on *iF* estimates of variables of interest was explored by comparing group means. The nonparametric Kruskall-Wallis rank sums test (or *K*-test) was used to test the null hypothesis of equal population medians, with the conventional Type-I error rate (α) of 0.05. As the probability distribution of the *K* statistic only approximates the chi-square distribution when the sample size is adequate (at least > 5), the results of comparisons of medians with $N < 5$ are to be treated with caution. In instances when the null hypothesis was rejected, the Tukey-Kramer honestly significant difference (HSD) test was employed to compare all possible pairs of means (and still control for the overall error rate of 0.05).

3.2.2. Episodic sources

During the cumulative observational monitoring periods for all seven houses, there were 59 instances when an indoor source event resulted in a PN peak. Each peak is labeled with a unique code. The first two characters of the code identify the house site at which the peak was observed. The third character of the code is a letter, starting with "a" for the first observed peak at each site. In some cases a peak contained sub-peaks that were then distinguished via a number in the fourth position of the code.

Intake fractions are assessed for 50 of the 59 peaks. In two instances, as shown in Table 3.5, overlapping pairs of peaks (H1f and g, and H6e1 and e2) were merged for the purposes of the *iF* analysis. Seven peaks were excluded for the following reasons: (a) emission estimates were unavailable, because monitoring commenced after the start of the source episode (H0a, H4a, H5e); (b) exposure estimates were unavailable, because emissions occurred in a location in the house that was not treated in our model as being part of the well-mixed exposure zone (H2f2, H4f, H4i); or (c) the first-order loss coefficient was very high (~10 h^{-1}), indicating that the characteristic residence time was too low for the well-mixed assumption to be reasonable (H4c).

For each source event, the attributable number of particles inhaled is determined as the product of the appropriate breathing rate estimate and the attributable particle number concentration ($N_{net}(t)$) integrated over the exposure period. The mass emitted is modeled as the product of the first order loss parameter ($k+a$), house volume (V), and $N_{net}(t)$ integrated over the full duration of the peak (assuming the attributable N_{net} is zero prior to and following the designated episode start and end times). The resulting expression for estimating *iF* is shown in equation (3.2). The integrals in the numerator are evaluated for the awake (*aw*) and asleep (*as*) periods of occupancy that coincide with the episode *i*, for resident *j*, of house site *h*. The integral in the denominator is evaluated over the full event.

$$iF_{h,i,j} = \frac{Q_{b,j,aw}\int_{aw,j} N_{net}(t)dt + Q_{b,j,as}\int_{as,j} N_{net}(t)dt}{V_h(k+a)_i\int_i N_{net}(t)dt} \quad (3.2)$$

The expression in equation (3.2) is simplified by defining a new parameter, *F*, which represents the exposure integral normalized by the emissions integral. The parameter *F* is evaluated separately for *aw* and *as* periods, as shown in equation (3.3).

$$iF_{h,i,j} = \frac{Q_{b,j,aw}F_{j,aw} + Q_{b,j,as}F_{j,as}}{V_h(k+a)_i} \quad (3.3)$$

If an occupant is present and either awake or asleep for the entire duration of a source event, equation (3.3) is simplified as shown in equation (3.4), which is identical to the basic expression in equation (3.1) except for the addition of the loss-rate parameter *k*:

$$iF_{h,i,j} = \frac{Q_{b,j}}{V_h (k+a)_i} \tag{3.4}$$

3.2.3. Continuous sources

Only one continuous source was identified in this study, natural gas pilot lights on the stove at house sites H1 and H3. For this source, the attributable mass inhaled is assessed as the product of the average, steady-state concentration owing to the source, N_{pilot}, multiplied by the appropriate breathing rate estimate and the exposure duration (assessed separately as T_{aw} and T_{as} for awake and asleep periods, respectively). The attributable number emitted is assessed as the product of the average emission rate, E_{pilot}, and the duration of the observational monitoring period, T_{obs}. The resulting expression for evaluating *iF* is shown in equation (3.5):

$$iF_{pilot,h,j} = \frac{Q_{b,j,aw} N_{pilot,h} T_{aw,j} + Q_{b,j,as} N_{pilot,h} T_{as,j}}{E_{pilot,h} T_{obs,h}} \tag{3.5}$$

The parameters E_{pilot} and N_{pilot} are related (based on material-balance principles, and assuming well-mixed conditions and steady values of governing parameters) as shown in equation (3.6) and discussed in Nazaroff et al. (2010):

$$N_{pilot,h} = \frac{E_{pilot,h}}{V_h (k+a)_{pilot,h}} \tag{3.6}$$

Substituting equation (3.6) into equation (3.5), and representing the ratio between the exposure (awake or asleep) duration and observational monitoring duration using a newly defined parameter *P* (which is analogous to *F*, above), the *iF* expression in equation (3.5) can be rewritten so it is independent of *E* and *N*, as shown in equation (3.7):

$$iF_{pilot,h,j} = \frac{Q_{b,j,aw} P_{aw,j} + Q_{b,j,as} P_{as,j}}{V_h (k+a)_{pilot,h}} \tag{3.7}$$

At site H1, separate $k+a$ values were assessed for each of three different building configurations. The analysis in Chapter 2 relies on the separate estimates to assess values of N_{pilot} – and hence exposures – that are specific to building configuration. In the present analysis, to simplify the analysis, a single, representative estimate of $k+a$ is employed for the site.

3.2.4. Input parameters

These input parameters are needed for *iF* evaluations: inhalation rates during awake and asleep states, house volume, first-order particle number loss coefficient, and the parameters *F* and *P* that account for partial occupancy during a source event and during the observational monitoring period, respectively. Methods used to assess values of each parameter are discussed in §3.2.4.1 – §3.2.4.4.

3.2.4.1. Inhalation rate (Q_b)

A person's volumetric inhalation rate, which may also be referred to as an inspiration, ventilation, or breathing rate, is an important parameter for assessing intake fractions because it governs the relationship between concentrations in the breathing zone and inhalation intake. Intake fractions have a direct, positive, linear relationship with inhalation rates. The inhalation rate is a function of the body's oxygen requirement, which in turn depends on the degree of physical exertion, body size, age, and health status. To manage the temporal and between-person variability in these variables, Q_b is commonly estimated for subpopulations defined on the basis of demographic parameters such as age and gender, which serve as proxies for the other influencing variables. Moreover, rather than point estimates, it is common to define distributional parameters for Q_b for each subpopulation (Allan et al., 2008).

To estimate intake fractions for indoor sources, we require estimates of short-term breathing rates as an input. The use of long-term estimates would be inappropriate for the present study because they do not allow us to incorporate information we possess on time spent asleep versus awake, and because they are based on activities individuals habitually conduct in all locations rather than just at home. Moreover, Q_b and episodic source use are both intimately associated with human activities, and thus correlated for the person conducting a source activity. Of the three approaches that have been used previously to generate estimates of breathing rates, only two – the time-activity-ventilation (TAV) approach (Allan et al., 2008) and metabolic energy conversion (MEC) approach (Layton, 1993; USEPA, 2009) – yield short-term, activity-specific estimates. The third approach, based on doubly-labeled-water (DLW) measurements (Brochu et al., 2006a,b; Stifelman, 2007), is considered the most reliable but is exclusively suited to long-term estimates.

The present analysis relies on estimates generated by the MEC approach, which is based on the principle that the amount of oxygen required for the energy expenditure (EE) associated with an activity can be used to estimate air intake. Individual, activity-specific inhalation rates are estimated as the product of EE, oxygen uptake per unit of energy produced (H), and ventilator equivalent (VQ) (Layton, 1993). The EE associated with an activity is estimated as the product of the basal metabolic rate (BMR), and the metabolic equivalent value (MET) assigned to the activity. The MET, in turn, is a dimensionless ratio of the activity's assigned metabolic rate to a person's BMR, and ranges from 0.9 for sleep to >6 for high intensity activities such as sports or farming (Layton, 1993; USEPA, 2009). Justifications for our choice of approach, and implications for the results (including a comparison with estimates based on the TAV approach), are discussed in Appendix 3.A.1.

The short-term Q_b estimates used as inputs in the present study are sorted by demographic group and activity class ("asleep" or "awake") as summarized in Table 3.2 (USEPA, 2009). The estimates in Table 3.2 are reasonable when compared with measurements

based on the doubly labeled water (DLW) approach. For example, using the short-term breathing estimates reported in Table 3.2, a female aged 41-51 y who sleeps 8 h/d and is awake and engaged in "light intensity activities" for 16 h/d would have a daily inhalation rate of 13.4 m^3/day. The DLW-based mean inhalation rate estimate for females aged 20 to 60 y is similar, at 13.6 m^3/day (Brochu et al., 2006b).

Table 3.2. Short-term breathing rate estimates based on a metabolic approach, sorted by demographic group and activity level.

Demographic Group	**Asleep (MET = 0.9) Q_b (L/min)**								
	Mean	**Percentiles**							**Max**
		5	**10**	**25**	**50**	**75**	**90**	**95**	
Male Child 3-6 y	4.36	3.06	3.30	3.76	4.29	4.86	5.54	5.92	7.67
Male Child 6-11 y	4.61	3.14	3.39	3.83	4.46	5.21	6.01	6.54	9.94
Female 21-31 y	3.89	2.54	2.74	3.13	3.68	4.44	5.36	6.01	9.58
Female 31-41 y	4.00	2.66	2.86	3.31	3.89	4.54	5.28	5.77	8.10
Female 41-51 y	4.40	3.00	3.23	3.69	4.25	4.95	5.66	6.25	8.97
Female 51-61 y	4.56	3.12	3.30	3.72	4.41	5.19	6.07	6.63	8.96
Male 21-31 y	4.73	3.16	3.35	3.84	4.56	5.42	6.26	6.91	11.2
Male 31-41 y	5.16	3.37	3.62	4.23	5.01	5.84	6.81	7.46	10.9
Male 41-51 y	5.65	3.74	4.09	4.73	5.53	6.47	7.41	7.84	10.8
Male 51-61 y	5.78	3.96	4.20	4.78	5.57	6.54	7.74	8.26	11.8
Demographic Group	**Awake (1.5 < MET ≤ 3.0) Q_b (L/min)**								
	Mean	**Percentiles**							**Max**
		5	**10**	**25**	**50**	**75**	**90**	**95**	
Male Child 3-6 y	11.4	9.20	9.55	10.2	11.1	12.3	13.4	14.0	19.7
Male Child 6-11 y	11.6	8.95	9.33	10.2	11.3	12.8	14.6	15.6	21.8
Female 21-31 y	10.6	7.75	8.24	9.1	10.2	11.7	13.4	14.3	21.5
Female 31-41 y	11.1	8.84	9.30	10.0	10.9	11.9	13.1	13.9	17.4
Female 41-51 y	11.8	9.64	10.0	10.7	11.6	12.7	13.9	14.5	17.7
Female 51-61 y	12.0	9.76	10.2	10.9	11.8	13.0	14.2	14.9	17.9
Male 21-31 y	13.0	9.68	10.2	11.3	12.4	14.0	16.5	17.7	27.2
Male 31-41 y	13.6	10.6	11.1	12.0	13.3	14.8	16.5	18.1	25.5
Male 41-51 y	14.4	11.2	11.8	13.0	14.1	15.6	17.4	18.3	23.0
Male 51-61 y	14.6	11.1	11.6	13.0	14.4	15.9	18.0	19.4	25.5

Source: USEPA, 2009. Values are unadjusted for body weight. "Sleep or nap" (MET = 0.9) estimates used to represent Q_b during sleep. "Light intensity activities" (1.5 < MET ≤ 3.0) estimates chosen to represent "Awake Q_b". This activity level includes activities such as food preparation and clean up, clothes washing, indoor play, talking/reading, childcare, personal hygiene tasks, and passive sitting.

In Table 3.3, the 21 study occupants are classified into demographic groups that match the classifications in Table 3.2. Breathing rates for each were assigned accordingly. Study subjects spanned most of the major demographic groups, with the notable exception that there were no female children, no seniors, and no infants at any of the sampled sites.

Table 3.3. Demographic classification of the 21 study subjects, for purposes of assigning breathing rate estimates.

Demographic group	Occupant ID
M 3-6	H1R4, H2R3, H2R4, H4R3, H4R4
M 6-11	H1R3, H3R3
M 21-31	H6R2
M 31-41	H1R2, H2R2, H3R2, H6R3
M 41-51	H4R2
M 51-61	H0R2
F 21-31	H2R1, H5R1, H6R1
F 31-41	H1R1, H3R1
F 41-51	H4R1
F 51-61	H0R1

3.2.4.2. House volume (V)

The volume of an indoor environment is an important parameter influencing exposure to contaminants released indoors, because a larger volume offers the potential for greater dilution of emitted compounds, and consequently lower exposure. Intake fraction has an inverse relationship with the volume through which pollutants are mixed following their release. The mixed volume is expected to be associated with the physical dimensions of an indoor space, but is influenced by additional parameters such as the volume occupied by furniture or occupants, and internal airflow characteristics. The airflow, in turn, depends on factors such as the state of doors and windows, operation of fans, and temperature and pressure gradients.

In the present analysis each house was treated as one or two well-mixed compartments. At two of the two-storey sites, H2 and H4, the observed concentration profiles indicated that emissions on one storey did not significantly influence concentrations on the other. Therefore, at these sites each storey was treated as an independent, well-mixed zone. The volume of each mixed zone is recorded in Table 3.4, and was assessed in two steps at each site. First, physical dimensions of each room (length, width, height) were measured manually by researchers and used to generate an estimate of the room volume. Second, 9% of the volume was subtracted to account for furniture and large objects, and to thus convert the measured volume into a "ventilated" volume estimate. The volume occupied by furniture and large objects was estimated on the basis of a study conducted in four detached houses located in the San Francisco Bay area (Hodgson et al., 2004). In that study, careful measurements were made of the room envelope and of large objects (including furniture), to assess the difference between the physical and the ventilated volume. Results from that study showed that on average, per site, the difference between the two measures of volume was 9% (N = 4, range = 8.1-10.2%, standard deviation = 0.9%).

Table 3.4. House volume.

Site	Volume based on linear dimensions (m^3)	Ventilated volume [a] (m^3)
H0	320	291
H1	315	287
H2	53, 250 [b]	48, 228
H3	200	182
H4	199, 186 [b]	181, 169
H5	420 (276, 144) [c]	382 (251, 131)
H6	314	286

[a] Correction factor: 9% subtraction from volume based on linear dimensions.
[b] Volumes of first and second storey, respectively.
[c] For analysis of peak due to ironing, upstairs/downstairs volumes considered separately (up: 144 m^3; down: 276 m^3); otherwise, the whole house was treated as a single well-mixed zone.

3.2.4.3. Particle first-order loss rate (k+a)

The intake fraction is inversely proportional to the first-order loss-rate coefficient, $k+a$. The faster the rate of loss, the less likely a particle is to be inhaled. For episodic sources, event-specific first-order loss-rate coefficients were estimated as the slope of the natural log of $N_{net}(t)$ versus time during the immediate post-emissions period, or as the weighted average of two slopes, assessed for the start and end of the episode. Values of $k+a$ associated with each peak are recorded in Table 3.5. Five of the episodic peaks were not amenable to the extraction of a $k+a$ estimate, either because emissions continued to occur during the decay period (e.g., for cleaning products), or because the peak was too small for quantitative analysis of the decay period (e.g., for wall-heater emissions). In these instances, a nominal loss coefficient (1 h^{-1} for cleaning products used at site H5 and 1.6 h^{-1} for four wall-heater emission peaks at site H2) was chosen to assess the associated intake fraction.

The decay coefficient of particles emitted from pilot lights was assessed, for site H3, as a best-fit coefficient based on the application of a material-balance model to data from a controlled experiment at the site. At site H1 the indoor particle loss rate varied significantly during the observational monitoring period, according to the building configuration, as is summarized in Table 3.5. Therefore a mean decay coefficient for pilot lights at this site was assessed as the harmonic mean of $k+a$ values estimated for each of three distinct building configurations, weighted by the occupant-average exposure duration corresponding to each configuration.

Table 3.5. Summary of $k+a$ estimates used to assess pilot lights iF at site H1.

Site	Configuration	$k+a$ (h^{-1})	Exposed duration (h)			
			R1	R2	R3	R4
H1	All closed	0.34	17	18	17	17
	Central air system on (with filtration)	0.75	31	24	31	31
	Window open	0.35	1.5	2.0	1.5	1.5
	Average [a]	0.51				

[a] Harmonic mean value weighted by occupation-average exposure durations

3.2.4.4. Occupancy and time-activity patterns

The parameters P and F were defined to be indicators of partial exposure to particles emitted indoors from continuous and episodic sources, respectively, owing to incomplete occupancy during the event and its aftermath. They assume values between 0 and 1, with the two extremes representing either zero exposure to the source or presence for the full duration of the influence of the source. As indicated by equations (3.3) and (3.7), P is the ratio between the awake or asleep exposure durations ($T_{aw,i,j}$ or $T_{as,i,j}$), and the observational monitoring duration (T_{obs}). The parameter F can be expressed as the product of two ratios – a duration ratio and a concentration ratio – as shown in equation (3.8b).

$$F_{aw,i,j} = \frac{\int_{aw,j} N_{net}(t)dt}{\int_{i} N_{net}(t)dt} \tag{3.8a}$$

$$F_{aw,i,j} = \frac{(\overline{N_{net}})_{aw,i,j}}{(\overline{N_{net}})_{i}} \times \frac{T_{aw,i,j}}{T_i} \tag{3.8b}$$

The derivation of equation (3.8b) starts with a presentation of F based on its definition as a ratio of two integrals (equation (3.8a)), one assessed for the period during which occupant j is awake that overlaps with the duration of episode i, and the other assessed over the full duration of the episode. Note that the subscript aw in equation (3.8b) can be replaced with as to assess F during the time spent asleep, so the equation (and this discussion) applies equally to awake and asleep periods. The transformation from equation (3.8a) to (3.8b) relies on the substitution of the integral of N_{net} with the average N_{net} during the integration period multiplied by the duration of integration. The "concentration ratio" in the final expression is the average PN concentration attributable to event i, while occupant j is awake or asleep, divided by the average attributable PN concentration for the entire episode.

3.3. Results and discussion

3.3.1. Episodic sources

3.3.1.1. Individual and aggregate intake fractions

Reported in Table 3.6 are individual and aggregate intake fractions for the 50 quantifiable episodic source events recorded over 26 days of observational monitoring at the seven house sites. Aggregate intake fractions span a range of about 20×, from 0.7×10^{-3} to 16×10^{-3}. As demonstrated by the cumulative distribution plot presented in Figure 3.1, aggregate iF values associated with the 50 events conform well to a lognormal distribution with a GM of 3.8×10^{-3} and a GSD of 2.2. The corresponding arithmetic mean ± standard deviation are $(4.9 \pm 3.3) \times 10^{-3}$. As the average number of residents per site is 3 (range 1-4), the average individual iF is ~3× smaller than the average aggregate iF. Exposure during "awake" hours accounts for (on average across all events) 95% of intake. Awake hours dominate intake both because many indoor

sources are tied to activities, which are conducted when occupants are awake, and also because breathing rates are higher when occupants are awake than when they are asleep.

The influence on *iF* of house-specific characteristics, source-type, and human factors is discussed in §3.3.1.3 - §3.3.1.5.

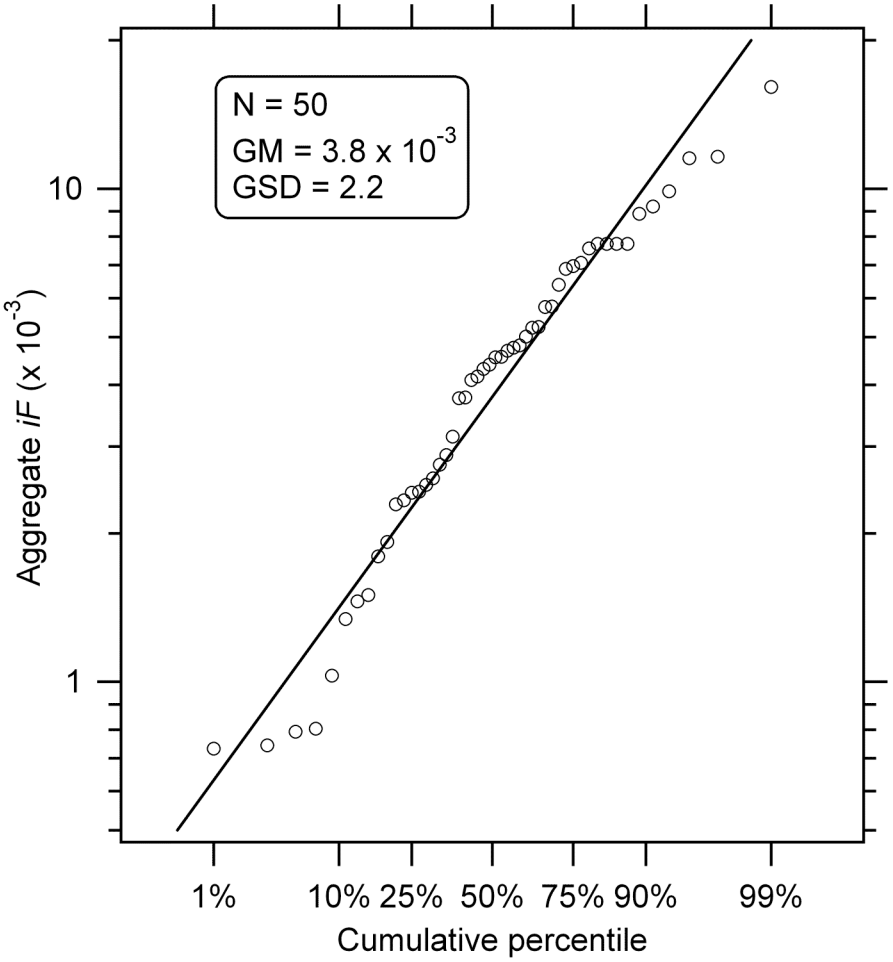

Figure 3.1. Cumulative probability distribution of *iF* estimates for 50 episodic indoor source events observed during 26 days of observational monitoring over an ensemble of seven house sites. The straight line represents a lognormal distribution with the parameter values (GM = 3.8 $\times 10^{-3}$, GSD = 2.2) computed from the data and reported in the box.

Table 3.6. Individual and aggregate intake fractions for the 50 quantifiable episodic source events observed over 26 days of monitoring at the seven house sites. [a, b]

				Intake fraction ($\times 10^{-3}$)						
	Peak ID	**Source**	**Details**	**R1**	**R2**	**R3**	**R4**	**All**	**RSD** [c]	***k+a*** **(h^{-1})**
1	H0b	Electric range	Boil water	4.8	n/a			4.8	0.10	0.51
2	H0c	Electric range	Cook rice, stir fry veg.	1.9	n/a			1.9	0.10	1.3
3	H0d	Electric range & natural gas furnace	First-use of furnace; boil water	1.5	n/a			1.5	0.10	1.7
4	H0e	Electric range & toaster	Boil potatoes	2.7	1.4			4.1	0.14	0.93
5	H0f	Natural gas furnace	Second-use of furnace	2.1	2.5			4.6	0.13	1.2
6	H0g	Electric range toaster	Boil water	1.4	3.0			4.3	0.13	1.0
7	H0h	Natural gas furnace	Third-use of furnace	n/a	1.5			1.5	0.11	2.0
8	H0i	Electric range	Cook ramen noodles	n/a	2.4			2.4	0.12	1.1
9	H0j	Electric range & toaster	Pasta, exhaust fan on	n/a	3.1			3.1	0.11	0.96
10	H1a	Gas oven	Melt wax	1.6	0.0	1.6	1.6	4.8	0.09	1.5
11	H1b	Gas stove	Boil water	1.4	0.27	0.60	0.57	2.9	0.11	1.6
12	H1c	Gas stove & toaster oven	Boil water, cook pasta	0.60	0.78	0.53	0.51	2.4	0.10	3.6
13	H1d	Gas stove	Stir-fry	3.1	2.5	3.1	3.0	12	0.10	0.76
14	H1e	Gas stove & toaster oven	Boil water	1.3	2.2	1.2	1.1	5.8	0.10	1.3
15	H1fg	Gas stove and oven, candles		1.4	1.2	1.4	1.3	5.2	0.10	1.7
16	H2a	Gas stove	Frying egg	0.23	1.6	1.3	1.3	4.4	0.11	2.3
17	H2b	Heater, wall unit		1.7	2.2	1.9	1.9	7.7	0.22	1.6
18	H2c	Heater, wall unit		1.7	2.2	1.9	1.9	7.7	0.22	1.6
19	H2d	Heater, wall unit		1.7	2.2	1.9	1.9	7.7	0.22	1.6
20	H2e	Heater, wall unit		1.5	2.0	1.7	1.7	6.9	0.10	1.8
21	H2f	Heater, wall unit		3.8	4.9	3.7	3.7	16	0.10	0.67
22	H2g	Heater, wall unit		1.1	2.2	1.9	1.2	6.4	0.15	1.6
23	H2h	Heater, wall unit		1.7	2.2	1.9	1.9	7.7	0.22	1.6
24	H2i	Gas stove	Cooking carrots	0.67	1.3	1.1	0.73	3.8	0.16	3.0,1.1
25	H3a	Gas stove	Meat and noodles	2.2	2.7	2.2		7.1	0.11	1.7
26	H3b	Gas stove		1.8	1.4	1.5		4.7	0.11	2.2,1.9
27	H3c	Gas stove		0.016	2.3	0.017		2.3	0.16	2.0
28	H3d	Gas stove	Onions, meat, and noodles	2.1	2.6	2.2		7.0	0.11	1.7
29	H3e	Gas stove		1.6	1.4	1.1		4.2	0.12	2.0,1.9
30	H4b	Toaster oven		2.2	2.7	2.1	2.1	9.2	0.10	1.8
31	H4d	Gas stove	Burned tortilla	2.4	2.9	2.3	2.3	9.9	0.10	1.6

32	H4e	Gas stove & and toaster oven	Boil water	2.2	1.1	2.1	2.1	7.6	0.16	1.7
33	H4g	Gas stove	Boil water	2.1	2.6	2.1	2.1	8.9	0.10	1.8
34	H4h	Gas stove	Boil water	1.1	1.3	1.1	1.1	4.5	0.10	3.6
35	H4j	Toaster oven		2.8	3.4	2.7	2.7	12	0.10	1.3
36	H5a	Gas stove		1.0				1.0	0.17	1.6
37	H5b	Iron		0.74				0.74		
38	H5c	Gas stove & cleaning products		1.3				1.34	0.25	1.0
39	H5d	Iron		0.73				0.73		
40	H5f	Cleaning products & microwave		2.5				2.5	0.17	0.66
41	H6a	Gas stove & rice cooker		0.0	0.0	0.80		0.80	0.11	3.6
42	H6b	Gas stove	Frying	1.5	1.8	1.9		5.2	0.11	1.5
43	H6c	Candle		0.39	1.4	0.52		2.3	0.11	1.9
44	H6d	Gas stove	Frying	1.7	1.7	2.4		5.8	0.11	1.2
45	H6e	Gas stove and toaster oven	Boil water	0.42	1.1	1.1		2.6	0.11	2.8,1.9
46	H6f	Gas stove	Frying	1.2	1.5	1.0		3.8	0.16	1.6
47	H6g	Gas stove	Boil water	1.2	1.5	0.0		2.8	0.13	1.8
48	H6h	Toaster oven		0.0	0.67	1.1		1.8	0.13	1.7
49	H6i	Stove	Frying, boil water	0.0	0.077	0.71		0.79	0.76	1.5
50	H6j	Stove and grill		1.4	1.8	1.9		5.0	0.11	1.5

[a] R1=Adult female, R2=Adult male, R3/R4=Male child (except for H6; at that site, R3=adult male)

[b] For a portion of the observational monitoring period at sites H0 and H3 one or more occupants was away from the home overnight. In those instances, the observational monitoring duration per occupant was assessed as the total monitoring period, minus 24 h per day not slept at home. Occupant absences that clearly fit within 24 h "travel absences" are excluded from consideration in this study. In other words, instead of recording the *iF* corresponding to an event/occupant pair as zero, for an event that occurred during a "travel absence," it is marked as "n/a."

[c] Approximate relative standard deviation of aggregate *iF* estimates.

3.3.1.2. Assessment of uncertainty

The error associated with individual episodic source *iF* estimates is approximated as a function of input parameters. For this purpose, equation (3.3) is simplified to a form wherein the input parameters are uncorrelated. The simplification involves lumping "awake" and "asleep" breathing rates into a single category (which is assigned an error equal to the error of the "awake" breathing rate). This step allows P_{aw}+P_{as} and F_{aw}+F_{as} to be considered as single terms. This lumping was deemed reasonable because it simplifies the error analysis and makes it more transparent, while having a minimal impact on the outcome. Errors associated with the two ironing-related peaks at site H5 were not quantified, as the procedure to assess *iF* for those peaks differed from our standard protocol.

Relying on the simplified function and Gaussian error propagation, the error (or approximate standard deviation) associated with intake fraction estimates for each peak *i* and occupant *j* is calculated using the quadratic rule for products and ratios as:

$$\varepsilon_{IF,i,j} = \sqrt{\varepsilon_{Qb,aw,j}^2 + \varepsilon_V^2 + \varepsilon_{k+a,i}^2 + \varepsilon_{F,aw+as,i,j}^2} \qquad (3.9)$$

The variable ε in equation (3.9) is the relative error, or the approximate relative standard deviation, associated with the input parameter identified by the subscript. The relative errors associated with aggregate *iF* estimates were assessed using a similar approach, i.e. by invoking the simplifying assumptions noted and propagating errors in input parameters. Procedures used to assess approximate values of ε for the four input parameters are discussed in Appendix 3.A.2.

Approximate relative standard deviations for 48 of the 50 aggregate episodic-source *iF* estimates are summarized in Table 3.6. The estimated error exceeded 25% for only one source event: peak H6i. Relative errors associated with individual *iF* estimates exceeded 25% (ranging from 45% to 350%) for one or more residents for six peaks: H2g, H2i, H3c, H4e, H6f and H6i. The highest fractional errors were associated with occupants who were present for a small fraction of a peak. In these cases, uncertainty about the occupant entry or exit time had the potential to change the exposure (and hence the *iF*) by up to a factor of 4. If the six less-robust assessments (and two ironing episodes) are excluded, the arithmetic mean, standard deviation, geometric mean, GSD, and range of *iF* estimates are not markedly changed. The moderate errors indicate that within the constraints of model assumptions, the results are reasonably robust.

The quantitative error analysis described in equation (3.9) does not incorporate approximation errors that arise from use of a model and subjective judgment involved in decisions such as identifying a peak start and end time, or whether a peak should be characterized via a single or multiple decay coefficients. Some of the approximations employed in this analysis are that (i) the house is modeled as a single, well-mixed compartment; (ii) model input parameters are treated as temporally invariant; and (iii) indirect exposure assessment techniques are used to model personal exposures.

The assumption of well-mixed conditions, applied in the present study to assess exposures and emissions, causes the true variability in individual and aggregate *iF* values to be underestimated. The degree of underestimation is likely to be much greater for individual estimates, as individual differences will, to some extent, average out in estimates of aggregate *iF*.

On an individual basis, there are likely to be patterns of under- or over-estimation of *iF* across similar events, owing to intentional behaviors and preferences. The degree to which the variability is underestimated depends on two factors: the spatial variability in concentrations in the house, and the occurrence of extremes of proximity between the source and exposed individuals. The spatial variability would be increased by the following conditions: interior doors are closed, especially when the isolated zone has enhanced ventilation or filtration; the central ventilation system and ceiling fans are off; the house is evenly heated, so thermal and pressure gradients are minimized and the rate of airflow between rooms is low; emitted particles have a high loss rate. In contrast, spatial variability is decreased by thermal energy releases within the house, as these would enhance mixing by means of natural convection. Such releases were associated with a large proportion of indoor source use episodes. Examples of extremes of proximity between the source and receptor are: an individual is behind a closed door, or in a high-ventilated zone distant from the emissions; the activity associated with emissions systematically brings a person close to a source, as occurs during cooking, cleaning, or ironing (in these instances, the effect of the exposure error may be magnified by an accompanying error in the breathing rate, which is likely underestimated for a person engaged in active tasks).

A review of the literature indicates that the effect of spatial variation on exposure can be substantial and, in a study of secondhand tobacco smoke (SHS) exposure, the unadjusted single-zone model generally overestimated the multi-zone nonsmoker exposure to particles (Klepeis and Nazaroff, 2006a). The range in *f* is expected to be greater for UFP than for fine particle mass (the indicator used to measure SHS), as UFP are more dynamic. A decision-tree presented by Hellweg et al. (2009) also suggests conditions under which the well-mixed model may be inadequate: the emission is into a space larger than a single, small room (<100 m^3), effective mechanical ventilation and thermal mixing are absent, and people are exposed in the near-field and are not highly mobile.

Whereas for exposures the error associated with a single-zone well-mixed model is related to spatial variability and the location and mobility of humans, for emissions (when they are assessed as described in this paper) the error depends on spatial variability and the location of instruments relative to sources. Since instruments remain stationary and are deliberately located in a zone that was deemed, for typical sources, to be most representative of average conditions in the house, the error in the emissions estimate is likely to be relatively small. Exceptions are when sources were unusually proximate or distant from measurement devices, which would imply reported emissions were over- or under-estimates, respectively. Such instances were uncommon during the present study.

3.3.1.3. House-specific characteristics

House-specific factors expected to influence *iF* values are the volume, which dilutes emitted particles and reduces their probability of being inhaled, and features that influence particle removal, such as the air exchange rate, filtration, and components of the particle deposition velocity that are site dependent, such as the surface area to volume ratio. Source-specific factors, and human factors such as the number of residents and their activity patterns and breathing rates, may also contribute to the difference in *iF* values across sites if these factors influence *iF* and differ systematically across sites.

Figure 3.2 presents aggregate *iF* estimates, sorted by house site, for the seven houses. Table 3.7 presents mean intake fractions per house site, for the seven monitored sites, H0-H6.

The number of estimates per site ranges from 5 (H3 and H5) to 10 (H6). The box-and-whisker plots in the figure depict the median, interquartile range, and 10th and 90th percentile estimates per site. Median aggregate *iF* values per site span roughly an order of magnitude, ranging from 1.0×10^{-3} at H5, to 9.1×10^{-3} at H4. The population medians are statistically unequal ($p < 0.0001$) showing that on average the house site had a significant influence on *iF*. A comparison of pairs of means showed that the means for H2 and H4 are significantly higher than the means for H0, H5, and H6.

The variability in aggregate *iF* estimates, as indicated by the relative standard deviation (RSD), is high and similar amongst homes and between episodes within a home (between-house RSD = 0.5; within-house RSD = 0.3-0.6). The between-house RSD was assessed as the standard deviation of per-site arithmetic mean (AM) *iF* values divided by the mean obtained by linearly averaging the seven per-site AMs. The within-house RSD was assessed as the standard deviation of per-episode *iF* values per house, divided by the mean *iF* per house site.

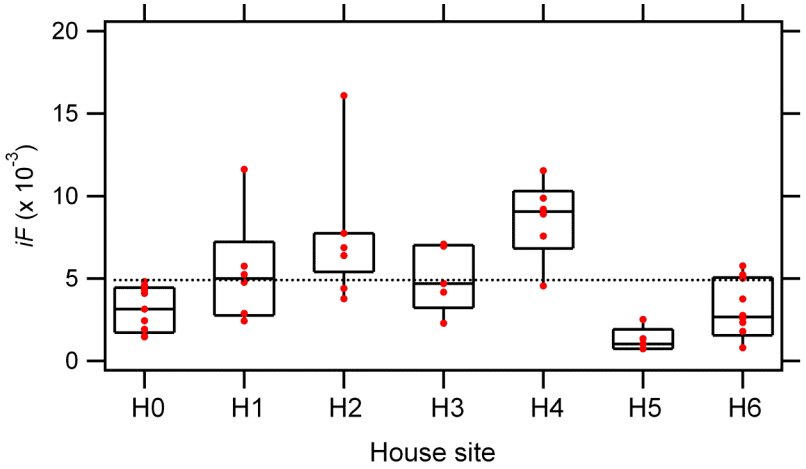

Figure 3.2. Aggregate *iF* estimates sorted by house site. Each marker represents the aggregate *iF* associated with a single event, and there are 5-10 quantified events per house site. The box-and-whiskers depict the median, interquartile range, and 10th and 90th percentile values per group. The different in medians across sites is statistically significant ($p < 0.0001$).

Table 3.7. Summary statistics (arithmetic means and standard deviations) for aggregate and individual intake fractions assessed for the 50 episodic source events at the seven house sites.

	Aggregate		**Individual**	
House site	***N***	**AM ± SD (× 10^{-3})**	***N***	**AM ± SD (× 10^{-3})**
H0	9	3.1 ± 1.4	12	2.4 ± 1.0
H1	6	5.4 ± 3.3	24	1.4 ± 0.9
H2	9	7.6 ± 3.5	36	1.9 ± 0.9
H3	5	5.0 ± 2.0	15	1.7 ± 0.8
H4	6	8.6 ± 2.4	24	2.2 ± 0.6
H5	5	1.3 ± 0.7	5	1.3 ± 0.7
H6	10	3.1 ± 1.8	30	1.0 ± 0.7

Possible interactions between the influence of source-specific and human factors, and house-type, are discussed in the next two subsections. The potential contribution of variations in volume (V) and air exchange rate (λ) to the difference in iF across sites is assessed by combining volume and air exchange rate into a single independent parameter, $V\lambda$ (which is equivalent to the building ventilation flow rate, Q). Harmonic mean air exchange rates summarized in Table 2.5 are treated as representative values for each site. The value of Q ranges from 52 $m^3 h^{-1}$ at H0 to 315 $m^3 h^{-1}$ at H6. A linear regression analysis of the mean per-site aggregate iF versus Q (Figure 3.3a) shows that there is no systematic association between the estimated ventilation flow rate and iF ($r^2 = 0.03$). Part of the reason for the lack of correlation may be that the air-exchange rate has significant temporal variation. The effect of the volume, which is invariant with time, is also assessed via a linear regression analysis (Figure 3.3b). Results show a strong inverse relationship between the house volume and average aggregate iF per site.

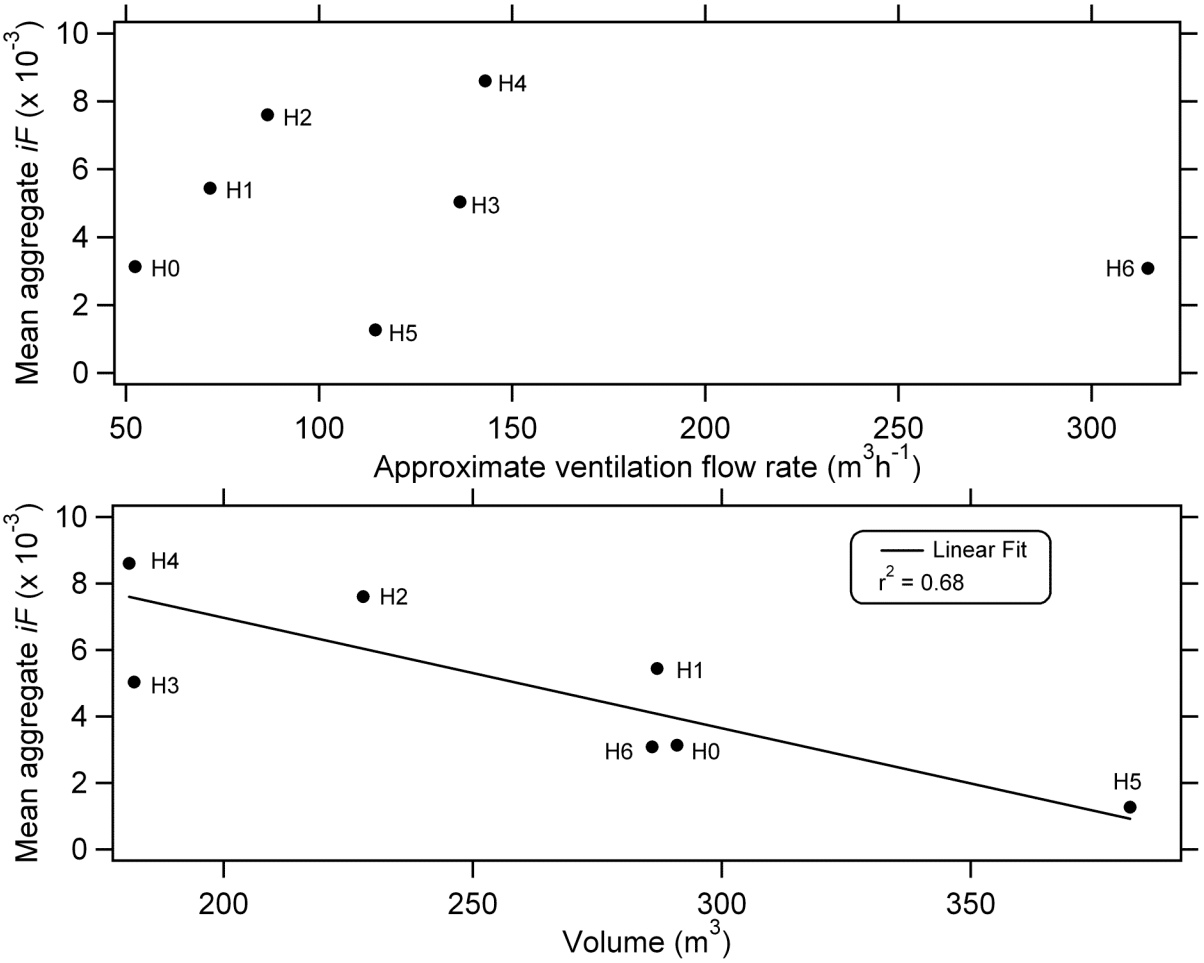

Figure 3.3. Average iF estimates sorted by house site. In Fig 3.3a (upper panel), the house is identified by its approximate ventilation flow rate, Q (volume × air exchange rate). In Fig 3.3b (lower panel), the house is identified by its estimated volume. Each marker represents the mean aggregate iF per house site.

3.3.1.4. Influence of source type

Source-specific factors that influence intake fraction may be direct or indirect. A potential direct influencing factor is the loss rate (k) owing to processes other than ventilation, of particles emitted from the source. For ultrafine particles, k is dominated by deposition (on fixed surfaces or on other particles), and the rate of deposition is related to particle size. Therefore, sources that emit smaller ultrafine particles are expected to be associated with lower iF values than sources emitting at the larger end of the ultrafine size range.

An indirect association of iF with source type may also occur when source groups are correlated with building configurations, activity patterns, or meteorological conditions, which in turn influence iF. For example, if clothes are habitually ironed during the afternoon when most occupants are away and windows are open, ironing may be associated with systematically lower iF values than sources habitually used when most occupants are present, or when the house configuration favors a lower air-exchange rate.

Table 3.8 presents a summary of mean individual and aggregate intake fractions for the 36 peak events that were associated with identifiable single activities. The population means shown in Table 3.8 span approximately an order of magnitude from 0.7×10^{-3} for a steam iron ($N = 2$) to 8.6×10^{-3} for emissions from a wall furnace ($N = 7$). Figure 3.4 presents the 36 aggregate iF estimates for single events, sorted by source-type. The seven medians depicted in Figure 3.4 are statistically unequal ($p = 0.01$). However, the validity of this finding is blunted by the inadequate sample size for most source categories ($N < 5$ for five of the seven sources). Moreover, the type of source is strongly correlated with house site. For instance, an iron was used only at site H5 and all seven instances of use of the wall furnace are associated with site H2. When the effects of house-site and source-type on iF are considered simultaneously, source-type is no longer a significant variable influencing iF (whereas house-site remains so).

These results show that for the peak events in our sample, source-type did not exert a direct influence on iF. In other words, particle loss rates did not vary systematically by source-type. An indirect association between source-type and iF is evident in our data, and appears to be associated with house-specific and human factors such as the house volume, and number of residents per house and their activity patterns in relation to individual sources. For example, the low iF associated with ironing is linked to the large volume and low occupancy at H5, as well as to the tendency of the H5 occupant to iron in the morning and leave for work soon after. However, comments on underlying reasons for the indirect effect are tentative owing to the small sample sizes (<5) associated with five of the seven source categories. In contrast to the lack of association between source-type and iF reported in this chapter, Zhang et al. (2010) found systematically higher iF for ultrafine particles emitted from gas stoves compared to UFP from electric stoves when both were operated at medium temperatures. The difference was effaced at high temperatures.

Table 3.8. Aggregate and individual intake fractions for quantifiable peak events at the seven houses associated with identified single activities. [a]

	Aggregate *iF* ($\times 10^{-3}$)		Individual *iF* ($\times 10^{-3}$)	
Emission source	***N***	**AM ± SD**	***N***	**AM ± SD**
Gas stove	17	5.3 ± 2.8	64	1.5 ± 0.8
Furnace, central air	2	3.0	3	2.0 ± 0.5
Candle	1	2.3	3	0.78 ± 0.6
Toaster oven	3	7.5 ± 5.1	11	2.0 ± 1.0
Electric stove	4	2.5 ± 1.6	4	2.5 ± 1.6
Furnace, wall	7	8.6 ± 3.3	28	2.2 ± 0.9
Steam iron	2	0.73	2	0.73

[a] Standard deviations are only noted for $N > 2$.

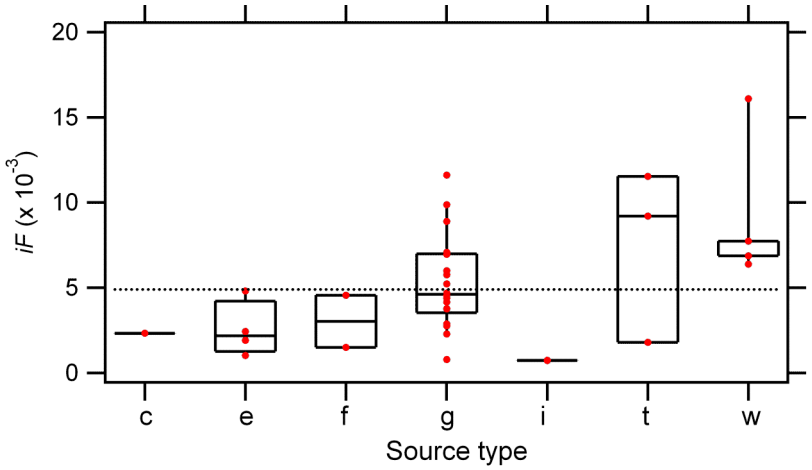

Figure 3.4. Aggregate *iF* estimates sorted by source type, where c = candle, e = electric stove, f = central-furnace, g = gas stove, i = iron, t = toaster oven, and w = wall-furnace. Each marker represents the aggregate *iF* associated with a single event, and there are 1-17 quantified events per source type. The box-and-whiskers depict the median, interquartile range, and 10th and 90th percentile values per group. Population sizes vary widely, with $N < 5$ for most groups, which complicates the use of statistical methods to compare population medians.

3.3.1.5. Human factors

Human factors that influence *iF* include the number of occupants, their breathing rates and time-activity patterns. Individual intake is reduced when an occupant is asleep, owing to a reduced breathing rate, and is zero when an occupant is absent. Trends in breathing rates presented in Table 3.2 also predict that, on average, intake is greater for males compared with females, and increases with age (up to 60 y) within gender groups (USEPA, 2009). Human factors (excluding the number of residents) were the cause of variations in individual *iF* values between residents of a house. An indicator of the variation is the ratio of the minimum individual *iF* to the maximum individual *iF* for an episode. This ratio ranged from 0 to 0.84

across the 45 episodes at homes with more than one resident. The low value of the mean ratio (0.55) indicates that human factors have a significant influence on individual intake fractions.

The influence of human factors on aggregate *iF* was assessed indirectly, by comparing our "measured" aggregate *iF* estimates with a hypothetical set of *iF* estimates. The hypothetical *iF* values assume that all household occupants are present and awake for the full duration of each source event, and breathe at the same rate, 14 L/min, which is at the high end of breathing rate estimates used as an input in our sample, applicable to an adult male, 31-51 y, engaged in light intensity activities). With these assumptions, the expression for the aggregate *iF* per event simplifies to: 14 L/min × number of residents ÷ house volume ÷ $k+a$ associated with the source event. The discrepancy between hypothetical and measured *iF* is an indicator of the influence in the present study of demographic differences and varying occupancy patterns – which are collectively referred to as "human factors" in the discussion below.

Measured and hypothetical *iF* estimates were compared via a single parameter, least-squares best fit linear regression, as presented in Figure 3.5. Each symbol on the plot represents an indoor peak episode ($N = 48$). The two ironing events are excluded from this comparison because equation (3.3) is not applicable to them. On average, measured *iF* values are 30% lower than hypothetical *iF* values (range: 4% greater to 90% lower). This result implies that the combined influence of partial occupancy and reduced breathing rates (relative to the 14 L/min benchmark) owing to demographic differences and reduced activity during sleep is to reduce intake fractions to roughly two-thirds of the value obtained without taking these factors into account. It is hard to predict, on the basis of data from this field study, whether the well-mixed assumption biases the average result. That is, if we had personal monitoring data to assess exposure, whether we would find the difference between the measured and hypothetical *iF* was on average systematically greater than or less than the 30% estimated here.

This study allows a preliminary assessment of the influence of demographic differences on intake fraction. Our sample included three demographic groups: adult females, adult males, and male children (3-11 y old). Three behavior trends that have the potential to influence indoor intake fractions and may have demographic associations, are the amount of time spent at home, fraction of time spent at home asleep, and time spent engaged in activities that emit particles. On average, individuals in the three groups ($N = 7$ per group) spent the same amount of time at home (16.8 h/d – 17.2 h/d). Adult males and females spent, on average, a similar amount of time at home asleep (8.0 h/d – 8.2 h/d). However, children spent a greater portion of their at-home time asleep (average = 10 h/d). The time spent asleep by adults versus children is similar to the average parameters of a large California survey (adults: $N = 1579$, AM = 8.0 h/d; children: $N = 1200$, AM = 10.5 h/d) (Wiley et al., 1991). The third factor cannot be evaluated because the amount of time each individual spent on activities that emit particles was not recorded.

On average, there were not large differences in *iF* based on age and gender. But sleeping more than the adults caused *iF* values for children to be reduced for 11 of the 26 source events at homes with children. The percent reduction in *iF* owing to sleep varied widely, from 0.5% for one case (an 11 y old for peak H3d) to 62% for another case (a 5 y old for peak H1b). On average, the percent reduction was moderate (16%). However, the true reduction in intake owing to sleep is likely to be greater than indicated by these figures, as all are based on exposures assessed with a monitor placed in the main living area. As all 11 peaks were associated with sources located in the kitchen (cooking), living room (heater) or dining room (candles), the sources are closer to the monitoring instruments than they are to the children in the bedroom. Hence, while the percent reductions in intake due to sleep reported here are associated

with the reduced breathing rate during sleep, the true reduction is likely also dependent on the association between being asleep and being located away from sources.

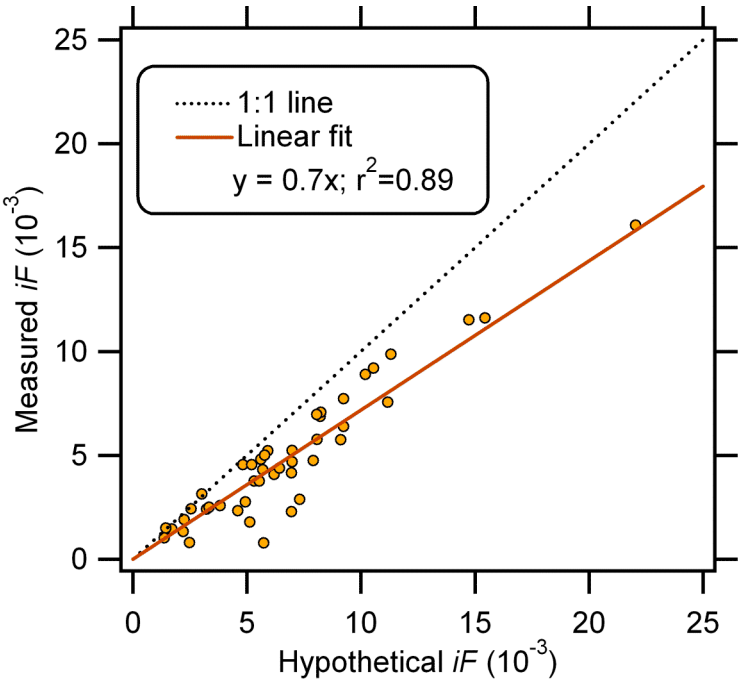

Figure 3.5. Each plotted symbol represents an indoor peak episode. Hypothetical *iF* = (number of household occupants) × (Q_b = 14 L/min) ÷ (house volume) ÷ (*k*+*a* associated with episode). The ~30% reduction, on average, in measured versus hypothetical *iF* owes to partial occupancy, and reduced breathing rates relative to 14 L/min owing to demographic factors or altered activity patterns (i.e., sleep).

3.3.2. Continuous sources

Reported in Table 3.9 are intake fraction estimates associated with the use of a continuous emissions source, unvented pilot lights, at houses H1 and H3. The aggregate *iF* for this source at H1 is 9.0×10^{-3}. Individual *iF* values at that site span a narrow range, from 2.1×10^{-3} to 2.4×10^{-3}. Inter-individual differences are dominated by differences in the fraction of time spent asleep: the two children spent the most time asleep, and the adult male spent the smallest fraction of time asleep. At H3, the aggregate *iF* is 3.7×10^{-3}, and the range of individual *iF* values is 1.0×10^{-3} (for the adult female) to 1.6×10^{-3} (for the adult male). At H3 the range in individual *iF* values is somewhat wider than at H1, owing to a greater disparity between occupants in the amount of time spent at home. This difference occurred because the adult female's routine included leaving the house during business hours, while the adult male and the child remained at home.

Table 3.9. Individual and aggregate intake fractions for UFP emissions from unvented natural gas pilot lights (associated with the range and oven) at sites H1 and H3.

Site ID	Mean $k+a$ (h^{-1})	Obs dur. (h)	Fraction awake				Fraction asleep				Intake fraction (10^{-3})				
			R1	R2	R3	R4	R1	R2	R3	R4	R1	R2	R3	R4	All
H1	0.51	67	0.38	0.30	0.25	0.25	0.36	0.35	0.49	0.49	2.3	2.4	2.1	2.1	9.0
H3	1.89	77, 53 [a]	0.42	0.55	0.38		0.29	0.32	0.38		1.0	1.6	1.1		3.7

[a] Observational monitoring duration is computed as the total monitoring period, minus 24 h per day not slept at home. Therefore the observational monitoring duration for occupants R1 and R3 is 24 h shorter (53 h) than the duration for occupant R2 (77 h).

A factor accounting for the difference in continuous-source *iF* values between H1 and H3 is the first-order particle loss rate, $k+a$. There is an approximately 4× difference in $k+a$ estimates for pilot lights obtained for the two sites. This difference is influenced by the difference in ventilation conditions between the two houses. As summarized in Table 2.5, the harmonic mean AER at H3 (0.75 h^{-1}) is 3× the harmonic mean AER assessed for H1 (0.25 h^{-1}).

At both H1 and H3, "awake" exposures contributed more to aggregate *iF* values than did "asleep" exposures, by 54% and 79%, respectively. At H1 occupants were awake for a smaller fraction of time than they were asleep; so awake exposures dominated only because the greater time spent asleep was trumped by the higher "awake" breathing rates. At H3 occupants were awake for a larger fraction of their at-home hours than they were asleep, so the effect of the time spent awake was compounded by the higher "awake" breathing rates.

As was the case for episodic sources, use of the well-mixed model is anticipated to dampen inter-individual differences in continuous-source *iF* estimates. However, the effect is likely less pronounced for continuous-source *iF* values compared to episodic-source intake fractions, because differences owing to spatial patterns of occupancy will be averaged out over the period of days. For continuous source *iF* estimates, the main source of model-related error is expected to be associated with the use of a single, time-invariant $k+a$ estimate to characterize the occupied component of the full observational monitoring period. An indication of the potential influence of the temporal variability in $k+a$ is obtained by looking at estimates of the air exchange rate obtained under varying conditions at each site. At H1, estimates range from 0.20 to 0.34 h^{-1}; both estimates were obtained from periods when the bathroom window was open. At H3, estimates range from 0.45 h^{-1} (all doors and windows closed) to 2.2 h^{-1} (conditions unknown).

3.4. Conclusions

Aggregate intake fractions estimated for a continuous indoor emission source – unvented pilot lights associated with the range and oven – were similar to aggregate intake fractions for episodic source events. However, the inter-individual variability in *iF* values spanned a greater range for the episodic source events (RSD: 0.08-2) than for continuous indoor emissions (RSD: 0.08-0.3). This outcome makes sense because it is common for occupancy patterns to differ more among residents on the short time-scale associated with episodic source peaks; the

differences are dampened when they are averaged over a time scale of days, which – being the monitoring period – is the relevant period for continuous emissions in this study. Exposures during "awake" hours dominated intake fractions both for episodic and for continuous sources, but they did so more strongly for episodic sources because episodic sources occurred more commonly when occupants were awake than asleep.

A comparison of episodic *iF* values across events, sites, and demographic groups showed that the house site had a significant influence on *iF*, with higher values associated with sites with a greater number of residents and a smaller volume. In Chapter 2, we saw that the type of source has a significant effect on emissions of and exposures to ultrafine particles. However, source-type was not demonstrated to have an independent effect of substance on *iF*. Human factors – occupancy and sleep patterns, and age/gender plus awake/asleep specific breathing rates – led to substantial inter-individual differences in *iF* for episodic sources, and for continuous source exposures at site H3 (but not at site H1). Assuming that all occupants are present and awake during the period under the influence of indoor source emissions can lead to a significant over-estimation in determining aggregate *iF* values.

Comparing the results presented in Chapters 2 and 3 shows that distinct (though overlapping) sets of factors influence concentrations of UFP in microenvironments, exposures to UFP in microenvironments, and intake fractions associated with those exposures. Residential pollutant intakes estimated in this study are typically higher than would be predicted by the product of the average residential concentration × average residential breathing rate, owing to spatial and temporal correlations between indoor concentrations, occupant density, and breathing rate. This result has been demonstrated earlier for intake of motor vehicle emissions (e.g. Marshall et al., 2003).

Our findings are consistent with limited prior research, which shows intake fractions for indoor releases are on the order of one in a thousand. The range in aggregate *iF* obtained in this study – (0.7-16) × 10^{-3} – falls within the range of estimates for indoor *iF* for particles presented in the peer-reviewed literature (as summarized in Table 3.1). The highest individual *iF* estimate associated with cooking obtained in this study (4.8 × 10^{-3}) compares well with the maximum individual *iF* for ultrafine particles emitted from cooking activities (2.3 × 10^{-3}) reported by Zhang et al. (2010). However, as the present study uses empirical data on occupancy and age/gender differentiated breathing rate estimates to assess *iF*, the range of individual *iF* estimates associated with cooking presented in this study is wider than the range reported by Zhang et al. (2010).

In theory, as modeled by Lai et al. (2000), particles at the smaller end of the ultrafine particle size range have a higher deposition velocity compared to accumulation mode particles, and should be associated with correspondingly lower *iF* values. However, the *iF* estimates in this study do not differ systematically from prior estimates for particles measured on a mass basis (the majority of which consider $PM_{2.5}$, which is typically dominated by the accumulation mode). As our particle metric (total number count) did not focus on the lower end of the ultrafine particle size range (i.e. d_p < 20-30 nm) and includes particles with a range of deposition velocities, perhaps it is not surprising that a distinct "ultrafine" signal did not dominate over the influence of other factors such as house volume and occupancy patterns.

This study used microenvironmental monitoring and time-activity data to model emissions and exposures. As a next step, it would be valuable to collect independent data on exposures and emissions – i.e., to assess exposures using the direct method and to evaluate

emissions as was done in the present study. That approach would have the effect of capturing the full variability in exposures amongst occupants of a house.

3.5. References

Allan M, Richardson GM, Jones-Otazo H, 2008. Probability density functions describing 24-hour inhalation rates for use in human health risk assessments: an update and comparison. *Human and Ecological Risk Assessment* **14**, 372-391.

Bennett DH, McKone TE, Evans JS, Nazaroff WW, Margni MD, Jolliet O, Smith, KR, 2002. Defining intake fraction. *Environmental Science and Technology* **36**, 206A-211A.

Brochu P, Ducré-Robitaille JF, Brodeur J, 2006a. Physiological daily inhalation rates for free-living individuals aged 1 month to 96 years, using data from doubly labeled water measurements: a proposal for air quality criteria, standard calculations and health risk assessment. *Human and Ecological Risk Assessment* **12**, 675-701.

Brochu P, Ducré-Robitaille JF, Brodeur J, 2006b. Physiological daily inhalation rates for free-living individuals aged 2.6 months to 96 years based on doubly labeled water measurements: comparison with time-activity-ventilation and metabolic energy conversion estimates. *Human and Ecological Risk Assessment* **12**, 736-761.

Chen QY, 2009. Ventilation performance prediction for buildings: a method overview and recent applications. *Building and Environment* **44**, 848-858.

Chiang TA, Wu PF, Wang LF, Lee H, Lee CH, Ko YC, 1997. Mutagenicity and polycyclic aromatic hydrocarbon content of fumes from heated cooking oils produced in Taiwan. *Mutation Research/Fundamental and Molecular Mechanisms of Mutagenesis* **381**, 157-161.

Dockery DW, Spengler JD, 1967. Indoor-outdoor relationships of respirable sulfates and particles. *Atmospheric Environment* **15**, 335-343.

Donaldson K, Stone V, 2003. Current hypotheses on the mechanisms of toxicity of ultrafine particles. *Ann 1st Super Sanità* **39**, 405-410.

Evans JS, Wolff SK, Phonboon K, Levy JI, Smith KR, 2002. Exposure efficiency: an idea whose time has come? *Chemosphere* **49**, 1075-1091.

Garza KM, Soto KF, Murr LE, 2008. Cytotoxicity and reactive oxygen species generation from aggregated carbon and carbonaceous nanoparticulate materials. *International Journal of Nanomedicine* **3**, 83-94.

Hellweg S, Demou E, Bruzzi R, Meijer A, Rosenbaum RK, Huijbregts MAJ, McKone TE, 2009. Integrating human indoor air pollutant exposure within life cycle impact assessment. *Environmental Science and Technology* **43**, 1670-1679.

Hodgson AT, Ming KY, Singer BC, 2004. Quantifying object and material surface areas in residences. Report LBNL-56786, Lawrence Berkeley National Laboratory, Berkeley, CA.

Humbert S, Manneh R, Shaked S, Wannaz C, Horvath A, Deschenes L, Jolliet O, Margni M, 2009. Assessing regional intake fractions in North America. *Science of the Total Environment* **407**, 4812-4820.

Ilacqua V, Hänninen O, Kuenzli N, Jantunen MF, 2007. Intake fraction distributions for indoor VOC sources in five European cities. *Indoor Air* **17**, 372-383.

Klepeis NE, Nazaroff WW, 2006a. Modeling residential exposure to secondhand tobacco smoke. *Atmospheric Environment* **40**, 4393-4407.

Klepeis NE, Nazaroff WW, 2006b. Mitigating residential exposure to secondhand tobacco smoke. *Atmospheric Environment* **40**, 4408-4422.

Ko YC, Lee CH, Chen MJ, Huang CC, Chang WY, Lin HJ, Wang HZ, Chang PY. Risk factors for primary lung cancer among non-smoking women in Taiwan. *International Journal of Epidemiology* **26**, 24-31.

Lai ACK, Thatcher TL, Nazaroff WW, 2000. Inhalation transfer factors for air pollution health risk assessment. *Journal of the Air and Waste Management Association* **50**, 1688-1699.

Layton DW, 1993. Metabolically consistent breathing rates for use in dose assessments. *Health Physics* **64**, 23-36.

Marshall JD, Riley WJ, McKone TE, Nazaroff WW, 2003. Intake fraction of primary pollutants: motor vehicle emissions in the South Coast Air Basin. *Atmospheric Environment* **37**, 3455-3468.

Meijer A, Huijbregts MAJ, Reijnders L, 2005. Human health damages due to indoor sources of organic compounds and radioactivity in life cycle impact assessment of dwellings. *International Journal of Life Cycle Assessment* **10**, 309-316.

Nazaroff WW, 2004. Indoor particle dynamics. *Indoor Air* **14 (Suppl. 7)**, 175-183.

Nazaroff WW, 2008. Inhalation intake fraction of pollutants from episodic indoor emissions. *Building and Environment* **43**, 269-277.

Nazaroff WW, Bhangar S, Mullen NA, Hering SV, Kreisberg NM, 2010. Ultrafine particle concentrations in schoolroom and homes, Final Report, Contract No. 05-305, California Air Resources Board, Sacramento, CA. Available at http://www.arb.ca.gov/research/apr/past/indoor.htm.

Neas LM, Dockery DW, Ware JH, Spengler JD, Speizer FE, Ferris BG, 1991. Association of indoor nitrogen dioxide with respiratory symptoms and pulmonary function in children. *American Journal of Epidemiology* **134**, 204-219.

Nel A, Xia T, Mädler L, Li N, 2006. Toxic potential of materials at the nanolevel. *Science* **311**, 622-627.

Russo JS, Khalifa HE, 2010. CFD assessment of intake fraction in the indoor environment. *Building and Environment* **45**, 1968-1975.

See SW, Balasubramanian R, 2008. Chemical characteristics of fine particles emitted from different gas cooking methods. *Atmospheric Environment* **42**, 8852-8862.

Smith KR, 1993. Fuel combustion, air pollution exposure, and health: the situation in developing countries. *Annual Review of Energy and the Environment* **18**, 529-566.

Stifelman M, 2007. Using doubly-labeled water measurements of human energy expenditure to estimate inhalation rates. *Science of the Total Environment* **373**, 585-590.

USEPA, 2009. Metabolically derived human ventilation rates: a revised approach based on upon oxygen consumption rates. National Center for Environmental Assessment, US Environmental Protection Agency, Washington, DC, EPA/600/R-06/129F.

Wallace L, 1989. Major sources of benzene exposure. *Environmental Health Perspectives* **82**, 165-169.

Wiley JA, Robinson JP, Cheng YT, Piazza T, Stork L, Pladsen K, 1991. Study of children's activity patterns, Final Report, Contract No. A733-149, California Air Resources Board, Sacramento, CA.

Zhang QF, Gangupomu RH, Ramirez D, Zhu YF, 2010. Measurement of ultrafine particles and other air pollutants emitted by cooking activities. *International Journal of Environmental Research and Public Health* **7**, 1744-1759.

Zhou Y, Levy JI, 2008. The impact of urban street canyons on population exposure to traffic-related primary pollutants. *Atmospheric Environment* **42**, 3087-3098.

3.A. Appendix

3.A.1. Comparing two sources of data for short-term inhalation rates

3.A.1.1. Results and discussion

The inhalation rate estimates used in the present study are presented in Table 3.2. For comparison, estimates based on direct measurement techniques (Allan et al., 2008) are presented in Table 3.A.1. The two sets of estimates are not directly comparable because of imperfect overlap in age bins and, for the "awake" state, the metabolic activity (MET) classification bins. Instead, the breathing rates that would be assigned to each occupant using each method, are compared. Direct measurement estimates exceed metabolic estimates for all occupants except toddlers (7 months – 4 y). The difference is most pronounced for "asleep" estimates, which are greater by 68% to 113%. "Awake" estimates are greater by 4% to 30%. For the three toddlers in the study, the direct estimates are 3 – 35% lower than the metabolic estimates.

Since the "asleep" estimates vary more strongly between the two methods than do the "awake" estimates, the continuous-source *iF* results – which, on average, have a higher relative contribution from "asleep" periods than do the episodic *iF* – are more sensitive to the choice of breathing rate estimates. A sensitivity analysis shows that if the Q_b estimates in Table 3.A.1 were used in the present study instead of the estimates in Table 3.2, the mean episodic source aggregate *iF* would increase by only 8%. The relative standard deviation would decrease slightly, from 0.67 to 0.63. Decreased variability is explained by the reduction in the number of age bins per gender category. The continuous source aggregate *iF* increases more substantially, by 37% for H1, and 27% for H3.

The relative merits and drawbacks of the methods underlying each set of estimates is briefly discussed below. This discussion provides context and justification for the choice of the USEPA (2009) data as inputs in the present study. In the direct (or TAV) approach, the flow of air through a face mask is monitored as subjects perform a variety of staged activities over a defined period of time. The main advantage of the minute-ventilation data presented by Allan et al. (2008) are that they are based on direct experimental measurements and so do not require assumptions about the energy expenditure associated with activities or about population distributions of parameters used to convert EE to an inhalation rate (such as the BMR). There are, however, several disadvantages from the perspective of our research goals: (1) Data for adults are lumped in to a single category rather than being age-specific, causing some loss in resolution. (2) The interpolation scheme chosen to fill gaps in the dataset requires assumptions about EE to assign MET values to activities, thus negating one of the advantages of this method. (3) In the present study we are interested in at-home activities which generally encompass MET values of 0.9 to 5. However, the interpolation equation used by the authors was generated with activities spanning MET values from 1-17 thus excluding the lower end of our range of interest and being subject to undue influence from the high-end estimates. (4) The treatment of uncertainty is unsophisticated relative to the technique used by USEPA (2009) to assess metabolic Q_b, with a uniform coefficient of variation (COV) selected for all means (Allan et al., 2008; Allan and Richardson, 1998).

An attractive feature of the USEPA (2009) metabolic approach is its reliance on activity patterns compiled in the NHANES (1999-2002) dataset, which is designed to be nationally representative, to generate inhalation rate distributions for a range of exertion levels and age and

gender groups. The USEPA (2009) estimates extend down to MET=0.9 and are individually specified for each decade of adulthood. They rely on an updated method to assess the ventilator equivalent (VQ), that takes account of the variability of this parameter across demographic groups. The main limitation is that the BMR data used may not be representative of non-Caucasians (Allan et al., 2008). The USEPA (2009) approach was validated via a comparison with estimates based on the DLW method, which has a rated error of ±5% (Brochu et al., 2006).

Table 3.A.1. Short-term breathing rate estimates based on direct-measurement techniques, sorted by demographic group.

Demographic group	**Q_b for MET=0.9 (L/min)**	**Awake Q_b (L/min)**
Male Toddlers (7 mo-4 y)	4.2 ± 1.5	7.5 ± 2.6
Male Children (5-11 y)	7.7 ± 2.7	13 ± 4.4
Female Adults (20-59 y)	8.28 ± 2.9	13 ± 4.6
Male Adults (20-59 y)	9.5 ± 3.3	15 ± 5.3

Source: Allan et al., 2008. Q_b estimates for "asleep" state calculated via empirical equations with a MET input of 0.9. Activity Level 3 estimates chosen to represent "Awake Q_b". This level is defined as "light activity dominated by moderate movements or periods of rest interspersed with greater activity and with METs typically in the 2-4 range". Standard deviations estimated as mean × coefficient of variation (COV). The 90th percentile of COV values obtained from the literature (0.35) was chosen for all age and gender groups. All estimates were noted as being lognormally distributed.

3.A.1.2. References

Allan M, Richardson GM, 1998. Probability density functions describing 24-hour inhalation rates for use in human health risk assessments. *Human and Ecological Risk Assessment* **4**, 379-408.

Allan M, Richardson GM, Jones-Otazo H, 2008. Probability density functions describing 24-hour inhalation rates for use in human health risk assessments: An update and comparison. *Human and Ecological Risk Assessment* **14**, 372-391.

Brochu P, Ducré-Robitaille JF, Brodeur J, 2006. Physiological daily inhalation rates for free-living individuals aged 2.6 months to 96 years based on doubly labeled water measurements: Comparison with time-activity-ventilation and metabolic energy conversion estimates. *Human and Ecological Risk Assessment* **12**, 736-761.

USEPA, 2009. Metabolically derived human ventilation rates: a revised approach based on upon oxygen consumption rates. National Center for Environmental Assessment, US Environmental Protection Agency, Washington, DC, EPA/600/R-06/129F.

3.A.2. Errors in input parameters

3.A.2.1. Inhalation rate

The primary reference (USEPA, 2009) denoted the spread in short-term Q_b estimates by presenting a range of percentile values for each mean. A lognormal distribution provided a reasonable fit to the percentiles shown, for each gender/age group. Hence, the standard deviation (SD) for each group was assessed as the SD of the normal distribution that best fit the log-transformed data in that group. The relative standard deviation (RSD) was assessed as the SD/mean of log-transformed data. For "awake" distributions the RSD ranged from 0.13 to 0.19 (mean RSD = 0.15), so $\varepsilon_{Qb,aw}$ was estimated as 0.15. The RSD for "asleep" distributions was lower (0.06).

3.A.2.2. Volume

The standard deviation of volume estimates used in the present investigation is not precisely known. It depends on both the error in measurements of physical dimensions and on variability in the volume occupied by large objects across sites. The latter is likely more variable than indicated by Hodgson et al. (2004), owing to the heterogeneity in the dimensions and types of homes included in the present sample; hence, it is likely to dominate the overall error. Therefore, the error in house volume measurements was approximated as being equal to the mean fractional volume of large objects measured by Hodgson et al. (2004), 0.09 (or, equivalently, ± 5%), so ε_V is approximated as 0.05.

3.A.2.3. Particle first-order loss rate

The error associated with first-order loss rates was approximated by considering the goodness-of-fit of the models (i.e. linear regression slopes) used to estimate the rates. The relative standard deviations of slopes/rates assessed for peaks linked with a single $k+a$ estimate range from 0.008 to 0.1. Most of the RSD values (all but one) lie below 0.05, so the error is approximated as ± 5% ($\varepsilon_{k+a} \sim 0.05$). The following exceptions apply. When a nominal loss coefficient was used to assess the iF, the nominal $k+a$ was deemed highly uncertain and was assigned an error of ± 20%, or $\varepsilon_{k+a} \sim 0.20$.

3.A.2.4. Time-activity patterns

The parameter F was defined as the product of duration and concentration ratios, where the numerators are exposure duration or average exposure concentration, and denominators are peak duration or average peak concentration. The denominators refer to well-defined quantities, so the error in F depends on errors in the exposure duration and mean exposure concentration. For both parameters, the underlying source of uncertainty is recall error, as exposure was modeled using occupant questionnaires. To assess the scale of the error, we require an indicator of the reliability of recall. The indicator chosen is the difference between reported and true entry or exit times, denoted as δ_t. A representative value of 7 min was chosen for δ_t, on the basis of 67

observed differences between self-reported entry or exit times and data from sensors on when an external house door was opened.

The influence of recall error was deemed to be negligible when sensor data were available to precisely define a time of entry or exit. When sensor data were not available to define an entry or exit the error in F was approximated as $2\delta_t$ and the relative error in F was characterized as $2\delta_t$ divided by the exposure duration, denoted T. The basis for this approximation is that δ_t/T is, by definition, the expected value of the relative error in the exposure duration owing to imperfect recall. As the exposure concentration error is difficult to precisely characterize (owing to its dependence on the shape of the peak in the zone influenced by an entry or exit), and because it is nonlinearly and nondeterministically but positively correlated with recall error, δ_t/T was multiplied by a factor of 2 to account for the influence of exposure concentration error.

3.A.2.5. Reference

Hodgson AT, Ming KY, Singer BC, 2004. Quantifying object and material surface areas in residences. Report LBNL-56786, Lawrence Berkeley National Laboratory, Berkeley, CA.

Chapter 4: Ozone levels in passenger cabins of commercial aircraft on North American and transoceanic routes

Reproduced in part with permission from Bhangar S, Cowlin SC, Singer BC, Sextro RG, Nazaroff WW, 2008, Ozone levels in passenger cabins of commercial aircraft on North American and transoceanic routes, *Environmental Science & Technology*, 42, 3938-3943.

4.1. Introduction

Passengers in aircraft cabins may be exposed to elevated ozone that originates naturally in the stratosphere, where it is formed and removed as per the Chapman cycle, which is driven by ultraviolet radiation from the sun. Stratospheric ozone is also removed via reactions with trace gases such as nitrous oxide and chlorofluorocarbons. In-cabin ozone depends on ambient levels, the presence or absence of an ozone control device, the rate of outdoor air supply, and the rate of ozone loss through within-cabin transformation processes, such as reactions with interior surfaces. Ozone levels outside the aircraft depend on flight altitude, tropopause height, and on meteorological processes that affect vertical mixing between the lower stratosphere and the upper troposphere. Exposure to ozone in cabin air has potential health significance for the flight crew and for the general flying population, which includes individuals who may be sensitive to respiratory health effects, such as infants and adults with cardiopulmonary conditions. Although an average person flies infrequently, the cumulative exposure to the population via this pathway is on the rise, as the passengers per year has quadrupled since the 1970s.

Ozone and its volatile reaction byproducts are associated with adverse respiratory and cardiovascular effects (Levy et al., 2001; Bell et al., 2006; Weschler, 2006; Jerrett et al., 2009). Semivolatile byproducts formed via reactions between ozone and human skin lipids may remain on the surface and serve as skin irritants (Wisthaler and Weschler, 2010). Acute effects from short-term inhalation exposure range from breathing discomfort, respiratory irritation, and headache for healthy adults (Strøm-Tejsen et al., 2008) to asthma-exacerbation and premature mortality for vulnerable populations (Gent et al., 2003; Bell et al., 2004). Chronic exposure effects may include enhanced oxidative stress (Chen et al., 2007), reduced lung function in young adults (Tager et al., 2005), and adult-onset asthma in males (McDonnell et al., 1999). Physical activity, as is undertaken by flight attendants, results in increased intake. There is no established threshold or "safe" level of exposure (Bell et al., 2006).

Real-time measurements made during flights in the 1960s and 1970s revealed that in-cabin ozone was commonly above 100 parts per billion by volume (ppbv), especially on flight routes through high latitudes (Brabets et al., 1967; Bischof, 1973; Perkins et al., 1979). In 1980, in response to these data and to associated health concerns for flight attendants (Reed et al., 1980), the Federal Aviation Administration (FAA) established standards (FAR 25.832 and FAR 121.578) designed to limit levels of ozone in airplane cabins (NRC, 2002). To comply with the regulations, many planes are equipped with "converters" that promote the decomposition of ozone in the ventilation supply air. Alternatively, airlines may comply by means of flight-route planning to reduce the probability of encountering elevated ozone. Not all planes are equipped

with converters and the probabilistic planning approach permits, by design, up to 16% of the flights to exceed the concentration standard. The ozone level in aircraft cabins is neither routinely monitored, nor has it been the subject of many research papers since the ozone standards were established. Spengler et al. (2004) present a survey of flight-integrated ozone levels on 106 segments. The presence or absence of an ozone converter was not confirmed. To our knowledge, real-time in-cabin ozone data have been published for just four flights since 1980 (MacGregor et al., 2008).

To address this data gap, we monitored ozone levels in the passenger cabins of 76 commercial flight segments between February 2006 and August 2007. Time-resolved (1-min) measurements were made using a portable UV-photometric monitor on many flights across the United States and on several transatlantic and transpacific flights. A range of narrow and wide body aircraft, with or without ozone converters, was sampled. Flight selection was substantially opportunistic, with some flights intentionally chosen to augment seasons or flight routes not otherwise well represented. Real-time sampling was undertaken to capture temporal trends within single flights, and because short-term elevated levels, which may be significant for public health, would be masked by flight-averaged sampling. The airlines operating the flights on which we sampled reported to us whether or not the plane was equipped with an ozone-control device. We estimated by direct observation the fractional occupancy of the cabin by passengers. Occupancy is of interest because chamber studies and studies in a simulated cabin and a simulated office (Wisthaler et al., 2005; Tamás et al., 2006; Weschler et al., 2007; Coleman et al., 2008; Wisthaler and Weschler, 2010) indicate that human skin oils constitute a significant sink for ozone (Nazaroff and Weschler, 2010). Our study objective was to assess in-cabin ozone, and factors that influence it, on northern hemisphere commercial passenger flights originating from or terminating in the United States, in all seasons.

4.2. Methods

4.2.1. In-flight sampling

Monitored flight segments were on participating airlines that, cumulatively, commanded more than 30% of the 2006 market share of US domestic air travel greater than approximately 4 hours in length (Bureau of Transportation Statistics, 2007). Permission to sample was secured in advance from the airlines, from the Federal Aviation Administration, and from the Transportation Safety Administration. Segments shorter than 3.5 h were excluded. Our sample was designed to include a range of routes and to be distributed across all seasons of the year. For a large majority of flights, airline personnel were notified of our intent to monitor at least one week in advance. They informed the captain and flight crew. For each monitored flight, a researcher with a purchased travel ticket carried on-board a portable ozone monitor (2B Technologies, Model 202). The monitor was packaged inside a hard-sided case that fit under the seat in front of the researcher. A sampling tube from the monitor was affixed to the seat back in front of the researcher to sample air in proximity to the researcher's breathing zone. In advance of the sampling campaign, the monitor underwent electromagnetic interference testing and was approved for use above a flight altitude of 10,000 ft. It required a 20-min warm-up period. Consequently, ozone data were collected from ~30 min after take-off until ~15 min before landing. For each segment, the researcher recorded the row number, the flight date, departure and arrival airports, departure and landing time, aircraft type, and the visually estimated

occupancy of the cabin. Whether that aircraft was equipped with an ozone control device was determined by consultation with airline personnel after monitoring.

4.2.2. Sampling method

The 2B Technologies Model 202 ozone analyzer is a single-beam photometer that works on the basis of absorption of 254-nm light by ozone (Bognar and Birks, 1996). A zero concentration reference sample is taken with each measurement and forms the basis for calculating an ozone concentration. Pressure and temperature sensors in the absorption cell record data required to compute mixing ratios. A 1-m coil of nafion tubing upstream of the ozone scrubber guards against adverse humidity effects (Wilson and Birks, 2006), and a filter protects the light cell from particle contamination. The analyzer samples air at the rate of 1.0 L/min and computes the ozone level every 4 s. The units used in this study were configured to retain data in the form of 1-min averages. The monitor has a detection range of 1.5 parts per billion by volume (ppbv) to 100 ppmv and, according to the manufacturer, is accurate to the greater of 1.5 ppbv or 2%.

Data were successfully acquired for 76 flight segments. On an additional ten segments, attempted monitoring was unsuccessful. A few samples were lost owing to instrument malfunction or accidental misuse. During early flight segments, instrument malfunction was related to problems with the display, solenoid valve, external charger, or data storage card. These issues were resolved by design changes to reduce uncontrolled static electricity and by replacing components. Other failures resulted from accidental toggling of the power switch, a sampling tube becoming dislodged from the pump during an airport security check, and failures related to datalogging. Minor instrument modifications and amended protocols for use prevented these issues from recurring.

On 11 of the monitored flights, supplementary, side by side ozone data were acquired with the active monitor and Ogawa passive ozone samplers. The goal of this effort was to make opportunistic use of the active monitoring field campaign to calibrate the Ogawa sampler for the air-cabin environment. The Ogawa monitor calibration study is described in Appendix 4.A.1.

4.2.3. Quality assurance

Prior to and in parallel with the in-flight sampling effort, the two units used in the study (designated 2B-1 and 2B-2) were tested under controlled conditions. Overall, the instruments performed satisfactorily. In October 2005, unit 2B-2 was tested in the simulated aircraft cabin facility at the Technical University of Denmark (DTU) against a recently calibrated ozone monitor (Dasibi, 1003-AH). Measurements made by the two instruments were closely correlated. In May 2007, an ozone analyzer was tested for pressure compensation at Lawrence Berkeley National Laboratory (LBNL). The tested unit was not one used for in-flight monitoring but shared the same make and model number and therefore served as a proxy. During this test, ozone was maintained at ~70 ppbv, while the pressure was reduced from 1 atm to 0.7 atm, and then increased back to 1 atm. The measurements showed no correlation with changes in pressure and were consistently within 10% of transfer standard readings. On two instances during our in-flight monitoring, units 2B-1 and 2B-2 were carried on board the same flight for duplicate measurements. On one flight, 4 h of data were collected, ozone levels were in the range 0-100

ppbv, and the correlation coefficient for a linear relationship between the two instruments was high, $r^2 = 0.98$. On a second flight, ozone levels averaged less than 5 ppbv, too close to the detection limit to allow for a meaningful comparison of response. Finally, on six occasions distributed through the duration of the study, the monitors were calibrated at six levels covering the range from 0 to 250 ppbv using a recently calibrated ozone analyzer (API, Model 1471 or Model 3824) as a transfer standard. Measurements from units 2B-1 and 2B-2 displayed a strong linear correlation ($r^2>0.9$) with transfer-standard readings. The 2B Tech units were consistently less sensitive to ozone: a linear regression analysis of 2B-1 and 2B-2 readings versus API readings resulted, for both monitors, in a mean slope of 0.9 ± 0.02 (mean ± standard error). Since this slope was consistent with that observed between 2B-2 readings and transfer standard readings in the DTU experiments, data collected in the field were adjusted by dividing all recorded values by 0.9 to correct for bias.

Occasional "spikes" – defined as an instance when the recorded change in ozone level in one minute exceeded 75 ppbv – were observed in data during July-Sept 2006. These were attributed to stray particle contamination in the light-absorption cell as they did not recur when the monitor's particle filter was reconfigured to be always present in-line. Subsequent spikes greater than 200 ppbv min^{-1} were present at a frequency of about one spike per flight segment on fewer than 30% of the segments monitored using 2B-2. They were absent from 2B-1-monitored flights at all times. Both types of spikes were treated as anomalous and deleted from data records.

4.2.4. Data analysis

Data were processed by computing, for each segment, peak one-hour, and sample-average ozone levels. Data from the 68 domestic flight segments were stratified into two groups based on the presence ($N = 22$) or absence ($N = 46$) of an ozone converter, and intergroup means were compared. Distributions of peak one-hour and sample-average ozone levels and of flight integrated ozone exposures were also determined for these two groups of domestic flights. Data from transoceanic segments ($N = 8$) were analyzed as a separate group. The with-converter segments were stratified into domestic and transoceanic routes and these groups were compared. For the domestic flight segments, the influence of additional variables of interest, including season, latitude, and occupancy, were analyzed by visual inspection and, for variables with clear influence, by means of a general linear regression model. Statistical significance was determined on the basis of the conventional 5% Type I error rate.

4.3. Results and discussion

Table 4.1 presents a summary of monitored flight segments by calendar quarter, organized by route type, the presence or absence of an ozone converter, and aircraft type. About half the samples in our data set were collected on Boeing 757 aircraft without ozone control devices on continental US routes. Eight were on transoceanic (6 transatlantic and 2 transpacific) routes on the 2-aisle Boeing 747, 767, or 777. All transoceanic flights were on aircraft with converters. Monitoring was approximately evenly distributed across the year but was most intensive in the second quarter and least intensive in the third quarter.

Table 4.1. Summary of 76 flight segments monitored.

Domestic without converter (*N* = 46)					
Aircraft type	**Number of aisles**	**Number of flights per quarter**			
		Q1	**Q2**	**Q3**	**Q4**
Boeing 737	1	2	1	1	
Boeing 757	1	9	13	8	8
Boeing 767	2	1		1	2

Domestic with converter (*N* = 22)					
Aircraft type	**Number of aisles**	**Number of flights per quarter**			
		Q1	**Q2**	**Q3**	**Q4**
Airbus 319	1	3	3	2	5
Airbus 320	1		2	1	
Boeing 747	2				1
Boeing 767	2		1		3
Boeing 777	2			1	

Transoceanic with converter (*N* = 8)					
Aircraft type	**Number of aisles**	**Number of flights per quarter**			
		Q1	**Q2**	**Q3**	**Q4**
Boeing 747	2	2	2		
Boeing 767	2				2
Boeing 777	2	2			

Figure 4.1 presents cumulative distributions of peak one-hour and sample average ozone levels obtained from the 68 domestic flight segments. Data from converter and nonconverter flights are plotted separately. The associated percentiles in the distribution are weighted to adjust for uneven sampling across the four quarters of the year. Weighting was done to minimize bias, as data from previous monitoring studies (Brabets et al., 1967; Spengler et al., 2004) show that ozone levels vary markedly through the year. The data conform reasonably to lognormal distributions and the weighted geometric means (GM) and geometric standard deviations (GSD) are presented for each distribution.

Peak-hour ozone levels on domestic flights exhibit an approximately 7× difference in central tendency (GM) between converter and nonconverter groups, and indicate that control devices are effective in limiting cabin ozone levels. The weighted GMs (GSDs, AMs) of peak one-hour ozone levels are 33 ppbv (2.3, 47 ppbv) for nonconverter flights, and 4.5 ppbv (1.4, 4.7 ppbv) for converter flights, respectively. For sample-average levels, the weighted GMs (GSDs, AMs) are 20 ppbv (2.1, 28 ppbv) for nonconverter, and 2.5 ppbv (1.4, 2.6 ppbv) for converter flights, respectively. The presence of an ozone converter is statistically significant in relation to cabin ozone levels for both peak one-hour ozone and sample-average ozone ($p < 0.0001$).

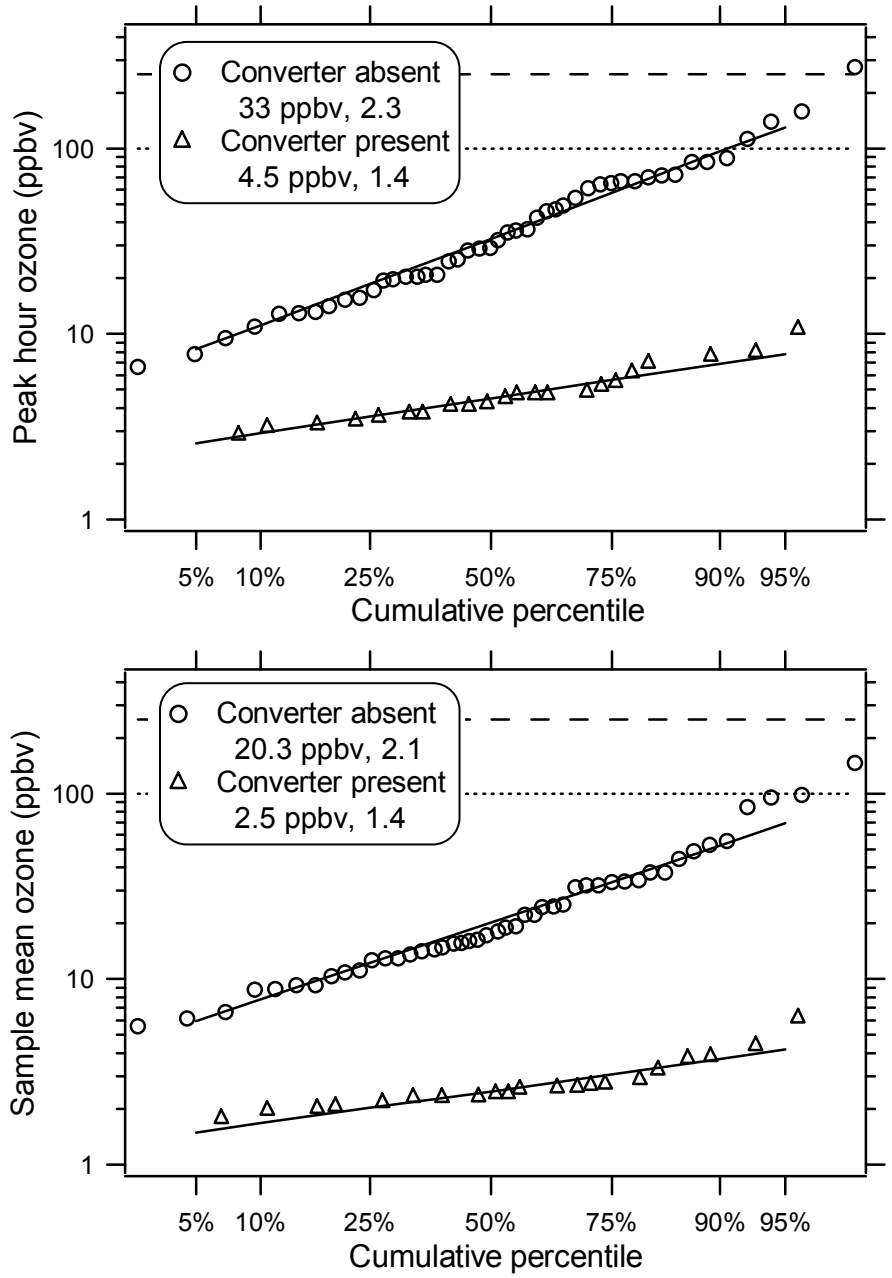

Figure 4.1. Weighted cumulative distributions of peak one-hour (upper frame) and sample-average (lower frame) ozone mixing ratios sampled in passenger cabins on 68 domestic US flight segments. Data are segregated by the presence or absence of an ozone converter. The weighted geometric mean and standard deviation, and the lognormal fits using these parameters, are presented for each distribution. Levels of 100 ppbv and 250 ppbv are indicated to facilitate comparison with levels specified in Federal Aviation Regulations (NRC, 2002).

Data from the eight transoceanic segments indicate that for aircraft equipped with converters, ozone levels on flights following long-haul, high-latitude routes span a greater range than they do on flights restricted to domestic routes (Figure 4.2). The peak one-hour ozone (GM

= 18 ppbv, GSD = 4.9, AM = 33 ppbv) and sample-average ozone (GM = 9.0 ppbv, GSD = 4.0, AM = 15 ppbv) on transoceanic flights were about 4 times higher than those on continental US flights with converters. This difference is statistically significant.

Flight-by-flight measurement results for domestic and transoceanic segments are presented in Tables 4.A.2 and 4.A.3 in Appendix 4.A.2.

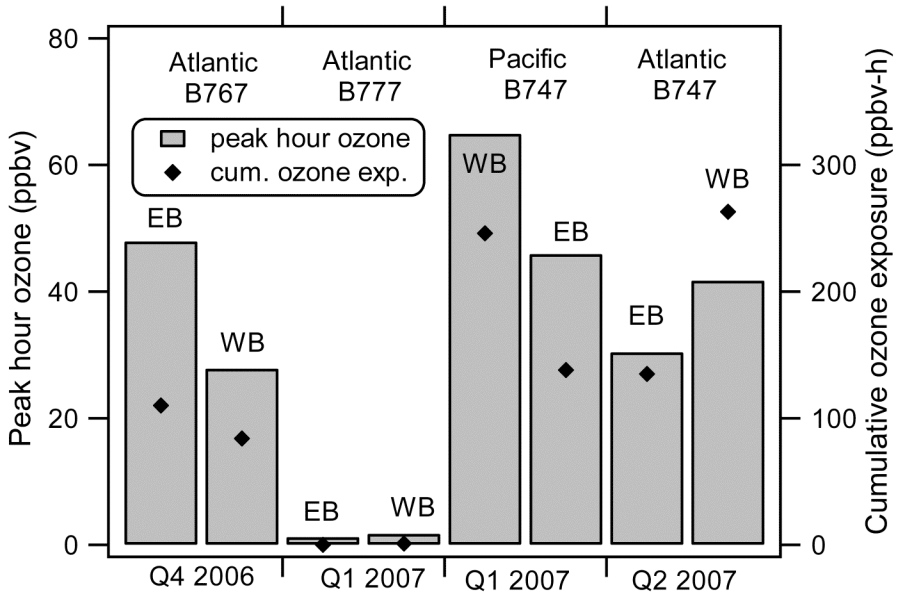

Figure 4.2. Ozone levels sampled on eight transoceanic flights. The shaded bars represent peak-hour ozone (left axis) for each flight segment and are labeled to indicate the flight route (Pacific or Atlantic), direction (eastbound or westbound), aircraft model, and the quarter and year of sampling. The diamonds denote cumulative ozone exposure (right axis) for each flight segment.

Flights with ozone converters consistently met the FAR for cabin ozone. As demonstrated by Figure 4.1, peak one-hour levels were very low – less than 10 ppbv – on domestic flights with converters. On transoceanic flights with converters ozone levels were higher, but considerably lower than levels measured before ozone converters were introduced (Perkins et al., 1979; Bischof et al., 1973; Brabets et al., 1967). Both Bischof et al. (1973) and Brabets et al. (1967) reported levels greater than 100 ppbv for 75% of the flight-time on long-haul flights in the spring. Using passive samplers to determine flight-average ozone levels, Spengler et al. (2004) found 3-hour average in-cabin ozone greater than 100 ppbv on 15 out of 42 transoceanic flights. However, 14 out of these 15 exceedances were on a Boeing 747-200. Only 20% of the aircraft of this model are estimated to be equipped with a converter (NRC, 2002). Aircraft in our sample of transoceanic flights belonged to newer models and were confirmed by airline personnel to have converters. The only other prior study involving one of these newer planes – a Boeing 767 – had results consistent with ours (Lindgren and Norbäck, 2002). This comparison raises the possibility that the difference between our results and those of Spengler et al. (2004) is a consequence of differences in the performance or availability of ozone

converters on different aircraft models. Aircraft type may also have contributed to differences within our transoceanic sample: ozone levels were highest on the older Boeing 747-400 aircraft which was introduced in 1988 (Boeing, 2007), and lowest on the more recently introduced Boeing 777. Overall, we expect the efficiency of a converter to be related to its design, and its age and maintenance schedule since efficiency can be degraded with use owing to fouling by contaminants in bleed air among other reasons.

Figure 4.1 illustrates that in-cabin ozone levels for domestic US flights are variable. While levels are consistently low on flights with converters, they range from low to high on flights without converters. Short-term levels are generally, but not always below the concentration limits specified in the Federal Aviation Regulations. Since the ozone FAR was introduced, no large-scale studies of real-time in-cabin ozone have been published. Results from a pilot-scale study (MacGregor et al., 2008) and from several studies where integrated samples were collected (Nagda et al., 1992; Lee et al., 1999; Spengler et al., 2004) are generally consistent with our observations.

Figure 4.3 presents distributions of in-cabin ozone exposures, expressed in ppbv-h, from the 68 domestic segments – divided into converter and nonconverter flights. This metric was chosen to facilitate comparison with a passenger's total ozone exposure during the course of routine activities when not flying. According to a recent analysis, estimates of total daily ozone exposure for various US urban populations are in the range 100-600 ppbv-h (Weschler, 2006). As demonstrated by Figures 4.2 and 4.3, 60% of exposures on our sample of transoceanic flights and 40% of exposures in our domestic nonconverter sample are in this range. In contrast, exposures from the domestic with-converter sample are well below this range, with a maximum of 26 ppbv-h. This result demonstrates that while exposures on aircraft can, in a few hours, reach levels comparable to what would be encountered on the ground over a day, converters on domestic flights are effective in reducing an occupant's ozone exposure to levels below those normally experienced when not flying.

In addition to ozone itself, exposure to the products of ozone-initiated chemistry is a potential concern in occupied aircraft cabins (Wisthaler et al., 2005; Weschler et al., 2007; Wisthaler and Weschler, 2010; Nazaroff and Weschler, 2010). Hence, the adverse health risks from ozone exposure in the cabin environment may be compounded by exposure to oxidation byproducts (Weschler, 2006). In a study conducted in a simulated, occupied airplane cabin, levels of the anticipated byproducts of ozone chemistry – aldehydes, ketones, and organic acids – increased to more than double their without-ozone level when the residual ozone was 60-75 ppbv (Weschler et al., 2007). Occupants and their clothing were responsible for the removal of >55% of the ozone in the cabin, owing to the reaction between ozone and human skin oils, most notably squalene (Weschler et al., 2007). A series of experiments conducted in a laboratory and simulated-office setting substantiated the finding that humans alter the mix and mixing ratios of ozone and ozone byproducts in indoor environments they occupy (Wisthaler and Weschler, 2010). Conditions favoring a higher exposure to oxidation products (and correspondingly reduced exposure to ozone) include a high occupant density, low air exchange rate, and high exposure duration (or contact time between ozone and humans) (Wisthaler and Weschler, 2010). Chamber studies show that the byproduct yield under aircraft cabin conditions ranges from 0.07 to 0.24 moles of volatile product per mole of ozone consumed (Coleman et al., 2008).

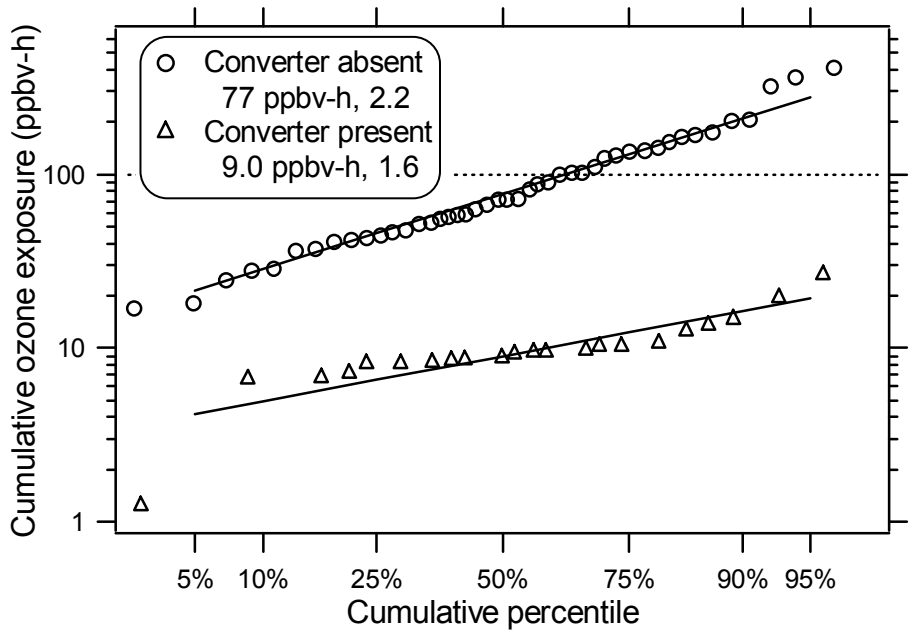

Figure 4.3. Weighted cumulative distribution of ozone exposure levels from 68 domestic flight segments. Ozone exposure, in ppbv-h, represents the time-averaged ozone level multiplied by the sample collection time. Data are segregated by the presence or absence of an ozone converter. The weighted geometric mean and standard deviation, and a lognormal fit using these parameters, are presented for each distribution. The 100 ppbv-h level is marked to facilitate comparison with the total daily ozone exposures of various US urban populations, which are typically in the range 100-600 ppbv-h (Weschler, 2006).

The presence of a residual ozone level of 60-80 ppb, and its associated byproducts, in a simulated cabin was associated with significant decrements in the self-reported symptoms of occupants (Strøm-Tejsen et al., 2008). The upper 15th percentile of exposures observed for domestic nonconverter flights in our sample were comparable to the ozone exposures in the simulated cabin studies (200-300 ppbv-h). This comparison indicates that exposure conditions that have been linked to byproduct formation and self-reported adverse health outcomes in a simulated cabin are encountered in some ordinary domestic flights on planes without converters. On planes with converters, exposures to byproducts are expected to be proportionately reduced as a consequence of the reduction in ozone entering the cabin.

Figure 4.4 depicts peak one-hour ozone for domestic flights plotted against time-of-year. For aircraft without converters, in-cabin ozone varies through the year in a cyclical manner. The size and statistical significance of the seasonal effect was determined by modeling the annual trend using a sinusoidal curve. In the model, peak one-hour ozone from domestic flights without converters served as the response variable (Y). The linear model has the general form shown in equation 4.1:

$$Y = \beta_0 + \beta_1 \sin(2\pi x_1 + \phi) \qquad (4.1)$$

Here β_0 is the annual mean. The continuous variable x_1 is the date, converted to a real number between 0.003 (January 1) and 1.0 (December 31). The magnitude of the seasonal effect is indicated by the relative size of $2\beta_1$ in relation to β_0. The times at which the maximum and minimum are attained are reflected in the value of ϕ. Fitting equation 4.1 to our data confirms that the seasonal effect is large and statistically significant (p=0.001) for domestic flights without converters. A least-squares best-fit sinusoidal curve for the nonconverter flights shows that ozone is expected to be highest in Feb-March, and lowest in Aug-Sept, with a difference of 73 ppbv. The finding of higher ozone in the winter and spring and lower ozone in the summer and fall was expected, as the tropopause height decreases in the hemisphere experiencing winter and spring, and rises in the summer and fall. Consequently, in the winter and spring there is a greater chance that flights at normal cruising altitudes will cross into the lower stratosphere and encounter elevated ozone. Ozone levels on domestic flights with converters were too low to manifest a clear trend.

The modeled trend in Figure 4.4 does not explain extreme values of peak one-hour ozone. Real time data from four domestic flight segments are displayed in Figure 4.5. The four frames (A-D) are arranged chronologically and provide a striking illustration of the effects on in-cabin ozone of both ozone converters and of a storm event. All four flights were monitored within the span of six days along domestic transcontinental US routes. On only the third flight was the monitored plane equipped with an ozone converter. Monitored levels of ozone are highest on the first segment, peaking at approximately 170 ppbv. They remain high but are reduced on subsequent nonconverter segments. Ozone is markedly reduced in the third segment (frame C), remaining below 10 ppbv at all times.

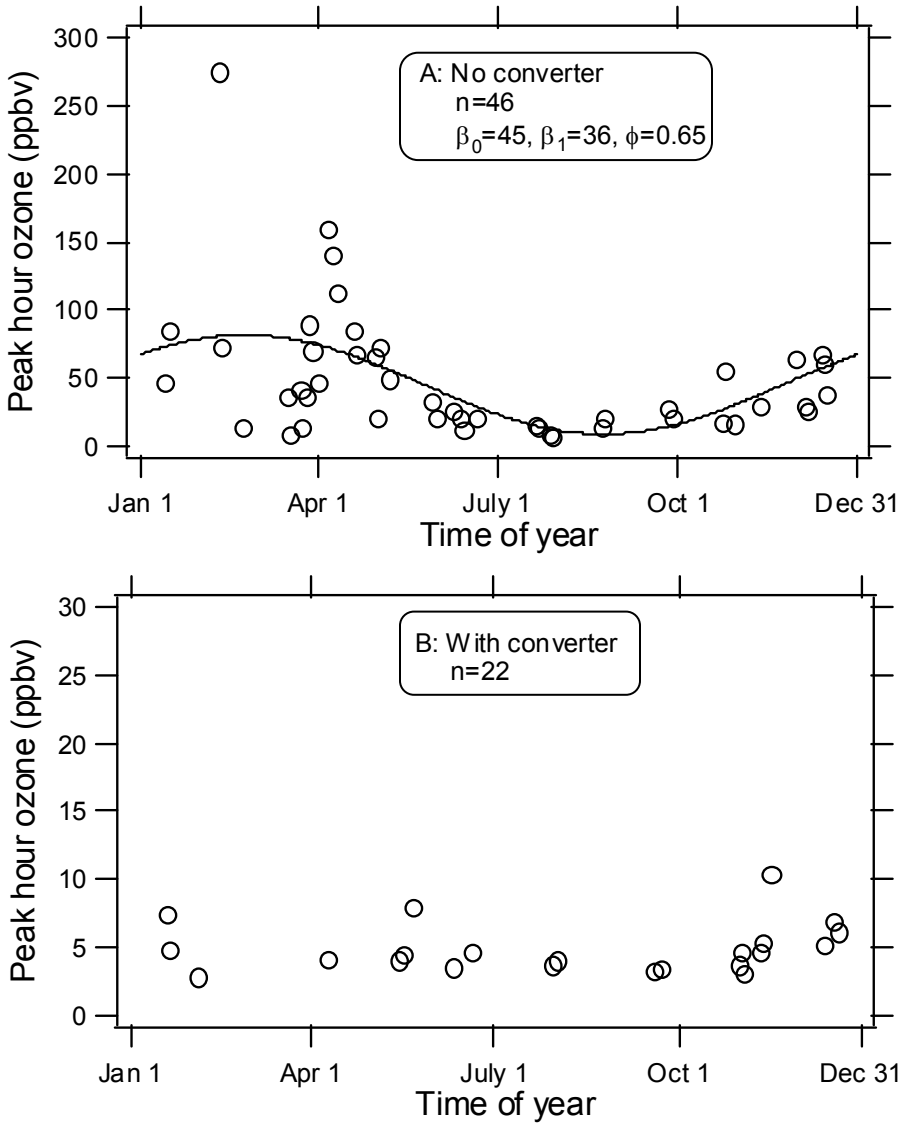

Figure 4.4. Peak one-hour ozone for domestic flights without converters (upper frame) and with converters (lower frame), plotted against time-of-year. A least-squares best-fit sinusoidal curve ($Y = \beta_0 + \beta_1(\sin 2\pi x + \phi)$) is included for the nonconverter sample.

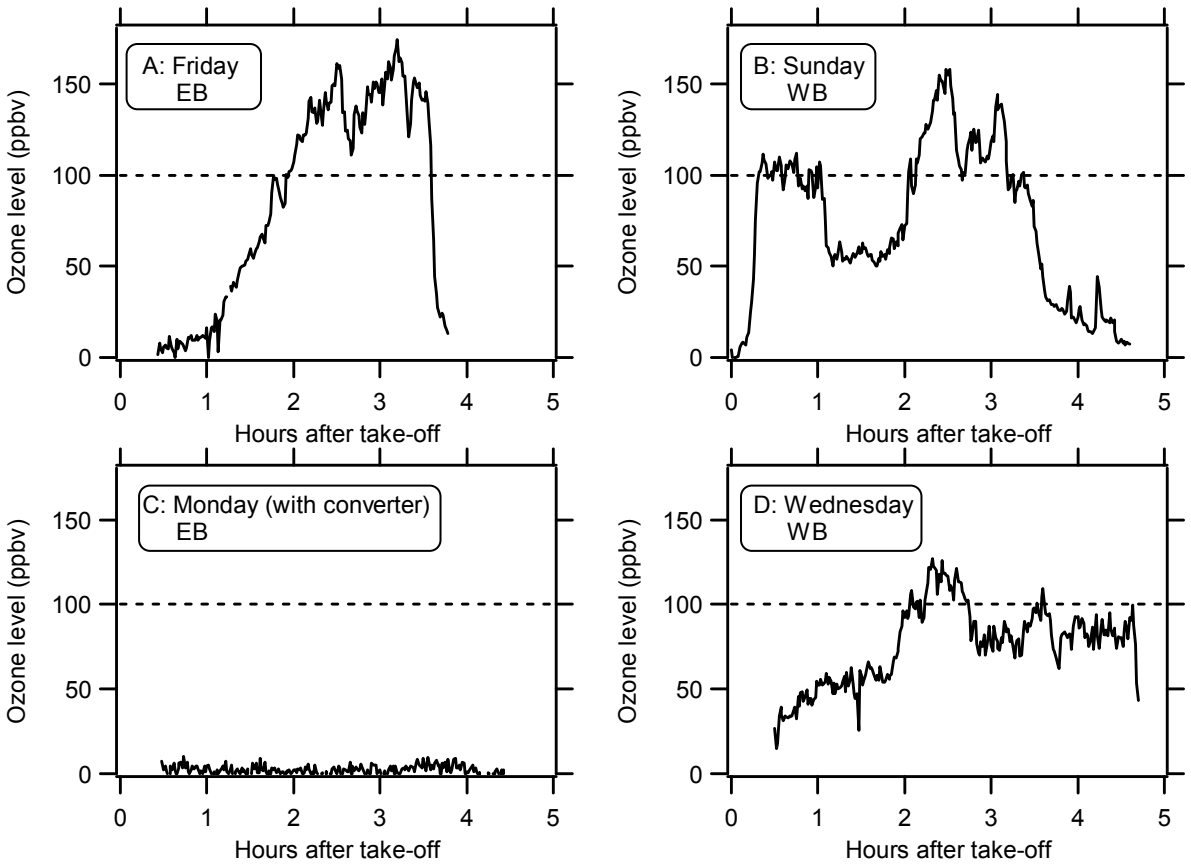

Figure 4.5. Real-time ozone data from four consecutive domestic transcontinental US segments monitored within a 6-day interval in April 2007, arranged chronologically in frames A-D. The direction (EB = eastbound or WB = westbound) is indicated for each segment. Frame C represents data from an aircraft equipped with an ozone converter; the three other flights were on planes without converters.

The flights in which the highest ozone levels were recorded were associated with significant winter storm events. On 6 April 2007, the day that the data in Figure 4.5A were collected, the New York Times reported that "one of the most widespread outbreaks of early April chill on record is enveloping most areas from the Plains to the East Coast." Forecasts through the next six days continued to highlight the eastern storm. The other flight segment exhibiting the highest ozone levels was sampled in February 2006, during a week similarly marked by heavy snow and frontal movement. We surmise that, while the mean variation in cabin ozone across seasons is tied to the established annual variability in the tropopause height, episodic winter and spring storm events appear to be a major driver causing the highest cabin ozone levels. A plausible explanation is the correspondence of these seasonal storms with tropopause folding events: periods when ozone-rich stratospheric air is injected into lower altitudes. Enhanced vertical mixing of this type can accompany cyclogenesis and the instigation of new weather systems. Appenzeller and Davies (1992) describe the structure, direction, and size of stratosphere-to-troposphere intrusions, the pressure and frontal systems that are associated

with them, and regions where the intrusions are favored at various times of year. Morgenstern and Marenco (2000), via an analysis of ambient airplane ozone measurements collected through the MOZAIC project, affirmed that outliers to the seasonal trend in wintertime ozone are associated with the North Atlantic storm track, an observation consistent with ours. In Chapter 5, I report on further investigations of atmospheric ozone levels along flight routes utilizing the MOZAIC data.

An effect owing to flight-route latitude is indirectly evident in a comparison of the domestic and transoceanic flight data, but not apparent within our domestic sample. In general, flights at higher latitudes are more likely to cross the tropopause, as the tropopause height diminishes from about 18 km at the equator to about 8 km at the poles (Seinfeld and Pandis, 1998). We observed this trend in the form of higher in-cabin ozone on transoceanic versus domestic routes, for converter-equipped aircraft. The domestic routes were restricted to latitudes south of about 50º N (with the exception of two round-trip flights to Anchorage, Alaska), whereas long-haul flights within the northern hemisphere typically follow polar routes, including latitudes north of 50º N. The lack of a clear latitude signal in our domestic data is expected, because although the tropopause altitude can demonstrate an approximately twofold variation across the United States in both vertical and horizontal directions, the change is not linear or constant with time (NCEP, 2007).

Higher-occupancy flights might be expected to have lower in-cabin ozone. Experiments in a simulated aircraft cabin (Tamás et al., 2006) showed that approximately 60% of in-cabin ozone removal could be attributed to human occupants. Our data do not clearly exhibit this effect. However, our analysis is constrained by the small number of sampled flights in which occupant density was low. On 53 out of 72 instances (33 out of 45 instances for domestic flights without converters), where data on occupant density was recorded by the researcher, the aircraft cabin was more than 80% full. Also, occupant density is correlated with season, as planes are more likely to be fully occupied in the summer and to have empty seats in the winter. Since the seasonal effect is strong and in the same direction as the anticipated effect owing to occupancy, and since the measured range in occupancy is narrow, the effect of occupancy on in-cabin ozone levels could not be separately resolved.

This field investigation adds substantially to the state of knowledge regarding ozone in the passenger cabins of commercial airplanes. Ozone levels were found to vary strongly with the presence or absence of an ozone converter and with season. For aircraft with converters, levels were elevated on flights following long-haul high-latitude routes relative to those restricted to domestic routes. We observed that the risk of elevated cabin ozone levels increases during winter-spring storms, suggesting that these are associated with hot spots of high ambient ozone in the mid-latitude air traffic corridor. Emerging epidemiological evidence indicates that ozone exposure can lead to an elevated risk of mortality with no threshold. In combination with evidence on within-cabin production of harmful volatile byproducts of ozone-initiated chemistry, these epidemiological data lend weight to the benefits of using ozone converters to reduce ozone exposure in all airplanes that fly at transcontinental cruise altitudes, even on those that fly on domestic routes.

4.4. References

Appenzeller C, Davies HC, 1992. Structure of stratospheric intrusions into the troposphere. *Nature* **358**, 570-572.

Bell ML, McDermott A, Zeger SL, Samet JM, Dominici F, 2004. Ozone and short-term mortality in 95 US urban communities, 1987-2000. *JAMA* **292**, 2372-2378.

Bell ML, Peng RD, Dominici F, 2006. The exposure-response curve for ozone and risk of mortality and the adequacy of current ozone regulations. *Environmental Health Perspectives* **114**, 532-536.

Bischof W, 1973. Ozone measurements in jet airliner cabin air. *Water, Air and Soil Pollution* **2**, 3-14.

Boeing. Commercial Airplanes. http://www.boeing.com/commercial. Accessed on November 16, 2007.

Bognar JA, Birks JW, 1996. Miniaturized ultraviolet ozonesonde for atmospheric measurements. *Analytical Chemistry* **68**, 3059-3062.

Brabets RI, Hersh CK, Klein MJ, 1967. Ozone measurement survey in commercial jet aircraft. *Journal of Aircraft* **4**, 59-64.

Bureau of Transportation Statistics. TranStats: the Intermodal Transportation Database. http://transtats.bts.gov/homepage.asp. Accessed on August 10, 2007.

Chen C, Arjomandi M, Balmes J, Tager I, Holland N, 2007. Effects of chronic and acute ozone exposure on lipid peroxidation and antioxidant capacity in healthy young adults. *Environmental Health Perspectives* **115**, 1732-1737.

Coleman BK, Destaillats H, Hodgson AT, Nazaroff WW, 2008. Ozone consumption and volatile byproduct formation from surface reactions with aircraft cabin materials and clothing fabrics. *Atmospheric Environment* **42**, 642-654.

Gent JF, Triche EW, Holford TR, Belanger K, Bracken MB, Beckett WS, Leaderer BP, 2003. Association of low-level ozone and fine particles with respiratory symptoms in children with asthma. *JAMA* **290**, 1859-1867.

Jerrett M, Burnett RT, Pope III CA, Ito K, Thurston G, Krewski D, Shi Y, Calle E, Thun M, 2009. Long-term ozone exposure and mortality. *The New England Journal of Medicine* **360**, 1085-1095.

Lee SC, Poon CS, Li XD, Luk F, 1999. Indoor air quality investigation on commercial aircraft. *Indoor Air* **9**, 180-187.

Levy JI, Carrothers TJ, Tuomisto JT, Hammitt JK, Evans JS, 2001. Assessing the public health benefits of reduced ozone concentrations. *Environmental Health Perspectives* **109**, 1215-1226.

Lindgren T, Norbäck D, 2002. Cabin air quality: indoor pollutants and climate during intercontinental flights with and without tobacco smoking. *Indoor Air* **12**, 263-272.

MacGregor IC, Spicer CW, Buehler SS, 2008. Concentrations of selected chemical species in the airliner cabin environment. *Journal of ASTM International* **5**, doi: 10.1520/JAI101639.

McDonnell WF, Abbey DE, Nishino N, Lebowitz MD, 1999. Long-term ambient ozone concentration and the incidence of asthma in nonsmoking adults: The Ahsmog study. *Environmental Research* **80**, 110-121.

Morgenstern O, Marenco A, 2000. Wintertime climatology of MOZAIC ozone based on the potential vorticity and ozone analogy. *Journal of Geophysical Research* **105**, 15,481-15,493.

Nagda NL, Koontz MD, Konheim AG, Hammond SK. 1992. Measurement of cabin air quality aboard commercial airliners. *Atmospheric Environment* **26A**, 2203-2210.

Nazaroff WW, Weschler CJ, 2010. Ozone in passenger cabins: concentrations and chemistry, Final Report, Office of Aerospace Medicine, Washington, DC. Available at www.faa.gov/library/reports/medical/oamtechreports/index.cfm.

NCEP Global Forecast System. Dynamic tropopause and surface; northern hemisphere; 7-day analysis. http://www.met.utah.edu/jimsteen/gfs/framesGFS.html. Accessed on November 19, 2007.

NRC (National Research Council) Committee on air quality in passenger cabins of commercial aircraft. *The Airliner Cabin Environment and the Health of Passengers and Crew.* National Academy Press, Washington, DC, 2002.

Perkins PJ, Holdeman JD, Nastrom GD, 1979. Simultaneous cabin and ambient ozone measurements on two Boeing 747 airplanes, Volume 1, US Department of Transportation, Federal Aviation Administration, Washington, DC. Available at ntrs.nasa.gov.

Reed D, Glaser S, Kaldor J, 1980. Ozone toxicity symptoms among flight attendants. *American Journal of Industrial Medicine* **1**, 43-54.

Seinfeld JH, Pandis SN. *Atmospheric Chemistry and Physics: From Air Pollution to Climate Change*, John Wiley & Sons, New York, 1998.

Spengler JD, Ludwig S, Weker RA, 2004. Ozone exposures during trans-continental and trans-pacific flights. *Indoor Air* **14 (Suppl 7)**, 67-73.

Strøm-Tejsen P, Weschler CJ, Wargocki P, Myskow D, Zarzycka J, 2008. The influence of ozone on self-evaluation of symptoms in a simulated aircraft cabin. *Journal of Exposure Science and Environmental Epidemiology* **18**, 272-281.

Tager IB, Balmes J, Lurmann F, Ngo L, Alcorn S, Kunzli N, 2005. Chronic exposure to ambient ozone and lung function in young adults. *Epidemiology* **16**, 751-759.

Tamás G, Weschler CJ, Bakó-Biró Z, Wyon DP, Strøm-Tejsen P, 2006. Factors affecting ozone removal rates in a simulated aircraft cabin environment. *Atmospheric Environment* **40**, 6122-6133.

Weschler CJ, 2006. Ozone's impact on public health: Contributions from indoor exposures to ozone and products of ozone-initiated chemistry. *Environmental Health Perspectives* **114**, 1489-1496.

Weschler CJ, Wisthaler A, Cowlin S, Tamás G, Strøm-Tejsen P, Hodgson AT, Destaillats H, Herrington J, Zhang J, Nazaroff WW, 2007. Ozone-initiated chemistry in an occupied simulated aircraft cabin. *Environmental Science and Technology* **41**, 6177-6184.

Wilson KL, Birks JW, 2006. Mechanism and elimination of a water vapor interference in the measurement of ozone by UV absorbance. *Environmental Science and Technology* **40***,* 6361-6367.

Wisthaler A, Tamás G, Wyon DP, Strøm-Tejsen P, Space D, Beauchamp J, Hansel A, Märk TD, Weschler CJ, 2005. Products of ozone-initiated chemistry in a simulated aircraft environment. *Environmental Science and Technology* **39**, 4823-4832.

Wisthaler A, Weschler CJ, 2010. Reactions of ozone with human skin lipids: sources of carbonyls, dicarbonyls, and hydroxycarbonyls in indoor air. *PNAS* **107**, 6568-6575.

4.A. Appendix

4.A.1. Determining an effective collection rate for the Ogawa passive ozone sampler for the aircraft cabin environment

4.A.1.1. Introduction

The technique of passive sampling for the quantitative detection of gaseous contaminants was introduced in 1973 for determination of nitrogen dioxide, sulfur dioxide, and water vapor (Górecki and Namieśnik, 2002). This method, which involves an assessment of the quantity of a gas transferred through a tube to a sorbent by molecular diffusion, has since been expanded to detect a range of contaminants including volatile organic compounds, carbon monoxide, formaldehyde, and ozone. Samplers based on this principle provide time-integrated measurements and are typically easy to use, inexpensive, small, light weight, unbreakable, create no noise, and do not need a power source. These features make them good candidates for the application considered here: the measurement of ozone in aircraft cabins.

Passengers or crew in aircraft cabins may be exposed to ozone when flight paths enter the lower stratospheric region. Recently, this issue has gained importance since ozone exposure has been associated with an increased risk of mortality down to relatively low levels with no apparent threshold (Bell et al., 2006). Passive sampling is a key to a large monitoring program that could, at moderate cost, elucidate factors that influence the level of ozone on airplanes. A passive sampling device for the measurement of ozone – the Ogawa badge – was developed in 1993 (Koutrakis et al. 1993). It does not require electromagnetic interference (EMI) certification for use on board and has been previously deployed to monitor in-cabin ozone (Spengler et al., 2004).

The Ogawa sampler contains two chambers holding collection filters protected by screens and a diffuser end cap. These filters are coated with a nitrite-based solution, and ozone oxidizes the nitrite to nitrate. The nitrate ion mass can be used to calculate the amount of ozone collected if the effective collection rate (ECR) of the sampler is known. The theoretical collection rate (TCR) is computed with the ozone diffusion coefficient and the dimensions of the sampler – the cross section area of diffusion (A) and the length (L) of the diffusion tubes – as shown in equation (A.1a). In equation (A.1b), the diffusion coefficient is expanded so its dependence on temperature (T) and pressure (P) are explicitly expressed.

$$TCR = \frac{DA}{L} \tag{4.A.1a}$$

$$TCR = \frac{\left(\frac{D'T^{1.5}}{P}\right)A}{L} \tag{4.A.1b}$$

The ECR, defined as the collection rate under real-world conditions, may be higher or lower than the TCR, depending on factors such as airflow conditions near the sampler and homogenous or heterogeneous reactions that can deplete the concentration of gas adjacent to the collector. For instance, an increase in the air speed near the sampler face reduces the effective diffusion length, L, and so increases the collection rate.

The mass of nitrate ion measured on the filter ($M_{NO3-,g}$) is converted to a molar concentration of ozone (M_{O3}) by dividing by sampling duration t, the molecular mass of nitrate (MW_{NO3-}), and the ECR (Koutrakis et al., 1993; Ogawa and Co., 2001) as shown in equation (A.2).

$$M_{O3} = \frac{M_{NO3-,g}}{t \times MW_{NO_{3-}} \times ECR} \tag{4.A.2}$$

The ideal gas law is applied to convert the molar concentration of ozone to a mixing ratio (Y_{O3}, ppb), by dividing by ($PR^{-1}T^{-1}$) as shown in equation (A.3):

$$Y_{O3,ppb} = \frac{M_{NO3-,g}}{t \times MW_{NO_{3-}} \times ECR \times \frac{P}{RT}} \times 10^9 \tag{4.A.3}$$

Equation (A.3) may be rewritten by defining a new parameter ECR_p, which is defined as the ECR multiplied by pressure and has units of $m^3\ h^{-1}$ atm, and substituting it for ECR in the equation. The pressure terms cancel, with the result shown in equation (A.4).

$$Y_{O3,ppb} = \frac{M_{NO3-}}{t \times MW_{NO_{3-}} \times ECR_p \times \frac{1}{RT}} \times 10^9 \tag{4.A.4}$$

The parameter ECR_p can be used in place of the ECR to convert the mass of nitrate to an ozone reading when a mixing ratio (rather than concentration) of ozone is sought. Equation (A.4) has the advantage, relative to equation (A.3), of enabling the mass of nitrate ion measured by the sampler to be converted to an ozone mixing ratio without requiring information about pressure conditions in the cabin. Hence, in the context of the assessment of an ozone mixing ratio, ECR_p is denoted as a "pressure independent" effective collection rate.

For the Ogawa sampler, the TCR at normal temperature and pressure is 24.5 $cm^3\ min^{-1}$ (Koutrakis et al., 1993). The ECR has been determined under a variety of conditions that include in a chamber and outdoors (Koutrakis et al., 1993) and during use as a personal monitor (Liu et al., 1994; Black, 2000). But the interior of an aircraft cabin is a distinctive environment, with a complex configuration of space, and with conditions that include a high air exchange rate and low pressure; so it is difficult to know, *a priori,* which of these environments it resembles most closely from the perspective of the ECR. The aim of this study was to calibrate the Ogawa sampler for the air-cabin environment by assessing ECR_p for the device for commercial passenger aircraft, at cruising altitudes.

4.A.1.2. Methods

4.A.1.2.1. Experimental protocols

Monitoring was conducted on 11 commercial passenger airline flights that ranged from 3 to 11 hours, and included domestic and transoceanic routes, over a two-month period between February and April 2007. Ozone was measured simultaneously with the Ogawa passive sampler and a UV-photometric real-time ozone analyzer (2B Technologies, Inc. Model 202). The active monitor was recently calibrated and so was treated as a transfer standard for this calibration effort. We aimed to obtain a comparison of the Ogawa sampler and active ozone measurements for a range of ozone levels. Therefore, we monitored during the northern hemisphere low-tropopause season when ambient ozone levels in the air-traffic corridor are most variable. To avoid intentionally including flights with very low mean ozone, domestic flights with control devices were excluded from the sample, as these were previously found to have flight-mean ozone levels of only a few ppb. Table 4.A.1 summarizes, for each flight segment, the aircraft type, and flight duration.

Protocols for in-flight active ozone sampling were described in §4.2.1. Briefly, a researcher placed the active monitor under the seat in front of her or him, in the economy cabin of the airplane. A sampling tube connected to the monitor was clipped to the seat back in front of the researcher to sample air close to the passenger breathing zone. The Ogawa monitor was affixed to the seat in front of the passenger, close to the sampling tube inlet of the active monitor. The passive sampler was not placed adjacent to a fleeced or cloth surface, to prevent its being located in an ozone-depleted boundary layer. The surface was covered with a paperboard backing before the sampler was pinned to it, or the sampler was attached such that there was at least 2.5 cm of air space separating it from the surface.

Table 4.A.1. Flight-by-flight measurement results for the 11 segments on which passive sampling was conducted.

No. [a]	Aircraft model	Conv-erter [b]	Sample duration (h)	Mean O_3 (ppb)	O_3 exposure (ppb-h)	Nitrate mass (μg) [c]
24	B737-300	N	4.0	6.1	24	0.056
30	B757	N	2.6	10.9	28	0.070
46	B737-300	N	3.7	12.8	47	0.12
47	B757	N	4.1	22.3	91	0.22
49	B757	N	3.6	17.2	63	0.094
51	B757-200	N	5.2	24.3	125	0.25
64	B757	N	4.0	32.1	129	0.36
69	B777	Y	6.3	-0.2	-1.4	0.026
70	B777	Y	10.2	0.1	1.1	-0.0079
74	B747-400	Y	7.8	17.9	139	0.30
76	B747-400	Y	8.2	30.0	246	0.48

[a] Passive sampling was conducted on a subset of flights described in Tables 4.A.2 and 4.A.3. The serial numbers link the data presented in the three tables.
[b] Y = converter present; N = converter absent. Ozone converters were present on all transoceanic flights, and absent on domestic flights.
[c] Measured nitrate mass minus the mean "blank" nitrate mass associated with the sample batch.

The sampler was assembled and handled according to the protocol described by Ogawa and Co. (2001). Briefly, coated pads were stored in a refrigerator prior to use. A "batch" was designated as the set of samples exposed over the month following their assembly date. Following assembly and prior to analysis, samplers were stored in individual dark, sealed vials at room temperature. Three blanks were assigned to each batch, and remained with their corresponding samplers but were not exposed. On board, field researchers were instructed to begin exposure once the transfer standard warm-up period was concluded, and to re-seal samplers when the active monitor was turned off. As a consequence, samples were collected during the portion of the flight above 10,000 ft.

Samples and blanks were analyzed via ion chromatography by Dr. Eva Hardigan (Research Triangle Institute, NC, USA). The analysis included duplicate measurements for quality control. The limit of detection (in μg nitrate) for each batch was computed as 3×(standard deviation of field blanks) following the method described by Koutrakis et al. (2003) and employed by Spengler et al. (2004). A background correction factor (in μg nitrate) was computed as the mean of the three blanks in each batch, and subtracted from each reading.

4.A.1.2.2. Data Analysis

The Ogawa readings were compared, via linear regression through the origin (Zar, 1999), to paired ozone exposure measurements. The regression slope, b, between the Ogawa reading (in g nitrate) and the ozone exposure ($Y_{O3} \times t$ in ppb-h) is interpreted as shown in equation (A.5), which is derived from equation (A.4b):

$$b = MW_{NO_{3-}} \times ECR_p \times \frac{1}{RT} \times 10^{-9} \qquad (4.A.5)$$

Central estimates of the ECR_p are assessed using the least-squares best-fit estimate of b (assuming in-cabin temperature, $T = 293$ K). Confidence intervals (95%) are calculated using the 95% upper and lower bound estimates of the slope (assuming the residuals are normally distributed and $\alpha(2) = 0.05$).

4.A.1.3. Results

Blank correction factors of 0.46 μg for batch 1 and 0.36 μg for batch 2 were subtracted from each reading. The limits of detection for batch 1 and batch 2 were 0.095 and 0.036 μg nitrate, respectively. Measurements (blank-corrected) ranged from –0.01 to 0.48 μg nitrate, corresponding to a range of ozone exposures, computed based on ozone measurements made by the active monitor, of –1.4 to 246 ppb-h. Negative values of mass nitrate or ozone are not physically meaningful; however, they have not been truncated to zero as they represent random measurement error and, as such, it is appropriate to include them in the regression.

Figure 4.A.1 presents a comparison between background-corrected Ogawa passive sampler raw readings (in g nitrate) and paired ozone exposure values based on readings from the active ozone monitor (in ppb-h ozone). The relationship between the two has a slope (M_{NO3-} per $Y_{O3}t$) of 2.1 ± 0.1 ng nitrate per ppb-h ozone (mean ± standard deviation). The corresponding

ECR_p, assessed from the slope according to equation (A.5), is 14 cm^3 min^{-1} atm (95% confidence interval: 12 to 15 cm^3 min^{-1} atm).

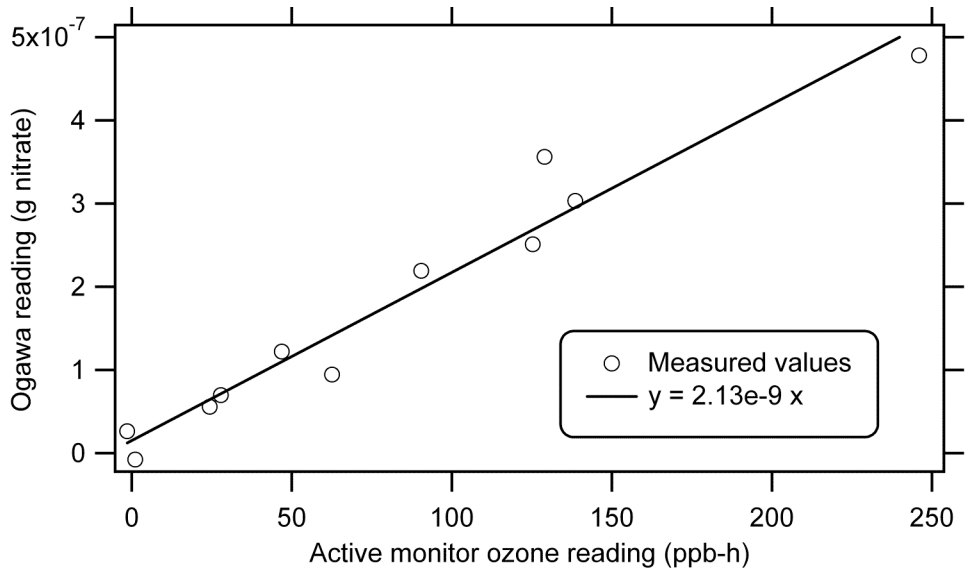

Figure 4.A.1. A comparison between background-corrected Ogawa passive sampler raw readings (in g nitrate), and ozone exposure values based on readings from the 2B Technologies' real-time ozone monitor when the two were simultaneously deployed. Exposure values are assessed from the period when the active monitor was on and warmed up, which corresponds the period when the Ogawa sampler was unsealed. The best-fit single-parameter regression slope is 2.1 ng nitrate per ppb-h ozone.

4.A.1.4. Discussion

The empirical ECR_p estimate assessed in this study can be converted to an ECR estimate by dividing by pressure. The 1-atm equivalent ECR is 14 cm^3 min^{-1}. At elevation, the pressure in the flight cabin is maintained at >0.75 atm. The equivalent ECR for P = 0.75 atm is 18.3 cm^3 min^{-1} (95% range: 16.4 – 20.3 cm^3 min^{-1}). ECR_p and ECR estimates are useful for converting nitrate mass to ozone mixing ratios and ozone concentrations, respectively (assuming exposure duration is known). The ozone exposure data that these estimates are based on span a moderate range: 0-246 ppb-h. Care must be taken when extrapolating to exposures far above this range.

Results from this calibration exercise reinforce the importance of accurate blank correction for unbiased interpretation of Ogawa passive sampler readings. The nitrate levels measured on blank samples in the present study were high – 0.36 to 0.46 μg nitrate – compared to levels obtained for exposed samples (0.45 to 0.94 μg nitrate). Spengler et al. (2004) measured similarly high blank nitrate levels of 0.70 to 2.6 μg. As a consequence, for low to moderate ozone exposures, a relatively small fractional error in the blank measurement could result in a substantial error in the corresponding ozone estimate.

The conversion from nitrate mass to ozone mixing ratio requires, in addition to estimates of the ECR_p and exposure duration, information on temperature. However as the influence of temperature on the conversion is negligible (Palmes and Gunnison, 1973) it is adequate, for the

flight-cabin environment, to assume that normal temperature (i.e. T = 293 K) conditions prevail. The main reason for a negligible dependence on temperature is that fractional changes in absolute temperature (i.e., measured in Kelvin) commonly encountered in the airplane cabin are small, few % or less. This result is also influenced by the finding from previous research that the dependence of diffusion coefficients on temperature is weaker than predicted by theory (Górecki and Namieśnik, 2002).

The Ogawa passive sampler was used to measure aircraft cabin ozone in one previous study. Spengler et al. (2004) used the device to survey 106 commercial passenger flight segments. That study used a nominal ECR of 21.6 cm^3 min^{-1} (and P = 0.75 atm), which is ~20% higher than the ECR determined in the present research. Based on differences in sampler placement and configuration, we deem it appropriate that the ECR for the Spengler et al. (2004) survey was greater than the estimate presented in this paper. Spengler et al. (2004) suspended samplers from the ceiling (so as to lie in the breathing zone of a potential passenger, and to not disturb local air velocities) above an unoccupied seat in the first-class cabin. Our field monitoring was conducted in the economy cabin with monitors clipped to the seat-back in front of the passenger. A monitor suspended in the air in the less densely occupied first-class cabin, without a passenger in its immediate proximity, is likely to be exposed to airflow that is less obstructed and, as a consequence, is likely to be associated with a higher ECR.

The influence of variables such as sampler placement (e.g. suspended from the air or clipped near a surface), location within the cabin, aircraft occupant density, flight altitude, and aircraft type on the ECR was not investigated in this study and has not been the subject of previous research. Hence, we cannot evaluate the spatial and temporal variability of the ECR within an airplane or its variability among flights. However, an approximate assessment of the anticipated variability and the factors that influence it is gauged by considering previous research on the influence of airflow on the ECR for passive samplers. Koutrakis et al. (1993) attribute the differences between estimates mainly to face velocity effects. Ogawa and Co. (2001) noted that during indoor monitoring, insufficient air movement has the effect of decreasing the ECR. In a similar assessment, Brown (2000) noted that in low wind-speed conditions, the analyte may not be replenished efficiently at the sampler surface, resulting in an increased effective diffusion path length; whereas in high wind conditions, the effective diffusion path length may be decreased by disturbance of the stagnant air layer.

The dependence of the ECR on airflow conditions and related parameters is demonstrated by the range of estimates obtained across monitoring applications. Outdoors, it is common for air speeds to be higher, and airflow to be unimpeded, relative to indoor environments, so one would expect higher ECRs. This expectation was confirmed in a study by Koutrakis et al. (1993), who report ECR = 29.0 ± 2.7 cm^3 min^{-1} (N = 37) for measurements made outdoors; and ECR = 18.1 ± 1.9 cm^3 min^{-1} (N = 20) in a laboratory chamber. The lowest ECR estimates in the literature, which were reported as being 9-38% less than 18.2 cm^3 min^{-1} (Liu et al., 1994), were associated with personal monitoring. The reduction was attributed to the ozone depletion attributable to reaction with clothing, dilution associated with human expiratory flow, and human activities blocking airflow around the sampler (Liu et al., 1994). Our ECR estimates – 18.3 cm^3 min^{-1} at reduced in-flight pressure conditions, and 14 cm^3 min^{-1} at 1 atm pressure – are comparable to those measured in personal monitoring studies and investigations in a chamber. As anticipated, they are much lower than estimates for outdoors.

This study represents the first field calibration of the Ogawa ozone passive sampler for the air cabin environment. A follow-up study with a larger sample size would be useful for obtaining estimates of ECR_p and ECR that have greater precision than is reported here.

4.A.1.5. References

Bell ML, Peng RD, Dominici F, 2006. The exposure-response curve for ozone and risk of mortality and the adequacy of current ozone regulations. *Environmental Health Perspectives* **114**, 532-536.

Black DR. *Development and application of a sensor for real-time microenvironmental and personal ozone measurements.* Dissertation, UC Berkeley, 2000.

Brown R, 2000. Monitoring the ambient environment with diffusive samplers: theory and practical considerations. *Journal of Environmental Monitoring* **2**, 1-9.

Górecki T, Namieśnik J, 2002. Passive sampling. *Trends in Analytical Chemistry* **24**, 276-291.

Koutrakis P, Wolfson JM, Bunyaviroch A, Froehlich SE, Hirano K, Mulik JD, 1993. Measurement of ambient ozone using a nitrite-coated filter. *Analytical Chemistry* **56**, 209-214.

Liu LJS, Olson MP, Allen GA, Koutrakis P, McDonnell WF, Gerrity TR, 1994. Evaluation of the Harvard ozone passive sampler on human subjects indoors. *Environmental Science and Technology* **28**, 915-923.

Ogawa & Co., USA, Inc. Protocol for ozone measurement using the ozone passive sampler badge. Revision 3.0. February 2001.

Palmes ED, Gunnison AF, 1973. Personal monitoring device for gaseous contaminants. *American Industrial Hygiene Association Journal* **34**, 78-81.

Spengler JD, Ludwig S, Weker RA, 2004. Ozone exposures during trans-continental and trans-pacific flights. *Indoor Air* **14 (Supp. 7)**, 67-73.

Zar JH. *Biostatistical Analysis.* Prentice-Hall, Inc., NJ, 1999.

4.A.2. Flight-by-flight measurement results

Tables 4.A.2 and 4.A.3 summarize, for the 76 successfully monitored flight segments, the aircraft model, whether or not a converter was present, and the time of year during which the flight was monitored. The 1-h peak ozone level and the sample mean ozone level (along with the sampling duration) are also reported for each flight.

Table 4.A.2. Flight-by-flight measurement results for domestic segments (*page 1 of 2*).

No. [a]	Aircraft model	Converter [b]	Quarter	Sample duration (min) [c]	One-hour peak ozone (ppb)	Sample mean ozone (ppb)
1	A 319	Y	Jan-Mar	186	3	2
2	A319	Y	Oct-Dec	298	3	2
3	A319	Y	Jul-Sep	216	3	2
4	A319	Y	Jul-Sep	172	3	2
5	A319	Y	Apr-Jun	237	4	3
6	B777	Y	Jul-Sep	222	4	3
7	A319	Y	Oct-Dec	312	4	0
8	A 320	Y	Jul-Sep	244	4	2
9	A319	Y	Apr-Jun	244	4	2
10	A 319	Y	Apr-Jun	237	4	2
11	A320	Y	Apr-Jun	259	4	2
12	B767-300	Y	Oct-Dec	210	5	3
13	B-767-400	Y	Apr-Jun	202	5	4
14	A319	Y	Oct-Dec	231	5	2
15	A 319	Y	Jan-Mar	252	5	2
16	B767-400	Y	Oct-Dec	202	5	3
17	A319	Y	Oct-Dec	182	5	3
18	A319	Y	Oct-Dec	270	6	3
19	B757	0	Jul-Sep	195	7	6
20	B767-300	Y	Oct-Dec	213	7	4
21	A319	Y	Jan-Mar	204	7	3
22	B757	N	Jul-Sep	153	8	7
23	A320	Y	Apr-Jun	264	8	4
24	B737-300	N	Jan-Mar	239	9	6
25	B747-400	Y	Oct-Dec	255	10	6
26	B757	N	Jul-Sep	268	11	9
27	B757	N	Jul-Sep	217	13	10
28	B737-800	N	Jul-Sep	248	13	9
29	B757	N	Jan-Mar	193	13	9
30	B757	N	Jan-Mar	153	14	11
31	B757	N	Jul-Sep	220	15	11
32	B757	N	Oct-Dec	219	16	13
33	B757	N	Oct-Dec	170	17	16
34	B757	N	Apr-Jun	216	20	16

Table 4.A.2. *cont.* (*p.2 of 2*).

No. [a]	Aircraft model	Converter [b]	Quarter	Sample duration (min) [c]	One-hour peak ozone (ppb)	Sample mean ozone (ppb)
35	B757	N	Apr-Jun	213	20	16
36	B757	N	Jul-Sep	308	20	14
37	B767-300	N	Jul-Sep	240	21	13
38	B757	N	Apr-Jun	231	21	15
39	B757	N	Jul-Sep	277	21	9
40	B757	N	Oct-Dec	277	25	15
41	B757	N	Apr-Jun	264	25	16
42	B757	N	Jul-Sep	199	28	25
43	B757	N	Oct-Dec	230	29	14
44	B757	N	Oct-Dec	236	29	18
45	B737-800	N	Apr-Jun	186	32	19
46	B737-300	N	Jan-Mar	219	36	13
47	B757	N	Jan-Mar	242	36	22
48	B757	N	Oct-Dec	345	37	19
49	B757	N	Jan-Mar	219	42	17
50	B757	N	Jan-Mar	242	46	25
51	B757	N	Apr-Jun	306	47	24
52	B757	N	Apr-Jun	237	49	22
53	B757	N	Oct-Dec	194	55	31
54	B757	N	Oct-Dec	249	61	32
55	B767-300	N	Oct-Dec	178	64	33
56	B757	N	Apr-Jun	246	65	38
57	B757	N	Apr-Jun	201	67	49
58	B767-300	N	Oct-Dec	240	67	34
59	B757	N	Jan-Mar	251	70	34
60	B757	N	Jan-Mar	237	72	44
61	B757	N	Apr-Jun	180	72	56
62	B757	N	Jan-Mar	321	84	38
63	B757	N	Apr-Jun	233	85	53
64	B757	N	Jan-Mar	240	89	32
65	B757	N	Apr-Jun	254	113	85
66	B757	N	Apr-Jun	297	141	99
67	B757	N	Apr-Jun	201	160	96
68	B767-300	N	Jan-Mar	169	275	146

[a] Flights ordered from lowest to highest peak-hour ozone level.
[b] Y = converter present; N = converter absent.
[c] The monitor was approved for use above a flight altitude of 10,000 ft. It required a 20-min warm-up period. Typically this meant excluding data from the first 30 min and last 15 min of the flight (where the flight is defined as the period from take-off to touch-down).

Table 4.A.3. Flight-by-flight measurement results for transoceanic segments (all had ozone converters).

No [a]	Aircraft model	Route	Quarter	Sample duration (min) [b]	One-hour peak ozone (ppb)	Sample mean ozone (ppb)
69	B777	Atlantic	Jan-Mar	378	1	0
70	B777	Atlantic	Jan-Mar	611	2	0
71	B767-ER	Atlantic	Oct-Dec	373	28	14
72	B747-400	Atlantic	Apr-Jun	557	30	15
73	B747-400	Atlantic	Apr-Jun	623	42	25
74	B747-400	Pacific	Jan-Mar	463	46	18
75	B767-300	Atlantic	Oct-Dec	406	48	16
76	B747-400	Pacific	Jan-Mar	491	65	30

[a] Flights ordered from lowest to highest peak-hour ozone level.
[b] The monitor was approved for use above a flight altitude of 10,000 ft. It required a 20-min warm-up period. Typically this meant excluding data from the first 30 min and last 15 min of the flight (where the flight is defined as the period from take-off to touch-down).

Chapter 5: Atmospheric ozone levels encountered by commercial passenger aircraft on transatlantic routes

5.1. Introduction

Ozone in the air traffic corridor poses a human health risk when it is introduced into passenger aircraft cabins via airplane ventilation systems. Elevated atmospheric ozone levels may be encountered by aircraft when they cross the tropopause and enter the lower stratosphere, or when meteorological processes cause ozone-rich air from the stratosphere to be injected into lower altitudes and to intersect with flight tracks. To assess the health risk associated with this exposure pathway and to evaluate control strategies, we need to increase our knowledge of in-flight ozone levels and the factors that influence exposure to ozone in the aircraft cabin environment. The investigation described in Chapter 4 addressed these objectives by quantifying ozone levels and exposures on 76 commercial flights either across the United States (68), across the Atlantic (6) or across the Pacific (2), in 2006-2007. The study showed that in-cabin ozone on domestic US flights varies as a function of season, differs with the presence or absence of ozone converters, and for flights without converters tends to be elevated during winter-spring storms. For aircraft with converters, levels were higher on transatlantic and transpacific flights compared to those occurring within the continental US.

Measurements of ozone made in passenger airplane cabins during flight are the most direct means of assessing in-cabin exposures. However at present, with no infrastructure in place for automatic in-cabin ozone monitoring, in-cabin data are expensive and time-consuming to acquire and are therefore scarce. Consequently, the present analysis seeks to elucidate an important factor influencing ozone exposures in aircraft: atmospheric ozone levels along commercial flight routes. This goal is accomplished via an analysis of ozone data collected by sensors installed outside aircraft, as part of the "and Water Vapor by Airbus In-service Aircraft" (MOZAIC) program.

Since 1994, automatic measurements of ozone have been made by MOZAIC aircraft on more than 30,000 commercial passenger flights along a range of routes across five continents, with a bias toward the North Atlantic flight corridor (Marenco et al., 1998). Previous research utilizing MOZAIC data has evaluated the effects of airplanes on atmospheric composition; identified and explained spatial and temporal ozone trends in the upper troposphere and lower stratosphere (UT/LS) region; assessed the frequency and features of cross-tropopause ozone flows; and evaluated existing three-dimensional chemistry and transport models (MOZAIC, 2010). While data from a previous aircraft campaign – the Global Atmospheric Sampling Program, GASP – were used to better understand in-cabin ozone trends in the 1970s (Perkins et al., 1979), the MOZAIC data have not yet been analyzed from a per-flight perspective to consider implications for human exposure to ozone in passenger cabins during flight.

The present study analyzes time-resolved ozone data collected by MOZAIC flights undertaken in 2000-2005, between Munich and selected destinations across the continental United States. The study objectives are to assess the influence of season, latitude, altitude, and tropopause folding events on ozone levels encountered by commercial passenger flights on transatlantic routes and to consider implications for exposures within the cabin.

5.2. Background: The tropopause

The tropopause marks the boundary between the troposphere and the stratosphere. The World Meteorological Organization defines the tropopause as the lowest level at which the temperature lapse rate decreases to 2 K km^{-1} or less (Stohl et al., 2003a). Alternate definitions of the tropopause characterize it as a zone marked by sharp transitions in ozone, water vapor concentration, or potential vorticity. Though the various definitions are broadly consistent, Stohl et al. (2003a) note the ozone tropopause is typically lower than the thermal tropopause. The representative mean height of the tropopause varies cyclically through the year, with a spring minimum and a fall maximum. The tropopause height also varies with latitude, with the annual average decreasing from about 15-18 km in the tropics to 6-8 km near the poles. The change in tropopause height with latitude is not linear or constant, but has sharp discontinuities; most notably, it jumps across the jet stream. Moreover, the tropopause height can fluctuate significantly around its mean trend over relatively short periods, because of meteorological processes that cause air exchange between the lower stratosphere and the upper troposphere (NRC, 2002).

Stratosphere to troposphere exchange (STE) events that perturb the tropopause from its average position are associated with mesoscale-level fluctuations and are most common (within the northern hemisphere) in the mid latitudes (30-60 °N). They are highly episodic, and classified into two types. Shallow STE, during which stratospheric air resides in the troposphere for < 6 h before returning to the stratosphere, account for more than 90% of cross-tropopause fluxes. Their occurrence has a weak amplitude seasonal cycle with a maximum in the spring, and relatively little zonal (i.e. longitudinal) variability. Deep exchanges, typically occurring via tropopause folds – defined as thin bands of stratospheric air intruding into the troposphere – account for only 1-2% of total fluxes. Their frequency has a strong seasonal cycle with a winter maximum and summer minimum. Tropopause folds usually occur in association with the development of a low pressure system and a cold front at the ground (Appenzeller and Davies, 1992); they are associated with cyclogenesis (Sprenger et al., 2003). Surface-based deep convection is linked to both extreme weather and to tropopause folds, so the latter may be used to improve weather forecasts (or equivalently, weather markers may serve as indicators of folding events). The intrusions follow distinct zonal patterns and are associated with the end of the Pacific storm track and the beginning of the Atlantic storm track, occurring with greatest frequency over the US west coast and the western North Atlantic. (Stohl et al., 2003b; Holton et al., 1995; El Amraoui et al., 2010; Morgenstern and Marenco, 2000).

5.3. Methods

5.3.1. The MOZAIC project

MOZAIC, an acronym for the measurement of ozone and water vapor by Airbus in-service aircraft, is a collaborative European field campaign initiated in 1993. The project involves the automatic, regular measurement of various airborne species by five passenger aircraft (Airbus Model A340) during routine commercial flight. Flights are monitored at the approximate frequency of 2,000 segments per year. The aircraft fly at cruising altitudes, spaced 0.3 km apart, that range from approximately 9.8 km to 12.5 km. The data are made accessible through international computer networks.

In Phase I of the campaign, ozone and water vapor were measured. Monitoring of carbon monoxide and oxides of nitrogen was added as part of a second phase. Additional monitored variables include position, temperature, pressure, and wind velocity. All measurements are made by sensors installed on the aircraft shell, just below the cockpit. Data are collected during flight at irregular intervals, at the approximate frequency of 0.25 Hz. Ozone was measured via dual beam ultraviolet absorption (detection limit 2 ppb; precision ± [2 ppb+2%]) (Law et al., 1998).

5.3.2. Data acquisition

Our team obtained access to the MOZAIC dataset in August 2007. We focused on flights involving a US city because (a) these comprised a large fraction of the global dataset (about 40%), and because (b) the present analysis aims to build on insights gained from the US field monitoring campaign described in Chapter 4. As shown in Table 5.1, amongst the ~10,000 flights involving US cities sampled between 1995 and 2005, the most frequented US cities were New York, Atlanta, and Chicago. The European cities most often flown to were Frankfurt, Brussels, and Munich.

Table 5.1. Number of flight segments in the MOZAIC database during 1995-2005, by year, and by US city involved (for the 8 US cities most frequently flown to). [a]

Year	Total global	Total US	NY	ATL	CHI	DAL	HOU	SF	CIN	LA
1995	1933	1083	493	58	28	101	81	94	0	4
1996	2323	854	465	46	6	172	84	50	0	14
1997	2721	1008	391	62	124	208	100	18	95	0
1998	2704	1057	353	102	62	202	163	16	155	0
1999	2651	1070	313	282	45	126	139	16	43	0
2000	2835	1170	237	286	187	78	124	12	4	2
2001	1880	828	313	50	254	48	40	8	0	4
2002	1636	611	255	0	194	32	20	18	0	0
2003	2552	838	208	112	260	60	42	16	12	10
2004	2544	1016	160	388	62	66	28	22	2	104
2005	1979	418	28	24	26	6	0	30	0	162
Total	25758	9953	3216	1410	1248	1099	821	300	311	300

[a] NY = New York, ATL = Atlanta, CHI = Chicago, DAL = Dallas, HOU = Houston, SF = San Francisco, CIN = Cincinnati, LA = Los Angeles.

The present analysis considers all flights between Munich and New York (NY), Chicago, and Los Angeles (LA), during the six-year period between 2000 and 2005. The period from 2000 to 2005 was selected as being reasonably representative of current conditions. New York, Chicago and LA were selected as they are major destinations, being the three most populous cities in the US. They represent an interesting blend of flight routes, as their locations encompass the eastern, central, and western US. Finally, they had approximately even sample sizes (NY = 361; LA = 274; Chicago = 432), and were monitored during all months of the year.

Flight segments with >10% data missing were excluded from the analysis. This reduced our sample sizes to: NY = 318; LA = 175; Chicago = 372.

5.3.3. Data analysis

Data were processed by computing the following summary statistics per flight segment: peak ozone, 1-hour peak ozone, and flight-average ozone; peak and flight-average altitude and latitude; mean altitude and latitude that coincide with the 1-h ozone peak; flight duration and the time-to-peak-ozone. Data from the 865 valid flight segments were stratified into six groups based on the route (Munich to LA, Chicago, or NY, and eastbound or westbound). Data were weighted to adjust for uneven sampling across the year, as described in Chapter 4, and weighted distributions of peak one-hour and flight-average ozone levels were determined for each group. Intergroup means were compared. The influence of time of year (i.e., season) and route on one-hour peak and flight-average ozone levels was analyzed by means of a general linear regression model. The effects of altitude and latitude were investigated indirectly, with the flight route serving as a proxy for their influence, and directly by assessing within-flight ozone trends. Statistical significance was determined on the basis of the conventional 5% Type I error rate.

5.4. Results and discussion

5.4.1. Comparing means

Figure 5.1 presents cumulative distributions of peak 1-hour and flight average ozone levels obtained from the 865 flight segments, stratified by route. The data conform reasonably to lognormal distributions, and weighted geometric means (GM) and geometric standard deviations (GSD) are presented for each distribution. Central tendencies of peak one-hour and flight-average ozone levels are in the ranges 355-415 ppb and 148-209 ppb, respectively. Across all 865 flights, ozone levels span an order of magnitude, with the 1-h peak and flight-average ozone ranging from approximately 90 to 900 ppb, and 50 to 500 ppb, respectively. Ozone levels are higher on westbound compared to eastbound routes. Of the three arrival city/departure city pairs, levels were highest for Munich/Chicago, and lowest for Munich/Los Angeles. The variations in ozone levels within each route are substantially greater than the variation across routes.

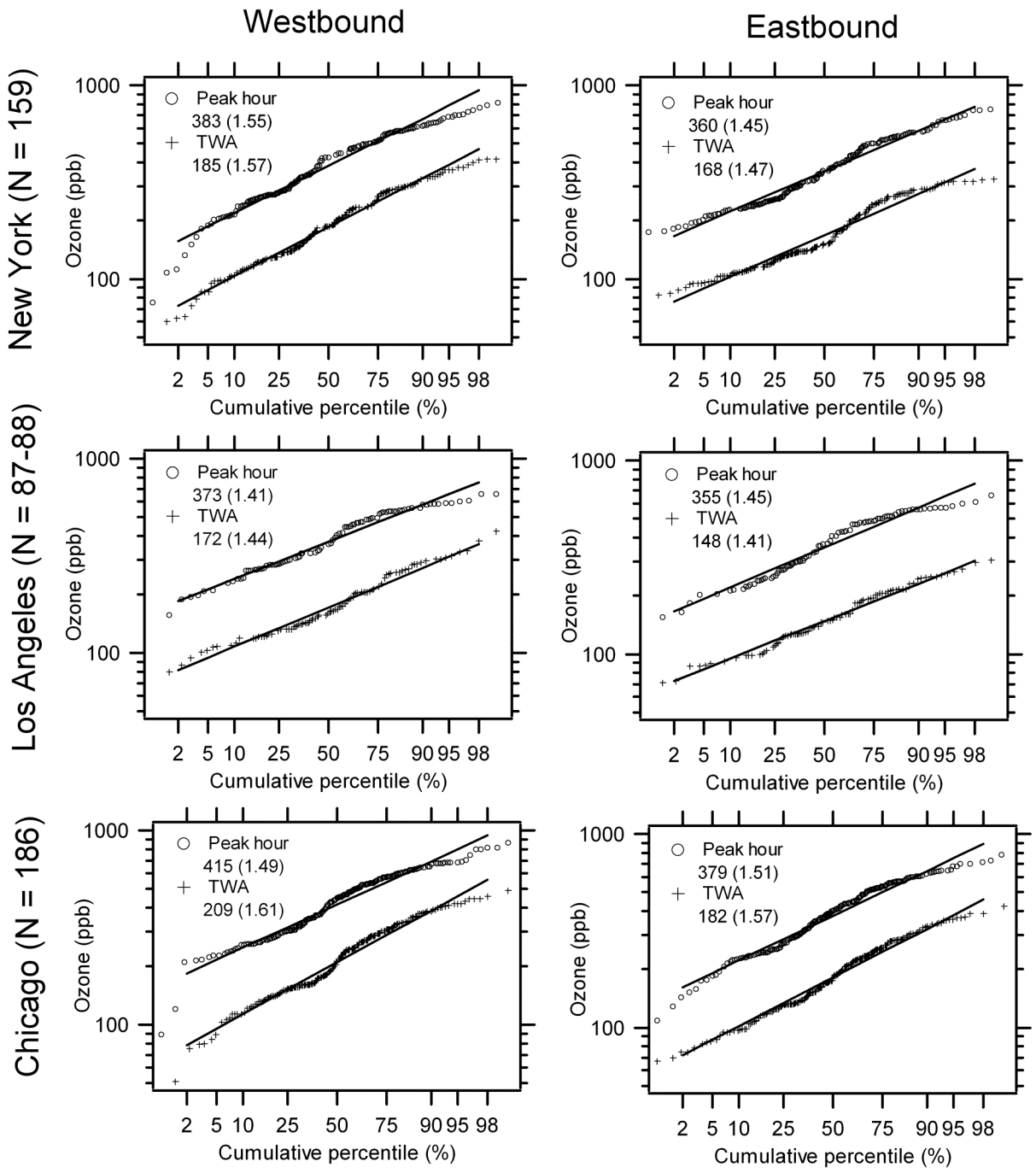

Figure 5.1. Weighted cumulative distributions of peak 1 h (upper trace) and sample-average (lower trace) ozone mixing ratios sampled outside passenger cabins of aircraft on six transatlantic routes. All flights either originated from or terminated in Munich. The weighted geometric mean and standard deviation and lognormal fits using these parameters are presented for each distribution. Data apply for the years 2000-2005.

5.4.2. Temporal effects

Figure 5.2a presents the peak 1-h ozone from the 865 flight segments, plotted against time-of-year. On all six routes, ozone varies through the year in a cyclical manner, and the timing and amplitude of the cycle is strikingly similar across routes. The degree of scatter about the mean trend also varies through the year. As summarized in Table 5.3, the value of an indicator of this scatter, the relative standard deviation of per-flight peak 1-h ozone levels, is about half as large in May-July than in Dec-Feb.

The size and statistical significance of the seasonal effect, and of the effect of the route direction (eastbound or westbound) and US arrival or departure city (LA, NY, or Chicago) on the annual mean, were determined by modeling the annual trend using the regression model shown in Equation (5.1):

$$Y = \beta_0 + \beta_1 \sin(2\pi x_1 + \phi) + \beta_2[WB] + \beta_3[LA] + \beta_4[NY] \qquad (5.1)$$

Here the response variable (Y) is the peak one-hour ozone and β_0 is the annual mean. The continuous variable x_1 is the date, converted to a real number between 0.003 (January 1) and 1.0 (December 31). The magnitude of the seasonal effect is indicated by the relative size of $2\beta_1$ in relation to β_0. The times at which the maximum and minimum are attained are reflected in the value of ϕ. The effect of the route on the annual mean is encompassed in the last three terms. For westbound routes, $WB = 1$; for eastbound routes, $WB = 0$. Similarly, $LA = 1$ for flights to or from Los Angeles, and $NY = 1$ for flights to or from New York.

Least-squares best-fit values of model parameters are summarized in Table 5.2. The sinusoidal curves described by the model are shown in Figure 5.2b. The coefficient of determination for the model fit is $r^2 = 0.98$. Results in Table 5.2 and Figure 5.2b show that the seasonal effect is large and statistically significant. The peak 1-h ozone in the flight corridor is expected to be highest in April and lowest in October-November, with a difference of 360 ppb between the two times of year. Table 5.2 also summarizes parameter values obtained by fitting equation (5.1) to flight-average ozone levels ($r^2 = 0.98$). The seasonal cycle is consistent across the two metrics – peak 1-hour and flight-average ozone – in terms of the timing of the annual high and annual low ($\phi = 6.0$ to 6.1 radians). The predicted annual mean, and the amplitude of the seasonal cycle, is half as large for flight-average ozone levels compared to peak 1-h ozone levels. The size and direction of differences in ozone levels between the six flight routes are discussed later in this section, in the context of observations about spatial (latitude, longitude, altitude) trends in flight-corridor ozone levels.

The finding of higher ozone in April and lower ozone in October-November was expected, based on previous research on in-cabin and flight-corridor ozone. Brabets et al. (1967) measured in-cabin ozone inside 285 aircraft on routes across the US, Canada, and the North Atlantic. The percent of flight time during which ozone levels were elevated above 100 ppb was greatest in March-April, and zero between August and November. Spengler et al. (2004) report in-cabin ozone levels to be greater during the winter and spring than in the summer and fall, in a survey of 106 flight segments on domestic US, Pacific, and southeast Asian routes. In our field study of in-cabin ozone, reported in Chapter 4, a sinusoidal curve fitted to data from the 46 domestic flights without ozone converters predicted maximum levels in Feb-March and minimum levels in Aug-Sept ($\phi = 0.65$ radians). Finally, data reported by NRC (2002) on ozone

levels at flight altitudes for selected months and latitudes are also consistent with the observed trend in terms of the timing of the annual cycle, and the magnitude of differences between ozone levels in the spring and the fall.

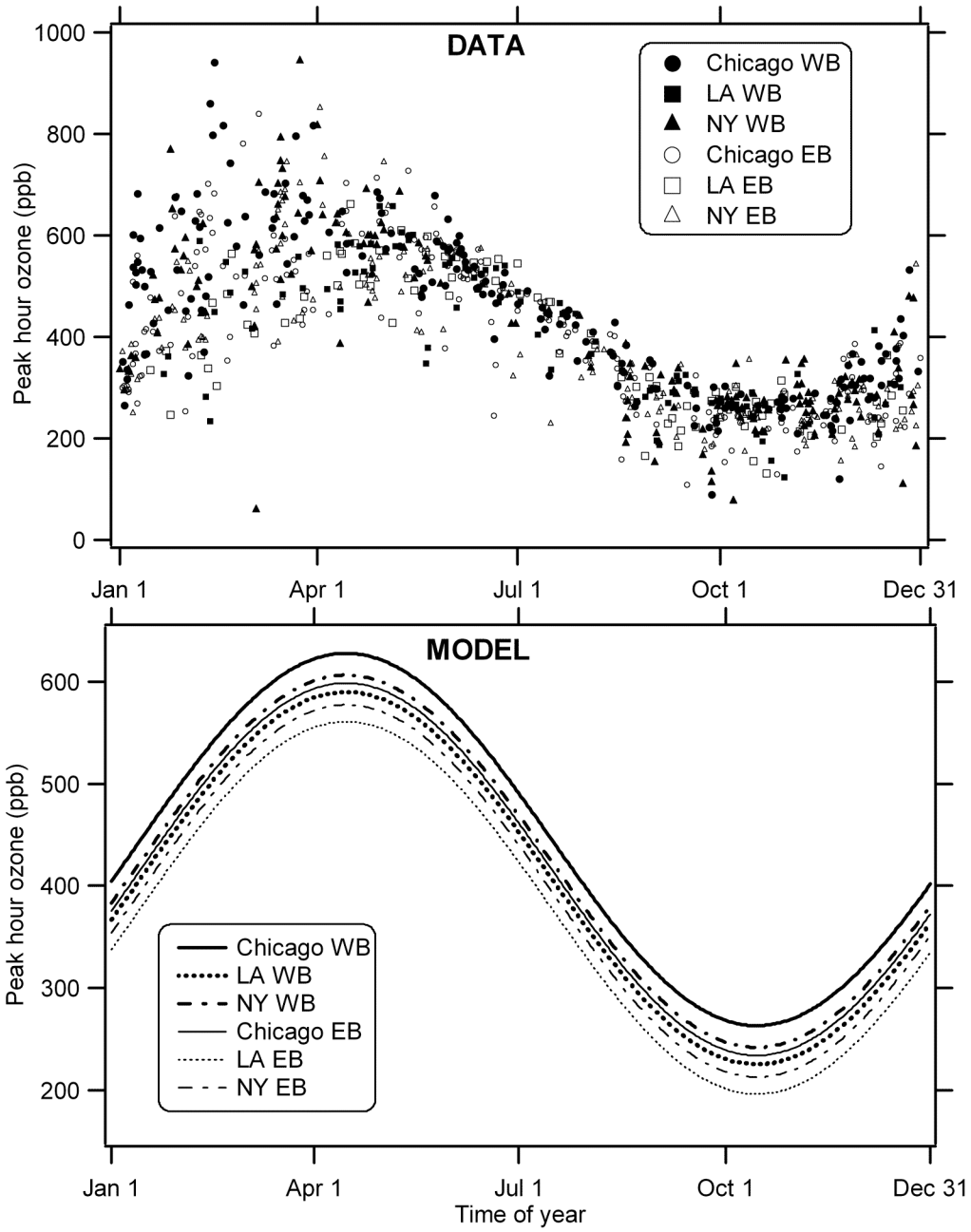

Figure 5.2. Peak atmospheric 1-h ozone encountered by aircraft on westbound (WB) and eastbound (EB) flights between Munich and each of three US cities, plotted against time-of-year. Data are presented in Fig. 5.2a (upper panel). Least-squares best-fit sinusoidal curves (Equation (5.1)) are fit to data corresponding to each route, and presented in Fig. 5.2b (lower panel). Note that the two plots have different y-axis scales.

Table 5.2. Summary of least-squares best-fit parameters for the model in Equation (5.1).

Effect	Parameter	Peak 1-h ozone		Time-weighted average ozone	
		Size	***p*-value**	**Size**	***p*-value**
Annual mean	β_0	416 ppb	<0.0001	203 ppb	<0.0001
Season (amplitude)	β_1	182 ppb	<0.0001	92 ppb	<0.0001
Season (phase shift)	ϕ	6.0 radians	<0.0001	6.1 radians	<0.0001
Westbound – Eastbound	β_2	29 ppb	<0.0001	28 ppb	<0.0001
LA – Chicago	β_3	-38 ppb	<0.0001	- 40 ppb	<0.0001
NY – Chicago	β_4	-21 ppb	0.04	- 19 ppb	<0.0001

A plot of model residuals (measured ozone minus modeled ozone) versus time-of-year (Figure 5.3) indicates that in addition to the mean seasonal trend – which is captured well by sinusoidal curves – there is an association between season and positive outliers to the model. This correlation between positive outliers and time-of-year is further highlighted in Table 5.3, which summarizes the fraction of flights per month with peak 1-h or flight-average ozone model residuals greater than 100, 200, and 300 ppb. Figure 5.3 and Table 5.3 demonstrate that very high ozone levels (defined as measured levels that exceed model predicted values by >100 ppb), occur with the greatest frequency in February.

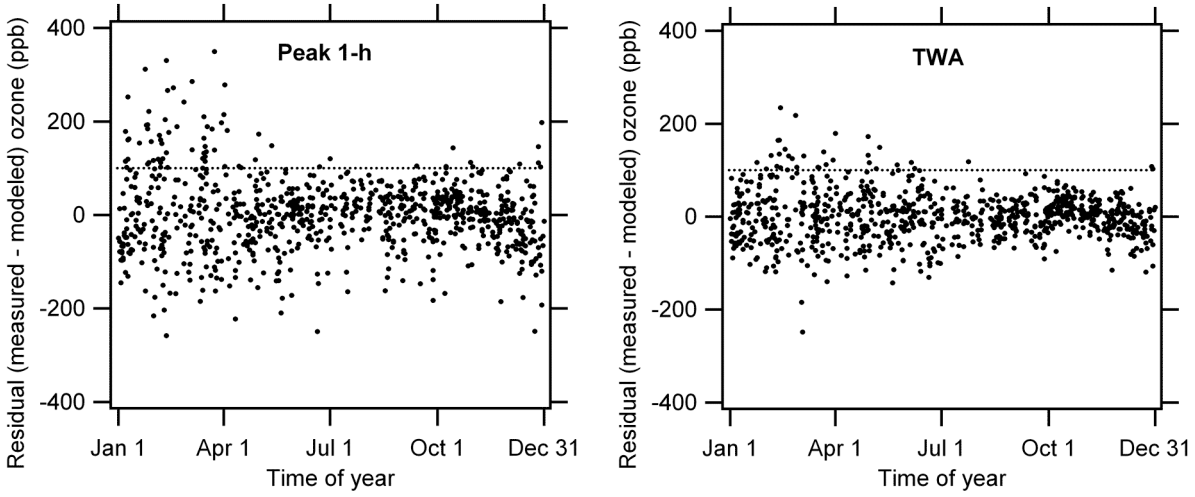

Figure 5.3. Model residuals (measured ozone minus modeled ozone) versus time-of-year for peak 1-h and flight-average ozone (N = 865). The dotted line at 100 ppb is intended to guide the eye, and shows that positive outliers to the model (where measured minus modeled ozone exceeds +100 ppb) occur most frequently around February and March.

Table 5.3. The percentage of flights per month with peak 1-h or flight-average ozone model residuals greater than 100, 200, and 300 ppb (blank cells imply a value of 0%).

	RSD [a]	Peak 1-h model residuals (%)				Flight-average model residuals (%)		
		100-200 ppb	200-300 ppb	>300 ppb	>100 ppb	100-200 ppb	> 200 ppb	>100 ppb
January	0.28	18	2	1	21	1		1
February	0.28	17	6	3	27	19	3	22
March	0.23	16	3	1	21	8		8
April	0.15	7	3		10	4		4
May	0.14	3			3	5		5
June	0.12	2			2	3		3
July	0.13	2			2	2		2
August	0.19							
September	0.23	1			1			
October	0.19	6			6			
November	0.19							
December	0.27	6			6	3		3
Annual	**0.38**	**7**	**1**	**0.5**	**8**	**4**	**0.2**	**4**

[a] The relative standard deviation of 1-h peak ozone levels measured on each flight segment during the month indicated.

A twofold effect of season on ozone levels encountered by aircraft is therefore observed. (1) Levels vary in a cyclical manner throughout the year, as would be expected by the reduction in the mean tropopause height in the hemisphere experiencing winter and spring, compared to the summer and the fall. Consequently winter and spring seasons produce a higher chance that flights at normal cruising altitudes will cross into the lower stratosphere and encounter elevated ozone. The mean trend predicts that levels are highest in April and that the scale of the high-low season difference is ~400 ppb for peak 1-h ozone, and ~200 ppb for flight-average ozone. (2) Overlaid on the seasonal cycle is a tendency for the flight to encounter, sporadically, unexpectedly high ozone levels in periods approximately between January and April. In February, the month with the highest frequency of very high ozone, 20-30% of flights encounter peak 1-h and flight-average levels that exceed the model-predicted level by more than 100 ppb. The time of year when very high ozone levels are most frequent coincides with the season when deep stratosphere to troposphere exchanges (STE) have been observed to occur at a maximum frequency, which suggests that these exchanges may account for the observed outliers.

This hypothesis linking very high ozone to STE is supported by observations from the in-cabin monitoring study as discussed in Chapter 4. The highest ozone level recorded during that study was also measured in February and also constituted a strong outlier to the mean seasonal trend in cabin-ozone levels. In that instance, the peak 1-h ozone exceeded the level predicted on the basis of season by ~200 ppb, and the flight it was measured on coincided with a major storm. We hypothesized that the storm was linked to a tropopause folding event and that the associated enhanced vertical mixing was the cause of the unusually high ozone. This hypothesis is further supported by the spatial pattern of very high ozone observations, as discussed below.

5.4.3 Spatial effects

In Figure 5.4a, locations where peak ozone levels were encountered are plotted for the 51 flights in Jan-Mar where peak 1-h ozone residuals exceeded 100 ppb. In Figure 5.4b, all ozone measurements made on these 51 flights are mapped on a latitude/longitude grid. The spatial distribution of the points on Figures 5.4a and 5.4b broadly support the hypothesis linking very-high ozone and deep STE, as northern hemisphere deep STE are known to occur most frequently over the US west coast and the western North Atlantic, in the 30-60º N latitude band (Stohl et al., 2003b).

Figure 5.4b shows that the 51 flights in Jan-Mar with very high ozone did not encounter consistently higher ozone with an increase in flight latitude, as might be expected based on the mean decrease in the tropopause height from the tropics to the poles. Instead, ozone levels encountered by the aircraft demonstrate a distinctly zonal pattern, with a tendency to be highest in the region described by the meridians 40-80º W, and parallels 40-60º N. If this region is conceived of as a rectangle, its edges are described approximately by the southern tip of Greenland and northwestern corner of Hudson Bay to the north, and Pennsylvania to the south. To assess the degree to which the zonal pattern in Figure 5.4b is specific to flights with peak 1-h ozone model residuals > 100 ppb, an analogous map is presented for all the flights in our sample from the month of June ($N = 66$; Figure 5.5). June was chosen as a representative period to assess latitude-related ozone trends that are largely independent of the influence of stratosphere-to-troposphere exchanges, because ozone levels in June are fairly well predicted by the seasonal model (i.e., the sets of peak 1-h and flight-average ozone levels measured in June have few positive outliers).

Figure 5.5 supports the observation that within the range of latitudes sampled, there is no monotonic association between latitude and ozone; instead, the spatial distribution of ozone appears to vary by zone. In June, elevated levels are distributed across most regions encompassed by the flight tracks investigated, with a band of relatively low ozone in a region that roughly corresponds to the plains states in the continental US, and that extends as far as northern Manitoba, Canada. A similar zonal pattern of low ozone on flight tracks overlaying the plains states was observed by Brabets et al. (1967). The lack of an association between ozone levels and latitude demonstrated in Figure 5.5 is consistent with the lack of a latitude-related trend in ozone levels observed for non-converter flights within the continental US in the in-cabin field study. In that study, ozone levels on transatlantic and transpacific flights (all of which had ozone converters) were found to be higher than levels on flights with converters on continental US routes. Interpreting those findings in light of the observed trend in Figure 5.5 suggests that the difference could be explained as a regional effect, rather than occurring solely as a consequence of differences in latitude across the two sets of flights.

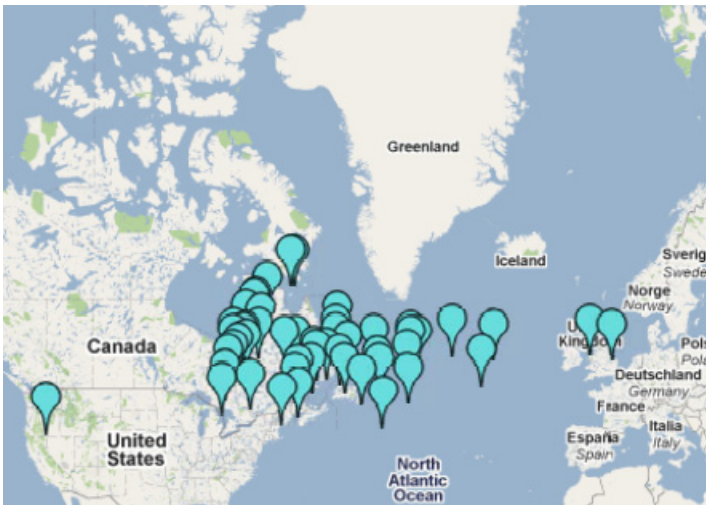

Figure 5.4a. Locations where peak ozone levels were encountered, for the 51 flights (out of 225) between Munich and Chicago, NY, and LA in Jan-Mar with peak 1-h ozone model residuals exceeding 100 ppb.

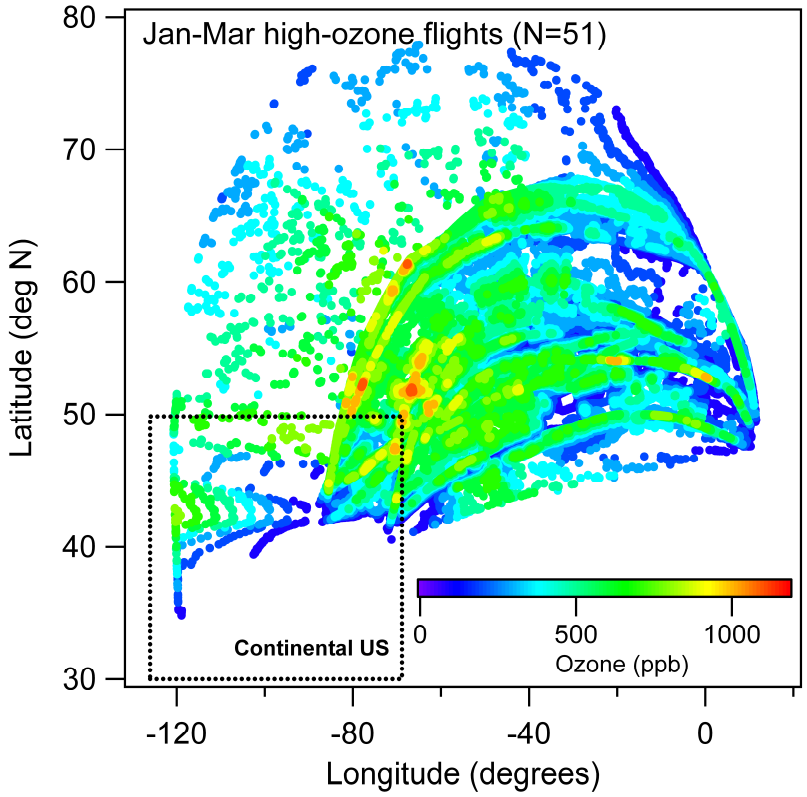

Figure 5.4b. Ozone levels measured along flight tracks, for the 51 flights (out of 225) between Munich and Chicago, NY, and LA in Jan-Mar with peak 1-h ozone model residuals exceeding 100 ppb. The highest levels are clustered in the 40-60º N latitude band, and particularly around the western North Atlantic region, which is also the zone where deep stratosphere-to-troposphere exchanges are most frequent. The rectangle tracing the approximate location of the continental United States is intended to guide the eye.

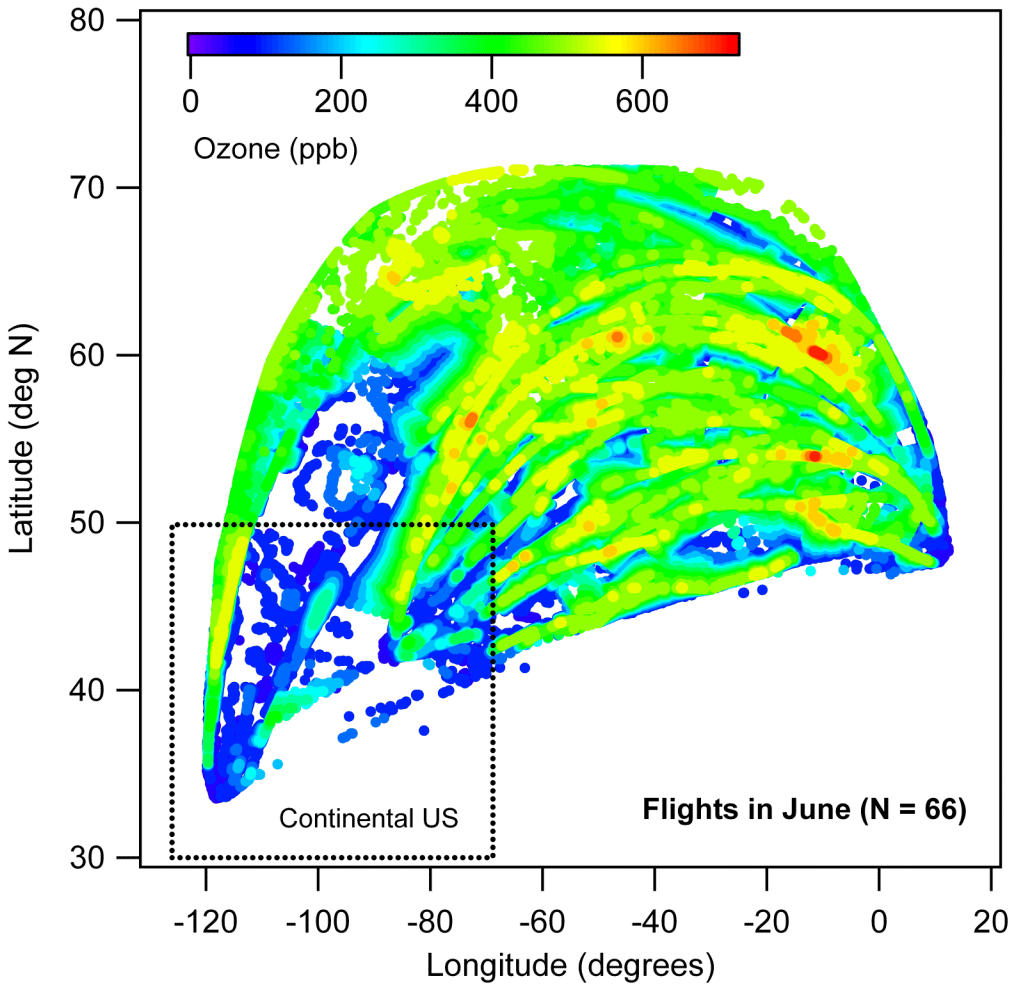

Figure 5.5. Ozone levels measured along flight tracks for the 66 MOZAIC flights between Munich and Chicago, NY, and LA monitored in June. The rectangle tracing the approximate location of the continental United States is intended to guide the eye.

The lack of a consistent, monotonic association between latitude and ozone explains why, as summarized in Table 5.2, we observe higher ozone levels on flight routes to Chicago and NY, compared to flights to Los Angeles. Based on between-flight differences in latitude alone, ozone levels are expected to increase in proportion to the east-west span of a route (within a hemisphere), because longer flights venture further north to trace greater circle routes. However, in fact, by traversing higher latitudes, flights between Munich and LA avoid much of the "high ozone" area centered around the western North Atlantic, and therefore encounter lower ozone on average than flights between Munich and Chicago or Munich and New York.

The influence of altitude on ozone levels encountered by flights is assessed by between-flight and within-flight comparisons, discussed in turn below. First, to assess the contribution of

altitude to differences in peak 1-h and flight-mean ozone levels encountered by the 865 flights in our sample, the linear regression model residuals are plotted against altitude. Figure 5.6a presents peak 1-h ozone model residuals, plotted against the mean altitude corresponding to the 1-h peak on each flight segment. Figure 5.6b presents flight-average ozone model residuals, plotted against each corresponding flight-mean altitude. Figures 5.6a and 5.6b show that the association between model residuals and altitude is, though weak, consistent and positive (linear regression coefficient of determination $r^2 = 0.2$) and suggestive of a link between altitude and flight-corridor ozone that is not accounted for by the model. The slopes of each fit suggest a mean variation on the scale of 70 ppb ozone per km increase in cruising altitude for both peak 1-h and flight-average ozone. An approximate comparison shows that this ~70 ppb value is consistent with data on the annual mean vertical distribution of ozone presented by NRC (2002). In Figure 3-1 of the NRC report (reproduced below as Figure 5.7), ozone levels at 50º N latitude (converted to mixing ratio units by assuming altitude-specific values of *P* and *T* for the "US standard atmosphere") vary from ~100 ppb at 9 km (*P* = 30.7 kPa, *T* = 230 ºK) to ~290 ppb at 11.5 km (*P* = 20.9 kPa, *T* = 217 ºK), a difference of ~73 ppb per km increase in flight altitude.

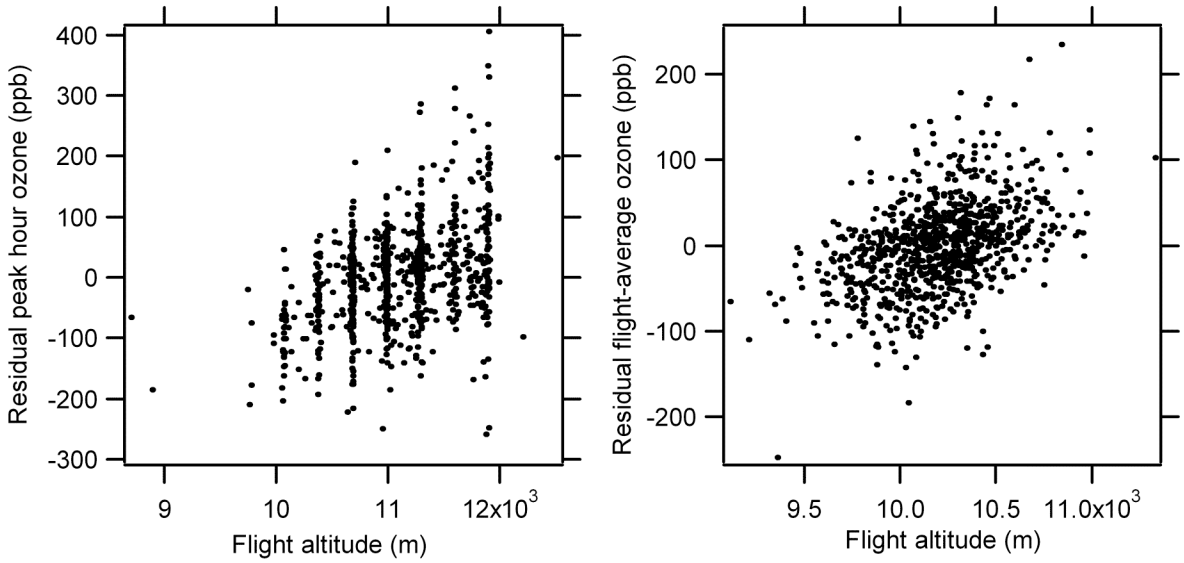

Figure 5.6. Peak 1-h ozone model residuals versus the mean altitude corresponding to the 1-h peak on each flight segment (a, left panel), and flight-average ozone model residuals versus the corresponding flight mean altitude (b, right panel). The weak (i.e. associated with a low coefficient of determination) but positive linear trend in each figure indicates an association between the flight altitude and ozone that is not accounted for by the model, equation (5.1).

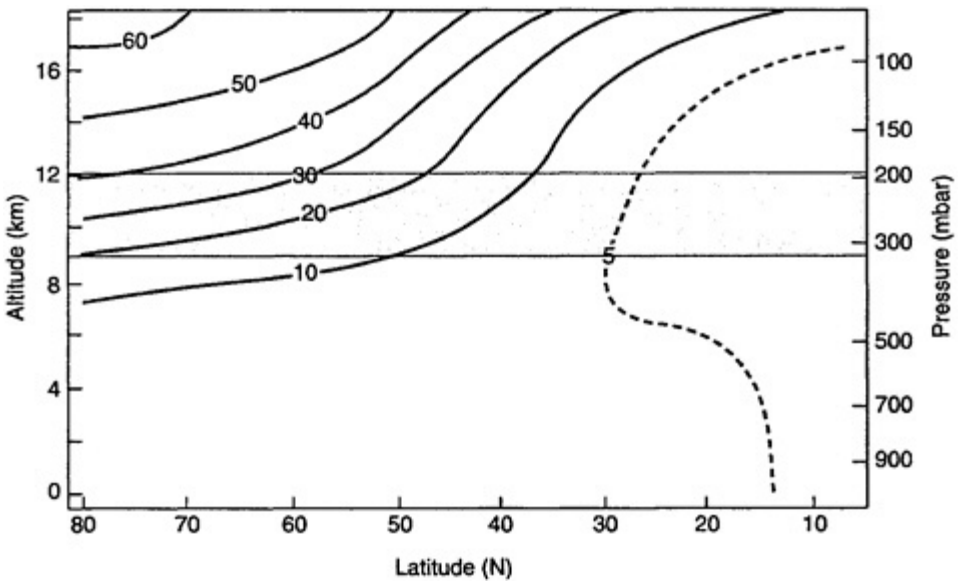

Figure 5.7. Annual mean vertical distribution of ozone (10^{11} molecules per cubic centimeter) over North America. Figure reproduced from NRC (2002).

Second, to assess the contribution of altitude to differences in ozone levels encountered during each flight, the mean flight altitude is compared with the mean altitude at which the 1-h peak is logged, by route (Figure 5.8). As flights typically gain altitude with time during a flight (until just before descent), the fraction of flight time that elapses before the 1-h ozone peak is achieved is also summarized, by route (Table 5.4), as a second indicator of the influence of altitude on within-flight ozone levels. Table 5.4 and Figure 5.8 show that the 1-h ozone peak for each flight segment is, on average, encountered during the second half of a flight (55 – 68% into the flight) on both eastbound and westbound routes, when the flight altitude (i.e. 1-h average coinciding with the 1-h ozone peak) is 0.7 – 1 km greater than the mean flight altitude.

The trends encapsulated in Figure 5.8 and Table 5.4 suggest the flights in our sample were, on average, more likely to encounter elevated ozone when they gained altitude on their journey between Munich and the US. The effect of altitude relative to effects of the other spatial coordinates (i.e. latitude/longitude) is further resolved by translating the average time-to-peak parameter into an average "distance", in terms of flight hours, from Munich (Table 5.5). Table 5.5 reveals a distinct eastbound versus westbound difference in the average "location" of the 1-h ozone peak per flight. For flights *to* Munich, the 1-h ozone peak was encountered 3.2 – 3.6 h flight time from Munich. For flights *from* Munich, the 1-h ozone peak was encountered significantly further away – 5.0 – 6.9 h from Munich – with the distance from Munich scaling in relation to the duration of the flight.

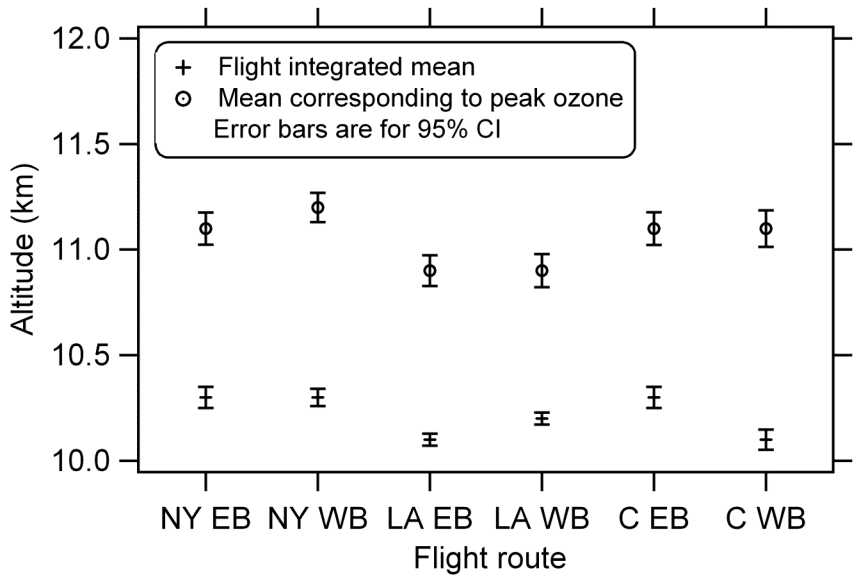

Figure 5.8. The mean flight-average altitude (10.1 – 10.3 km), and the mean altitude at which peak 1-h ozone levels are logged (10.9 – 11.2 km), for the six flight routes investigated.

Table 5.4. The fraction of flight time elapsed before the 1-h ozone peak is logged, by route.

Route	**Avg. flight duration (h)**	**Avg. time-to-peak** [a]	***N***
Chicago EB	8.1	0.55 ± 0.22	186
LA EB	10.8	0.68 ± 0.16	87
NY EB	8.1	0.56 ± 0.23	159
Chicago WB	9.3	0.64 ± 0.20	186
LA WB	11.8	0.59 ± 0.17	88
NY WB	8.5	0.59 ± 0.22	159

[a] Expressed as a fraction of the flight duration

Table 5.5. The mean "distance" from Munich when the 1-h ozone peak is logged, by route.

Route	**"Location" of 1-h ozone peak** [a]
Chicago EB	3.6 ± 1.8
LA EB	3.5 ± 1.7
NY EB	3.2 ± 1.7
Chicago WB	6.0 ± 1.9
LA WB	6.9 ± 2.1
NY WB	5.0 ± 1.9

[a] The location is indicated in terms of flight time out of Munich, in hours

The flight times/distances in Table 5.5 are evidence of the combined influence of two spatial trends in ozone levels encountered by aircraft. (1) Flights encounter peak levels of ozone in the latitude/longitude zone that corresponds to the 3 – 7 h "distance" from Munich. As the flight speed is approximately 850 km h^{-1}, this corresponds to about 2500 km to 6000 km away from Munich along flight tracks (for sample flight tracks, see Figure 5.9). This spatial zone is centered around the western North Atlantic, further supporting the hypothesis that ozone in the flight corridor varies by zone, rather than monotonically with latitude. (2) Within the latitude/longitude zone of high atmospheric ozone levels, differences in the location of the peak are sensitive to differences in flight altitude. Therefore EB flights, which attain their maximum altitude closer to Munich, have a corresponding tendency to log their highest ozone exposures closer to Munich. The reverse is true for WB flights. This difference may explain the trend for ozone levels to be higher, overall, on WB flights than on EB flights. For WB flights, the high flight altitude coincides with the latitude/longitude zone observed to have the highest atmospheric ozone levels, so the two effects reinforce one another. For EB flights, the high altitudes along flight tracks occur closer to Europe where atmospheric ozone levels at flight altitudes are not quite as high.

To illustrate the combined effects of latitude, longitude and altitude on ozone levels encountered by aircraft, Figures 5.10a and 5.10b present the ozone data from all flights in June, and from the 51 flights in Jan-Mar with very high ozone, resolved into four altitude bins: <9.6 km, 9.6 – 10.6 km, 10.6 – 11.5 km, and > 11.5 km. The association between altitude and ozone is much stronger for the Jan-March high ozone flights mapped in Figure 5.10b, compared to the flights in June mapped in Figure 5.10a. For both sets of flights, the highest bracket of ozone levels (roughly, those greater than 600 ppb) are only observed at altitudes greater than 10.6 km. For the flights in June, there is no clear trend of increasing ozone with altitude above 10.6 km. For the very-high ozone flights, however, there is a further association between ozone and altitude in the > 10.6 km bracket, whereby levels greater than ~1000 ppb are present above 11.5 km.

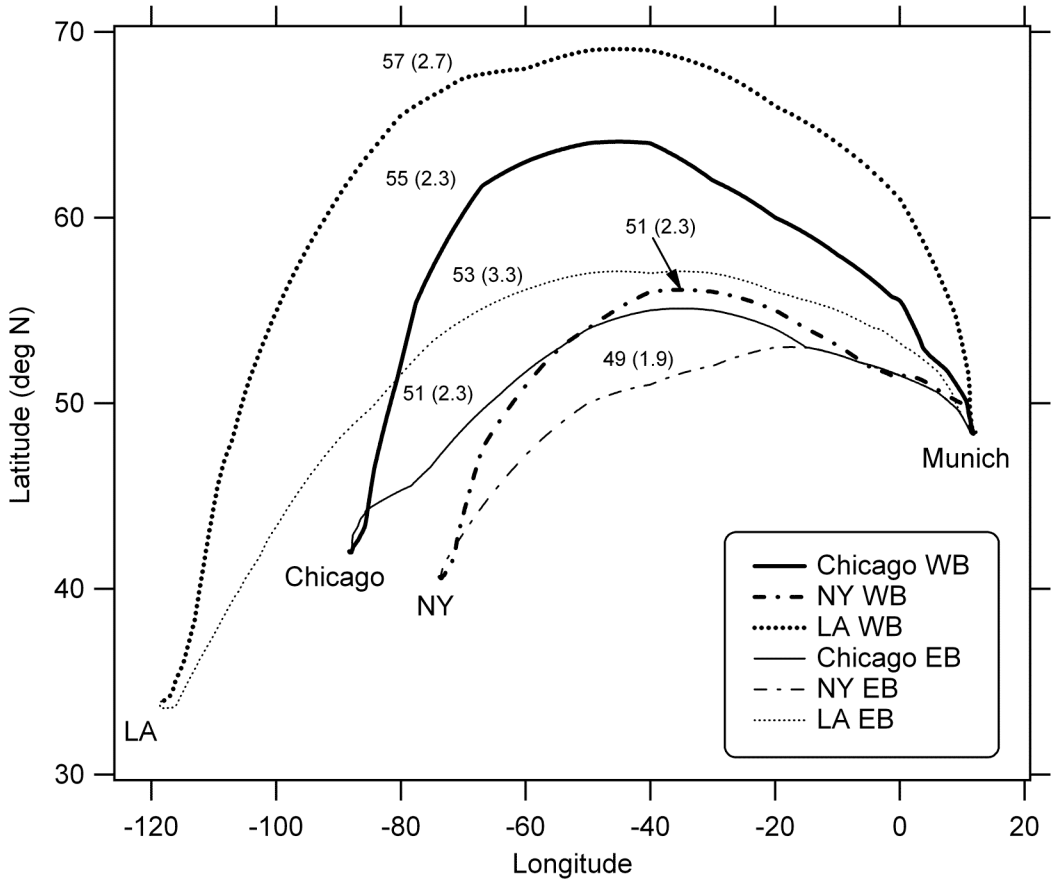

Figure 5.9. Sample flight tracks for the route between Munich and each of three US cities. The tracks shown correspond to flights selected at random from a period also selected at random: June-July 2005. For all routes, westbound tracks trace higher latitudes compared to eastbound tracks, and flights going further West fly at higher latitudes. The numbers indicated near each trace are the average (standard deviation) flight latitudes for all flights on that route.

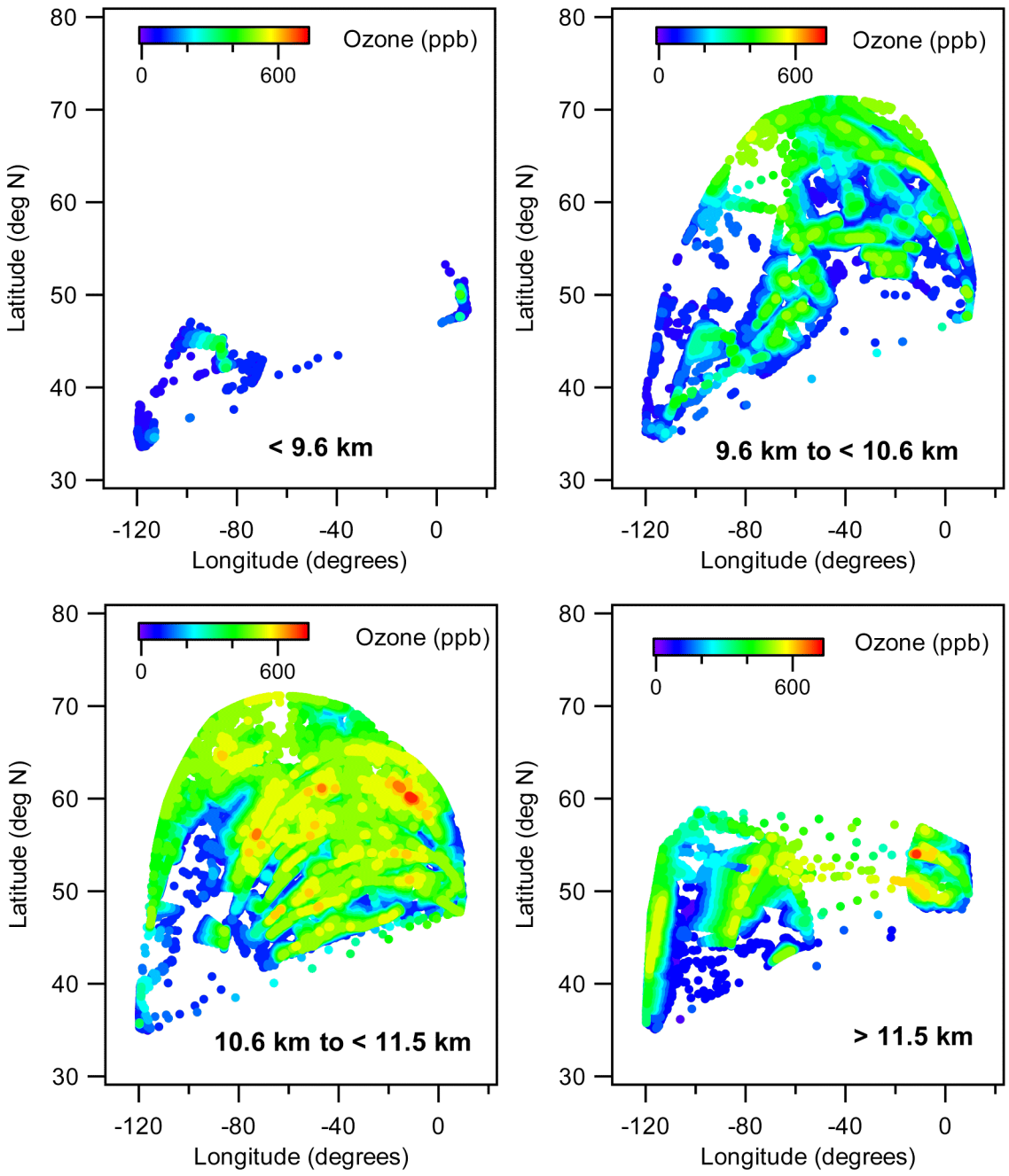

Figure 5.10a. Ozone levels measured along flight tracks for the 66 MOZAIC flights between Munich and either Chicago, NY, or LA monitored in June. Measurements range from 0-725 ppb, and are grouped into four bins, according to altitude.

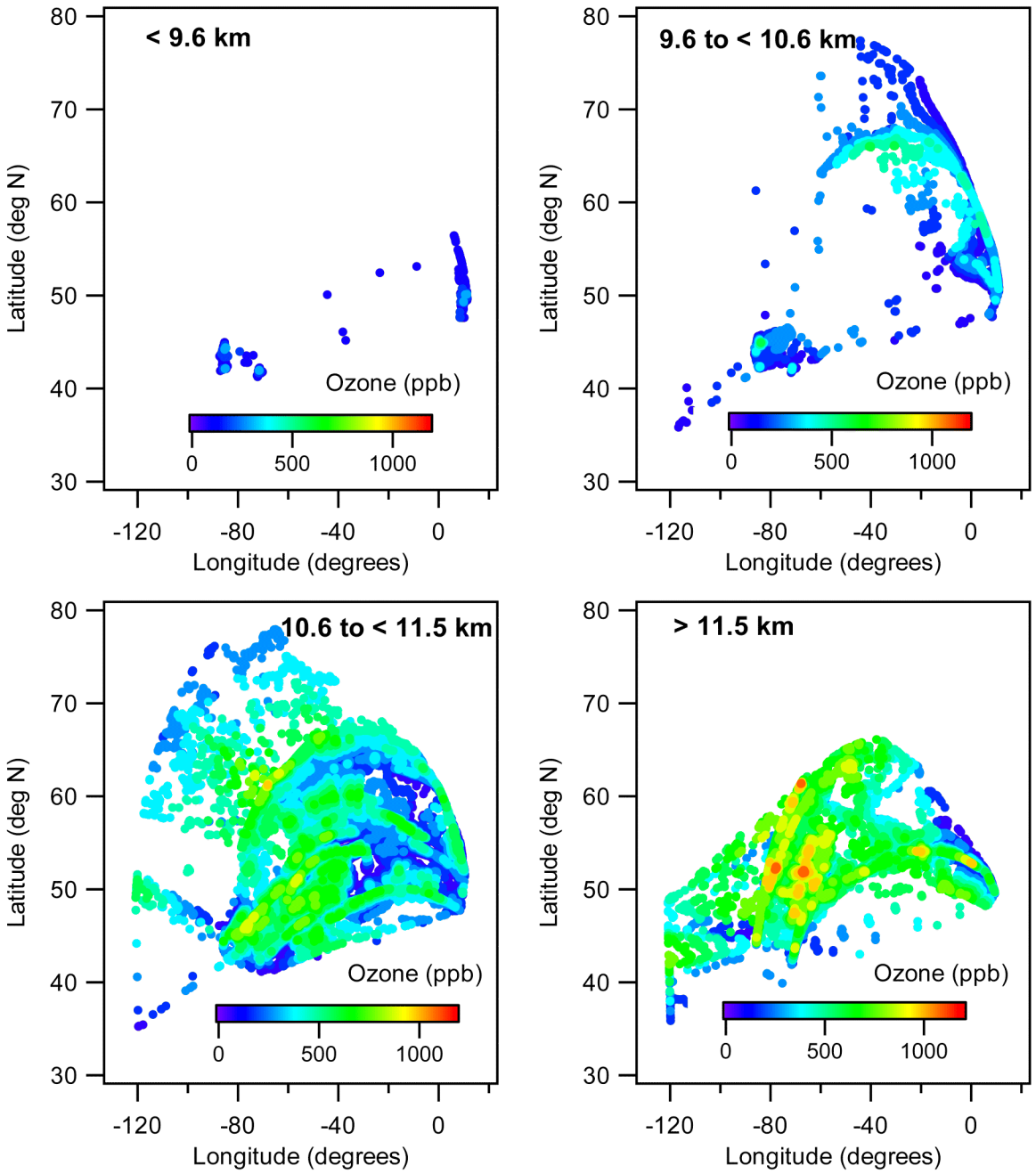

Figure 5.10b. Ozone levels measured along flight tracks for the 51 MOZAIC flights between Munich and either Chicago, NY, or LA with very high ozone, monitored in Jan-Mar. Measurements range from 0-1200 ppb, and are grouped into four bins, according to altitude.

5.5. Implications for in-cabin ozone exposures

This investigation reinforces the expectation that flights on transatlantic routes routinely encounter very high ozone levels, with annual means of approximately 200 and 400 ppb for flight-average and 1-h peak ozone, respectively. Without a control device (a catalyst or "converter") to remove ozone from the ventilation air before it enters the cabin, corresponding in-cabin levels of ozone and ozone reaction byproducts would be unacceptably high – especially between February and June – and could commonly exceed the limits specified in Federal Aviation Regulations (FAR 25.832 and FAR 121.578).

A parameter known as the "retention ratio" (or R-value) is defined as the indoor proportion of outdoor ozone in the absence of a control device. The R-value enables in-cabin ozone levels to be estimated, given the range of flight-corridor ozone levels reported in this study. The R-value depends on cabin surface materials, occupant density, the surface area to volume ratio, and the design and operation of the aircraft ventilation system. Nastrom et al. (1980) report R-values between 0.47 and 0.83, based on a study where cabin and ambient ozone levels were measured simultaneously. More recently, R-values in the range 0.2-0.4 were calculated by Coleman et al. (2008), based on chamber experiments measuring ozone consumption on materials found in aircraft cabins, combined with a common range of cabin air-exchange rates and expected friction velocities. For demonstrating compliance with FAA ozone regulations, aircraft can be assigned a default R-value of 0.7 (NRC, 2002).

Based on R = 0.7, in-cabin peak 1-h and flight-average ozone levels on the 865 flights investigated would be expected to range from approximately 60 to 600 ppb, and 35 to 350 ppb, respectively. With this default R-value, flight-average ozone levels would exceed 100 ppb on more than 95% of flights between February and June. The high ozone levels would be accompanied by correspondingly high levels of ozone reaction byproducts. According to chamber-experiments, the total byproduct yield is predicted to range from 0.07 to 0.24 moles of products volatilized per mole of ozone consumed (Coleman et al., 2008). The byproduct yields during experiments in an occupied simulated cabin exceeded the range of values predicted by the chamber experiments, at 0.25 to 0.30 moles of product volatilized per mole of ozone consumed (Weschler et al., 2007). The mix and mixing ratio of oxidized species formed depends in part on occupancy conditions in the cabin. Human skin oils, most prominently squalene, react with ozone to generate characteristic products that desorb to the gas phase or, if they are less volatile, remain on the skin. Owing to reactions occurring on the body envelope, levels of byproducts in the breathing zone are expected to be greater than average levels in the cabin. (Wisthaler and Weschler, 2010; Nazaroff and Weschler, 2010).

As flights on transatlantic routes are routinely equipped with ozone converters (in response to the introduction of the FARs limiting cabin ozone), this illustration serves both to demonstrate the exposures avoided through use of the converters, and to define worst-case scenarios for conditions where a converter is absent or fails to perform adequately. The next illustration considers in-cabin levels of ozone that might be expected on the current fleet of aircraft plying transatlantic routes. When new, converters on these aircraft have an expected ozone destruction efficiency (η) of 90-98% (NRC, 2002). If the aircraft in our sample are modeled as having a converter with $\eta = 0.95$, and R = 0.7, ozone levels in the cabin are effectively controlled, with predicted in-cabin flight-average and 1-h peak ozone levels less than 18 ppb and 33 ppb, respectively, across all 865 flights investigated.

However, the efficiency of the catalysts is degraded with use, and they are subject to replacement or maintenance once the efficiency drops below 60% (Hunt et al., 2010). At η = 60%, our results indicate that in-cabin ozone exposures could be substantial. For example, with $\eta = 0.60$ and R = 0.7, 97% of flights in February-June (and 55% of all flights) would have a predicted in-cabin peak 1-h ozone level exceeding 100 ppb; 6% of all flights would have in-cabin flight-average ozone levels exceeding 100 ppb. These observations highlight the importance not only of equipping transatlantic flights with converters, but also of ensuring they function well throughout their service life.

5.6. Conclusions

This investigation adds to the state of knowledge regarding ozone encountered by commercial passenger airplanes during flight, on transatlantic routes. Ozone levels were found to vary strongly and consistently with season, with maximum levels observed in April, and minimum levels in October. The spatial and temporal distribution of the highest bracket of ozone levels encountered by aircraft in our sample suggests these may be associated with intermittent tropopause folding, which occurs most frequently in the winter months, in the western North Atlantic region. For the routes investigated, flights at higher latitudes did not encounter systematically higher ozone than flights at lower latitudes. Instead, the relatively moderate differences between ozone levels observed on each of the six routes were linked to the combined influence of zonal (i.e. latitude/longitude) ozone trends, and flight altitude. As airplanes gain altitude with time during a flight, and because flights at higher altitudes are more likely to encounter elevated atmospheric ozone levels, the 1-h ozone peak per flight was observed, on average, during the second half of each flight segment.

Though this investigation included only transatlantic routes, maps of the spatial distribution of ozone along the flight routes studied allow a glimpse into levels of ozone in the flight corridor overlaying a portion of the continental US and thus provide a perspective on ozone levels that might be encountered on domestic routes as well. The results show that even on domestic routes (which are frequently traversed by aircraft without ozone converters), elevated ozone at levels of hundreds of ppb is routinely encountered, especially in a zone near the central west US, and in the northeast quadrant of the country (Figure 5.4b and 5.5). Therefore the present investigation supports the case made in Chapter 4 for the benefit of using ozone converters to reduce ozone exposure in all airplanes capable of transcontinental flight, even those only used on domestic routes.

Flight route planning is one strategy airlines can use to comply with ozone FARs. Data to aid with planning efforts are based on statistical summaries of atmospheric ozone as a function of altitude, latitude, and month (NRC, 2002). The results presented here indicate that planning-based risk management techniques may be effective in predicting ozone trends based on month and altitude. However, in addition to being based on mean trends in the position of the tropopause, planning should take account of the intermittent influence of tropopause folding events, especially when considering ozone that might be encountered in the winter months. Moreover, our results suggest that within the transatlantic flight corridor, latitude is not associated monotonically with ozone, so flight-route planning based on expected latitude trends may not be particularly effective.

5.7. References

Appenzeller C, Davies HC, 1992. Structure of stratospheric intrusions into the troposphere. *Nature* **358**, 570-572.

Brabets RI, Hersh CK, Klein MJ, 1967. Ozone measurement survey in commercial jet aircraft. *Journal of Aircraft* **4**, 59-64.

Coleman BK, Destaillats H, Hodgson AT, Nazaroff WW, 2008. Ozone consumption and volatile byproduct formation from surface reactions with aircraft cabin materials and clothing fabrics. *Atmospheric Environment* **42**, 642-654.

El Amraoui L, Attie J-L, Semane N, Claeyman M, Peuch V-H, Warner J, Ricaud P, Cammas J-P, Piacentini A, Josse B, Cariolle D, Massart S, Bencherif H, 2010. Midlatitude stratosphere-troposphere exchange as diagnosed by MLS O_3 and MOPITT CO assimilated fields. *Atmospheric Chemistry and Physics* **10**, 2175-2194.

Holton JR, Haynes PH, McIntyre ME, Douglass AR, Rood RB, Pfister L, 1995. Stratosphere-troposphere exchange. *Reviews of Geophysics* **33**, 403-439.

Hunt EH, Reid DH, Space DR, Tilton FE. Commercial airliner environmental control system. www.boeing.com/commercial/cabinair/ecs.pdf. Accessed on September 15, 2010.

Law KS, Plantevin PH, Shallcross DE, Rogers HL, Pyle JA, Grouhel C, Thouret V, Marenco A, 1998. Evaluation of modeled O_3 using Measurement of Ozone by Airbus In-Service (MOZAIC) data. *Journal of Geophysical Research-Atmospheres* **103**, 25,721-25,737.

Marenco A, Thouret V, Nédélec P, Smit H, Helten M, Kley D, Karcher F, Simon P, Law K, Pyle J, Poschmann G, Von Wrede R, Hume C, Cook T, 1998. Measurement of ozone and water vapor by Airbus in-service aircraft: the MOZAIC airborne program, an overview. *Journal of Geophysical Research-Atmospheres* **103**, 25,631-25,642.

Morgenstern O, Marenco A, 2000. Wintertime climatology of MOZAIC ozone based on the potential vorticity and ozone analogy. *Journal of Geophysical Research-Atmospheres* **105**, 15,481-15,493.

MOZAIC, 2010. Measurement of ozone, water vapor, carbon monoxide and nitrogen oxides by Airbus in-service aircraft. Papers making use of MOZAIC data. http://mozaic.aero.obs-mip.fr/web/features/publications.html. Accessed on August 25, 2010.

Nastrom GD, Holdeman JD, Perkins PJ, 1980. Measurements of cabin and ambient ozone on B747 airplanes. *Journal of Aircraft* **17**, 246-249.

Nazaroff WW, Weschler CJ, 2010. Ozone in passenger cabins: concentrations and chemistry, Final Report, Office of Aerospace Medicine, Washington, DC.

NRC (National Research Council) Committee on air quality in passenger cabins of commercial aircraft. *The Airliner Cabin Environment and the Health of Passengers and Crew.* National Academy Press, Washington, DC, 2002.

Perkins PJ, Holdeman JD, Nastrom GD, 1979. Simultaneous cabin and ambient ozone measurements on two Boeing 747 airplanes, Volume 1, US Department of Transportation, Federal Aviation Administration, Washington, DC. Available at ntrs.nasa.gov.

Spengler JD, Ludwig S, Weker RA, 2004. Ozone exposures during trans-continental and trans-pacific flights. *Indoor Air* **14 (Suppl 7)**, 67-73.

Sprenger W, Maspoli MC, Wernli H, 2003. Tropopause folds and cross-tropopause exchange: a global investigation based upon ECMWF analyses for the time period March 2000 to February 2001. *Journal of Geophysical Research* **108** (D12), STA 3-1-11.

Stohl A, Bonasoni P, Cristofanelli P, Collins W, Feichter J, Frank A, Forster C, Gerasopoulos E, Gäggeler H, James P, Kentarchos T, Kromp-Kolb H, Krüger B, Land C, Meloen J, Papayannis A, Priller A, Seibert P, Sprenger M, Roelofs GJ, Scheel HE, Schnabel C, Siegmund P, Tobler L, Trickl T, Wernli H, Wirth V, Zanis P, Zerefos C, 2003a. Stratosphere-troposphere exchange: a review, and what we have learned from STACCATO. *Journal of Geophysical Research* **108** (D12), STA1-1-15.

Stohl A, Wernli H, James P, Bourqui M, Forster C, Liniger MA, Seibert P, Sprenger M, 2003b. A new perspective of stratosphere-troposphere exchange. *Bulletin of the American Meteorological Society* **84**, 1565-1573.

Weschler CJ, Wisthaler A, Cowlin S, Tamás G, Strøm-Tejsen P, Hodgson AT, Destaillats H, Herrington J, Zhang J, Nazaroff WW, 2007. Ozone-initiated chemistry in an occupied simulated aircraft cabin. *Environmental Science and Technology* **41**, 6177-6184.

Wisthaler A, Weschler CJ, 2010. Reactions of ozone with human skin lipids: sources of carbonyls, dicarbonyls, and hydroxycarbonyls in indoor air. *PNAS* **107**, 6568-6575.

Chapter 6: Conclusions

6.1. Summary of findings

The research presented in this dissertation explores inhalation exposures to two dynamic air pollutants in two important settings: ozone in aircraft cabins and ultrafine particles (UFP) in residences. Administrative and technological challenges have limited prior efforts to acquire time-resolved data under normal occupied conditions on these two pollutant-environment pairs; such data are important for understanding human exposures and consequent health risks. Hence, our knowledge of these two exposure circumstances has been based more on measurements of ambient concentrations, concentrations measured in unoccupied or controlled indoor environments, or on historical data than on current data acquired in the presence of humans engaged in habitual activity patterns. This dissertation addresses the knowledge gap by presenting new field data acquired under normal use conditions from occupied microenvironments. Observed pollutant trends are modeled for the purposes of assessing and apportioning exposure and to assess the importance for indoor concentrations and exposures of variables such as outdoor levels, ventilation characteristics, indoor sources, pollutant dynamics, human factors and control strategies. Study findings can be applied to assess and more effectively control health risks associated with each exposure scenario and to suggest conditions under which interventions are likely to have the greatest public health impact.

Residences were studied because people spend a large proportion of time in their own homes. As a consequence, exposures that occur indoors at home have the potential to contribute significantly to total daily exposures and hence to adverse health outcomes resulting from air pollutant exposure. Moreover, several sources and sinks of ultrafine particles occur uniquely in residences. And owing to their use in an enclosed space in close proximity to humans, residential sources can lead to high cumulative and peak exposures. Results from the field investigation of ultrafine particles in California residences presented in Chapter 2 reinforce and substantiate the expectation that residential exposure to ultrafine particles cannot be characterized by ambient measurements alone. Reasons include (1) the importance of indoor sources and (2) variations in the indoor proportion of outdoor particles across sites and as a function of several variables that change with time during the day and year. Owing to the association between occupancy and UFP levels indoors, residential exposures also cannot be characterized by average indoor concentrations alone. Levels measured in homes were, on average, 1.7× greater during occupied relative to unoccupied hours because occupants, when present and awake, engage in activities that emit particles.

In Chapter 2, the "indirect" method was used to quantify occupant exposures and a model based on the principle of material balance was developed and applied to apportion exposures among source categories. The geometric mean time-average residential UFP exposure concentration for 21 study subjects in seven monitored homes was assessed as 14,500 particles per cm^3 (GSD = 1.8). The average exposure duration (i.e. time spent at home) was 17 ± 1.7 h/d (mean ± standard deviation). Episodic indoor source activities, most notably cooking, caused the highest peak exposures and most of the variation in exposure among homes. The average contribution to residential exposures from indoor episodic sources was 150% of the contribution

from particles of outdoor origin. A previously uncharacterized continuous indoor source – unvented natural-gas pilot lights – contributed 10-19% to exposure for the two households where present.

Activities and appliances observed to be sources of ultrafine particles indoors included "continuously emitting" combustion devices such as gas stoves or candles; heated surfaces that could be characterized as "sudden-burst emitters" such as an electric-stove or a vented furnace; and cleaning with terpene-based products in the presence of sufficient quantities of ozone to generate particles by secondary formation. Mean source strengths per episode ranged from 2-3 $\times$ 10^{12} particles for low-emitting sources (e.g., a steam iron, clothes dryer, and wall-furnace) to 26-41 $\times$ 10^{12} particles for high-emitting sources (e.g., a candle, central air furnaces, and gas stoves). The first-order particle loss-rate coefficient, representing removal by all processes, had a geometric mean of 1.6 h^{-1} (GSD = 1.5) and did not vary systematically across source types.

The intrusion of outdoor particles and emissions from indoor continuous sources determined the baseline particle level indoors. The indoor proportion of outdoor particles (*IPOP* or infiltration factor) ranged, on average, from 0.1 to 0.5 across sites (mean = 0.4). As such, values of the *IPOP* were found to be lower for ultrafine particles than values previously reported for fine particle mass, as would be expected for this more dynamic species. Making houses more airtight can provide better protection from outdoor particles but also leads to higher exposures to particles generated indoors. When present, active filtration or air treatment was seen to be an effective means of reducing the persistence of particles from outdoors and indoors alike.

In Chapter 3 semi-empirical intake fractions quantifying source-to-receptor relationships were assessed for episodic indoor source events and continuous sources observed during the field study described in Chapter 2. Estimates of the aggregate (i.e., summed over all occupants) intake fraction spanned an approximately 20-fold range, from 0.7 $\times$ 10^{-3} to 16 $\times$ 10^{-3}. The geometric mean aggregate *iF* for the 50 episodic source events analyzed was 3.8 $\times$ 10^{-3}. As the mean number of residents per site was three, individual intake fractions were approximately three times smaller than aggregate *iF*. The reported range in values is consistent with limited prior research showing that intake fractions for indoor releases are approximately one in a thousand. Exposures during "awake" hours dominated the intake associated with episodic sources because episodic indoor sources are tied to human activities.

A comparison of episodic intake fractions across events, sites, and demographic groups showed that the house site had a significant influence on *iF*, with higher *iF* associated with sites with a smaller volume per resident. Human factors, such as occupancy and sleep patterns, and the variability in the breathing rates linked to age and gender, caused substantial variations between individual *iF* assessed for each episodic source event. The *iF* for children, for episodic source events, was 16% lower on average than the corresponding *iF* for adults owing to a greater number of hours spent asleep. Aggregate intake fraction estimates were ~30% less than they would have been if activity patterns and demographic differences were ignored and all occupants were treated as being present and awake throughout indoor emission episodes. In Chapter 2, we observed the type of source had a significant effect on emissions of and exposures to ultrafine particles. However, source-type was not demonstrated to have an independent effect on *iF* under the conditions sampled.

In Chapters 4 and 5 the focus of this dissertation shifted from buildings to transportation vehicles, and from ultrafine particles to ozone. The transportation environment studied, passenger cabins of commercial aircraft during flight, has several exposure-relevant features that are distinct from residences. The air-cabin microenvironment is, compared to houses, more

densely occupied. Occupants spend much less time in this environment than they do in their own homes, but when present they do not have the options of leaving or of significantly modifying their local environment if conditions become unfavorable. Air-traffic routes take airplanes into the upper troposphere and lower stratosphere, while houses are located in the atmospheric boundary layer, and are as such exposed to different airborne constituents and temperature/relative humidity conditions. Finally, houses typically have a lower air exchange rate compared to airplane cabins, although the volume flow rate of ventilation air per occupant is generally higher in residences than in aircraft cabins.

In Chapter 4, results are presented from a field campaign that represents the largest published survey since 1980 of time-resolved ozone levels in aircraft cabins during flight. A few monitoring surveys on a similar or larger scale were conducted in the 1960s and 1970s, but data from those studies are not representative of conditions currently experienced by passengers in economy cabins, both because of the significant changes to aircraft design and operation since 1980, and because in the early surveys monitoring was not conducted in the main cabin, in close proximity to passengers.

The novel field data presented and interpreted in Chapter 4 show ozone levels vary with season, as was expected owing to the mean seasonal changes in the tropopause height. In-cabin levels also varied strongly with the presence or absence of an ozone "converter" or control device. Levels on aircraft without converters, all of which were on domestic routes, were moderate on average with a geometric mean peak 1-h ozone of 33 ppb (GSD = 2.3). Converters were effective at reducing in-cabin ozone, so that the peak 1-h ozone level on domestic flights with converters did not exceed 10 ppb. For aircraft with converters, levels were elevated on flights following long-haul, transoceanic routes relative to those restricted to domestic routes. Aircraft type may have contributed to differences within our transoceanic sample; newer aircraft models appear to have more efficient converters. Individual in-cabin ozone exposures, expressed in units of concentration × time, were in the range 100-600 ppb-h for 40-50% of transoceanic flights (with converters) and domestic flights without converters. On a few domestic non-converter flights ozone levels were very high and the 1-h peak and sample mean exceeded 100 ppb. These high-ozone flights coincided with major storms, which appeared to be indicators of tropopause folding events that were the likely drivers of the high ozone.

As in-cabin ozone data are scarce and as ozone in the cabin originates in the air outside, the investigation in Chapter 4 was augmented by a study of atmospheric ozone levels collected as part of the MOZAIC monitoring campaign. Results from analysis of MOZAIC data are presented in Chapter 5 and substantiate the finding from Chapter 4 that ozone levels encountered by aircraft vary with season. As with the in-cabin data, the effect of season was observed to have two important components, consisting of (1) a mean annual trend that is plausibly explained by mean seasonal changes in the tropopause height and predicts maximum levels in the spring, and (2) a tendency for the highest bracket of ozone levels that are outliers to the mean trend to cluster in the winter. The spatial and temporal distribution of the high ozone levels suggests, as did the highest levels measured inside the cabin, that they are associated with intermittent tropopause folding that occurs most frequently in the winter months in the western North Atlantic region and around the central west US.

In addition to providing insight into temporal trends in ozone levels encountered by commercial passenger aircraft, Chapter 5 builds on the findings in Chapter 4 by elucidating spatial trends. Contrary to expectations, within the 40º – 80º north latitude band spanned by the US and transatlantic flight corridors, there was no consistent or monotonic association between

ozone and latitude. Hence the analysis of MOZAIC data suggests that the higher ozone on long-haul versus domestic US routes observed during the in-cabin monitoring study is better explained by regional location trends, rather than by the higher latitudes traversed by the transatlantic flights alone. While the in-cabin data were not conducive to resolving the effect of flight altitude on ozone exposures, the MOZAIC analysis showed a mean – though highly variable – increase of approximately 70 ppb in the atmospheric ozone level per km gain in flight altitude.

An analysis of the portion of the MOZAIC data that intersects with domestic US airspace substantiated the finding, suggested in Chapter 4, that elevated ozone levels (> 100 ppb) are routinely encountered by aircraft even on domestic routes. Atmospheric ozone levels over 100 ppb were common at flight altitudes in the winter and spring months, especially in a zone around the western United States and in the northeast quadrant of the country. As anticipated, in-cabin ozone levels on domestic flights without converters were, overall, substantially lower than atmospheric ozone levels measured by MOZAIC flights. However, the difference between atmospheric and in-cabin levels may not represent a public health benefit, as emerging research indicates that the reduction in ozone in the cabin environment occurs at the cost of forming potentially harmful volatile and semivolatile gaseous- and condensed-phase oxidation products. These findings reinforce the benefit of using ozone converters even on domestic routes to protect passengers from exposure to in-cabin levels of ozone and ozone oxidation byproducts that would be associated with the presence of ozone in the incoming ventilation air.

6.2. Opportunities for future research

Indoor (or, equivalently, in-cabin) sources were, from the perspective of the primary pollutants evaluated in this dissertation, present and important for ultrafine particle exposures in homes and absent for ozone in aircraft. However, ozone in airplane cabins is associated with a class of pollutants generated in the interior space that is of concern: ozone oxidation byproducts. Section 6.2.1 proposes research to look more closely at indoor episodic sources of ultrafine particles in residences and at the in-cabin formation of ozone oxidation byproducts in airplanes.

While episodic sources of ultrafine particles discussed in this dissertation have been previously investigated to some degree, the characterization of emissions and exposures associated with a continuous indoor source – natural gas pilot lights – was a novel contribution. As this source has not been well studied, §6.2.2 suggests research aimed at investigating it further.

The studies presented in this dissertation used microenvironmental monitoring and data on occupancy patterns to model exposures. As such, reported exposures do not account comprehensively for the effects of spatial variability in concentrations within the interior environments studied. As a next step, it would be valuable to combine personal and microenvironmental monitoring in a single study, discussed in §6.2.3, to accomplish the following goals with respect to the study on ultrafine particles in homes: (a) validate the use of the indirect exposure assessment method, (b) evaluate the full impact of pollutant and human dynamics on exposure, and (c) obtain improved intake fraction estimates by assessing exposure and emissions independently.

Finally in §6.2.4 an avenue of research is suggested that explores ways to incorporate advances in knowledge in disciplines outside of air quality and exposure science to improve our understanding of present and expected future trends for in-cabin ozone.

6.2.1. Indoor sources

6.2.1.1. Residential exposure to ultrafine particles from cooking

Cooking was the most important indoor source of ultrafine particles in the monitored homes described in Chapter 2, in terms of cumulative contributions to exposure. The frequency of cooking and the primary cooking fuel (gas versus electric) were the main drivers of exposure variability across sites and between residents within a site. It would be useful to assess the degree to which the reported findings – concerning the magnitude of exposures associated with cooking and the importance of cooking compared to other indoor sources – can be generalized to geographical regions and population groups beyond the ones directly studied.

This question might profitably be approached in two stages. First a review of the literature, in light of variables observed to be important for residential exposure to particles from cooking (compared to other sources), could aid in classifying populations as being more or less vulnerable to exposures from cooking emissions. The described classification could also provide a basis for an initial assessment of the anticipated inter-population variability. Variables that might be targeted include:

- The type of fuel (electric or gas) used for cooking, as natural gas appliances were associated with higher emissions and exposures than electric appliances.
- The presence of a particle filter or treatment device associated with the air handling system, as this would reduce the residential component of total daily exposures.
- The number of occupants, as a greater number of residents could necessitate longer and more frequent cooking.
- The house volume, as a smaller volume implies less dilution of emitted particles.
- Outdoor levels of UFP and the *IPOP*, as higher exposures to particles of outdoor origin could diminish the relative importance of particles emitted during cooking.
- Demographic attributes (e.g. age and gender). We did not observe a difference in exposures between men and women. However, such a difference might be observed in populations that have a gender-bias in terms of the amount of time spent engaged in cooking. For children, the longer duration of time spent asleep compared to adults could serve a protective function by removing them from the zone of active cooking emissions.

Second, on the basis of the review, two populations hypothesized to have high and low fractions of residential UFP exposures attributable to cooking activities could be selected for a comparative monitoring study. The exercise could aid with control efforts by helping to identify conditions under which cooking emissions matter for exposure and variables that mediate their influence. A comparative study of the type described would also have the benefit of helping to identify subpopulations most vulnerable to exposure to ultrafine particles from cooking. Identifying these populations could, in turn, inform a health risk assessment or intervention study targeting indoor sources.

To properly evaluate the importance of cooking emissions for ultrafine particle exposures it is also necessary to evaluate whether ultrafine particle emissions from cooking, apart from contributing to exposure, pose a human health risk. To address this issue three questions might be usefully considered. First, from an epidemiological perspective, can UFP generated by cooking and other indoor sources be lumped with UFP from outdoor sources? If so, does the

residential component contribute meaningfully to total daily exposures to ultrafine particles? Second: while at home, people are exposed to "spiky" levels of freshly emitted particles from indoor sources, and to lower and more steady levels of an "aged" population of particles originating outdoors. Looking only at residential exposures, how do the health effects of particles from the two source categories compare? Third, a bottom-up approach could look at the size distribution and composition of UFP generated from cooking and use these parameters as indicators of their toxicity. The question of whether ultrafine particles generated by cooking matter for health could also be directly investigated through a controlled human study, where an acute health outcome (such as heart rate variability) could be measured in an exposed and an unexposed group.

6.2.1.2. In-cabin exposure to ozone byproducts

In the studies presented in Chapters 4 and 5, in-cabin and atmospheric ozone were investigated independently of each other. To our knowledge only one prior study (Perkins et al., 1979; Nastrom et al., 1980) has monitored the two parameters simultaneously on a large sample of flights, thus offering insight into the empirical relationship, under in-flight conditions, between atmospheric and in-cabin ozone levels. Simultaneous atmospheric and in-cabin monitoring was accomplished by adding an in-cabin monitoring component to the GASP aircraft monitoring campaign. This enabled the assessment of values of the retention ratio for two different aircraft types under five different operating conditions, on more than 300 flight segments.

There is a need to update the findings obtained by Perkins et al. (1979) as conditions in aircraft have changed since the 1970s. Long-haul commercial passenger aircraft are now routinely operated with ozone catalytic converters that were absent before 1980, the outside air ventilation rate has been reduced by approximately a factor of two, and the average occupant density has increased. Moreover recent research has advanced our understanding of a corollary of ozone surface removal, the formation of ozone oxidation byproducts, which is a piece of the story linking atmospheric and in-cabin ozone that was previously unknown.

Preliminary research has investigated the formation of ozone reaction byproducts and resulting health effects via experiments conducted in a chamber and in a simulated aircraft cabin. A field study investigating the formation of byproducts under normal, occupied conditions constitutes an important next step. It is especially crucial that byproduct formation be investigated in the presence of exposed people as human skin surfaces form a substrate for ozone reactions, and thus the presence and density of humans has an effect on their exposures. New research that investigates the formation of byproducts under in-flight conditions was initiated in 2008 (Weisel et al., 2010), and simultaneous ozone and ozone byproduct data have so far been acquired from 40 domestic and international flights. Ozone levels on the flights varied from below 20 ppb to greater than 100 ppb, and the oxidation products nonanal, decanal and 6-methyl-5-hepten-2-one (6-MHO) were routinely detected.

The research by Weisel et al. (2010) provides a strong platform for a large scale study of in-cabin exposure to ozone byproducts that could be modeled in part on the GASP and MOZAIC aircraft campaigns. In the proposed research, one or more commercial, passenger, B-757 aircraft (without ozone converters) would be outfitted with outside and in-cabin ozone monitoring equipment designed to automatically sample time-resolved levels of ozone on routine transcontinental US flights. The resulting large sample of atmospheric and in-cabin ozone levels

would enable the assessment of a robust retention ratio under conditions currently prevalent in aircraft chosen to be reasonably representative of the commercial passenger fleet. Ozone byproducts could then be sampled episodically, on a subset of monitored flights, to provide insight into the yield and mix of byproducts per mole of ozone consumed in the cabin. These parameters could in turn be linked to factors such as the cabin occupant density, and aircraft operating conditions. This study would advance our understanding of the importance of atmospheric ozone trends relative to other variables influencing the exposure of cabin occupants to ozone and ozone byproducts. It would form a strong basis for evaluating whether the current Federal Aviation Regulations limiting in-cabin ozone are adequately health protective.

6.2.2. Ultrafine particle emissions from natural gas appliance pilot lights

Reported in this dissertation are particle number emission rates, first-order decay coefficients and exposures for continuously burning pilot lights associated with a cooking range and oven. The pilot lights were present at two sites. The stoves at these sites were of the same make and model: they were antique Wedgewood stoves that had 4 pilots each (two for the range and two for the oven). Emissions and exposures associated with this source were found to be significant for the occupants of sites where it was present. The precise prevalence of natural gas pilot lights – which would, along with emissions and exposure estimates, serve as an indicator of their importance – could not be assessed. However, a Department of Energy analysis that assumes 18% of gas-range consumers purchase equipment with constantly burning pilots suggests piloted ranges are still in wide use (NARA, 2007).

It would be worthwhile to evaluate a wider set of piloted stoves, ovens and other appliances, to obtain a regionally or nationally representative distribution of ultrafine particle emission rates for this source category. To facilitate future research, the ability of gaseous copollutants such as nitrogen oxides and carbon monoxide to serve as indicators of the presence and particle number emission rate of pilot lights might also be evaluated.

The proposed research – which could be conducted in the field or in a laboratory – combined with a review of the prevalence of the use of pilot lights would facilitate an assessment of the importance of pilot lights compared to other residential sources of ultrafine particles. As a corollary the exposure benefit of phasing out pilot lights could be estimated, which might add momentum to a trend already underway, motivated by the intent to save energy. Results from the proposed investigation could also help researchers studying UFP in homes to gauge the importance of taking emissions from piloted appliances into account, to avoid misattributing indoor baseline exposures to outdoor particles.

6.2.3. Direct versus indirect exposure assessment

A study similar to the investigation in Chapter 2, with the addition of a personal monitoring component, could help to validate the "indirect" method used in this dissertation and to define its limitations for the exposure scenario under study. As the indirect exposure assessment method has distinct benefits compared to the direct method, the proposed study would make a methodological contribution by facilitating its use.

Results on UFP exposures in homes presented in Chapters 2 and 3 provided preliminary evidence of the influence of pollutant and human dynamics on exposure. With the addition of a

personal monitoring component, the impact on exposure of spatial variability in concentrations, ultrafine particle removal processes, and the movement of individuals through the house could be more accurately assessed. A comparison of direct and indirect exposure assessment results could provide insight into conditions under which the indirect method is more or less reliable.

While our intake fraction analysis did not demonstrate a difference in *iF* associated with source type, such a difference might emerge if personal monitoring were employed to assess exposure and if some sources systematically require closer proximity than others. For instance, "active" cooking that requires a cook to remain close to a range is expected to result in exposures to elevated breathing-zone concentrations (relative to those recorded by the area monitor) and hence greater *iF* than "passive" cooking such as use of the oven or water boiling.

6.2.4. Lessons from other disciplines

The investigations in Chapters 4 and 5 address the issue of ozone in aircraft cabins from the perspective of exposure scientists with a primary expertise in indoor air quality. It would be valuable to supplement that perspective with advances in knowledge from other disciplines that are concerned with commercial passenger aircraft and with atmospheric ozone. These disciplines include transportation, meteorology, atmospheric chemistry, and climate change.

Lessons from research under way in these areas could help in the interpretation of trends observed in an air-cabin ozone exposure study, and in anticipating future changes. Examples of such research areas include: (a) research on the relationship between stratospheric intrusions, the occurrence of deep convection, and weather systems, (b) predicted changes in the tropopause height as a consequence of global warming, (c) innovations in ozone catalytic converter design, (d) changes in aircraft design and operation, such as a shift from the use of bleed air for ventilation to bleedless systems, and (e) projected increases in flight altitude bands.

6.3. References

NARA, 2007. Federal Register, November 15, 2007. Office of the Federal Register, National Archives and Records Administration (NARA). Available at http://www.gpoaccess.gov/fr/.

Nastrom GD, Holdeman JD, Perkins PJ, 1980. Measurements of cabin and ambient ozone on B747 airplanes. *Journal of Aircraft* **17**, 246-249.

Perkins PJ, Holdeman JD, Nastrom GD, 1979. Simultaneous cabin and ambient ozone measurements on two Boeing 747 airplanes, Volume 1, US Department of Transportation, Federal Aviation Administration, Washington, DC. Available at ntrs.nasa.gov.

Weisel CP, Weschler C, Mohan K, Alimokhtari S, 2010. Ozone and its byproducts in aircraft cabins. Abstract submitted to Indoor Air, 2011.